University of **Strathclyde**
Science

WestCHEM

Synthesis and Characterisation of Novel Organic Semiconductors

A thesis submitted to the Department of Pure and Applied Chemistry, The University of Strathclyde, in fulfilment of the regulations for the Degree of Doctor in Philosophy in Chemistry

Irina Afonina

2011

ACKNOWLEDGEMENTS

TO MY SON DMITRI WITH LOVE

ABSTRACT

Organic semiconductors (OSCs) attract considerable attention from blue-chip companies and research communities as potential substitutes of inorganic counterparts in electronic devices.

Thiophenes are one of the most extensively studied and highly topical classes of electron-rich OSCs. Linked compounds are known for their photoluminescent and conducting properties. On the other hand, *fused* thiophenes (FTs), both as small molecules and conducting polymers containing these blocks, demonstrate a different approach to broaden and improve the properties of this family of materials.

FTs are highly ordered structures, with good potential for high charge-mobilities. Simultaneously, they are more environmentally resistant than many other OSCs, due to their wider HOMO-LUMO gaps. The review regarding these interesting materials and recent literature examples are presented in Chapter 1.

During the course of my PhD research work several novel diindenodithioenothiophene (DITT) based molecular and polymeric materials were prepared and investigated. The parent compound (**77**), obtained through a multistep synthesis, comprises a central dithienothiophene-core and symmetrically attached indene-moieties at both sides. It was found to be sparingly soluble and in order to enable further synthetic manipulations was successfully derivatised with solubilising groups (**78**). Further oxidation of the thienyl sulfur to the corresponding sulfone afforded a highly photoluminescent compound (**79**). These three materials were characterised in terms of their chemical structure and properties. The findings are discussed in Chapter 2 along with the results of the performance of an OFET device, which was fabricated with **77** as the active semiconductor.

77

78

79
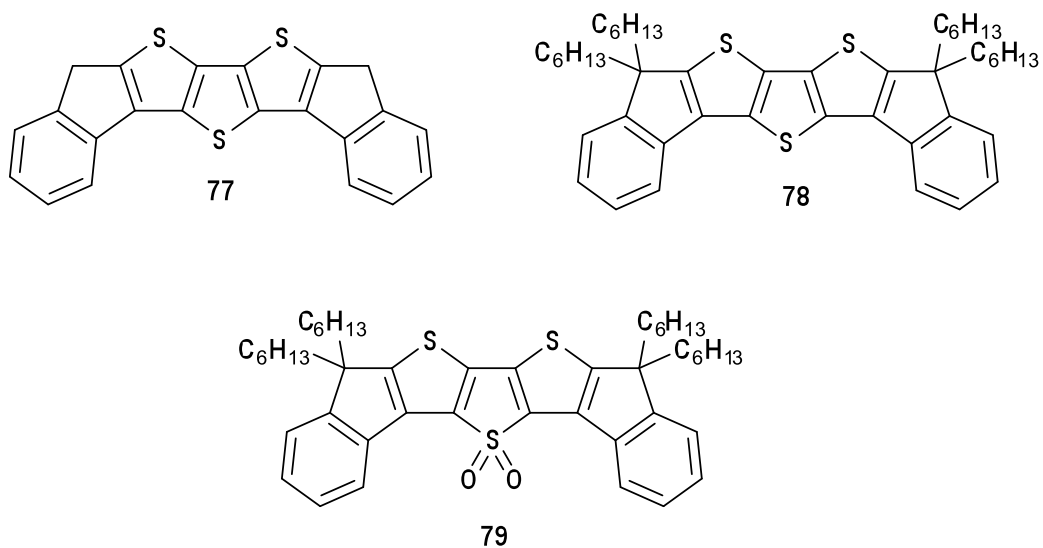
Further work with the DITT-based materials involved polymerisations of **78** and **79** *via* a Yamamoto protocol and also copolymerisations of **78** with the fluorene and *para*-phenylene derivatives achieved through Suzuki polycondensations. The details of the synthetic procedures are described in Chapter 3. Chapter 4 presents the results of the property investigations of the synthesised polymers.

ABBREVIATIONS

AFM	Atomic Force Microscopy
BDT	2,2'-Bidithieno[3,2-*b*:2',3'-*d*]thiophene
BTEAI	Benzyltriethylammonium Iodide
CP	Conjugated Polymer
CT	Charge Transfer (transport)
CV	Cyclic Voltammetry
D-A	Donor-Acceptor
DCM	Dichloromethane
DITT	Diindenodithienothiophene
DMSO	Dimethyl Sulfoxide
DPh-BTBT	2,7-Diphenyl[1]benzothieno[3,2-b][1]-benzothiophene
DSC	Differential Scanning Calorimetry
DTT	Dithienothiophene
EDOT	Ethylenedioxythiophene
E_F	Fermi Level
E_g	Band Gap
EI	Electron Impact (Ionisation)
EL	Electroluminescence
ES	Electrospray Ionisation
eV	Electron-volt
FAB	Fast Atom Bombardment
FET	Field Effect Transistor
FF	Fill Factor
FT	Fused Thiophene
GPC	Gel Permeation Chromatography
HMDS	Hexamethyldisilazane
HOMO	Highest Occupied Molecular Orbital
HT	Head-to-Tail
ICT	Intramolecular Charge Transfer
IR	Infrared

LDA	Lithium Diisopropylamide
LUMO	Lowest Unoccupied Molecular Orbital
M	Molar
***m*-CPBA**	*meta*-Chloroperoxybenzoic Acid
MALDI	Matrix–Assisted Laser Desorption Ionisation
MO	Molecular Orbital
mol	Moles
MS	Mass Spectrometry
n-doped	Negatively doped
NBS	*N*-Bromosuccinimide
NMR	Nuclear Magnetic Resonance
OFET	Organic Field Effect Transistor
OLED	Organic Light Emitting Diode
OPV	Organic Photovoltaic Device
OSC	Organic Semiconductor
OTFT	Organic Thin Film Transistor
OTS	Octyltrichlorosilane
p-doped	Positively doped
P3HT	Poly(3-hexylthiophene)
PA	Polyacetylene
PAN	Polyaniline
PAT	Polyalkylthiophene
pBTTT	Poly(4,4-dialkyl-2,2-bithiophene-*alt*-thieno[3,2-*b*]thiophene)
Pc	Phthalocyanines
PCBM	Phenyl-C_{60}-butyric acid methyl ester
PCE	Power Conversion Efficiency
PDI	Polydispersity Index
PDI*	Perylene Diimide
pDTT	Poly(dithienothiophene)
PEDOT	Poly(ethylenedioxythiophene)
PF	Polyfluorene
PL	Photoluminescence
PLED	Polymer Light Emitting Device

PLQY	Photoluminescence Quantum Yield
PPA	Polyphosphoric Acid
ppm	Parts per Million
PPP	Poly-*para*-phenylene
PPV	Poly-*para*-phenylenevinylene
PPy	Polypyrrole
PSC	Plastic (Polymer) Solar Cells
PSS	Polystyrene Sulfonic Acid
PT	Polythiophenes
pTT	Poly(thieno[3,2-*b*]thiophene)
SAM	Self-assembled Monolayer
SPC	Suzuki Polycondensation
TCNQ	Tetracyano-p-quinodimethane
TCSPC	Time Correlated Single Photon Counting
TFT	Thin Film Transistor
TGA	Thermal Gravimetric Analysis
TH-DITT	Tetrahexyl-diindenodithienothiophene
THF	Tetrahydrofuran
TIPS	Triisopropylsilyl
TLC	Thin Layer Chromatography
TMEDA	Tetramethylethylenediamine
TMTSF	Tetramethyl tetraselenafulvalene
TOF	Time-of-Flight
TTF	Tetrathiafulvalene
UV	Ultra Violet
V_{oc}	Open Circuit Voltage
XRD	X-ray Diffraction

CONTENTS

CHAPTER 1

CHAPTER 1

INTRODUCTION

This work was conducted under the supervision of Professor Peter J. Skabara and was dedicated to the synthesis of novel organic semiconductors and investigation of their electrochemical properties. Organic semiconducting materials have been extensively studied in the last 50-60 years and resulted in significant progress within the industry of electronic devices, allowing the world to benefit from more efficient, practical, durable and sustainable technologies. Rapidly increasing demand for high performance electronics and smart energy-saving solutions dictates the search for alternative materials, such as organic semiconductors.

Organic semiconductors are materials that can conduct electric charges upon excitation triggered by, *e.g.*, applied voltage or solar/UV irradiation. They are presented by various aromatic systems and several distinct groups of conjugated polymers. In the following chapters, some essential principles and fundamental properties of these materials will be outlined, revealing the elegance and rationality behind the recent and future progress.

1.1. Conductivity

Conductivity is the ability of a material to transport an electrical charge. This ability lies in the electronic structure of the material and band theory is usually used to explain the fundamental properties.[1,2,3] Band theory is based on a model of three bands: filled, valence and conducting. The valence band presents the highest occupied level in a molecule's electronic structure, whereas the conducting band refers to the lowest unoccupied level.

Electrical conductivity is temperature dependent and there are two main types of conductors (Figure 1):

- **Metallic conductor** (conductivity decreases with an increase in temperature)
- **Semiconductor** (conductivity increases with an increase in temperature).
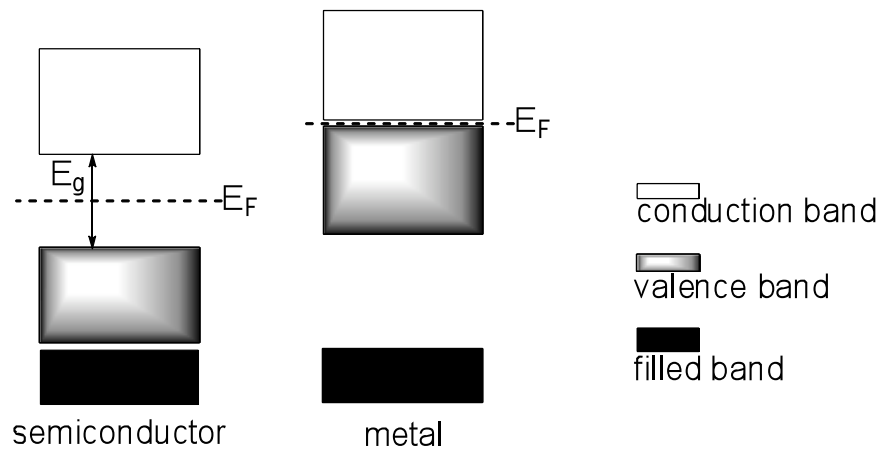
Figure 1. Energy bands according to band theory (E_F = Fermi level, E_g = energy gap)

The electronic structure of a metal includes at least one partially filled level and that means that there is no energy gap between the highest occupied level – Fermi level, E_F, and the lowest unoccupied level. Electrons can pass almost freely between the bands and thereby sustain electrical conductivity. A decrease in conductivity with an increase in temperature is attributed to the increased movements of the atoms within the lattice, promoting chaotic collisions of the electrons and, hence, resulting in less efficient charge transport.

Because of the electronic nature of semiconductors, they can only contain completely filled and completely empty bands, which leads to an energy gap, E_g, between the highest occupied (valence) and the lowest unoccupied (conducting) levels. To overcome this gap some initial energy is required, *e.g.*, thermal, which would allow the electrons to excite across the gap and populate the empty orbitals of the conducting band and thus, transport electrical charges.[1-3]

Some materials possess a very large energy gap between the bands and very few electrons are able to promote to the upper band at ordinary temperatures, which results in no electrical conductivity. Such materials are referred to as **insulators**.[1-2]

Thus, semiconductivity depends on the number of charge carriers within the solid structure of a material. For improved charge transfer, so-called **doping** can be applied. The main idea of doping is to introduce an additional energy level (band) between the existing bands that would provide additional assistance with electron or hole transport and hence, increase of conductivity. There are two types of doping: p- and n-doping (Figure 2).
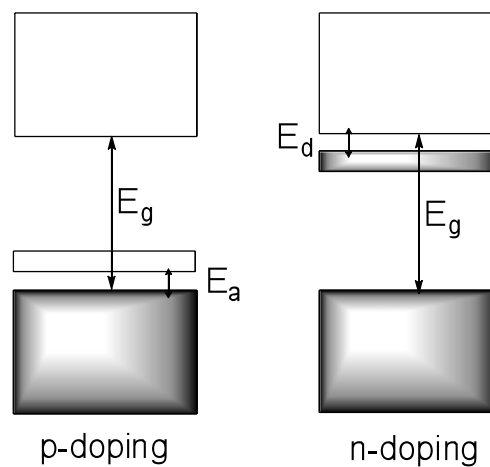
Figure 2. p-and n-doping of a semiconductor

p-Doping means that positive charges – holes, have been created by incorporation of a more electron deficient (acceptor) band, E_a, just above the valence level. Electrons can now move between these holes, create new holes and provide an enhanced conductivity as a result. **n-Doping** is achieved when a donor band, E_d, is incorporated by injection of additional electrons (negative charges). E_d, placed beneath the conduction band, increases the supply of mobile electrons and in turn, the conductivity.

At this point, it is worth mentioning that there is one more type of conductivity. Superconductivity is a very complicated physical process, which in the past was commonly achieved with metals at low temperatures.[3] Presently, this can be achieved at much higher temperatures and with materials other than metals. Superconductivity

can be observed when a material shows no resistance at its critical temperature. Electrical circuits made of a superconductor suffer no power loss and no current decay.

Overall, the material's ability to conduct depends directly on its chemical structure: provision of the charge carriers, and intermolecular interactions in its solid state are responsible for the efficient charge transport required for conductivity. One of the most important characteristics of a semiconductor is therefore charge-carrier mobility, which defines this ability as a numerical value.

1.2. Charge-carrier Mobility

Inorganic semiconductors, such as silicon, have highly crystalline, three-dimensional structures, formed by strong covalent bonds. This causes the formation of true bands and charge transport is only limited by the physical conditions of the crystal solid (impurities, vibration, etc.). In contrast, organic semiconductors are more disordered. They have only weak intermolecular interactions *via* van der Waals forces, S⋯S or S⋯O interactions, hydrogen bonds and π-π interactions and usually do not form proper bands. They generally can be considered as wide-gap semiconductors (band gaps of 1.4 eV and over) down to insulators (band gaps above 3 eV) in traditional, that is, inorganic semiconductor terms. Hence, charge delocalisation occurs only within the π-conjugated backbone of a molecule or to π-orbitals of the closest molecules.[1, 4]

Although the exact mechanism is not yet fully understood, there is a model which seems to give a general idea of the charge transfer in these disordered organic materials: the so-called, hopping process.[4] By this model, the charge transport is seen as a continuous reduction-oxidation (insertion-removal of the charge carriers) process of the molecules, where:

- electrons are transferred from an anion radical of a molecule to a neutral molecule through the LUMO, and
- hole transport is realised by electron transfer from a neutral molecule to a cation radical through the HOMO.[4-5]

There are several types of electronic devices that are able to utilise properties of organic CT-materials. In general, the three main types include OLEDs (organic light-emitting diodes), OFETs (organic field effect transistors) and OPVs (organic photovoltaic devices). The less common device types are sensors and lasers. All of them operate in different manners, but in each case are fully dependent on effective charge transfer provided by a charge-transporting material – the organic semiconductor. In turn, the performance of an organic semiconductor in an electronic device depends mainly on the efficiency of charge transfer by the charge-carriers (electrons or holes) within the π-conjugated system.

Therefore, one of the most significant qualities describing an organic material is its charge-carrier mobility, which is particularly important if the intended application is in an OFET device.

Charge-carrier mobility can be measured experimentally by several methods:
- **TOF** (time-of-flight): measures charge-carrier transit time through a thin layer of the organic material sample, placed between two electrodes. The sample is initially irradiated by a laser pulse in proximity of one of the electrodes. Then, generated holes or electrons migrate towards the other electrode, where the current is recorded as a function of time.
- **FET – configuration**: the material of interest is incorporated into an OFET and its performance is analysed.
- **Diode configuration**: the sample is analysed in a diode.
- **PR-TRMC** (Pulse Radiolysis Time-Resolved Microwave Conductivity) is a non-contact technique. The charges are generated in the bulk of the sample directly by a pulse of highly energetic electrons. This way, a low density of free carriers is produced and their transport characteristics are determined as a frequency of microwave radiation, resulting from changes in electrical conductivity.

Charge-carrier mobilities can be influenced by many factors, such as purity of the sample, molecular packing, level of disorder, size/molecular weight, temperature, pressure and electric field. Amongst the above mentioned techniques, the TOF-method

and the analysis of an OFET performance are the most common ways to determine the potential efficiency of an organic semiconductor in an electronic device.[6]

1.3. Common Electronic Devices

Organic semiconductors find more and more applications and substantial progress is being made in the industrial development of electronic devices. Not so long ago organic electronics were mainly a subject of research, but now blue-chip companies, such as IBM, Sony, Kodak, Philips, Sanyo, Siemens, DuPont, BASF, CDT, Merck and many others, put a lot of effort into improving the prototypes, constructing new devices, utilising the electrochemical properties of these materials, striving for better performance, stability, long lifetime and reliability.

As mentioned previously, the three main types of electronic devices for utilising organic semiconductors are OLEDs, OFETs and OPVs. Their basic working principles are summarised here.

1.3.1. OLEDs

OLEDs are commonly known as flat displays, screens, etc., and considered to be the most advanced among the three types of electronic devices. They can offer low drive voltage, brightness of colours, fast response and easy manufacturing over large surfaces. OLEDs work on applied voltage between the cathode and the anode and are usually composed of hole-transporting (conductive) and electron-transporting (emissive) layers of organic materials (Figure 3).
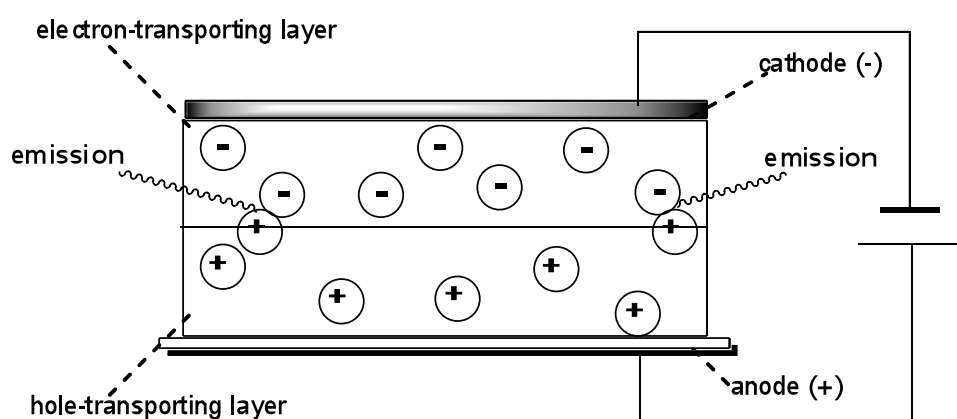
Figure 3. Working principle of OLEDs

The operation of OLEDs builds on an initial charge injection from the anode and the cathode, which promotes charge transport through the organic layers following an exothermic recombination of holes and electrons within the layers. This results in excited states of the molecules and follows by rapid relaxation in the form of emission of fluorescence or phosphorescence.[5, 7]

The hole-injecting anode is usually presented by a highly conductive, stable and transparent indium tin oxide (ITO) film, deposited on the polished glass substrate. The cathode is responsible for efficient electron injection into the organic layer and should be preferably made of low-work-function metals, *e.g.*, In, Mg, Ca or alloys: Mg:Al and Al:Li. Organic layers can be made with both small molecule materials and polymers as long as high quality, defect-free films with controlled thickness can be obtained and remain stable for long periods of time.[4]

Today, OLEDs are commercially used in smaller TV screens, displays of mobile phones and digital cameras, car audio systems, etc. In the future we will be able to take more advantage of ultra-thin, bright, low power consumption and lightweight OLED based devices. Although, despite the overall accessibility, the main difficulties in manufacturing of such products are limited lifetimes of the organic materials (blue emitters, in particular), recrystallisation of the film layers and formation of non-emissive dark spots. Also, sensitivity of the emissive materials to water and air poses another problem and proper encapsulation of the device is required.

1.3.2. OFETs

Transistors, based on inorganic semiconductors, such as silicon and gallium arsenide, are utilised on huge industrial scale for their small size and high conductivity. Organic transistors, on the other hand, have a great potential of easy, low cost manufacturing and flexibility, but so far cannot measure up in stability and charge mobilities.[8]

Figure 4 gives a schematic representation of an OFET device. It consists of conductors: gate, source and drain electrodes; an insulator – gate dielectric, and an organic semiconductor as an active body. The gate dielectric or insulator can be made of an

inorganic material, such as SiO₂ or an organic polymer insulator, *e.g.*, poly(methyl methacrylate); its function is to control the flow of electrons. Electrons flow between the source and drain electrodes, which are often made out of metals: gold, platinum or silver.
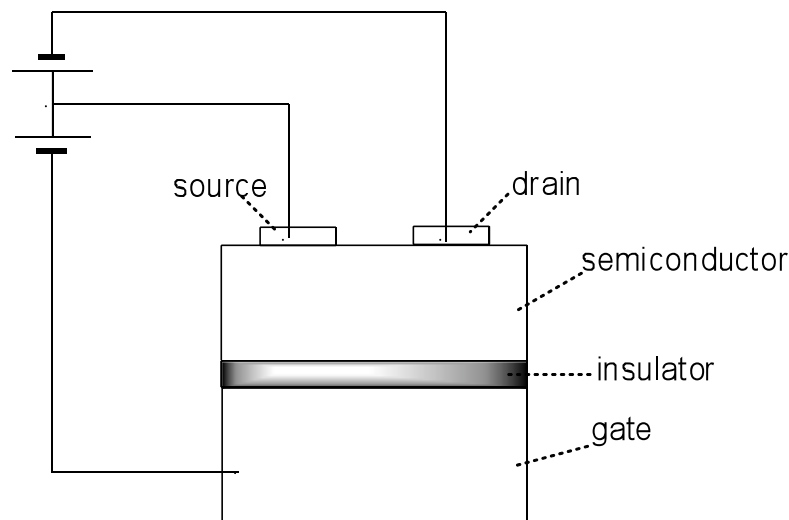
Figure 4. Structure of an OFET (top contact configuration)

The off-mode of an OFET is defined by a very small flow of current between the source and the drain when no voltage is applied. An on-mode takes place when, for instance, a negative voltage is applied (at the gate electrode), which triggers the formation and accumulation of charge carriers (holes, in this case) at the interface with the insulator. Thus, hole transport occurs from the source to the drain electrodes and this makes a p-channel device. In similar fashion, application of positive voltage, promotes transport of electrons and this is an n-channel device.[5]

OFETs are used as switches for different purposes, for instance, in display back panels and another major application – radio frequency identification tags for diverse objects.

1.3.3. OPVs

Photovoltaics is a technology for utilising solar energy as one of few clean and sustainable energy sources. Photovoltaic devices are known as solar cells and they perform direct conversion of sunlight into electricity. Since the task of finding efficient

alternative energy sources becomes more serious and the demand for manufacturing of capable photovoltaic cells grows stronger, there is no wonder that this field receives a lot of attention.

The first generation solar cells, consisting of a single p-n junction diode were made using the silicon wafer and this is still the dominating technology. The second generation is based on using thin films of inorganic semiconductors, such as silicon of different morphologies, cadmium telluride, copper indium selenide/sulfide. These cells have generally lower efficiencies, but their manufacturing costs are also lower. The increasing demand for silicon makes production of traditional solar cells more expensive therefore alternative materials for harvesting solar radiation are required. Thus, the third and fourth generations of solar cells involve extensive use of organic semiconducting materials, often polymers,[9] and nanoparticles.

The first organic solar cell was made in the middle of the 1980s by Tang and co-workers.[10] It was constructed from copper phthalocyanine and a perylene derivative and had a power conversion efficiency of 1%. Also, it was one of the earliest applications of an organic optoelectronic device.

Organic PV cells consist of thin films of organic photoactive materials between two metal electrodes. The working process of an OPV cell can be considered as just the opposite of the OLED's (Figure 5).[5] It starts with sunlight absorption by the organic material and formation of excited states known as excitons. The generated excitons further migrate, separate at the p-type/n-type interface and promote charge transport to the electrodes, where the charge collection occurs.[7]
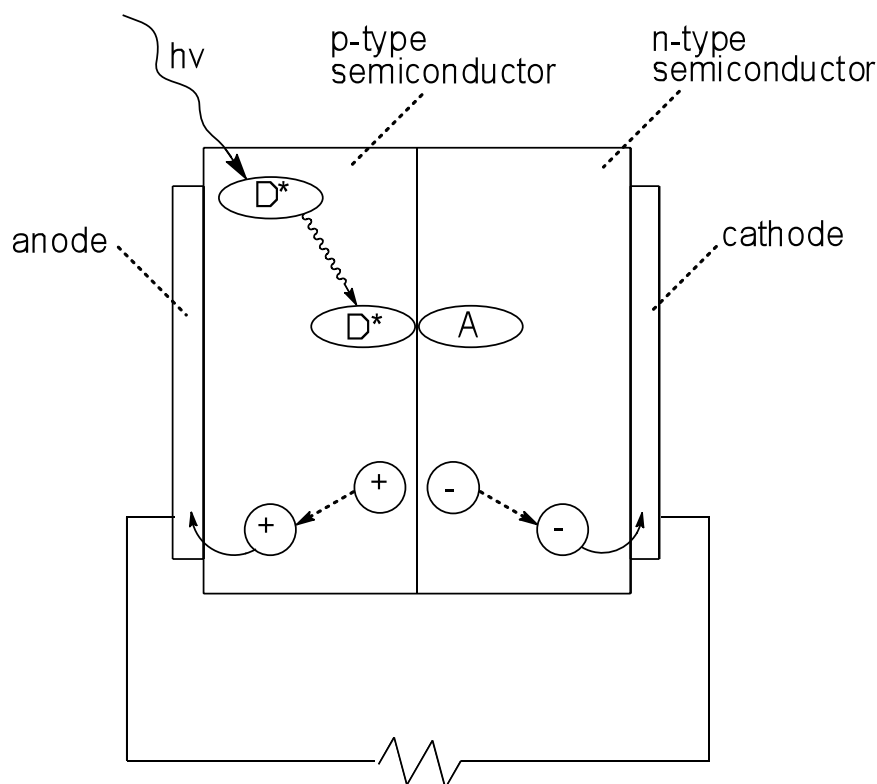
Figure 5. Working process of *pn*-heterojunction OPVs[5]

There are a few difficulties in the manufacture of organic solar cells on an industrial scale. Firstly, the energy conversion efficiency remains low, even the best OPV to date converts only at 7.4% rate.[11] Secondly, many organic materials undergo degradation upon exposure to UV light and because of their highly unsaturated nature, they are sensitive towards oxidation and moisture.[12] Despite that, research work keeps going forward and new methods and materials can be applied in the future. For more in depth information, Günes, Neugebauer and Sariciftci have published an extensive review on third and fourth generation solar cells.[13]

1.4. Organic Semiconductors

1.4.1. Background

Organic charge-transfer (CT) materials used for applications in electronic devices can be semiconductors or metals. Organic semiconductors are mostly π-electron materials with remarkable abilities for charge-carrier generation and transfer, light absorption and emission, electroluminescence (EL), magnetism, etc.[5,6, 14,15] These abilities arise from extensive delocalisation of π-electrons within the π-bonded framework of these materials. Thus, with an initial formation of charge-carriers (electrons or holes), these effects can be achieved. In turn, the ability of the organic materials to transfer electrons or holes depends mainly on their highest occupied molecular orbital (HOMO) and lowest unoccupied molecular orbital (LUMO) energies, the gap and interactions between them. To find application in an electronic device, an organic material must be readily accessible for easy redox processes: that is, to be able to easily donate or accept electrons in a reversible manner. The electrons are donated from the HOMO and accepted into the LUMO in order to form stable redox states. The possible candidate material needs to possess HOMO and LUMO levels within an accessible potential range – the gap between the orbitals must be considerably narrow.

There are two ways to reduce the HOMO-LUMO gap in an organic material for the purpose of tailoring its electrochemical properties:[16]

- extension of π-conjugation in the molecule, which is readily applied in the case of π-conjugated polymers
- synthesis of a D-A compound, where D (π-electron donor with high HOMO level) and A (π-electron acceptor with low LUMO level) are bound through conjugation, which in the case of small molecules provides a better option to control the gap between the orbitals.

Organic semiconductors are flexible, lightweight and can be modified chemically for the desired properties. They can be manufactured and processed in solution, which lowers the production costs by replacing expensive methods, such as vacuum deposition techniques and lithography required for silicon-based materials. These qualities make organic materials suitable candidates for a broad range of applications in

optoelectronic devices such as OLEDs[17] – *e.g.*, displays, screens; OFETs[14,18,19,20] – radio frequency identification tags; solar cells[9, 21] and lasers.[22]

Organic conductive charge-transfer complexes have been a field of extensive research for the past 50 years. Perylene (**1**), discovered in the 50s, was one of the first showing high conductivity, displaying blue fluorescence and is used in OLEDs.[23]

1
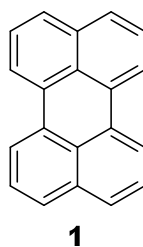
In 1973, Ferraris *et al.* managed the synthesis of the TTF-TCNQ donor-acceptor complex (**2**) – the first true organic metal characterised by its metallic properties at temperatures as low as 54 K.[3,24]

2
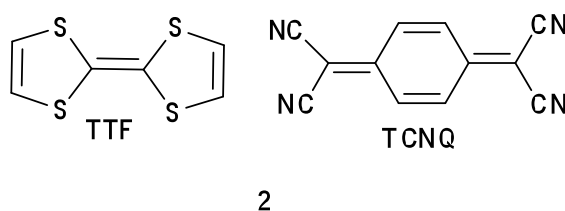
In 1979, Bechgaard *et al.* observed superconductivity for a number of tetramethyltetraselenafulvalene (**3**) based salts, $(TMTSF)_2X$, where X was an inorganic monovalent anion (PF_6^-, AsF_6^-, SbF_6^- , etc.) at low temperatures and applied pressure.[3,25] Later, he discovered $(TMTSF)_2ClO_4^-$, a complex that remained superconductive under atmospheric pressure.[26]

3
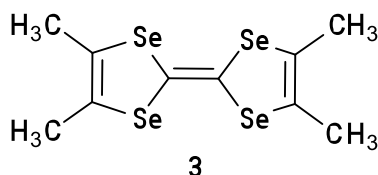
Among the first conducting polymers, Weiss *et al.*[27] in 1963 found that iodine-doped polypyrroles produced high conductivity, but their work was not widely acknowledged.

Research in the area of organic conducting materials continued both in academia and industry. The 2000 Nobel Prize in Chemistry was awarded to A. Heeger, A. MacDiarmid and H. Shirakawa for their earlier discovery of highly conducting iodine-doped polyacetylenes in the late 1970s.[28]

The research and development of potent organic charge-transfer materials is important and beneficial. They are probably not going to fully replace their inorganic analogues in the very near future, but can efficiently complement them. Utilising the remarkable properties of organic materials in electronic devices opens up new possibilities and provides cost effective options for excellent performance.

1.4.2. Representative Classes

Organic conducting materials are represented by a broad range of π-compounds, from small molecules and oligomers to high molecular weight polymers.[5,6] Small molecules have well-defined structures and weight and usually need to be deposited by vapour methods, such as sublimation, in low or high vacuum. On the other hand, polymers are processed from solution by, *e.g.*, spin-coating or inkjet printing and because of their dispersion properties they make good materials for glass surfaces.[8] Polymeric materials are often mechanically resistant and suitable for flexible applications.

Some of the most studied and used materials will be listed in the following sections.

1.4.2.1. Molecular Semiconductors and Oligomers

1.4.2.1.1. Tetrathiafulvalene

Tetrathiafulvalene (TTF) is a known electron donor. Its derivatives and salts are probably the most studied conducting and superconducting materials so far. The interest in TTF is based on its electrochemical properties, that arise from the ability to reversibly donate two electrons and in this way generate a stable open shell cation radical and a dication (Scheme 1).
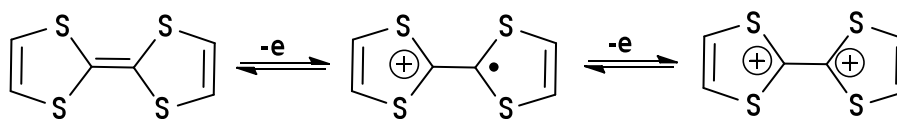
Scheme 1. Redox states of TTF

These two states are stabilised by the aromatic resonance of the TTF molecule and are responsible for its conducting and even superconducting characteristics.

Because of its chemical structure, TTF and its derivatives are also able to take part in some very organised intermolecular arrangements with other molecules bearing other properties and together contributing to complex, so-called supramolecular structures. Supramolecular arrangements are non-covalent, mutual interactions between the molecules, based on van der Waals forces, hydrogen bonding and other weak interactions. These interactions are also partially responsible for the π-stack formation and conducting properties of TTF charge transfer salts. Derivatisation of TTF increases the dimensionality of the entire molecule or complex, which can lead to supramolecular arrays with distinct properties.

As mentioned previously, one of the tactics to narrow the HOMO-LUMO gap of an organic CT-material is to synthesise a D-A complex. This approach is somewhat more reliable for a molecular conductor, such as TTF, since both HOMO and LUMO can be adjusted individually. Some common acceptors are represented by other aromatic systems – benzene rings, phthalocyanines, benzoquinones, porphyrins, TCNQs, etc., in

either a conjugated or non-conjugated manner. Fullerene (C_{60}) is a known acceptor and can be connected with TTF in various ways.[16,29]

Some TTF based macrocyclic D-A systems are able to spontaneously self-assemble and disassemble in controlled redox processes. This is a popular subject of research because of the potential application of these materials as sensors, switches and in nanotechnology. Among such D-A structures, there are several TTF-fullerene complexes, both as self-assembling non-covalent formations[30] and as covalently linked dyads and triads.[31,32]

TTF with appropriate "partners" and/or derivatisation can exhibit qualities suitable for a variety of devices, but a large-scale industrial manufacturing of such is a matter of future development. In the research field, however, some prototypes and experimental devices have been built, among which OFETs seem to attract a lot of attention.[33]

The range of potential applications of TTF-based compounds is rather broad. New materials are being prepared and tested for their conducting,[34] superconducting,[35] magnetic,[15,36] and optical[37] properties.

A group of dumbbell-shaped, mechanically interlocked molecules, developed by F. Stoddart known as rotaxanes, present another area of interest for application as molecular machines and switches.[38]

Also, TTF can be applied in the design of sensors as reported by Zhang *et al.*[39] where a TTF-anthracene dyad with two attached boronic acid groups, showed a distinct selectivity towards fructose.

1.4.2.1.2. Oligoacenes

Oligoacenes (**4**) – polycyclic aromatic hydrocarbons, present a group of widely investigated materials and have found a broad application in organic electronic devices.[6]

4
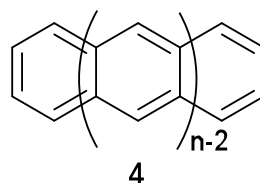
Pentacene (**4a**, n = 5) has a well-defined crystal structure and is known to be a p-semiconductor (a hole-transporter) possessing high charge-carrier mobilities. Pentacene thin films have wide use in OFETs and thin-film transistors.[40,41] Also, a recent report of a pentacene-C_{60} photovoltaic device showed that fabrication of the cell with a layer of nanoimprinted pentacene resulted in a 5-fold improvement in power conversion efficiency *versus* a cell with no nanoimprinting.[42]

4a
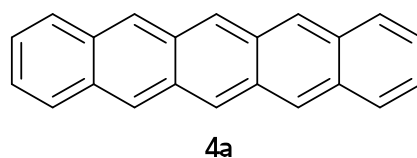
Tetracene-derivative, rubrene (**4b**), is another high hole-mobility material. It is also known as a sensitiser in chemoluminescence and used for yellow glow emission in light sticks. A high performance OLED device using rubrene as one of the components was also reported.[43]

4b
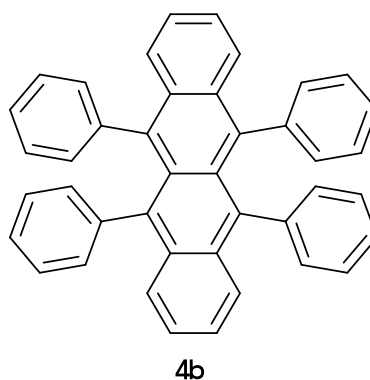
1.4.2.1.3. Oligothiophenes

Oligothiophenes (**5**, n = 2-6, 8) are another well-known family of aromatic p-type semiconductors, consisting of linked thiophenes and representing a variety of

heterocyclic, aromatic, planar and electron-rich molecules. Many of them are highly crystalline compounds with well-defined structures.[5]

5
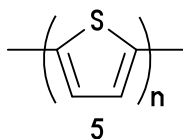
These materials have been extensively investigated in terms of their structure,[44,45,46] properties[47,48,49] and applications in OPVs, OLEDs[17] and OFETs.[18,19,20,50] Selenium analogues[51,52] of oligothiophenes have also been synthesised.

1.4.2.1.4. Phthalocyanines

Phthalocyanines (**6**) are highly aromatic structures. Their properties can be varied by the incorporation of different metals (M) into the central cavity or other peripheral substituents.

6
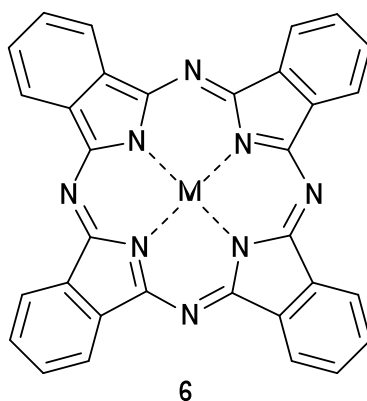
Some phthalocyanines (Pc) behave as discotic liquid crystals and are known for their ability to adopt different crystalline forms.[6] Examples include zinc phthalocyanine (M = Zn) and magnesium phthalocyanine (M = Mg). Phthalocyanines are p-type semiconductors and are used in OLEDs, OFETs and OPVs.[5,6]

1.4.2.1.5. Perylene

Perylene (**1**) and its derivatives, combined with other materials are useful in OLEDs.[53] Soluble derivatives of perylene diimide (PDI*) have been tested for use in OFETs.[54] Linked with such electron withdrawing groups as imide or anhydride, perylenes make good n-type semiconductors.[5-6]

1.4.2.1.6. Fullerene

Fullerene (**7**, C_{60}) and its derivatives are widely used as electron acceptors in donor-acceptor CT-complexes for photovoltaics and OFETs.[55] It is also, a well known material in nanoscience, mainly for its ability to form various nanostructures, *e.g.*, nanotubes, and possessing extraordinarily high hole-mobility within those.[6,56]
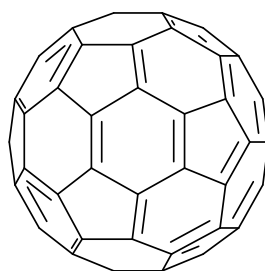
7

1.4.2.2. Conducting Polymers

Conducting polymers present a huge group of organic semiconductors. Their ability to form thin films, electronic properties that can be tailored to specific needs, ease of production and other valuable properties make them very attractive in the research community and feasible in many industrial applications.

Since the 1940s polymers have been used as simple insulating plastics to replace other materials like wood or metal. During the 1970s, in the search for an organic polymer with conducting properties, Shirakawa, MacDiarmid and Heeger *et al*. were able to successfully prepare polymers of acetylene, both in the *cis*- and *trans*-forms. The conductivities they observed initially were low, 1.7×10^{-5} S cm^{-1} and 4.4×10^{-5} S cm^{-1}

respectively, but increased dramatically, up to seven orders of magnitude, upon exposure to halogen vapours.[57]

Conducting polymers are characterised by a conjugated double bond framework – the π-system (Figure 6), which exists through the whole entity, which allows the delocalisation of the π-electrons and hence, results in conductivity.
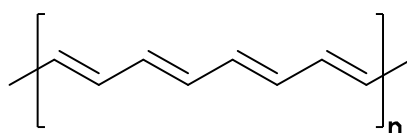
Figure 6. π-Framework of conducting polymer polyacetylene

The conductivity of many undoped polymers is usually low, making them insulators rather than conductors. Although with appropriate doping (both p- and n-types) conductivity can be increased by several orders of magnitude, for some highly conductive polymers it can even be increased to the levels of metallic conductivity, with the additional advantage of low weight and recyclability.[58]

The most common and useful classes are: polythiophenes (PTs), poly-*para*-phenylenes (PPPs), polyfluorenes (PFs), poly-*para*-phenylene-vinylenes (PPVs), polyacetylenes (PA) and polypyrroles (PPy). The structures of these polymers are presented in Figure 7. Some key points regarding these materials will be outlined in the following sections.
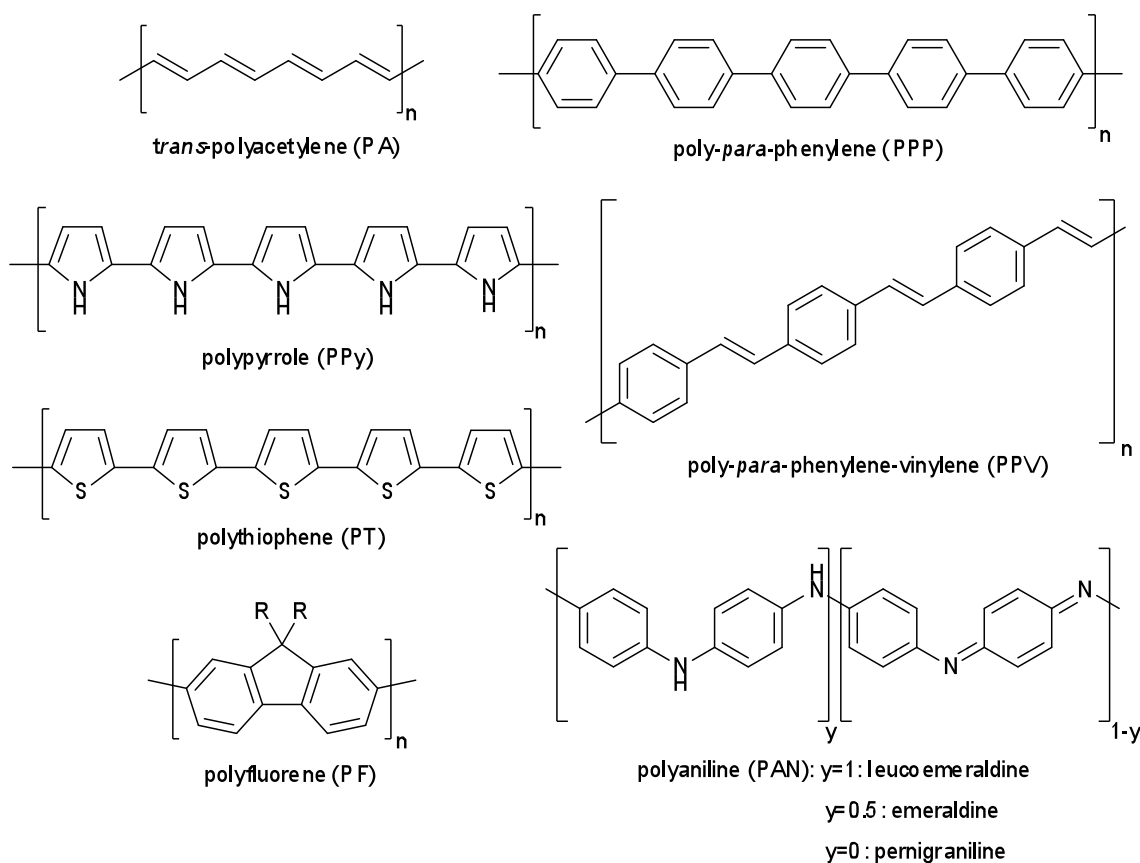
Figure 7. Common classes of conjugated polymers

1.4.2.2.1. Polyacetylenes (PAs)

Unsubstituted polyacetylene has a linear structure and belongs to the simplest among the conjugated polymers. The crystal structure of PA consists of rigid π-stacks as a result of strong interactions between the polymer chains. This makes PA infusible and insoluble in any kind of solvent. PA is obtained by polymerisation of acetylene and can be found in the *cis*- or *trans*-conformations. Both of them are considered to be planar.[59]

Polyacetylene's otherwise rather low conductivity can be varied over several orders of magnitude *via* doping,[57-58] but its sensitivity to moisture, air and light and insolubility make it unsuitable for application in optoelectronic devices.

The planar structure of PA is considered to be its most stable, but Akagi *et al.* aimed for the synthesis of PA films consisting of helical chains, using special solvents and a

Ziegler-Natta catalyst,[60] which was expected to add some optical and magnetic properties to PAs.

1.4.2.2.2. Polyaniline (PANs)

Polyaniline exists in several oxidation states, depending on the processing method (Figure 7). The three common states are: fully reduced – leucoemeraldine (y=1), partially reduced – emeraldine (y=0.5) and fully oxidised – pernigraniline (y=0). Emeraldine is the most commonly used form, since it is stable at room temperature, while leucoemeraldine is prone to oxidation and pernigraniline to degradation.[61]

Polyaniline is usually obtained by oxidative polymerisation with ammonium peroxydisulfate and soluble in many organic solvents. This makes it commercially available from common sources such as Fisher Scientific and Sigma-Aldrich Co.[58] Polymerisation can also be performed electrochemically.

Polyaniline in its emeraldine state is a rather poor conductor, but the conductivity can be considerably increased through doping with protic acids (Scheme 2), which results in highly conducting and insoluble salts. The whole doping process can be easily monitored by pH changes in solution, allowing variation of the dopant quantities until a desired extent of imine protonation is achieved. Dedoping is carried out with bases such as ammonium hydroxide.[58]
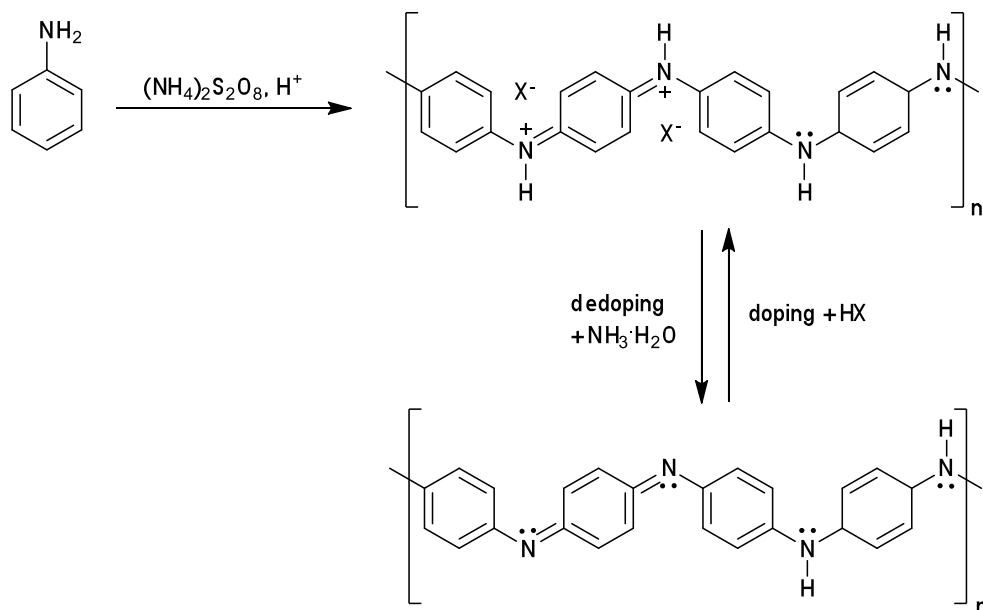
Scheme 2. Polymerisation of aniline and subsequent doping/dedoping[58]

Polyaniline salts are used as highly conductive powders, additives in photocopying and corrosion protection coatings.[62] Since PANs can be effectively tailored for specific needs in terms of their conductivity, PAN-based blends have wide industrial use, including applications in electronics (circuit boards), construction (antistatic floors), the automotive industry and many more.

With currently growing interest for nanomaterials, polyaniline has also been a subject of extensive investigations for its ability to form nanostructures, such as nanowires, nanorods, nanofibres and nanotubes.[63] Such structures may well contribute to a class of new functional materials with novel physical and electronic properties.

1.4.2.2.3. Poly-para-phenylene-vinylenes (PPVs)

There are two main ways to prepare PPVs – direct and precursor routes. Both methods involve condensation reactions of appropriately substituted benzenes, but the precursor route is suitable to make both soluble and insoluble materials, while the direct route is only used to obtain the soluble PPVs.

The precursor route (Scheme 3) involves the formation of a precursor polymer with saturated bonds, which allows the preparation of high quality, high molecular weight polymers.
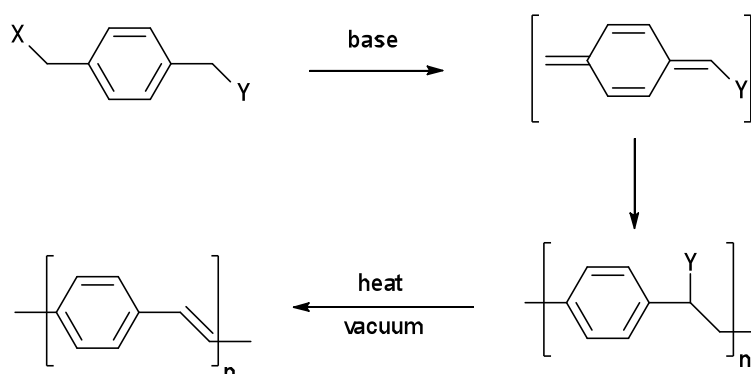
Scheme 3. Precursor route to PPVs[58]

The substituents X and Y (the leaving groups) can be varied, but the most commonly used method is the Gilch route, utilising α-halo-*para*-xylenes.[64]

The common problem with the precursor route is the formation of defects (impurities),[65] which is a highly undesirable feature, due to the potential negative impact on the optical and electronic properties of the polymers.

The direct route to PPVs proceeds through, *e.g.*, Heck coupling. The molecular weights of polymers obtained in this way are usually lower than with the precursor route. Among the advantages are: (a) the possibility for incorporation of functionalities as well as copolymerisation with other moieties and (b) relative freedom from defects.[58]

PPVs are typical semiconductors with conductivities that can be altered through substitution on the benzene rings and/or the double bonds. However, these materials, even with extensive doping, show conductivities that are too low to serve as conducting materials. Despite that, their luminescence properties (stable red, blue and green emissions) make them very useful in OLEDs. In fact, the first polymer-based OLED was constructed with PPV as an emissive layer by Friend *et al.*, in 1990.[66]

1.4.2.2.4. Poly-para-phenylenes (PPPs) and Polyfluorenes (PFs)

PPPs are known to produce blue electroluminescence (EL). Emission of blue light is very important for full colour light-emitting devices, because apart from the blue light itself, it can be transformed into red and green light *via* colour conversion.[67]

Pristine PPP is insoluble in organic solvents. Therefore, other approaches, like using non-conjugated precursor polymers[68] and electrochemical polymerisation of benzene[69] need to be employed to prepare defect-free thin films of PPP. Another way to increase the solubility of PPPs is to introduce substituents on the benzene rings, such as alkyl, alkoxy, ester, keto, etc., in so-called "hairy rod" (**10**) fashion. Synthetic approaches to these modified chains include coupling and cross-coupling reactions (Yamamoto, Suzuki and Stille) of various substituted aryls.[58]
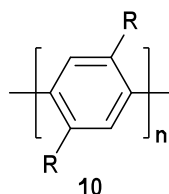
The main disadvantage of such derivatisation, however, is the decrease in conjugation between the polymer chains and, hence, reduction of EL efficiency, due to the steric bulkiness of certain substituents in the 2- and 5-positions of the benzene rings.

The solution of this problem was to force the polymer units into the coplanar conformations by bridging the neighbouring phenylenes with methylene links. Eventually, this approach resulted in the whole new group of ladder-PPPs (**11**, LPPPs).[70]

11
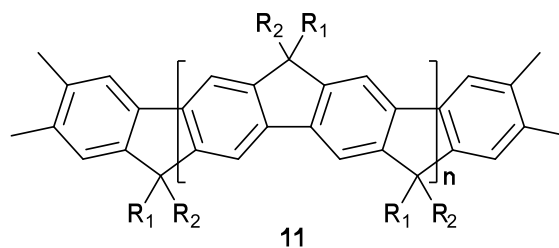
If the bridging occurs only every other phenylene-phenylene unit, then polyfluorene (PF) is obtained. PFs attract considerable attention for their particularly strong blue EL that can be used in OLEDs.[71]

The synthetic routes to PFs are mainly based on Suzuki-type cross coupling and Yamamoto-type homocoupling of various 9,9-substituted fluorenes, yielding high quality, high molecular weight polymers.[58,72]

The nature of the substituents in the 9-position of fluorenes (on the methylene carbon) can have a significant influence on the polymer's solid state packing and hence, its EL, charge mobility and thermal properties. For instance, incorporation of phenylene dendrons in the 9-position (**12**) demonstrates stabilised blue emission without a negative effect on the charge mobility.[73]

12
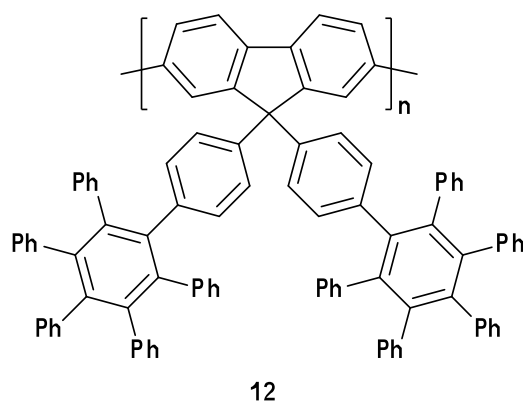
Copolymerisation of PFs with low band gap aromatic moieties significantly alters the emission spectrum. As was shown by Shim *et al.*,[74] a variation of ratio between 9,9-bis(2-ethylhexyl)fluorene and 2,5-bis(5'-bromothiophen-2-yl)-1-cyanovinyl)-1-(2''-ethylhexyl)-4-methoxybenzene could produce copolymers (**13**) with emission over the full color range, from blue to red, depending on values of x and y.

13
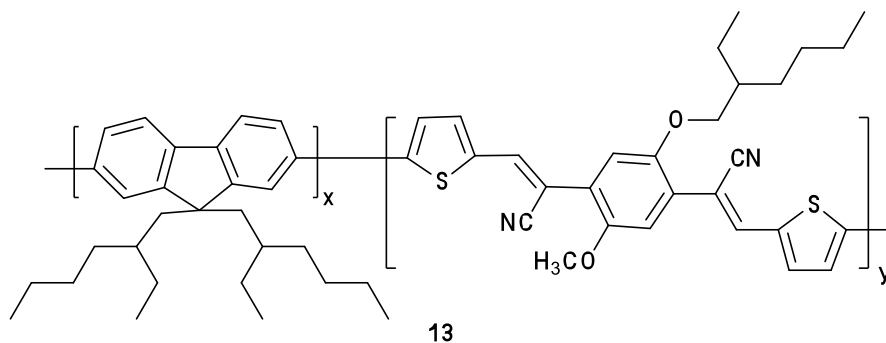
1.4.2.2.5. Polypyrroles (PPy)

Polypyrrole, as is the case with many other conjugated polymers, exhibits low conductivity in its pristine form. Still, like in the case of polyacetylene, it can be manipulated over several orders of magnitude, achieving a metal-type conductivity with doping (oxidation). With an increasing amount of dopant the band gap is narrowed, giving rise to a higher conductivity. Typically, polypyrrole can accommodate between 20 and 40 mol% of dopant to produce the maximum conductivity.[58]

Polypyrrole can be prepared chemically and electrochemically *via* oxidation of the pyrrole monomer. Electrochemical polymerisation, originally developed by Diaz *et al.*,[75] offers a clean and easy way for obtaining PPy, but is difficult to optimise and scale up.

Chemical polymerisation of pyrrole is carried out with an oxidising reagent, such as lead dioxide, quinones or ferric chloride and a dopant.[76] The conductivities of chemically obtained polymers are somewhat lower than that of the electrochemically prepared PPy. However, this method demonstrates more control over the polymerisation process, allows optimisation of the reaction conditions and is better suited for commercial production of PPy.

Unsubstituted polypyrrole is insoluble and infusible, which makes its processing rather difficult. To improve the solubility, substitution of the pyrrole monomer in the 1,3, 4-

positions prior to polymerisation can be applied. The common substituents are alkyl or alkoxy groups and the common rule is that any bulky moieties introduce steric interference, affecting planarity and π-interactions of the polymer chains, and hence reduce conductivity.

The processability of polypyrroles can be further improved by copolymerisation with, for instance, polythiophenes [77] and aniline.[78]

Unlike polyacetylenes, polypyrroles are more environmentally stable, which makes them important materials in various sensors,[79,80,81] rechargeable batteries[82] and OFETs.[83]

1.4.2.2.6. Polythiophenes (PTs)

Polythiophenes are considered to be one of the most important classes of conductive polymers. PTs are mostly used as semiconductors and are more environmentally stable than the majority of other CPs, both in the doped and undoped state. They can be soluble and have been used in a variety of devices, such as polymer LEDs,[84] sensors,[84] and solar cells.[85] However, the simplest member of this group – polythiophene – is insoluble and infusible, but shows good conductivity, stability and is quite cheap.

PTs can be prepared chemically and electrochemically. As in the case of polypyrroles, the chemical synthesis of simple PTs from thiophene monomers results in products with a number of defects from other coupling sites, apart from the desired 2,5-coupling.[86]

As mentioned previously, derivatisation is a widely used approach to modify physical and electrochemical properties of conductive polymers. The typical substituents on PT include alkyl- and alkoxy-groups in either the 3 or 4 (or both) positions. PTs, substituted with alkyl groups of various length in the 3-position, poly(3-alkylthiophenes (P3ATs, **14**), present a well-studied group of soluble, film forming polymers with interesting EL properties .

14
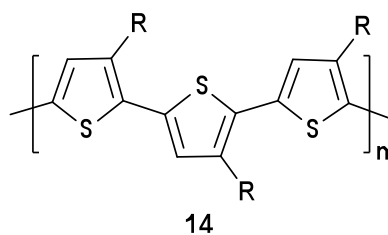
Typically, integrated alkyl groups dramatically increase the solubility of a polymer, but they also provide a certain degree of steric bulkiness, which compromises the packing of polymer chains, conjugation and, as a result, the conducting properties.

Additionally, substituted thiophene is no longer a symmetric molecule and during the polymerisation process there are several possibilities for couplings (Figure 8).
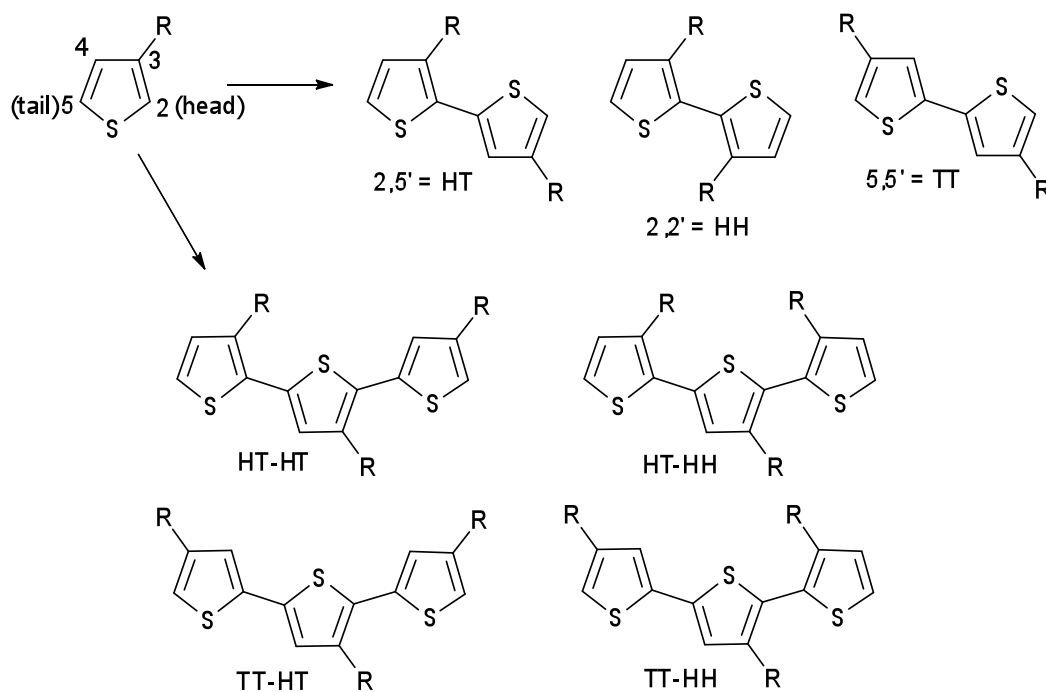
Figure 8. Regiochemical isomers of P3ATs[58]

The head-to-tail (HT) coupling is the preferable one for higher charge transport properties, because it provides the minimal steric crowding of the alkyl groups, allowing self-assembly in two dimensions, while the products of other couplings contribute to the increased disorder and loss of planarity of the polymer chains. Therefore, regioregularity becomes a very important quality of the prepared polymer.

With that in mind, the synthetic routes to PATs must possess considerable regioselectivity towards the desirable HT-coupling.

The three main methods for the synthesis of regioregular PATs are generally called the McCullough,[87] Rieke[88] and GRIM (Grignard metathesis)[89] routes. All three employ transition metal-based polymerising reagents, such as Ni(dppp)Cl$_2$ and yield almost exclusively the HT products. The difference between them is in the way of producing the asymmetric organometallic intermediates and the compatibility of functional groups, where the first two methods are limited to organolithium and organomagnesium tolerant ones. Generation of the organometallic intermediates occurs with either LDA and MgBr$_2$·OEt$_2$ (McCullough), highly reactive "Rieke Zinc" (Rieke) or any Grignard reagent available (GRIM).

PATs and other substituted analogues exhibit good EL properties, suitable for application in light-emitting devices. The nature of the substituent(s) influences the colour and intensity of the emission. For instance, pure P3ATs produce red electroluminescence and its intensity increases with the growing alkyl chain length. Among analogues, the cyclohexyl 3-substituted PT (**15**) emits green light. The same polymer with additional methyl group, inserted in the 4-position (**16**), produces blue emission.[71]

15   16
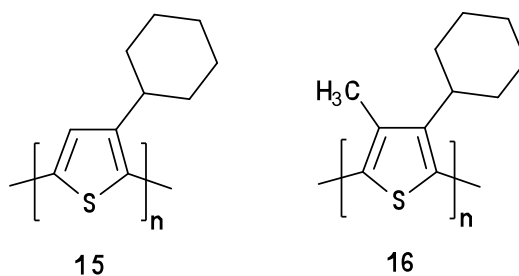
Another substituted PT, polyethylenedioxythiophene (PEDOT, **17**), with its cyclic dialkoxy-substituent is a well-known material, with an ordered structure possessing good conducting and hole-transporting properties.
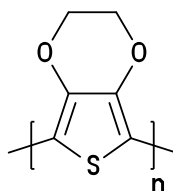
17

PEDOT is a patented product and as copolymer with PSS (polystyrene sulfonic acid) is known under the trade name Baytron® (Bayer AG Leverkusen). Baytron® has multiple applications, such as antistatic coatings of glass, conductive coatings, hole-injector in LEDs, solar cells, etc.[90]

1.5. Fused Thiophenes

As mentioned previously, oligo- and polythiophenes present a large, actively researched group of organic semiconductors. Fused thiophenes, both as small molecule materials and conducting polymers containing such blocks, represent another important research direction that demonstrates a different approach to vary and improve certain optoelectronic properties and hence, broaden the possibilities for further applications.

This PhD project was focused on this particular class of semiconducting materials. In the sections below, the general structure, synthesis and properties of fused thiophenes will be reviewed in more detail.

1.5.1. Structure of Fused Thiophenes

As known, high charge-carrier mobility is a crucial condition for efficient functioning of an organic electronic device. Increased π-stacking within the bulk of an organic semiconductor, provided by full and extended π-conjugation would fulfil this requirement. At the same time, increased π-conjugation often means: (a) lowered material solubility and therefore, processability and (b) narrowed HOMO-LUMO gaps that lead to decreased environmental resistance. Overall, improved charge mobility often leads to a less soluble and more degradation-prone semiconductor.[91]

Fused thiophenes (two to seven thiophene units) with their structure and degree of π-conjugation, can be seen as analogues of oligoacenes, *e.g.*, pentacene (Figure 9).[92]
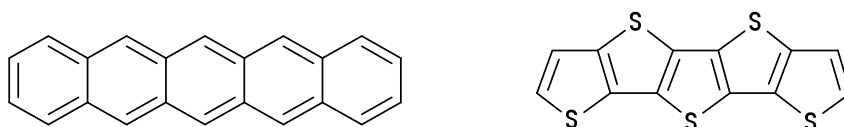
Figure 9. Pentacene and pentathienoacene

A high C:H ratio in the π-backbone, achieved through the fusion of thiophene rings, avoids interference from C—H bonds in the intermolecular interactions. This results in a better π-overlap between the molecules and further promotes the formation of π-stacks in the solid state.[93]

In contrast, linked oligothiophenes possess a lower C:H ratio and tend to adopt herringbone arrangements in the solid state. In their study, Matzger *et al.*[93] confirmed that with the increased degree of fusion (higher C:H ratio) in a series of β-linked oligothiophenes based on fused thiophenes units, the crystal packing tended to adopt the π-stacking arrangement rather than the herringbone. However, despite the notable trends, the latter arrangement is still rather common for some extensively substituted fused representatives as well.

Also, the fusion of thiophene rings leads to a rigid and planar core structure with low torsional flexibility and the *S*-density becomes significantly increased, stimulating efficient intermolecular interactions through additional chalcogen-chalcogen (*e.g.*, $S\cdots S$) contacts.

The HOMO-LUMO gaps of thienoacenes are rather large,[94] which provides for a better environmental stability in comparison with pentacene, which although is known for its high hole-mobility, faces limited solubility and degradation under ambient conditions.[95]

The above shows that fused thiophenes are highly ordered structures, with good potential for high charge-mobilities through π-stacking arrangements and, simultaneously, are more environmentally resistant than many other materials.[94,96]

1.5.2. Synthesis of Fused Thiophenes

The synthesis of fused thiophenes (thienoacenes) is more complicated than that of linked thiophenes. Because of this, there is a limited number of established methodologies and not all of them are universal enough to produce any desired number of fused units. An extensive review on the synthesis of diverse members of the thienoacene family have been recently published in a book,[90] covering thiophene-based organic materials. Some of the common approaches and methods will be outlined in this section.

The simplest fused thiophene species consists of two thiophene units. One of its most stable isomers thieno[3,2-*b*]thiophene can be prepared from commercially available 3-bromothiophene as a starting material (Scheme 4).[97]
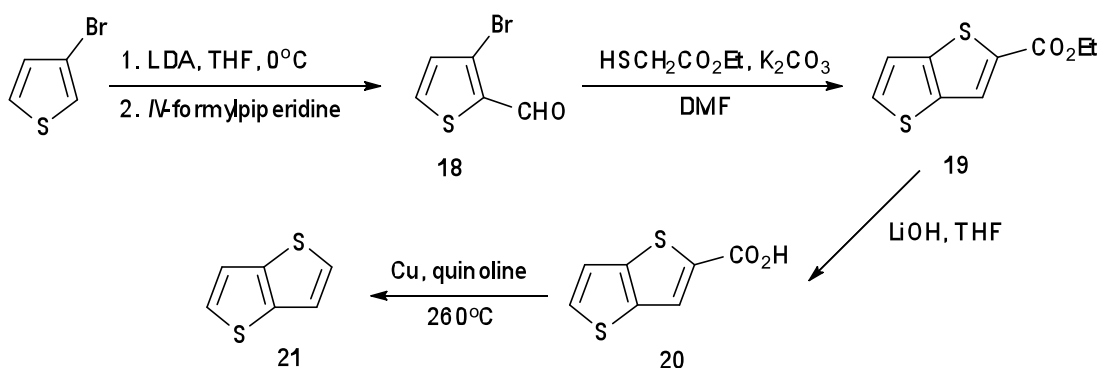
Scheme 4. Synthesis of thieno[3,2-*b*]thiophene.[97]

A whole range of various substituents can be introduced onto the thieno[3,2-*b*]thiophene core through subsequent bromination/lithiation of appropriate positions or *via* direct bromination of the acid **20**.[97]
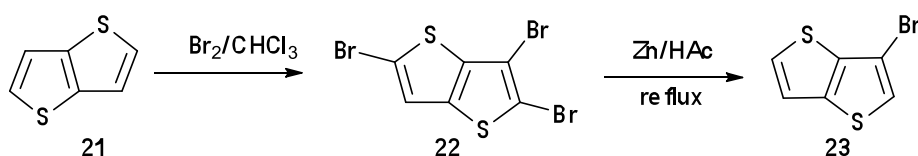
Scheme 5. Preparation of 3-bromothieno[3,2-*b*]thiophene

3-Bromothieno[3,2-*b*]thiophene (**23**, Scheme 5) can be used to obtain higher unsubstituted thienoacenes such as tetrathienoacene (**25**) and pentathienoacene (**27**) as described by Kobayashi *et al.*[98] and Xiao *et al.*[94] (Scheme 6).
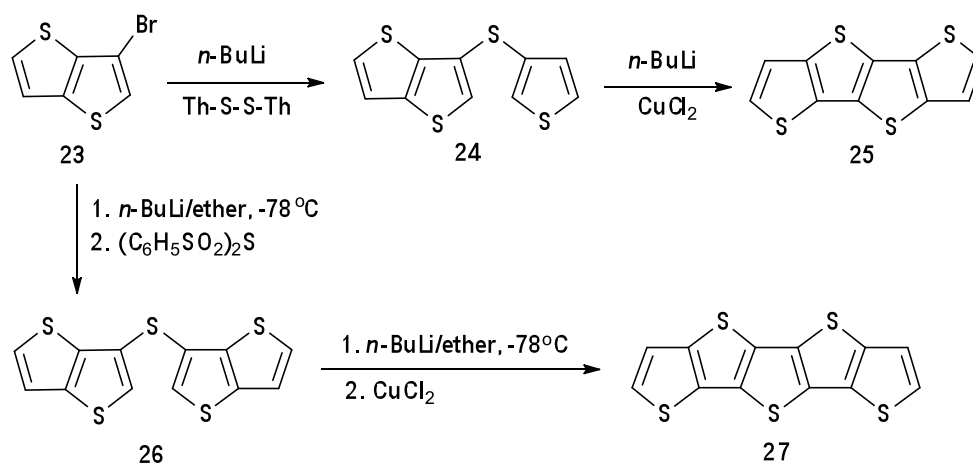
Scheme 6. Synthesis of tetrathienothiophene (**25**) and pentathienothiophene (**27**)

Another, more recent approach developed by Chen and co-workers[99] suggests a one-pot method for synthesis of a variety of unsubstituted and substituted thienothiophenes, including the tetramer (**25**). Although the reported yields are quite moderate, it seems tempting to replace the conventional multi-step procedures with less involved synthesis. The proposed method starts with lithiation of 3-bromothiophene, sulphur insertion and formation of intermediate (**28**), which is further reacted with appropriate lithiated (thieno)thiophene and ring closed with CuCl$_2$ (Scheme 7).
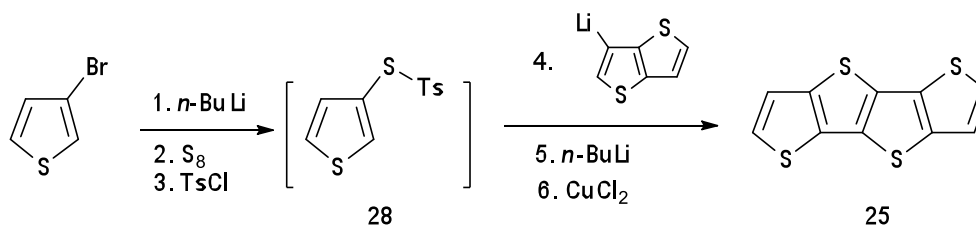
Scheme 7. One-pot [1+1+1] synthesis of tetrathienoacene [99]

Synthesis of even higher FTs becomes more complex, since the approaches applied for smaller members fail to produce desired larger systems. Higher thienoacenes, as a rule, also suffer from lower solubility than the simpler members, which complicates their isolation, further reactivity and processing.

Substitution with some solubilising groups such as alkyl chains, helps to resolve this issue although compromises the efficiency of interactions between the molecules, their packing in the solid state and hence, conductive properties. Synthetic approaches to

such small molecule materials were studied and developed by He and Zhang,[91] where the synthesis of, *e.g.*, alkylated seven-ring molecule posed a certain challenge. The seven-ring target was eventually achieved through "dimerisation" and condensation of an alkylated dithienothiophene (DTT) unit, which was prepared from the starting material 3,6-substituted thieno[3,2-*b*]thiophene. The entire multi-step procedure is rather specific and will not be outlined here. However, it is important to identify one more valuable building block, DTT – a thienoacene, consisting of three fused thiophene rings.

1.5.2.1. Synthesis of DTT

DTT is often used as a core for the synthesis of many thiophene-based materials. Unsubstituted, it can be obtained by the method described by Hellberg,[100] which is an improved version of the low yielding original procedure, developed by Jong and Janssen in 1971.[101] The method (Scheme 8) starts with halogen-lithium exchange of 2,3-dibromothiophene and oxidation with $CuCl_2$ to form 3,3'-dibromo-2,2'-bithiophene (**29**), which undergoes another halogen-lithium exchange followed by a ring-closure reaction using bis(phenylsulfonyl)sulfide to give the DTT (**30**) product in overall 53% yield.
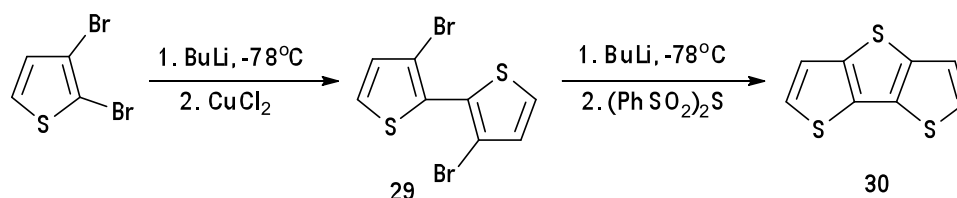
Scheme 8. Hellberg's synthesis of DTT [100]

A very similar approach to the above method, with only minor variations (Scheme 9) has been reported by Frère *et al.*[102] They used bis-thiophene as starting material that was tetra-brominated with NBS. The 3,3'-dibromo-2,2'-bithiophene (**29**) intermediate was obtained through selective debromination with zinc in acetic acid. The final step employs the same reactants as Hellberg's route.
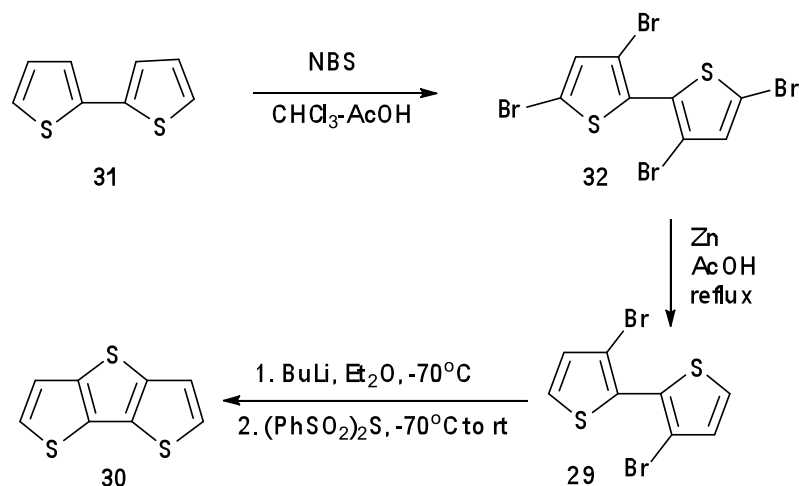
Scheme 9. Frère's synthesis of DTT

Another improved approach to the DTT system (Scheme 10) employed tetrabromothiophene (**33**) as starting material, which was initially dilithiated and quenched with 1-formylpiperidine to form dialdehyde (**34**). Further reaction with ethyl mercaptoacetate produced DTT-dicarboxylate (**35**), which was reduced with LiOH and the resulting dicarboxylic acid (**36**) was converted to DTT *via* decarboxylation reaction with copper in quinoline.[103] The overall yield of DTT was modest (47%), but the main advantages of this approach included: (a) easily synthesised starting material tetrabromothiophene *versus* 2,3-dibromothiophene, which is used in Hellberg's method but is difficult to obtain; (b) the expensive reagent bis(phenylsulfonyl)sulfide was not required.
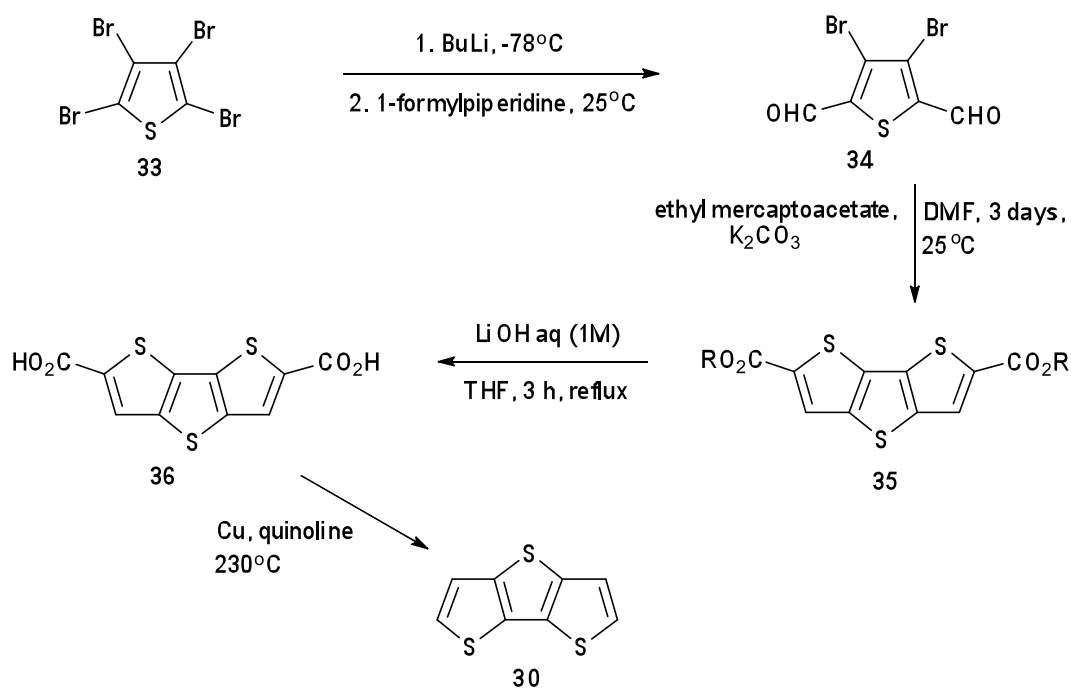
Scheme 10. Frey-Holme's synthesis of DTT[103]

The previously mentioned one-pot approach[99] to tetrathienoacene (**25**) was also used to prepare DTT (**30**), replacing thieno[3,2-*b*]thiophen-3-yllithium (step 4) with thiophen-3-yllithium (Scheme 7). However, the reported yields were only around 30%.

1.5.3. Functionalised FTs, Their Properties and Applications

Substitution of available positions on the flat and highly conjugated π-framework of FTs is a way to diversify the properties of these materials and therefore, the range of their applications in electronic devices.

Generally speaking, variation in the substituents provides possibilities for tailoring the HOMO-LUMO gaps of FT-based structures. It is more critical for the higher members, since the increased degree of conjugation and other π–interactions produce densely packed solid-state arrangements, which possess reasonably high charge-carrier mobilities, but simultaneously, the HOMO-levels rise and the stability towards oxidation can become a problem. In the following sections, a few examples of such work will be described.

1.5.3.1. DTT-based Small Molecule Materials

The DTT core is rather versatile for generating new materials, not least, due to its relative accessibility in terms of synthesis and acceptable solubility. Its flat, π-electron rich but not too dominating structure provides a good basis for various conducting compounds.

Bromination of DTT in the 5,5' (α) positions (**37**) can be achieved in quantitative yield by reaction with NBS. Lithiation of α-positions is easily accomplished with, *e.g.*, *n*-butyllithium. Either way, the activated molecule becomes open for various functionalisation possibilities.[104]

37
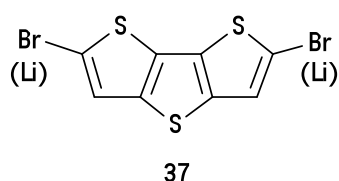
Attaching such simple moieties as phenyl, biphenyl and thiophene rings gives very interesting materials for organic thin film transistors (OTFTs) as reported by Liu and co-workers.[105] They performed Suzuki-coupling of dibromo-DTT and the corresponding boronic acids (Scheme 11). Investigation of the properties showed that the produced materials possessed high mobilities and on/off ratios with the highest values of 0.42 cm^2 V^{-1} s^{-1} and 5×10^6, respectively, measured for **38**. The HOMO-LUMO gaps were estimated to be around 3.0 eV, which indicated good device stability and was eventually confirmed by the characteristics of the corresponding devices. Also, compounds **38** and **39** showed high thermal stability. XRD of **40** showed a planar structure adopting a herringbone arrangement and the authors reasonably suggested that the other two materials have similar packing.
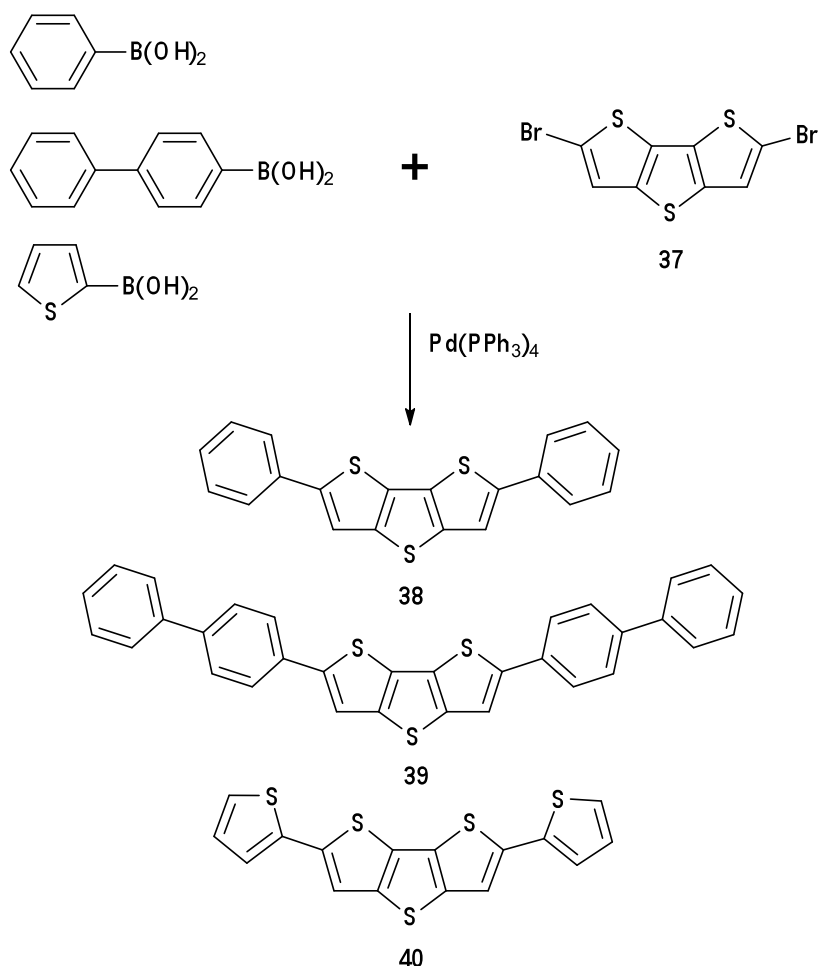
Scheme 11. Suzuki-coupling of DTT and phenyl, biphenyl and thiophene

The same laboratory has recently reported a synthesis of a family of styrene and 1-pentyl-4-vinylbenzene end-capped thienoacenes (**41**) achieved through Stille coupling.[106] The group reported a high mobility and on/off ratio for the styrene derivatives. The 1-pentyl-4-vinylbenzene end-capped member's mobilities suffered from the impact on film morphology, caused by the presence of the alkyl chains. Nevertheless, all new reported compounds were found to be thermally stable.
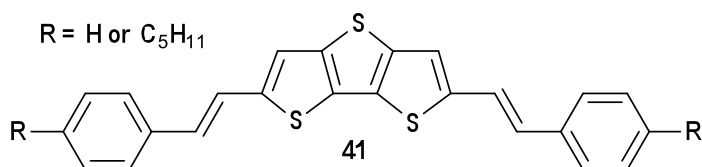
α-Linked DTT, 2,2'-bidithieno[3,2-*b*:2',3'-*d*]thiophene (BDT, **43**) also presents a considerable interest for application in organic TFTs.[96] This dimer is a typical p-type semiconductor and shows mobilities up to 0.05 cm^2 V^{-1} s^{-1} and a high on/off ratio close to 10^8. These properties are most likely to arise from its closely packed face-to-face π-stacking solid-state structure. BDT is thermally stable up to 350°C and sublimes well. Also, the wide HOMO-LUMO gap (2.8 eV) suggests good environmental stability. BDT is obtained from α-mono-lithiated DTT, which "dimerises" upon oxidative coupling with ferric acetylacetonate (Scheme 12).
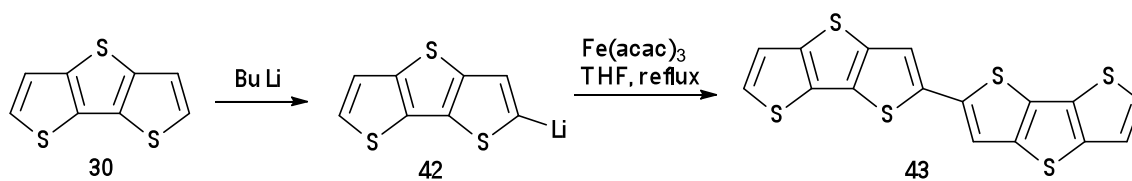
Scheme 12. Synthesis of BDT

There is a limited number of FT-based n-type semiconductors for OTFT applications, although incorporation of suitable electron-withdrawing moieties could result in an interesting scope of materials of such type.

An illustrative example was the recently published work by Chen *et al.*,[99] where they synthesised and investigated properties of several DTT derivatives, bearing electron-poor substituents (Scheme 13). However, the perfluorobenzoyl substituted candidate (**44**) and its asymmetric version (**45**), showed the highest charge-carrier mobilities of 0.0015 cm^2 V^{-1} s^{-1} and 0.03 cm^2 V^{-1} s^{-1}, respectively and were the only electron (n-type) transporters in this reported family of DTT derivatives.
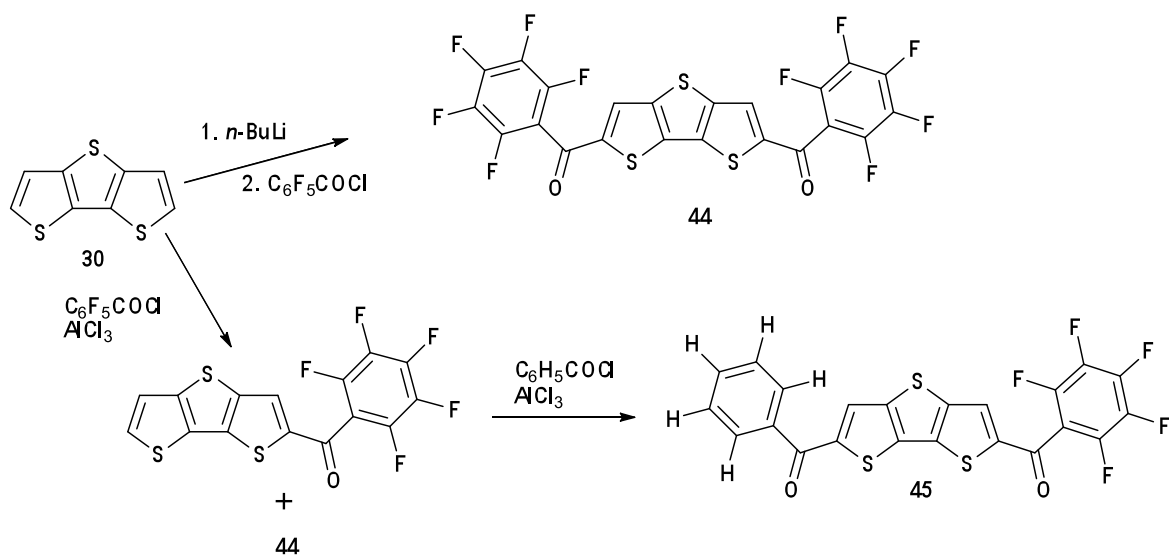
Scheme 13. Synthesis of n-type DTT-based semiconductors

As can be seen, DTT derivatives are widely investigated as small molecule materials for applications in OFETs or OTFTs. However, oxidation of the thienyl sulfur atom to the corresponding sulfones generates a fantastic family of photoluminescent materials, which have been shown to be suitable for OLEDs. This direction was extensively researched by Barbarella and co-workers[107] over several years. They focused on the synthesis of such dioxy-DTT based compounds, investigated the "tunability" of their emission and the mechanisms of PL in such structures. Their approach was built on the fact that similar (dioxide) linked oligothiophenes, although exhibiting high PL quantum yields in the solid state or in viscous media, lost the majority of their emission strength while being in dilute solutions. The reason for such behaviour seemed to originate from the conformational flexibility of linked structures, where the rotational energies can be very low. The consequence of such freedom is the loss of PL through non-radiative patterns during the relaxation of excitons that form upon UV illumination. Therefore, a more rigid core was expected to have less impact on the PLQY caused by these effects.

The synthesis of several DTT-based sulfones was thus performed (Scheme 14) and their optical properties and structural arrangements were investigated.[107]
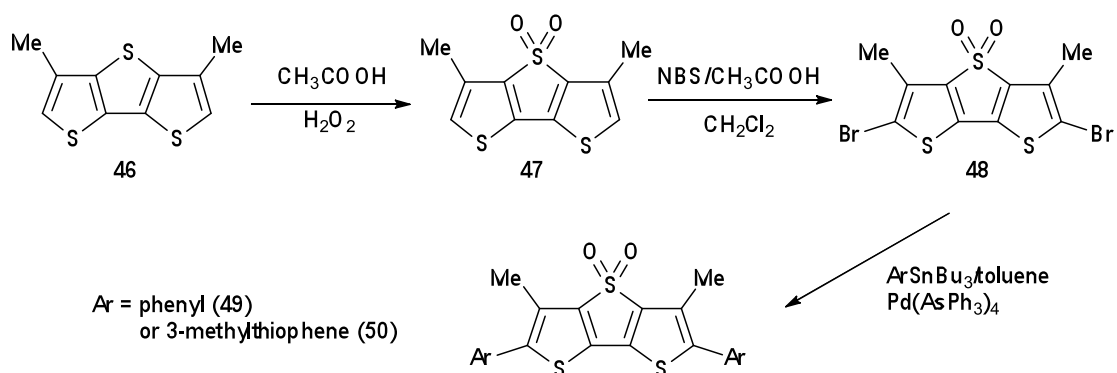
Scheme 14. Synthesis of *S,S*-dioxy DTT based materials

3,5-Dimethyl-DTT **46** was prepared according to standard procedures from 3-bromo-4-methyl-thiophene. Sulfone **47** was obtained *via* oxidation with hydrogen peroxide in acetic acid. *meta*-Chloroperoxybenzoic acid (*m*-CPBA) can also be used for this purpose.[108] Stille coupling afforded additional derivatisation to compounds **49** and **50**. These interesting materials were found to exhibit remarkably high PLQYs in solution – 85% for derivatives **49** and **50** and 77% for compound **47**. However, photophysical investigation of their powders revealed a significant drop in the PLQYs to 48%, 24% and 16% respectively, due to PL-quenching. The authors suggested that a possible explanation of such a drop was in the build-up of excimers – rather weakly emissive states. In turn, the formation of excimers could be attributed to close intermolecular packing in the solid states, which was observed for these materials.

Despite the large difference, the PLQYs of both solutions and powders of sulfones **47**, **49** and **50** are still rather high and much higher than those observed with the best conventional oligothiophenes.

Apart from the well-studied PL-properties, a very recent publication presents an investigation of the charge transport properties of a family of *S*-oxide and *S,S*-dioxide DTTs.[109] The materials (**51 a-b** and **52 a-b**) were obtained in the same manner as described in Scheme 14, with slightly different stannylated precursors for Stille coupling. Although the reported charge mobilities of these compounds were rather low, the authors remained enthusiastic and aimed for further optimisation of FET device fabrication.

51a

51b

52a

52b
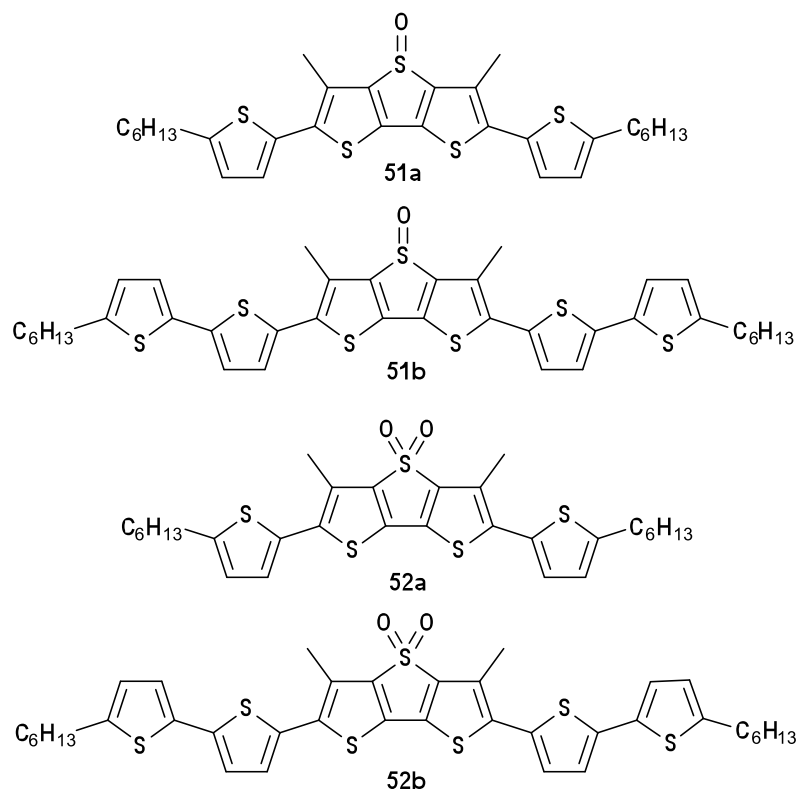
1.5.3.2. Other FT-based Small Molecule Materials

Thienothiophene, the simplest fused thiophene, is often used in various extended conjugated structures as a "spacer" or a rigid planar fragment. Materials containing this unit are mostly investigated for their charge transfer properties. One interesting example of such TT-containing materials (**56**), showing very high charge mobility and a high on/off ratio, was reported by Takimiya *et al.*[110] The synthesis (Scheme 15) started from commercially available disodium 4,4'-dinitrostilbene-2,2'-disulfonate (**53**), giving the corresponding 2,7-diamino compound (**54**) in 3 steps. Subsequent Suzuki coupling between phenyl boronic acid and **55** afforded the product 2,7-diphenyl[1]benzothieno[3,2-b][1]-benzothiophene (DPh-BTBT, **56**).
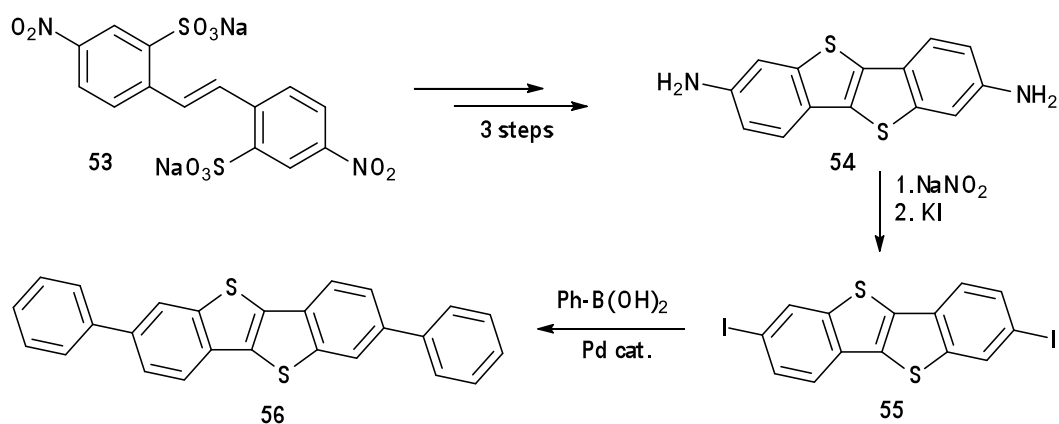
Scheme 15. Synthesis of DPh-BTBT (**56**)

DPh-BTBT was used in the fabrication of a number of thin-film OFET devices by vacuum deposition onto a Si/SiO$_2$ substrate with a variation of surface treatments: bare, octyltrichlorosilane (OTS) and hexamethyldisilazane (HMDS) and the substrate temperatures. The highest charge mobility of 2.0 cm^2 V^{-1} s^{-1} and on/off ratio of ~ 10^8 were observed on OTS treated Si/SiO$_2$ at 100°C, which is a respectable result for an OFET based on this type of material. Many of the fabricated devices showed good stability, which could be associated with the wide HOMO-LUMO gap of DPh-BTBT, which was measured to be 3.2 eV.

Another recent example of TT-based materials, exhibiting rather good p-type OFET characteristics, includes styrene or 1-pentyl-4-vinyl end-capped derivatives (**57**), which were synthesised *via* Stille coupling between 2,5-dibromo-TT and stannylated side groups.[106] The isolated materials possessed high thermal resistance and relatively wide HOMO-LUMO gaps (2.53 eV and 2.52 eV, respectively), which could suggest certain device stability.

R = H or C$_5$H$_{11}$
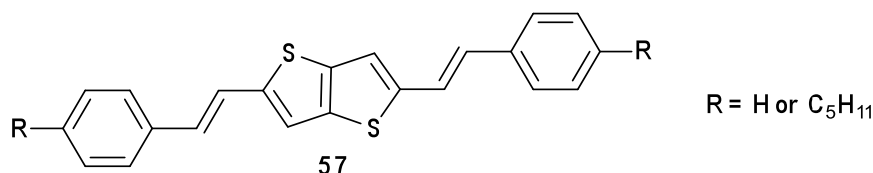
With the intention to introduce some n-type character into the oligothiophene core, a family of linked *S,S*-dioxide TT "dimers" (**58**) was prepared.[111] Their structural and

optical properties were investigated. The oxidation of the sulfur atoms was performed with *m*-CPBA, and the "dimerisations" were achieved through Stille couplings with appropriately stannylated TTs.
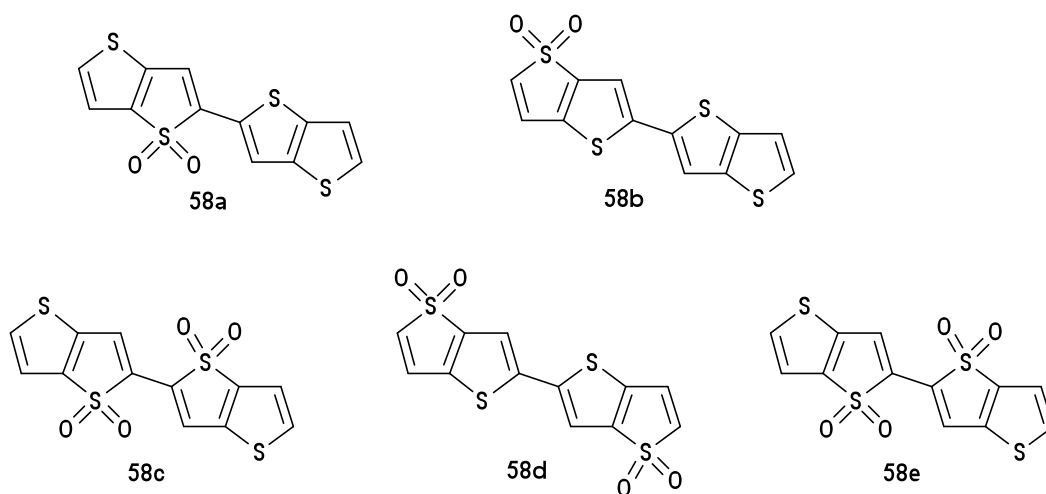
The materials were found as π-stacked dimers with varying solid-state packing motifs. The intermolecular distances depended mainly on the number and position of the sulfone-functionalities within each molecule. These materials were intended as possible candidates for photovoltaics, but require further investigations of their properties.

A limited number of synthetic routes and difficulties associated with the preparation of higher thienoacenes (4–7 thiophene units) lead to a scarce selection of reported materials that incorporate such moieties. In addition, their generally low solubility in common organic solvents obstructs further handling and processability. Insertion of various solubilising groups is therefore required.

He and Zhang[91] describe elaborated procedures towards didecyl ($C_{10}H_{21}$)-substituted four-, five- and seven-membered thienoacenes. These compounds were found to arrange in π-stacking motifs in their solid state and exhibit wider HOMO-LUMO gaps in comparison with oligoacene analogues, possibly due to the effects of sulfur atoms. Together with an observed high thermal stability and ability to form thin films, these thienoacenes can be promising candidates for, *e.g.*, OTFTs.

Triisopropylsilyl (TIPS) groups are also able to increase the solubility of high thienoacenes.[112] Introduced in the earlier synthetic steps, they appreciably facilitate the entire process, isolation of the fully fused products (heptathienoacene, in particular) and their further property investigations.

Yamagichi *et al.*[113] developed an unusual synthetic approach towards higher substituted thienoacenes through an intramolecular triple cyclization of bis (*o*-haloaryl)-diacetylenes (Scheme 16). The starting material **59** was treated with an excess of *t*-BuLi and elemental sulfur, undergoing double cyclisation through the formation of highly reactive electrophilic intermediates and additional cyclisation upon treatment with NaOH and oxidation with potassium ferricyanide(III), yielding the 1,2-dithiin product **60**. The dithiin derivative was further heated to high temperatures (250-300°C) in the presence of Cu nanopowder and resulted in the thienoacene (**61**) within a few minutes.
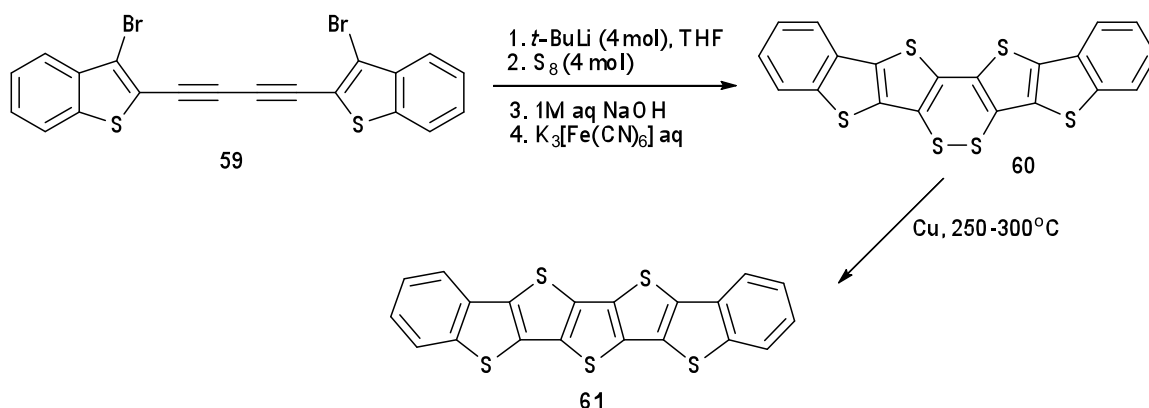
Scheme 16. Synthesis of benzoannulated heteroacene (**61**)

The solvent-free dechalcogenation in the final step is clearly very beneficial, since many higher thienoacenes suffer from low solubility and are, therefore, less practical in further synthesis. The entire approach can be considered as a convenient one-pot route, which in addition, is regiospecific in terms of the position of the six-membered dithiin ring in the product **60**.

Benzoannulated pentathienoacene **61** was found to adopt face-to-face π-stacking modes in its solid state. Its charge transport properties were also investigated by means of a

single crystal FET device.[114] The results showed a typical p-type FET performance with an average mobility of 0.4 $cm^2 V^{-1} s^{-1}$.

Later, the same group applied their own method to prepare four-, six- and an impressive eight-membered TIPS-functionalised thienoacenes (Scheme 17).[115] The latter (**63**) exhibits two reversible redox states and was suggested to be a promising candidate for OFETs, which is a subject of further investigations.
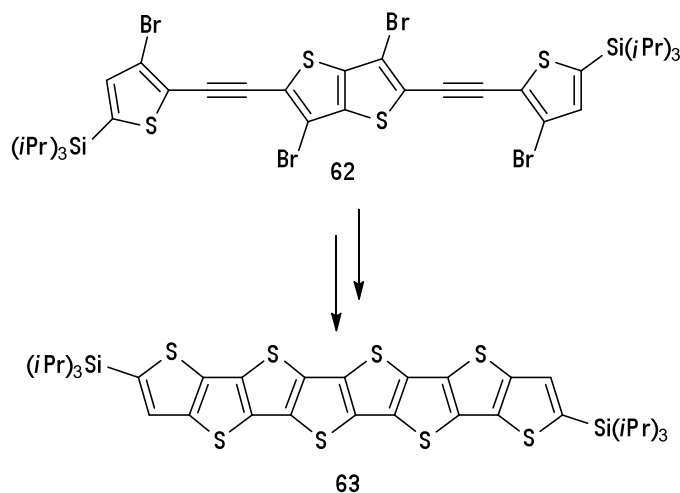
Scheme 17. Schematic synthesis of TIPS-octathienoacene (**63**)

There are other impressive examples of cyclic, helical and even more complex thienoacenes-based structures, although they understandably are investigated to lesser extent.[90]

1.5.4. FT-based Polymers and Their Applications

Polymers that contain FT blocks are readily utilised as solution-processable semiconducting materials in various transistors, plastic solar cells, sensors, etc., and therefore have been extensively researched for the past couple of decades.

The synthesis of polymers can be performed in various ways, depending on many variables such as, for instance, the availability and nature of the monomers (substituents present, crystallinity, solubility, etc.), expected molecular weight of the

polymer and polydispersity. Chemical and non-chemical methods can be employed, whereas amongst the latter electropolymerisation is probably the most common. Chemical methods of polymerisation will be reviewed in more detail in Chapter 3, while in this section, a few examples of thienoacene-based polymers and their property-dependent applications will be illustrated.

Many thiophene-containing polymers are made and studied with the intention of application in OFETs or OTFTs. They are generally considered to be good candidates for this purpose, since reasonably high charge mobilities and conductivities are expected due to their high π-conjugation within the polymer backbone and additional interchain interactions, facilitated by the presence of sulfur atoms, assuring closely packed π-stacked solid-state structures. Also, such polymers are often quite soluble in organic solvents, which could afford large-scale, cheap processing from solution. However, the mobilities exhibited by the polymeric materials are generally lower than the ones of small molecule semiconductors, due to a more disordered crystalline structure of their films. Homogeneity of the semiconducting layer (as a thin film) applied in the device is another important factor for achieving good FET performance and polymers, accommodating thienoacene moieties, are rather likely to exhibit consistent film morphologies.

The simplest member, poly(thieno[3,2-*b*]thiophene) (pTT, **64**), has a band gap of 2.0 eV and low conductivity (10^{-6}–10^{-3} S cm^{-1}) in its neutral state. Substitution with alkyl groups at the β-position (**65**) results in even lower conducting abilities, which is attributed to disrupted solid-state arrangements.[90]

64   65   66
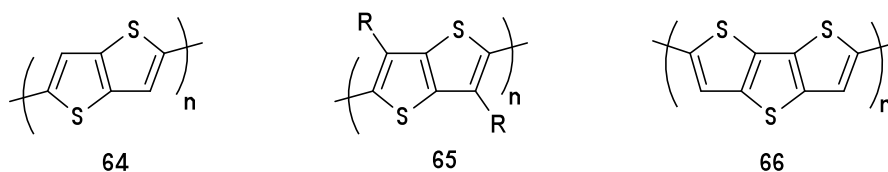
For comparison, the unsubstituted higher member – poly(dithienothiophene) (pDTT, **66**) shows a band gap of 1.8 eV and its conductivity is increased by orders of magnitude (3.1×10^{-3} – 1.1×10^{-2} S cm^{-1} for oxidised states),[90] indicating efficient

solid-state organisation, which is promoted by a planar and rigid core within the DTT repeat unit. This tendency of improved conductivity with increasing number of fused units could be interesting, but polymers of even higher thienoacenes (>3 thiophene units) are not common, most likely due to their insufficient solubility.

High charge mobilities were observed for a polymer consisting of alternating monomer units of thieno[3,2-*b*]thiophene and 4,4-dialkyl-2,2-bithiophene (pBTTT, **67**). The planarity of the repeat units allows close face-to-face π-stacking of polymer chains in so-called lamellae. *Anti*-arrangement of the sulfur atoms facilitates almost linear extension of the polymer backbone, while the alignment of the alkyl side chains (*e.g.*, −$C_{14}H_{29}$) creates an overall three-dimensional highly ordered organisation of the polymer film.[116] The polymer was synthesised *via* Stille cross-coupling between 2,5-bis(trimethylstannyl)thieno[3,2-*b*]thiophene and 5,5-dibromo-4,4-dialkyl-2,2-bithiophenes in the presence of the catalyst tris(dibenzylideneacetone)dipalladium(0), yielding pBTTT with a molecular weight between 20,000 and 30,000 g mol^{-1}.

67
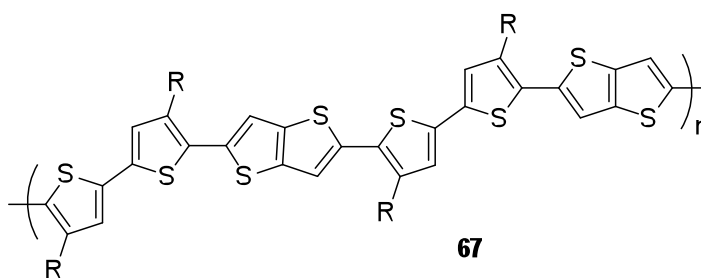
Good morphology of the polymer thin films was achieved on OTS-treated substrate surfaces with additional thermal annealing, which enabled the optimal transistor performance. Thus, the highest charge mobility, ~ 1 cm^2 V^{-1} s^{-1}, of the polymer in its undoped state was measured in a bottom-gate, bottom-contact OFETs with short channel length.[117] This result is one of the highest for polymers and can be compared with the charge transport characteristics of molecular semiconductors.

Other polymers, similar to pBTTT, have been made with alternating β-alkylated thieno[3,2-*b*]thiophene and thiophene, bithiophene and thienothiophene monomers. The highest mobility, up to 0.3 cm^2 V^{-1} s^{-1}, among these analogues was measured with the thiophene copolymer (**68**) in a bottom-gate device.[90]

68
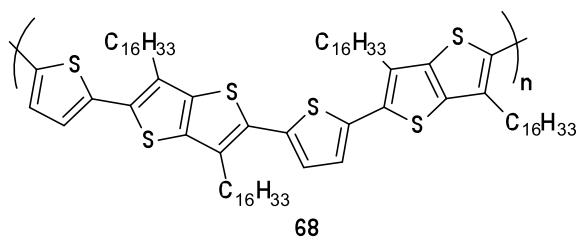
DTT is a valuable block in the design of polymeric semiconductors. Incorporation of this highly π-conjugated and planar core helps to achieve higher order in the interchain structure of polymers through enhancement of π-stacked arrangements and hence, increased charge mobility.

Thus, a polymer consisting of DTT and *N,N'*-dialkylated perylene diimide (PDI*) units was prepared (**69**).[118] Polymerisation was performed through Stille cross-coupling between a 1,7-dibromo derivative of PDI* and distannylated DTT monomers. The polymer was found to be thermally stable and soluble in several organic solvents. It showed good n-type FET performance with high electron mobility up to 1.3×10^{-2} cm^2 V^{-1} s^{-1} and on/off ratio $>10^4$ in a top-contact geometry device.

69

70
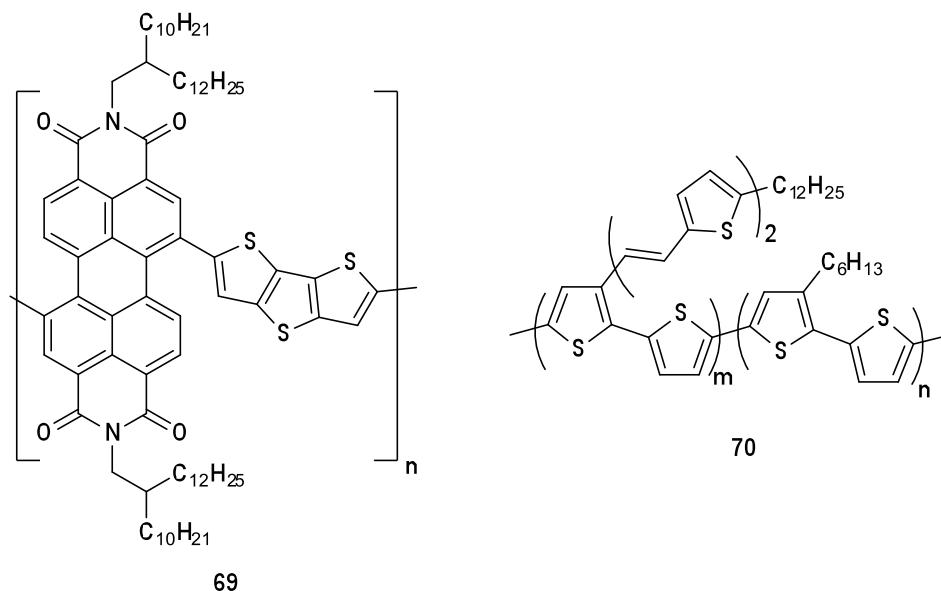
The broad absorption spectrum (to *ca.* 850 nm) of **69** was also recorded, which is a promising feature for application in photovoltaics. To investigate this, **69** was tested in a plastic/polymer solar cell (PSC) device as an electron acceptor in a 1:1 blend with electron donating bi(thienylenevinylene) substituted polythiophene (**70**). The power conversion efficiency (PCE) for the device was over 1%, which is a high value for an all-plastic solar cell.

A similar approach to manipulating the electrochemical properties of a polymer was used in the preparation of two DTT-based polymers by Zhang *et al.*,[119] where donor and acceptor moieties were merged for induced intramolecular charge transfer (ICT). The group reported the synthesis and properties of polymers with alternating units of β-didecyl DTT and benzothiadiazole (**71**) and DTT/benzothiadiazole linked with 3-dodecylthiophene (**72**). The polymers were obtained *via* Stille cross-coupling between appropriately functionalised monomers in the presence of Pd(PPh$_3$)$_4$ catalyst.

71   72
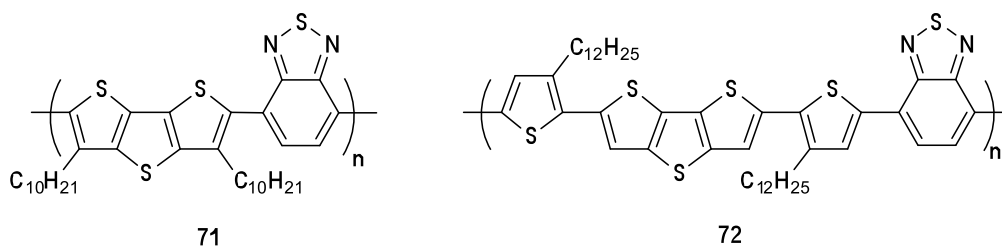
Each of the polymers showed good solubility in common organic solvents and could be processed from solution. Although didecyl chains on the DTT unit of **71** provided increased solubility of the material, the produced steric effect caused a highly twisted structure of the polymer and resulted in low molecular weight and early thermal degradation (160°C). Hindered structure of this polymer was also detected by UV-Vis spectroscopy, which showed absorption maxima of both solution and film in the blue region (λ_{max} 490 and 494 nm respectively). Due to the poor film-forming properties as the result of the polymer's twisted structure, its FET and photovoltaic characteristics could not be investigated.

Polymer **72**, on the other hand, was obtained in high molecular weight and showed good thermal stability with a T$_d$ of 347°C. Its films showed a significantly red-shifted,

in comparison to **71**, broad absorption with a peak maximum of 626 nm. OFET properties were investigated in a top-contact device with annealing at 100°C. The observed hole mobility was up to 8×10^{-5} $cm^2 V^{-1} s^{-1}$ and on/off ratio up to 6×10^3. The low values could be explained by the low homogeneity of the film, which was confirmed by AFM measurements. A bulk heterojunction PSC device was fabricated with a 1:4 (w/w) blend of **72** as an electron donor and solution processable PCBM as an acceptor. The PCE value of the cell was 0.17% and additional annealing did not help to improve the obtained result.

Linked polythiophenes, such as P3HTs, have been used in the fabrication of OPV cells as blends with the soluble fullerene derivative PCBM, achieving high PCEs.[120] A polymer consisting of repeat units of alkylated bithiophene and a DTT-block (**73**) was prepared by Luzzati and co-workers to investigate its solar cell performance.[121] A PSC device was constructed with blends of **73** and PCBM in different proportions: 50, 67 and 80% of the latter.

73
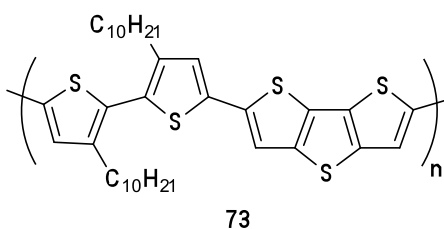
An increase in open circuit voltage (V_{oc}) values for these cells in comparison with similar P3HT-containing devices was observed and was consistent with the expectations for this type of donor polymer. However, the other important solar cell characteristic, the fill factor (FF, assigning for transport properties of the photogenerated charges), was significantly lower and associated with a low charge mobility of **73**. As a result, the obtained PCE-values were lower than initially expected − 0.64, 0.81 and 0.51% respectively, for each blend. An improvement of performance of such a PSC device could be achieved through an increase of the charge transport property of the donor polymer by, *e.g.*, decreasing the steric hindrance arising from the presence of long alkyl chains on the thiophene units.

There are a number of other polymeric materials for OPV applications, containing thiophene in a fused moiety in one of the repeat units (**74-76**). The synthesis of such polymers and subsequent investigation of their OPV characteristics was recently reported by Janssen *et al.*[122]
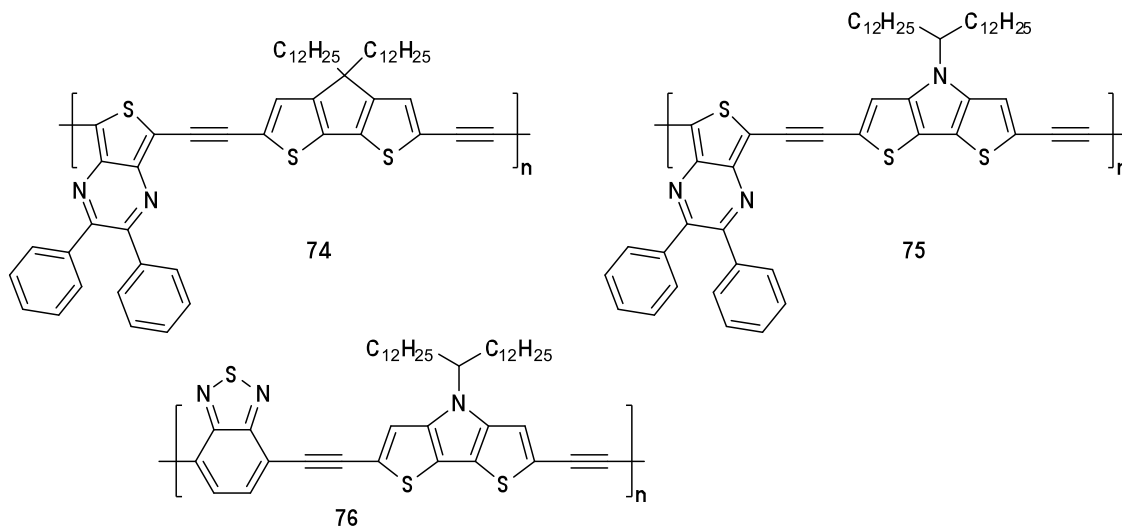
As can be seen, thienoacenes can offer numerous possibilities to a wide variety of molecular and polymeric semiconducting materials with promising properties. Fused thiophenes are versatile building blocks and attract a lot of attention within the relevant research communities.

REFERENCES

1.   Atkins, P. W., *"Physical Chemistry"*. Oxford: 1998.

2.   Smart, L.; Moore, E., *"Solid State Chemistry"*. Stanley Thornes: 1998.

3.   Williams, J. M.; Ferraro, J. R.; Thorn, R. J.; Carlson, K. D.; Geiser, U.; Wang, H. H.; Kini, A. M.; Whangbo, M.-H., *"Organic Superconductors (Including Fullerenes)"*. Prentice Hall: 1992.

4.   Richardson, T. H., *"Functional Organic and Polymeric Materials"*. Wiley: 2000.

5.   (a) Murphy, A. R.; Fréchet, J. M. J., *Chem. Rev.* **2007,** *107*, 1066-1096; (b) Shirota, Y.; Kageyama, H., *Chem. Rev.* **2007,** *107*, 953-1010.

6.   Coropceanu, V.; Cornil, J.; Filho, D. A. d. S.; Olivier, Y.; Sibley, R.; Brédas, J.-L., *Chem. Rev.* **2007,** *107*, 926-952.

7.   Brédas, J.-L.; Beljonne, D.; Coropceanu, V.; Cornil, J., *Chem. Rev.* **2004,** *104*, 4971-5003.

8.   Forrest, S. R.; Thompson, M. E., *Chem. Rev.* **2007,** *107*, 925.

9.   Krebs, F. C., *Solar Energy Materials & Solar Cells* **2009,** *93*, 394-412.

10.   Tang, C. W., *Appl. Phys. Lett.* **1986,** *48*, 183.

11.   Liang, Y.; Xu, Z.; Xia, J.; Tsai, S.-T.; Wu, Y.; Li, G.; Ray, C.; Yu, L., *Adv. Mater.* **2010,** *22*, E135-E138.

12.   Jørgensen, M.; Norrman, K.; Krebs, F. C., *Solar Energy Materials & Solar Cells* **2008,** *92*, 686-714.

13.   Günes, S.; Neugebauer, H.; Sariciftci, N. S., *Chem. Rev.* **2007,** *107*, 1324-1338.

14.   Reese, C.; Bao, Z., *Mater. Today* **2007,** *10*, 20.

15.   Coronado, E.; Day, P., *Chem. Rev.* **2004,** *104*, 5419-5448.

16.   Bendikov, M.; Wudl, F.; Perepichka, D. F., *Chem. Rev.* **2004,** *104*, 4891-4945.

17.   Mazzeo, M.; Pisignano, D.; Favaretto, L.; Barbarella, G.; Cingolani, R.; Gigli, G., *Synth. Met.* **2003,** *139*, 671.

18.   Kajii, H.; Okuya, H.; Sakakibara, A.; Ohmori, Y., *J. J. Appl. Phys.* **2005,** *44*, 1567.

19.   Kunugi, Y.; Takimiya, K.; Negishi, N.; Otsubo, T.; Aso, Y., *J. Mater. Chem.* **2004,** *14*, 2840.

20. Zen, A.; Pingel, P.; Jaiser, F.; Neher, D.; Grenzer, J.; Zhuang, W.; Rabe, J. P.; Bilge, A.; Galbrecht, F.; Nehls, B. S.; Farrel, T.; Sherf, U.; Abellon, R. D.; Grozema, F. C.; Siebbeles, L. D. A., *Chem. Mater.* **2007,** *19*, 1267.

21. (a) Lloyd, M. T.; Anthony, J. E.; Malliaras, G. G., *Mater. Today* **2007,** *10*, 34; (b) Mayer, A. C.; Scully, S. R.; Hardin, B. E.; Rowell, M. W.; McGehee, M. D., *Mater. Today* **2007,** *10*, 28.

22. Samuel, I. D. W.; Turnbull, G. A., *Chem. Rev.* **2007,** *107*, 1272-1295.

23. Donaldson, D. M.; Robertson, J. M.; White, J. G., *Proc. R. Soc. Lond. A Math. Phys. Sci.* **1953,** *220*, 311-321.

24. Ferraris, J.; Cowan, D. O.; Walatka, V. J.; Perlstein, J. H., *J. Am. Chem. Soc.* **1973,** *95*, 948.

25. Bechgaard, K.; Jacobsen, C. S.; Mortensen, K.; Pedersen, M. J.; Thorup, N., *Solid State Commun.* **1980,** *33*, 1119.

26. Bechgaard, K.; Carneiro, K.; Rasmussen, F. G.; Olsen, K.; Rindorf, G.; Jacobsen, C. S.; Pedersen, M. J.; Scott, J. E., *J. Am. Chem. Soc.* **1981,** *103*, 2440.

27. McNeill, R.; Siudak, R.; Wardlaw, J. H.; Weiss, D. E., *Aust. J. Chem.* **1963,** *16*, 1056-1075.

28. Chiang, C. K.; Fincher, J. C. R.; Park, Y. W.; Heeger, A. J.; Shirakawa, H.; Louis, E. J.; Gau, S. C.; MacDiarmid, A. G., *Phys. Chem. Lett.* **1977,** (39), 1098.

29. Perepichka, D. F.; Bryce, M. R.; McInnes, E. J. L.; Zhao, J. P., *Org. Lett.* **2001,** *3*, 1431-1434.

30. Nielsen, M. B.; Lomholt, C.; Becher, J., *Chem. Soc. Rev.* **2000,** *29*, 153-164.

31. Martin, N.; Sanchez, L.; Illescas, B.; Pérez, I., *Chem. Rev.* **1998,** *98*, 2527-2547.

32. (a) Allard, E.; Oswald, F.; Donnio, B.; Guillon, D.; Delgado, J. L.; Langa, F.; Deschenaux, R., *Org. Lett.* **2005,** *7*, 383-386; (b) Kreher, D.; Cariou, M.; Liu, S.-G.; Levillain, E.; Veciana, J.; Rovira, C.; Gorgues, A.; Hudhomme, P., *J. Mater. Chem.* **2002,** *12*, 2137-2159; (c) Prato, M.; Maggini, M.; Giacometti, C.; Scorrano, G.; Sandona, G.; Farnia, G., *Tetrahedron* **1996,** *52*, 5221-5234.

33. (a) Gao, X.; Wu, W.; Liu, Y.; Jiao, S.; Qui, W.; Yu, G.; Wang, L.; Zhu, D., *J. Mater. Chem.* **2007,** *17*, 736-743; (b) Mas-Torrent, M.; Rovira, C., *J. Mater. Chem.* **2006,** *16*, 433-436; (c) Rovira, C., *Chem. Rev.* **2004,** *104*, 5289-5317.

34. (a) Akutsu, H.; J.-i.Yamada; Nakatsuji, S.; Turner, S. S., *Solid State Commun.* **2006,** *140*, 256-260; (b) Laukhina, E.; Vidal-Gancedo, J.; Laukhin, V.; Veciana, J.; Chuev, I.; Tkacheva, V.; Wurst, K.; Rovira, C., *J. Am. Chem. Soc.* **2003,** *125*, 3948-3953; (c) Suzuki, W.; Fujiwara, E.; Kobayashi, A.; Fujishiro, Y.;

Nishibori, E.; Takata, M.; Sakata, M.; Fujiwara, H.; Kobayashi, H., *J. Am. Chem. Soc.* **2003,** *125*, 1486-1487.

35. (a) Kimura, S.; Maejima, T.; Suzuki, H.; Chiba, R.; Mori, H.; Kawamoto, T.; Mori, T.; Moriyama, H.; Nishio, Y.; Kajita, K., *Chem. Commun.* **2004**, 2454-2455; (b) Nishikawa, H.; Machida, A.; Morimoto, T.; Kikuchi, K.; Kodama, T.; Ikemoto, I.; Yamada, J.-i.; Yoshino, H.; Murata, K., *Chem. Commun.* **2003**, 494-495.

36. Enoki, T.; Yamazaki, H.; Okabe, K.; Enomoto, K.; Kato, T.; Miyazaki, A.; Ogura, E.; Kuwatani, Y.; Iyoda, M., *Synth. Met.* **2003,** *133-134* (501-503).

37. Bryce, M. R.; Green, A.; Moore, A. J.; Perepichka, D. F.; Batsanov, A. S.; Howard, J. A. K.; Ledoux-Rak, I.; Gonzalez, M.; Martin, N.; Segura, J. L.; Garin, J.; Orduna, J.; Alcala, R.; Villacampa, B., *Eur. J. Org. Chem.* **2001**, 1927-1035.

38. (a) Amabilino, D. B.; Stoddart, J. F., *Chem. Rev.* **1995,** *95*, 2725-2828; (b) Balzani, V.; Gomez-Lopez, M.; Stoddart, J. F., *Acc. Chem. Res.* **1998,** *31*, 405-414.

39. Tan, W.; Wang, Z.; Zhang, D.; Zhu, D., *Sensors* **2006,** *6*, 954-961.

40. Dimitrakopoulos, C. D.; Mascaro, D. J., *IBM J. Res. Dev.* **2001,** *45*, 11.

41. Pesavento, R. V.; Chesterfield, R. J.; Newman, R.; Frisbie, C. D., *J. Appl. Phys.* **2004,** *96*, 7312.

42. Nanditha, D. M.; Dissanayake, M.; Adikaari, A. A. D. T.; Curry, R. J.; Hatton, R. A.; Silva, S. R. P., *Appl. Phys. Lett.* **2007,** *90*, 253502.

43. Qiu, Y.; Gao, Y.; Wang, L.; Wei, P.; Duan, L.; Zhang, D.; Dong, G., *Appl. Phys. Lett.* **2002,** *81*, 3540.

44. Hotta, S.; Warangal, K., *J. Mater. Chem.* **1991,** *1*, 835.

45. Graf, D. D.; Campbell, J. P.; Miller, L. L.; Mann, K. R., *J. Am. Chem. Soc.* **1996,** *118* (5480).

46. Funaoka, S.; Imae, I.; Noma, N.; Shirota, Y., *Synth. Met.* **1999,** *101*, 600.

47. Bäuerle, P.; Segelbacher, U.; Maier, A.; Mehring, M., *J. Am. Chem. Soc.* **1993,** *115*, 10217.

48. Noma, N.; Kawaguchi, K.; Imae, I.; Nakano, H.; Shirota, Y., *J. Mater. Chem.* **1996,** *6*, 117.

49. Matsuura, Y.; Oshima, Y.; Y, Y. M.; Fujiwara, H.; Tanaka, K.; Yamabe, T.; Hotta, S., *Synth. Met.* **1996,** *82*, 155.

50.   Akimichi, H.; Waragai, K.; Hotta, S.; Kano, H.; Sakaki, H., *Appl. Phys. Lett.* **1991,** *58*, 1500.

51.   Inoue, S.; Nakanishi, H.; Takimiya, K.; Aso, Y.; Otsubo, T., *Synth. Met.* **1997,** *84*, 341.

52.   Kunugi, Y.; Takimiya, K.; Yamane, K.; Yamashita, K.; Aso, Y.; Otsubo, T., *Chem. Mater.* **2003,** *15*, 6.

53.   Jarikov, V. V.; Young, R. H.; Vargas, R.; Brown, C. T.; Klubek, K. P.; Liao, L.-S., *J. Appl. Phys.* **2006,** *100*, 0940907.

54.   Singh, T. B.; Erten, S.; Günes, S.; Zafer, C.; Turkmen, G.; Kuban, B.; Teoman, Y.; Sariciftci, N. S.; Icli, S., *Org. Electronics* **2006,** *7*, 480.

55.   Yang, C.; Kim, J. Y.; Cho, S.; Lee, J. K.; Heeger, A. J.; Wudl, F., *J. Am. Chem. Soc.* **2008,** *130*, 6444-6450.

56.   Dürkop, T.; Kim, B. M.; Fuhrer, M. S., *J. Phys.: Cond. Matter* **2004,** *16*, R553-R580.

57.   Shirakawa, H.; Louis, E. J.; MacDiarmid, A. G.; Chiang, C. K.; Heeger, A. J., *J. Chem. Soc., Chem. Commun.* **1977**, 578-580.

58.   Skotheim, T. A.; Reynolds, J. R., *"Conjugated Polymers"*. CRC Press: 2007.

59.   Tanabe, Y.; Kyotani, H.; Akagi, K.; Shirakawa, H., *Macromol.* **1995,** *28*, 4137-4178.

60.   Akagi, K., *Polymer Int.* **2007,** *56*, 1192-1199.

61.   Lu, W.; Fadeev, A. G.; Qi, B.; Mattes, B. R., *Electrochem. Soc.* **2004,** *151*, H33-H39.

62.   Kulszewicz-Bajer, I.; Zagorska, M.; Bany, A.; Kwatkowski, L., *Synth. Met.* **1999,** *102*, 1385.

63.   Li, D.; Kaner, R. B., *J. Am. Chem. Soc.* **2006,** *128*, 968-975.

64.   Gilch, H. G.; Wheelwright, W. L., *J. Polym. Sci. A-1* **1966,** *4*, 1337-1349.

65.   Becker, H.; Spteitzer, H.; Ibrom, K.; Kreuder, W., *Macromol.* **1999,** *32*, 4925-4932.

66.   Burroughes, J. H.; Bradley, D. D. C.; Brown, A. R.; Marks, R. N.; Mackay, K.; Friend, R. H.; Burns, P. L.; Holmes, A. B., *Nature* **1990,** *347*, 539-541.

67.   Tasch, S.; List, E. J. W.; Hochfilzer, C.; Leising, G.; Schlichting, P.; Rohr, U.; Geerts, Y.; Scherf, U.; Müllen, K., *Phys. Rev. B* **1997,** *56*, 4479-4484.

68.   Ballard, D. G. H.; Courtis, A.; Shirley, I. M.; Taylor, S. C., *J. Chem. Soc., Chem. Commun.* **1983**, 954.

69.   Tabata, M.; Satoh, M.; Kaneto, K.; Yoshino, K., *J. Phys. C* **1986**, *19*, L101-L105.

70.   Huber, J.; Müllen, K.; Salbeck, J.; Schenk, H.; Scherf, U.; Stehlin, T.; Stern, R., *Acta Polymerica* **1994**, *45*, 244-247.

71.   Kraft, A.; Grimsdale, A. C.; Holmes, A. B., *Angew. Chem. Int. Ed* **1998**, *37*, 402-428.

72.   Yamamoto, T.; Morita, A.; Miyazaki, Y.; Maruyama, T.; Wakayama, H.; Zhou, Z.-h.; Nakamura, Y.; Kanbara, T.; Sasaki, S.; Kubota, K., *Macromol.* **1992,** *25*, 1214-1223.

73.   Pogantsch, A.; Wenzl, F. P.; List, E. J. W.; Leising, G.; Grimsdale, A. C.; Müllen, K., *Adv. Mater.* **2002,** *14*, 1061-1064.

74.   Cho, N. S.; Hwang, D. H.; Lee, J.-I.; Jung, B.-J.; Shim, H.-K., *Macromol.* **2002,** *35*, 1224-1228.

75.   Diaz, A. F.; Kanazawa, K. K.; Gardini, G. P., *J. Chem. Soc., Chem. Commun.* **1979**, 635.

76.   Lee, J. Y.; Kim, D. Y.; Kim, C. Y., *Synth. Met.* **1995,** *74* (103-106).

77.   Cha, S.-K., *J. Polym. Sci. B Polym. Phys.* **1997,** *35*, 165-172.

78.   Fusalba, F.; Bélanger, D., *J. Phys. Chem. B* **1999**, *103*, 9044-9054.

79.   Lin, C. W.; Hwang, B. J.; Lee, C. R., *Mater. Chem. Phys.* **1998,** *55*, 139-144.

80.   Suri, K.; Annapoorni, S.; Sarkar, A. K.; Tandon, R. P., *Sensors Acutat B* **2002,** *81*, 277-282.

81.   Michalska, A.; Hulanicki, A.; Lewenstam, A., *Microchem. J.* **1997,** *57*, 59-64.

82.   Veeraraghavan, B.; Paul, J.; Haran, B.; Popov, B., *J. Power Sources* **2002**, *109*, 377-387.

83.   Lee, M. S.; Kang, H. S.; Joo, J.; Epstein, A. J.; Lee, J. Y., *Thin Solid Films* **2005,** *477*, 169-173.

84.   Andersson, M. R.; Olinga, T.; Mammo, W.; Svensson, M.; Theander, M.; Inganäs, O., *J. Mater. Chem.* **1999**, *9,* 1933-1940.

85.   Liu, J.; Tanaka, T.; Sivula, K.; Alivisatos, A. P.; Fréchet, J., *J. Am. Chem. Soc.* **2004,** *126,* 6550-6551.

86.   Roncali, J., *Chem. Rev.* **1992,** *92*, 711-738.

87.   McCullough, R. D.; Lowe, R. D.; Jayaraman, M.; Anderson, D. L., *J. Org. Chem* **1993,** *58,* 904-912.

88. Chen, T.-A.; Wu, X.; Rieke, R. D., *J. Am. Chem. Soc.* **1995,** *117*, 233-244.

89. Loewe, R. S.; Ewbank, P. C.; Liu, J.; Zhai, L.; McCullough, R. D., *Macromol.* **2001,** *34*, 4324-4333.

90. Perepichka, I. F.; Perepichka, D. F., *"Handbook of Thiophene-based Materials: Applications in Ogranic Electronics and Photonics".* Wiley: 2009; Vol. One: Synthesis and Theory.

91. He, M.; Zhang, F., *J. Org. Chem* **2007,** *72*, 442-451.

92. Kim, E.-G.; Coropceanu, V.; Gruhn, N. H.; Sanchez-Carrera, R. S.; Snoeberger, R.; Matzger, A. J.; Bredas, J.-L., *J. Am. Chem. Soc.* **2007,** *129*, 13072-13081.

93. San Miguel, L.; Porter III, W. W.; Matzger, A. J., *Org. Lett.* **2007,** *9*, 1005-1008.

94. Xiao, K.; Liu, Y.; Qi, T.; Zhang, W.; Wang, F.; Gao, J.; Qiu, W.; Ma, Y.; Cui, G.; Chen, S.; Zhan, X.; Yu, G.; Qin, J.; Hu, W.; Zhu, D., *J. Am. Chem. Soc.* **2005,** *127*, 13281-13286.

95. Yamada, M.; Ikemoto, I.; Kuroda, H., *Bull. Chem. Soc. Jpn.* **1988,** *61*, 1057-1062.

96. Li, X.-C.; Sirringhaus, H.; Garnier, F.; Holmes, A. B.; Moratti, S. C.; Feeder, N.; Clegg, W.; Teat, S. J.; Friend, R. H., *J. Am. Chem. Soc.* **1998,** *120*, 2206-2207.

97. Fuller, L. S.; Iddon, B.; Smith, K. A., *J. Chem. Soc., Perkin Trans.1* **1997**, 3465-3470.

98. Mazaki, Y.; Kobayashi, K., *Tetrahedron Lett.* **1989,** *30*, 3315-3318.

99. Chen, M.-C.; Chiang, Y.-J.; Kim, C.; Guo, Y.-J.; Chen, S.-Y.; Liang, Y.-J.; Huang, Y.-W.; Hu, T.-S.; Lee, G.-H.; Facchetti, A.; Marks, T. J., *Chem. Commun.* **2009**, 1846-1848.

100. Allared, F.; Hellberg, J.; Remonen, T., *Tetrahedron Lett.* **2002,** *43*, 1553-1554.

101. Jong, F. D.; Janssen, M. J., *J. Org. Chem* **1971,** *36*, 1645-1648.

102. Leriche, P.; Raimundo, J.-M.; Turbiez, M.; Monroche, V.; Allain, M.; Sauvage, F.-X.; Roncali, J.; Frère, P.; Skabara, P. J., *J. Mater. Chem.* **2003,** *13*, 1324-1332.

103. Frey, J.; Bond, A. D.; Holmes, A. B., *Chem. Commun.* **2002**, 2424-2425.

104. Ozturk, T.; Ertas, E.; Mert, O., *Tetrahedron* **2005,** *61*, 11055-11077.

105. Sun, Y.; Ma, Y.; Liu, Y.; Lin, Y.; Wang, Z.; Wang, Y.; Di, C.; Xiao, K.; Chen, X.; Qiu, W.; Zhang, B.; Yu, G.; Hu, W.; Zhu, D., *Adv. Funct. Mater* **2006,** *16*, 426-432.

106. Liu, Y.; Di, C.; Du, C.; Liu, Y.; Lu, K.; Qui, W.; Yu, G., *Chem. Eur. J.* **2010,** *16*, 2231-2239.

107. Barbarella, G.; Favaretto, L.; Sotgiu, G.; Antolini, L.; Gigli, G.; Cingolani, R.; Bongini, A., *Chem. Mater.* **2001,** *13*, 4112-4122.

108. Sotgiu, G.; Favaretto, L.; Barbarella, G.; Antolini, L.; Gigli, G.; Mazzeo, M.; Bongini, A., *Tetrahedron* **2003,** *59*, 5083-5090.

109. Santato, C.; Favaretto, L.; Melucci, M.; Zanelli, A.; Gazzano, M.; Monari, M.; Isik, D.; Banville, D.; Bertolazzi, S.; Loranger, S.; Cicoira, F., *J. Mater. Chem.* **2010,** *20*, 669-676.

110. Takimiya, K.; Ebata, H.; Sakamoto, K.; Izawa, T.; Otsubo, T.; Kunugi, Y., *J. Am. Chem. Soc.* **2006,** *128*, 12604-12605.

111. San Miguel, L.; Matzger, A. J., *J. Org. Chem* **2008,** *73*, 7882-7888.

112. Zhang, X.; Coté, A. P.; Matzger, A. J., *J. Am. Chem. Soc.* **2005,** *127*, 10502-10503.

113. Okamoto, T.; Kudoh, K.; Wakamiya, A.; Yamaguchi, S., *Org. Lett.* **2005,** *7*, 5301-5304.

114. Yamada, K.; Okamoto, T.; Kudoh, K.; Wakamiya, A.; Yamaguchi, S.; Takeya, J., *Appl. Phys. Lett.* **2007,** *90*, 072102.

115. Okamoto, T.; Kudoh, K.; Wakamiya, A.; Yamaguchi, S., *Chem. Eur. J.* **2007,** *13*, 548-556.

116. DeLongchamp, D. M.; Kline, R. J.; Lin, E. K.; Fisher, D. A.; Richter, L. J.; Lucas, L. A.; Heeney, M.; McCulloch, I.; Northrup, J. E., *Adv. Mater.* **2007,** *19*, 833-837.

117. Hamadani, B. H.; Gundlach, D. J.; McCulloch, I.; Heeney, M., *Appl. Phys. Lett.* **2007,** *91*, 243512.

118. Zhan, X.; Tan, Z.; Domarcq, B.; An, Z.; Zhang, X.; Barlow, S.; Li, Y.; Zhu, D.; Kippelen, B.; Marder, S. R., *J. Am. Chem. Soc.* **2007,** *129*, 7246-7247.

119. Zhang, S.; Guo, Y.; Fan, H.; Liu, Y.; Chen, H.-Y.; Yang, G.; Zhan, X.; Liu, Y.; Li, Y.; Yang, Y., *J. Polym. Sci. A* **2009,** *47*, 5498-5508.

120. Ma, W.; Yang, C.; Gong, X.; Lee, K.; Heeger, A., *Adv. Funct. Mater* **2005,** *15*, 1617-1622.

121. Millefiorini, S.; Kozma, E.; Catellani, M.; Luzzati, S., *Thin Solid Films* **2008,** *516*, 7205-7208.

122. Ashraf, R. S.; Gilot, J.; Janssen, A. J., *Solar Energy Materials & Solar Cells* **2010,** *94*, 1759-1766.

CHAPTER 2

CHAPTER 2

SYNTHESIS AND CHARACTERISATION OF NEW DIINDENODITHIENOTHIOPHENE (DITT) BASED MATERIALS

2.1. Introduction

Oligothiophenes, as a class of p-type organic semiconductors, attracts considerable interest for their potential applications in OFETs, OLEDs and photovoltaics.[1,2,3] This well-studied group of oligomers offers possibilities for fabricating electronic devices with higher stability, flexibility and lower cost of manufacturing.

Fused oligothiophenes are often seen as heteroatomic analogues of oligoacenes such as pentacene, which is known for its high hole mobility as a p-type semiconductor.[4] The study of new sulfur-containing fused structures is highly topical and concerns the development of synthetic methodologies,[5,6,7,8,9,10,11,12] investigation of structure and electrochemical behaviour[13,12] for utilisation in electronic devices, such as organic transistors[13,4,14,15] and light emitting diodes.[16,17]

Fused thiophenes show larger HOMO-LUMO gaps in comparison with, *e.g.*, pentacene and this leads to their higher environmental stability[5,16] and resistance to oxidation upon illumination. Also, fused thiophenes possess a rigid core structure with high planarity, which stimulates intermolecular assemblies in their solid state leading to highly ordered π-π stacking modes.[5-6,8,10,12-13,18] For comparison, linked oligothiophenes (and pentacene) adopt herringbone arrangements, which are less densely packed than the π-stacked structures and often show a lower degree of charge transport through the bulk material.[4, 6, 9, 19]

Generally, π-π stacking is favoured for high C:H ratio within the π-framework of the molecule and with thiophenes it can be achieved through the fusion of rings. At the same time, the higher density of sulfur within the fused molecule enables more effective intermolecular interactions,[6,7] thus promoting higher order of the solid state entity. Consequently, such ordered structures can accommodate more efficient charge transport along the π-stacking direction, which has a positive effect on the charge carrier mobilitiy – a crucial characteristic for performance of electronic devices, *e.g.*, OFETs.

The strong p-character of fused thiophenes can be altered chemically through thienyl *S,S*-oxidation to produce materials with pronounced electron-acceptor features. The lower LUMO-energies in such structures lead to the increase in their electron affinities and therefore enhanced electron acceptor properties. In addition, the electron delocalisation within the molecule increases,[20] which is beneficial from the charge transport point of view. Strong photoluminescence, both in solution and in the solid state, has been observed for a range of *S,S*-dioxy dithienothiophene derivatives,[21] which can be useful for the fabrication of emission based devices, such as OLEDs.

Dithienothiophene (DTT) is an important building block[22,23,24,25] for the development of fused thiophene-based semiconductors and offers possibilities for chemical diversity of materials for device applications. Herein, the synthesis of three new dithienothiophene based materials **77**, **78** and **79** is presented. Their electrochemical and photophysical properties were studied and will be discussed in this Chapter.
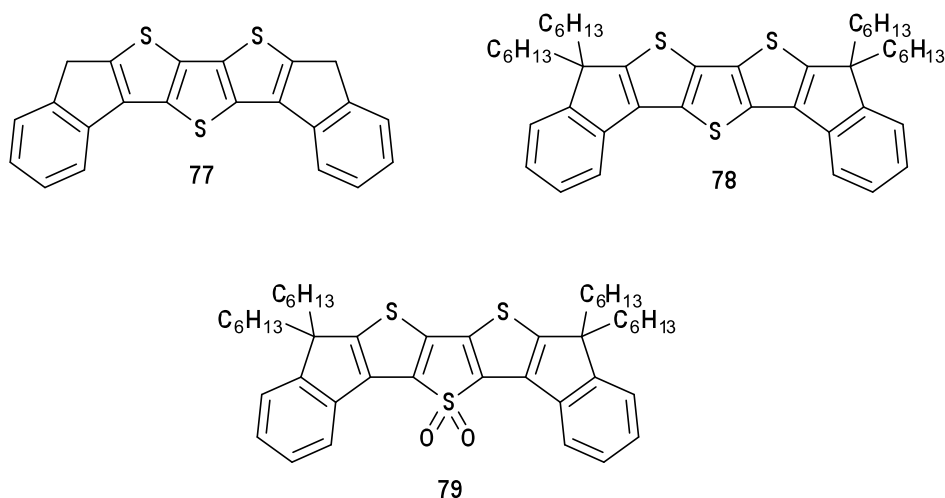
2.2. Results and Discussion

2.2.1. Synthesis

Scheme 18 depicts the synthetic route to the three new materials. The synthesis can be initiated with either **80** or **81** as starting materials. Compound **80** was prepared according to the previously reported procedures,[26] starting from CS_2 and 1,2-dibromoethane in seven steps. Compound **81**[10,27] is also known in the literature and was obtained in three steps starting from commercial thiophene. The synthetic strategy shown in Scheme 18 is more efficient in terms of yields when starting with compound **80**, but derivative **81** appears to be more synthetically viable and was accepted as the main starting point.
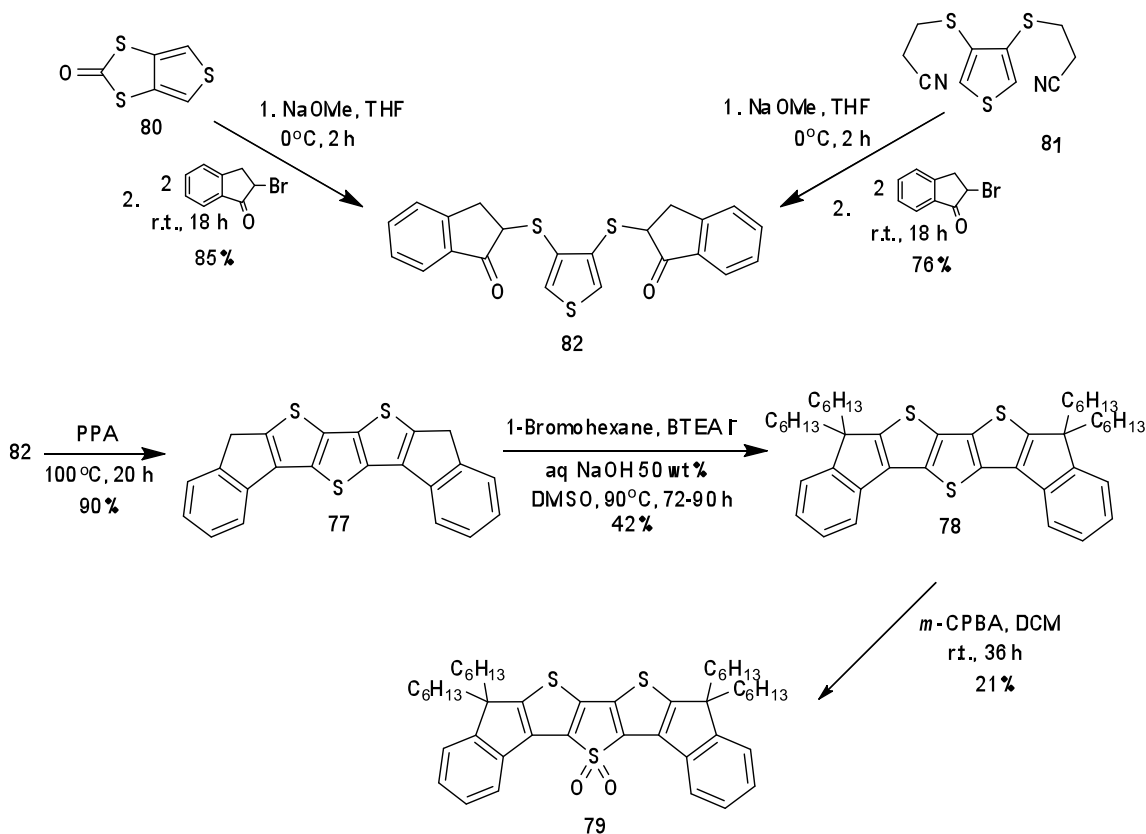
Scheme 18. Reactions and conditions for syntheses of compounds **77-79**

Diketone **82** was obtained as a mixture of diastereomers, which was confirmed by ^{1}H NMR. 2-Bromoindan-1-one (Aldrich, 90%) used in this reaction required additional purification by column chromatography (dichloromethane-petroleum ether, 1:2, then

dichloromethane) or distillation using Kügelrohr apparatus (3.5 mm Hg, 85°C), since the high content of impurities in the commercially available chemical resulted in the formation of by-products that were difficult to separate during subsequent purification procedures.

Cyclisation of diketone **82** into diindenodithienothiophene **77** was successfully achieved using polyphosphoric acid. A few attempts to use P_2S_5 as the ring closing reagent were made but, due to its reductive effect, significant quantities of dihydrobisindenothiophene were isolated. Purification of **77** was performed either by recrystallisation from boiling toluene or by vacuum sublimation at *ca*. 230°C and 0.3 mm Hg. The structure of **77** was confirmed by ^{1}H NMR spectroscopy, mass spectrometry and elemental analysis. The molecular structure of **77** was also determined by single crystal X-ray diffractometry. The solubility of **77** was found to be quite poor in most common organic solvents (dichloromethane, diethyl ether, THF, CCl_4 etc). It dissolved very sparingly in hot (or boiling) toluene, chloroform, chlorobenzene and DMSO. Improvement of the solubility was therefore an important goal and alkylation of the aliphatic positions was chosen for this purpose.

Insertion of four hexyl chains was challenging not only because of the poor solubility of **77**, but also due to the ineffectiveness of a number of bases used for its initial deprotonation. Applying bases such as butyllithium, NaOMe, LDA and tetrabutylammonium hydroxide under various conditions promoted extensive degradation of **77** and produced extremely low yields of **78**. Finally, **78** was obtained by using a 50 wt% solution of NaOH and an interphase catalyst. Column chromatography (petroleum ether, 40-60°C) was employed for purification.

The moderate yields of **78** could be the result of incomplete dissolution of **77** and possibly, its partial degradation due to the combination of the chosen solvent (DMSO) and the high reaction temperature (see Scheme 18). The demand for a more soluble derivative **78** was understandably high and further optimisation of the reaction conditions was required.

An attempt to use solution of potassium *tert*-butoxide as the base, THF as the solvent and no heating of the reaction mixture (Scheme 19), resulted in significantly increased yields of the alkylated product. The pure product recrystallised nicely from boiling acetone, affording a crystalline solid, which was much easier to handle in further work.
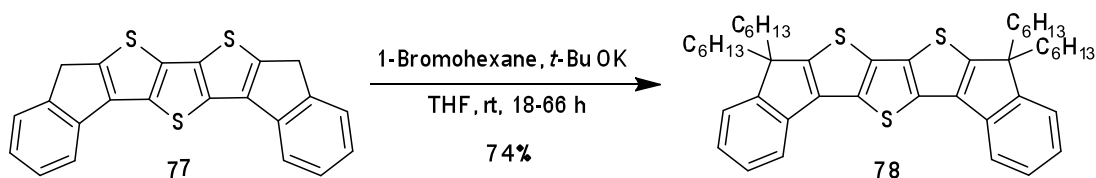
Scheme 19. Improved synthesis of **78**

The reaction was repeated several times. It was found that the prolonged reaction times did not result in any higher yields and the alkylation of **78** was completed already after 18 hours.

In search of a more efficient synthetic strategy to soluble diindenodithienothiophene-derivatives, an alternative route was explored (Scheme 20). The initial intention was firstly to construct the DTT-core according to the conventional method[22] starting with tetrabromothiophene and then to perform a Suzuki-coupling reaction between the substituted DTT-core **83** and TMS-phenylboronate component **84**. Further steps, involving alkylation (*via*, *e.g.*, Grignard reaction) and/or acid mediated cyclisation were anticipated to yield substituted and non-substituted DITT derivatives.
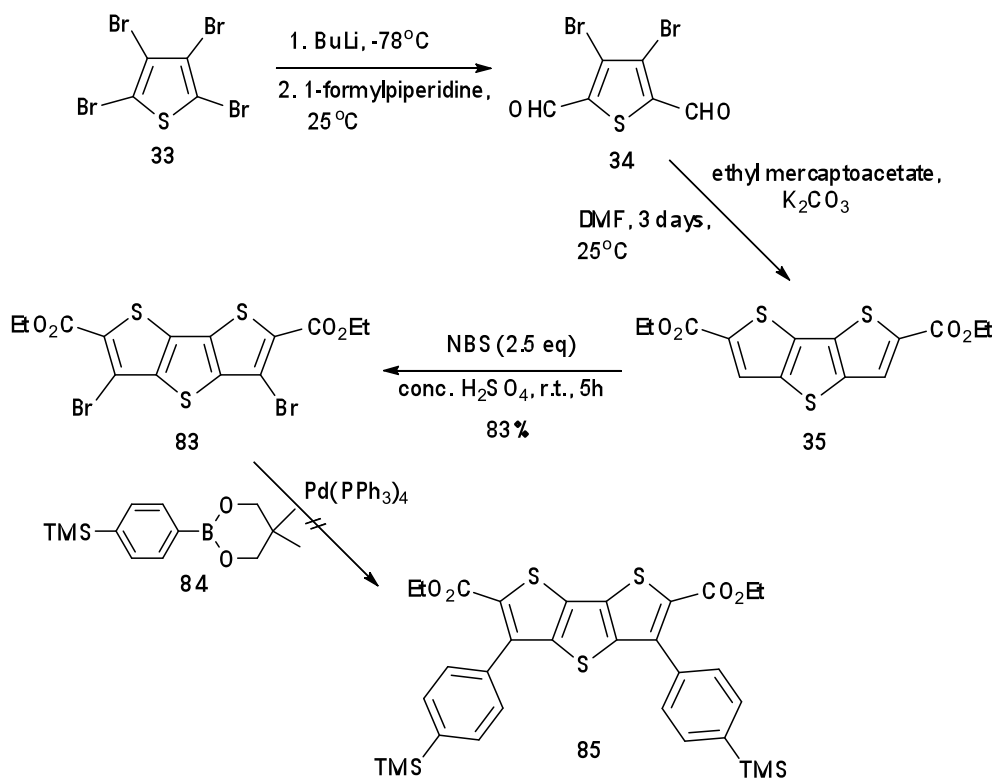
Scheme 20. Alternative route towards DITT derivatives (not successful)

Bromination of the less reactive β-positions of the compound **35** was additionally complicated by the presence of the electron withdrawing caboxylate groups. A few attempts resulted in either the recovery of unreacted starting material or the formation of inseparable mixtures of mono- and dibrominated **35**. Eventually, the desired derivative **83** was obtained with NBS/conc. sulfuric acid in 83% yield. The new compound was characterised by ^{1}H and ^{13}C NMR spectroscopy, mass spectrometry and elemental analysis.

Compound **84** was obtained according to known procedures[28] starting from 1,4-dibromobenzene (Scheme 21). In the first two steps, 4-(trimethylsilyl)phenylboronic acid **84a** was prepared and after that converted into the boronate **84** for the ease of further handling.
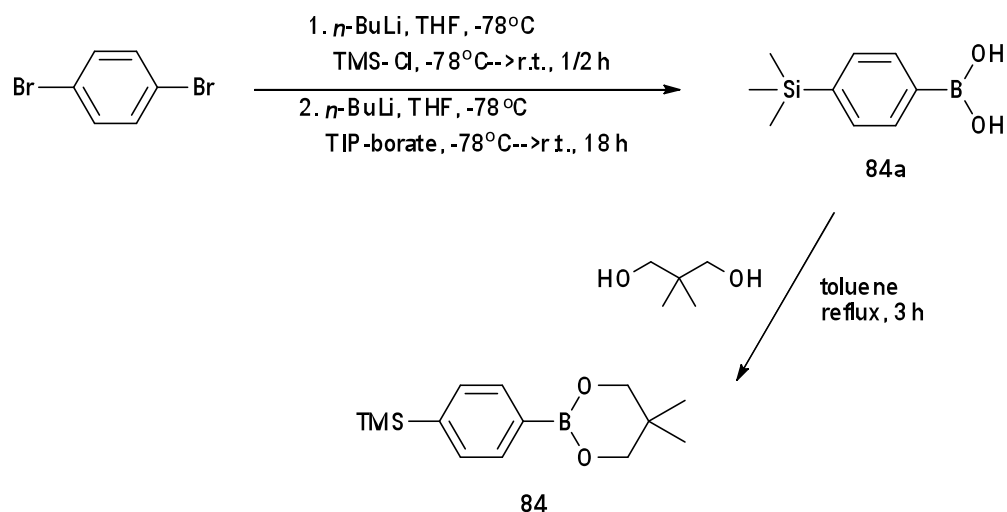
Scheme 21. Synthesis of compound **84**

Suzuki-coupling between **83** and **84** was attempted several times with varying conditions but each time produced complex mixtures of products. Consequently, very low yields of **85** (8–11%) were obtained after extensive column chromatography purification procedures. The development of this alternative route was therefore considered unsuccessful and the previous methods were used in further work.

Oxidation of **78** with *m*-CPBA produced a complex mixture of compounds and just over 20% of the highly photoluminescent product **79**. The pure material **79** was obtained by column chromatography (dichloromethane-petroleum ether, 1:3) followed by precipitation with acetonitrile. Mass spectrometry results indicated the presence of two oxygen atoms per molecule. ^{1}H and ^{13}C NMR spectroscopy confirmed the symmetry of the product, concluding that the oxygens are positioned on the central thiophene unit. This type of reactivity and regioselectivity have been shown previously in the oxidation of other DTT-derivatives.[25] Compound **79** is very soluble in most common organic solvents such as chloroform, dichloromethane, THF, petroleum ether, toluene and chlorobenzene and shows no signs of degradation under ambient conditions for periods of several months.

2.2.2. Electrochemistry

The electrochemical properties of materials **77**, **78** and **79** were investigated by cyclic voltammetry (CV) using dichloromethane as the solvent for oxidation and for the reduction of **79**. Tetrahydrofuran was required for the reduction of **77** and **78** at lower potentials. The supporting electrolyte was tetrabutylammonium hexafluorophosphate (0.1 M) and the potentials were referenced against the ferrocene/ferrocenium redox couple (Table 1 and Figure 10). Glassy carbon was used as the working electrode with platinum and silver wires as the counter and pseudo-reference electrodes, respectively. Oxidation and reduction cycles were performed separately to avoid complications in the CV due to possible side products arising from irreversible and quasi-reversible processes.

The electrochemical HOMO-LUMO gaps were calculated from the differences in the onsets of the first oxidation and reduction peaks. Using data referenced to the ferrocene/ferrocenium redox couple, HOMO and LUMO energies were calculated by subtracting the onsets from the HOMO of ferrocene, which has a known value of –4.8 eV. There is a good agreement between the optical and electrochemical estimates of the HOMO-LUMO gaps for all three compounds. Compound **79** shows a smaller electrochemical gap of 2.8 eV compared to **77** and **78** (3.3 and 3.5 eV, respectively).

Table 1. CV data for compounds **77-79**

	E_{ox} / V	E_{red} / V	HOMO[a] / eV	LUMO[a] / eV	Echem E_g / eV
77	0.72[i]	-2.86[i]	-5.4	-2.1	3.3
78	0.71/0.64	-2.95[i]	-5.4	-1.9	3.5
79	1.04/0.96	-2.03/-1.95	-5.7	-2.9	2.8

[a] HOMO and LUMO values were calculated from the onset of the first peak of the corresponding redox wave and referenced to ferrocene, which has a HOMO of -4.8 eV.
[i] Irreversible peak.
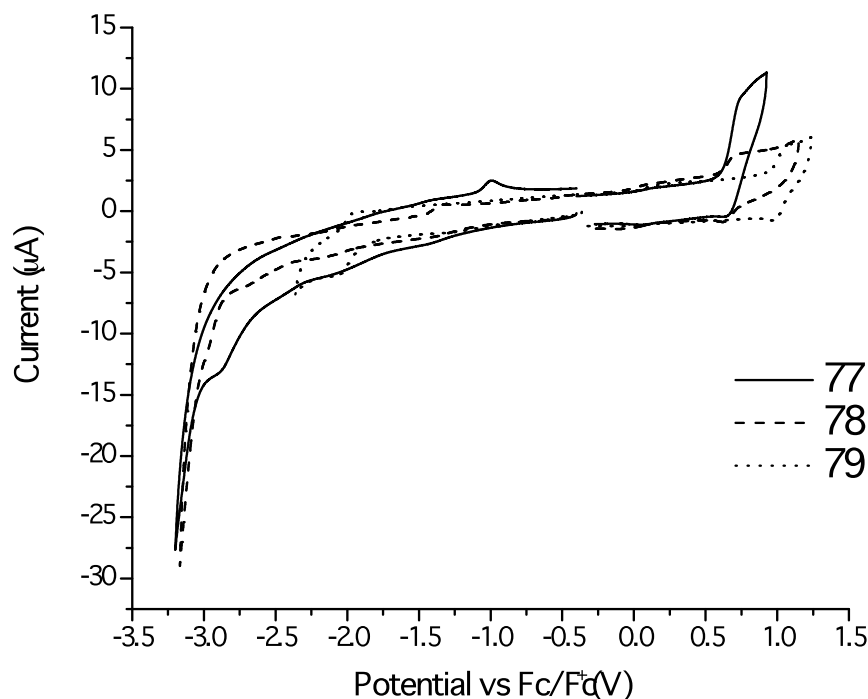
Figure 10. Cyclic voltammograms for **77-79**

Compounds **77** and **78** gave very similar redox potentials with the main difference being that the oxidation of **78** was reversible (**77**, E_{ox} = +0.72 V and **78**, $E_{ox}^{1/2}$ = +0.68 V, one electron wave for each compound). The hexyl chains blocking the α-positions of the indene unit in **78** stabilise the radical cation intermediate, so it is suspected that **77**$^{+\bullet}$ undergoes chemical decomposition through reactivity at this position. The reduction of both materials showed irreversible behaviour (**77**, E_{red} = −2.86 V and **78**, E_{red} = −2.95 V), indicating that the inclusion of hexyl chains did not stabilise the formation of radical anions.

The analysis of **79** showed reversible peaks for both oxidation and reduction processes ($E_{ox}^{1/2}$ = +1.00 V, $E_{red}^{1/2}$ = −1.99 V, one electron transitions). The increase in potential for the oxidation step was expected from the addition of the electron withdrawing sulfone group, but this adaptation of the structure gave the advantage of stabilising the reduction of the compound. Generally, the incorporation of thienyl *S,S*-dioxide units into oligothiophenes leads to compounds that are more readily reduced than the corresponding oligothiophenes.[29]

2.2.3. Absorption/Emission Studies

The UV-visible absorption spectra for all three compounds were measured in dichloromethane and are shown in Figure 11.
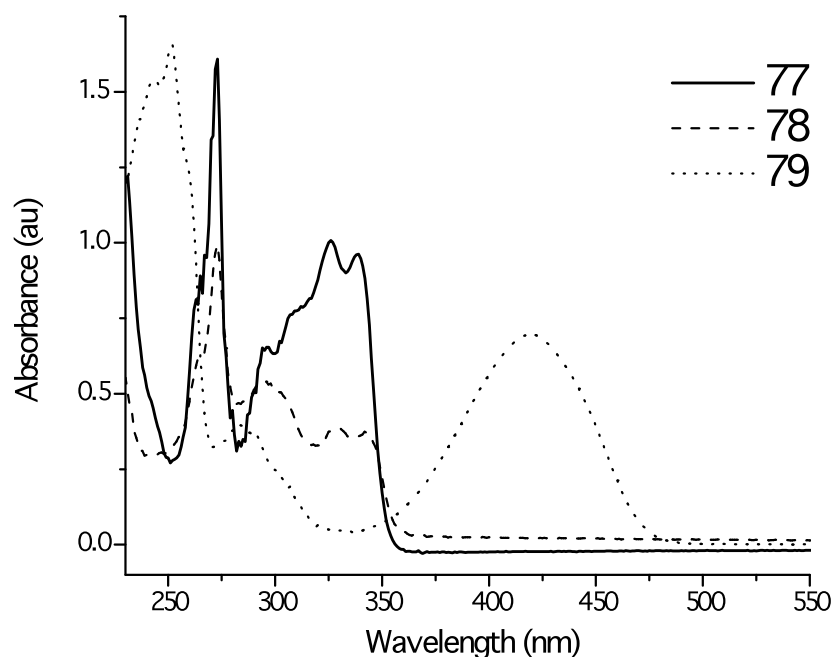
Figure 11. Absorption spectra of compounds **77-79**

Compounds **77** and **78** show fine structure in the spectra, indicative of rigid, planar structures. Both spectra are rather similar with absorption maxima at 284 and 273 nm for the π-π* transition, respectively. Compound **79** shows significant difference in comparison to the others; the main π–π* transition is red shifted by *ca.* 140 nm due to the electron withdrawing effect of the sulfone group, which narrows the HOMO-LUMO gap of the molecule. The smaller gap, in turn, lowers the energy required for the intramolecular charge transfer, which is seen as the red shifted absorption in the spectrum.

To further investigate the origin of this large bathochromic shift, a spectroscopic study with a range of solvents was conducted. Five solvents of varying solvation character (hexane, diethyl ether, tetrahydrofuran, dichloromethane and dimethyl sulfoxide) were

used to measure the λ_{max} of **79** (Figure 12 and Table 2). Positive solvatochromism, *i.e.*, an increase in λ_{max} and therefore a decrease in absorption energy, with the increasing solvation character of the chosen solvents, was observed as linear correlation (Graph 1), thus, indicating the possibility of an intramolecular charge transfer process within the molecule.
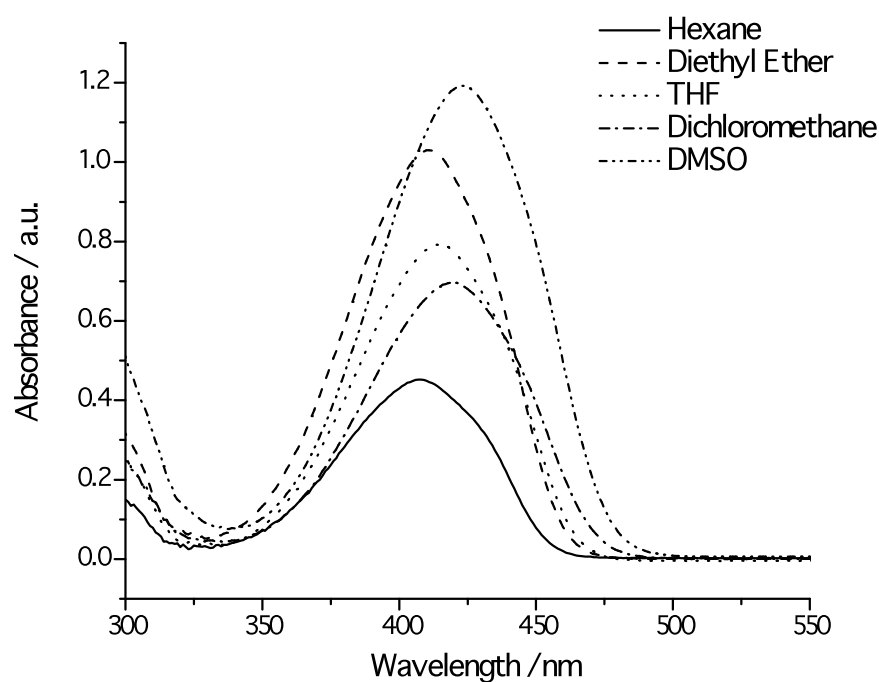
Figure 12. Solvatochromic effect of compound **79**

Table 2. Solvatochromic data of compound **79** in selected solvents with π^* values by Kamlet and Taft[30]

Solvent	π^*	$\lambda_{abs,max}$ / nm
Hexane	-0.08	407 (3.05)[a]
Diethyl Ether	0.27	411 (3.02)[a]
Tetrahydrofuran	0.58	414 (2.99)[a]
Dichloromethane	0.82	419 (2.96)[a]
Dimethyl sulfoxide	1.00	423 (2.93)[a]

[a] Values given in eV
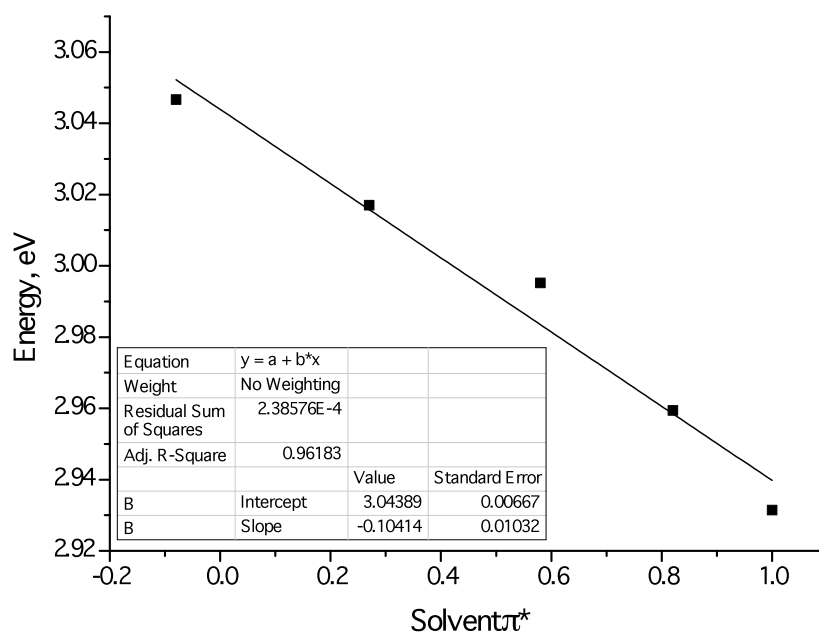
Graph 1. Dependency between the solvation character of selected solvents and the absorption energy (in eV) of **79**

The optical HOMO-LUMO gaps of compounds **77**, **78** and **79** were also determined from the absorption spectra. The edge of the longest wavelength band corresponds to the optical HOMO-LUMO gap and this value was similar for **77** and **78** (3.4 eV). Compound **79**, on the other hand, produced an optical HOMO-LUMO gap of 2.6 eV, which is consistent with the contribution from the sulfone group. The absorption data for all three compounds are presented in Table 3.

Table 3. Absorption data and optical HOMO-LUMO gaps for compounds **77-79**

	$\lambda_{abs, max}$ / nm	ε /mol^{-1} dm^{3} cm^{-1}	Optical $E_g{}^a$ / eV
77	284	34,300	3.4
78	273	56,600	3.4
79	419	32,100	2.6

[a]Optical HOMO-LUMO gaps determined from the onset of the highest wavelength absorption band (and given in eV).

Photoluminescence studies on **77-79** were also performed and the data are collated in Table 4. Solution studies of all three were performed in their diluted chloroform

solutions. Films of **78** and **79** were prepared on fused silica substrates by spin coating from chloroform solutions in a protected environment (glovebox). However, the insolubility of compound **77** did not allow sufficiently high concentrations to obtain spin-coated films and only solution study was possible in this case (Figure 13).

Table 4. PL data for compound **77-79**

	$\lambda_{em, max}$ / nm	PLQY (solution)	PLQY (film)
77	373	0.010	—
78	376	0.004	—
79	524	0.720	0.140
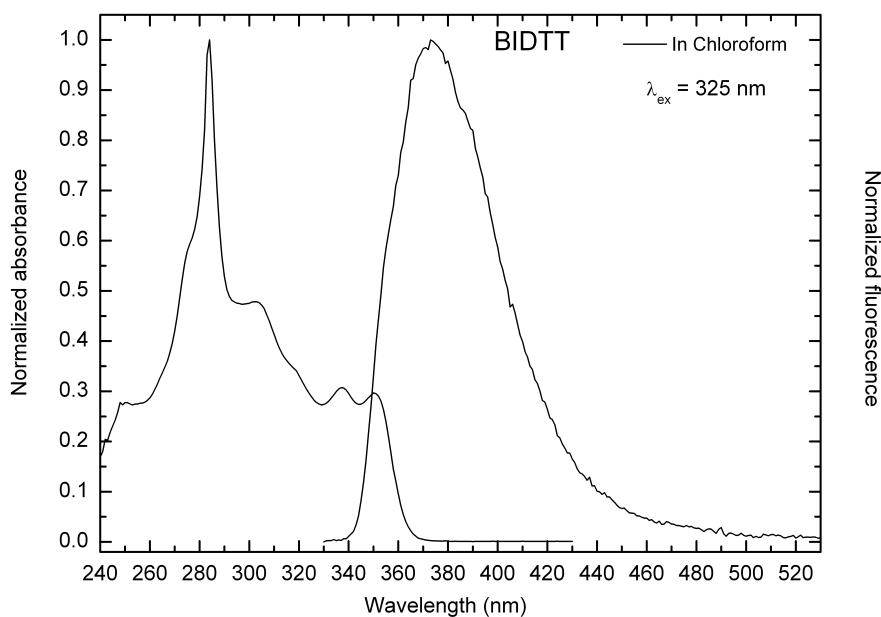
Figure13. Normalised absorption (left) and emission (right) spectra of **77** in chloroform solution

Although the solubility of **78** is increased by the introduction of the four hexyl chains, its emission properties are compromised and the photoluminescence quantum yield (PLQY) of its solution is rather low. The PLQY of films could not be measured due to their weak emission. The solution and film emission spectra of **78** are similar apart

from the additional peak produced by the film at 540 nm, indicating the presence of neutral weakly emissive states – excimers (Figure 14a).
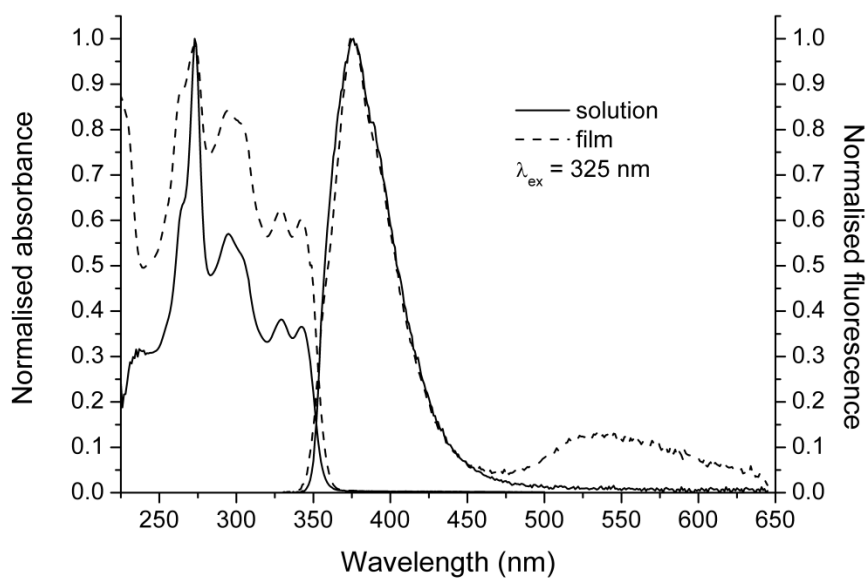
(a)
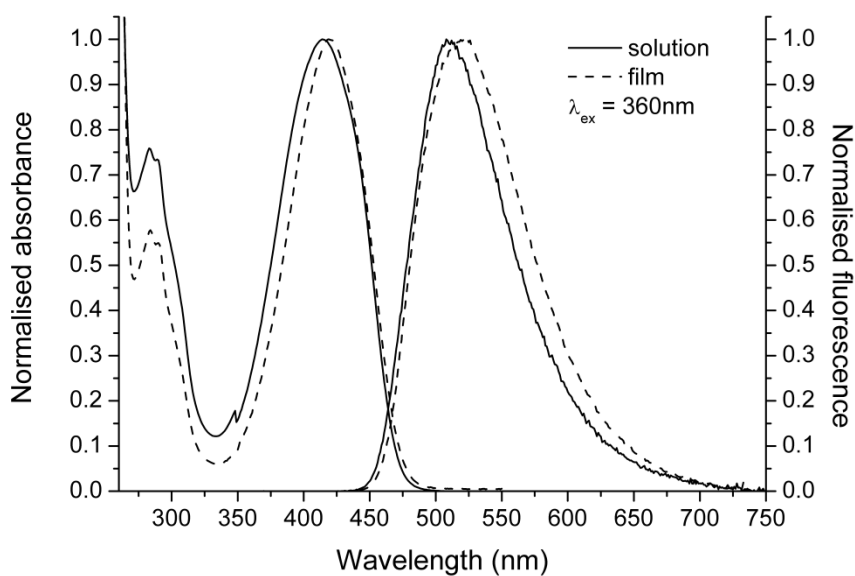
(b)

Figure 14. Normalised absorption (left) and emission (right) spectra in solution and thin-film for (a) **78** and (b) **79**

As can be concluded from Table 4, **77** and **78** produce rather weak blue emission, whereas compound **79** shows a strongly red shifted emission spectrum in the green

region (Figure 14b). Its emission efficiency is also stronger by orders of magnitude in contrast to the other two members. Compound **79** exhibits 0.72 PLQY in solution, which in comparison with *S,S*-dioxides of non-fused related oligothiophenes[31] is a significantly higher value for solution state PLQYs. Such emission behaviour of fused DTT-based sulfones was extensively studied by Barbarella *et al.*[16] and can be attributed to the restrictions of torsional flexibility in these rigid structures.

Further investigation of the photophysical solution characteristics of compound **79** was performed by time-resolved photoluminescence measurements (Figure 15). The study was aimed to determine the average lifetime of the excited states prior to photon release (relaxation) and hence define the nature of the observed emission. The lifetime of a photoluminescent molecule is defined by the rate of radiative and non-radiative processes that depopulate the excited states, and their ratio is determined by the PLQY of the material.

The time correlated single photon counting (TCSPC) setup was used to carry out the measurements. The setup uses a pulsed excitation source to excite the sample and the photons from the resulting emission are filtered by a monochromator before being detected by a micro-channel plate-photomultiplier. The time delay between the excitation pulse and the photon detection is converted into a voltage pulse. The amplitude of pulses is then plotted on a histogram and decay statistics can be calculated.

The PL decay of the material **79** in solution was found to be monoexponential, indicating the presence of a single emitting species, with a measured lifetime of 7.9 ns. When combined with the PLQY of 0.72, the natural radiative lifetime could be estimated to be 10.9 ± 1.1 ns.
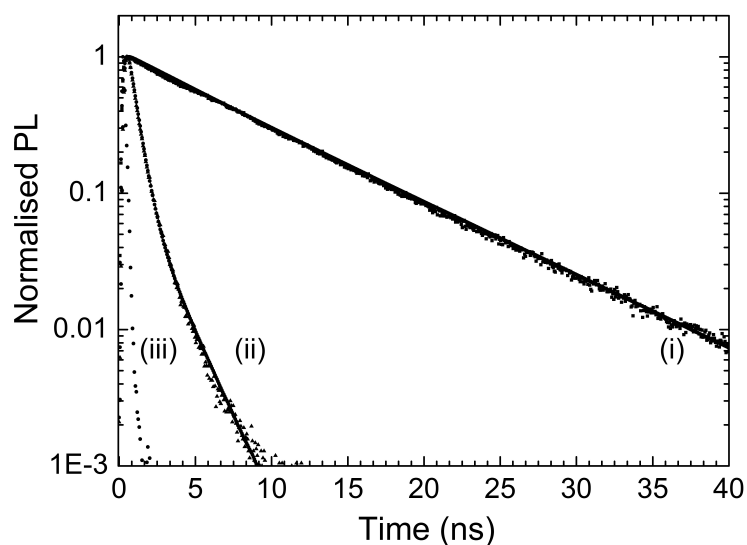
Figure 15. Normalised PL decay of **79** with λ_{ex} = 394 nm (i) in solution at λ_{em} = 524 nm (ii) in thin-film at λ_{em} = 510 nm and (iii) instrument response function

The PLQY of films of **79** was found to be dramatically lower than the solution value. The emission is quenched to a PLQY of only 0.14 due to formation of excimers that do not contribute to the overall emission. The PL decay in the film is much faster than that in solution as a result of rapid non-radiative decay, possibly due to formation of aggregates. It can be fitted by two exponentials, where the first component dominates the overall depopulation process (79%) with a lifetime of 500 ps. The remaining 21% belongs to a slower decay with a lifetime of 1.77 ns. Thus, the average lifetime was estimated to be 760 ps and together with the low film PLQY confirms the strong quenching of emission in the solid state, which is in line with the previously observed trend for *S,S*-dioxy DTT-based materials.[16]

2.2.4. X-Ray Crystallography

Single crystals of **77** were isolated by recrystallisation from boiling toluene. The asymmetric unit is shown in Figure 16a and consists of seven fused rings labelled A-G. The central rings A-C represent the dithienothiophene unit and the two benzene rings (F and G) are linked to this core *via* fused cyclopentadienes (D and E). The entire molecule is highly planar with the largest torsion angle in the structure being 2.19º within S(2)-C(3)-C(3)-C(11).

In the bulk, compound **77** forms one-dimensional π-π stacks (Figure 16b), in which adjacent molecules are inverted but otherwise eclipsed (Figure 16c). The curved shape of the molecule promotes the efficient overlapping of rings A, D and E within the stacks with π-π ring centroid distances of 3.49–3.52 Å. However, the inverted mode of the solid-state packing results in the lateral displacement of rings B and C in relation to the neighbouring molecule (Figure 16b) with therefore longer π-π distances of 3.87 and 3.95 Å, respectively. The benzene rings F and G that reside at the peripheries of the molecule, are affected by its curved structure in even larger degree, consequently showing π-π distances of 5.03 and 4.75 Å.
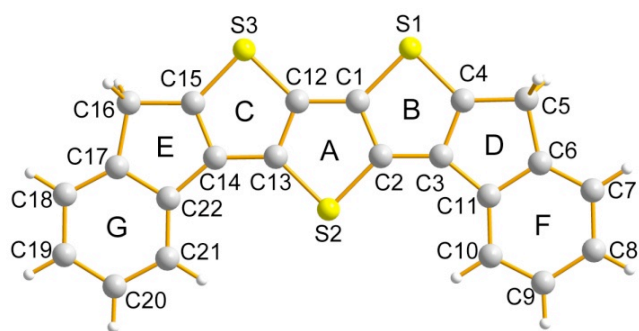
(a)
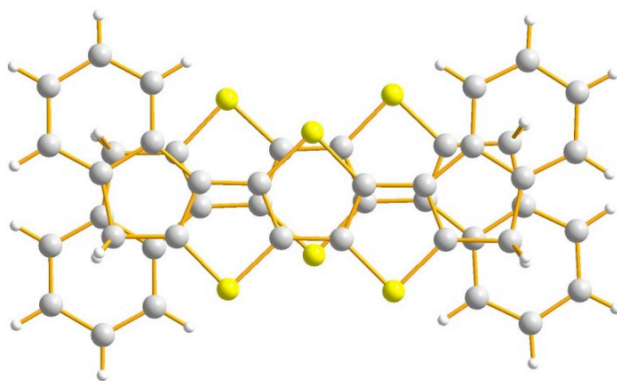
(b)
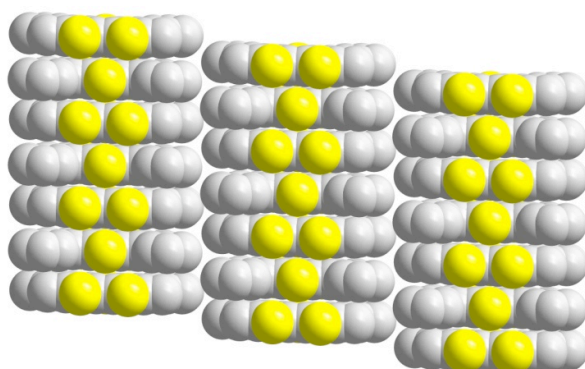
(c)

Figure 16. X-ray structures: (a) asymmetric unit of compound **77** with labels; (b) inversion between a dimer of **77** within the one-dimensional stacks; (c) space-filling diagram showing π-π stacking

2.2.5. Transistor Fabrication and Measurement

Despite the fact that the DTT-based materials **77-79** were designed for photonic applications, the flat nature of the core structure encouraged the investigation of their charge transport properties. Compound **77** was of particular interest, since absence of the hexyl substituents favours the formation of more ordered solid-state packing. Thus, field-effect transistors were fabricated from compound **77** using heavily doped Si^{++} substrates as the gate electrode and a 200 nm thermally oxidised SiO_2 layer as the gate dielectric. Using conventional photolithography, gold source and drain electrodes were defined in a bottom-contact configuration to give a channel length (L) of 15 µm and width (W) of 20 mm. The SiO_2 layer was treated with the low surface energy SAM hexamethyldisilazane (HMDS) to passivate the surface. A 50 nm layer of the organic semiconductor **77** was then deposited by vacuum sublimation at a base pressure of 10^{-9} bar and a rate of 1 Å s^{-1}.

Figure 17 shows a polarised optical microscope image of material **77** vacuum deposited onto the HMDS treated Si/SiO₂ substrate, after annealing for 2 and 4 hours at 125ºC. As can be seen, the prolonged annealing on the HMDS-treated surface had a positive effect on the quality of the layer through the formation of larger crystals. Good crystallinity of the semiconductor in an OFET device is usually highly desirable as an indicator of more ordered and potentially better performing material. For this purpose, thermal annealing is a very common technique, which allows the molecules to arrange in crystal structures with a smaller number of defects and in a more continuous manner.
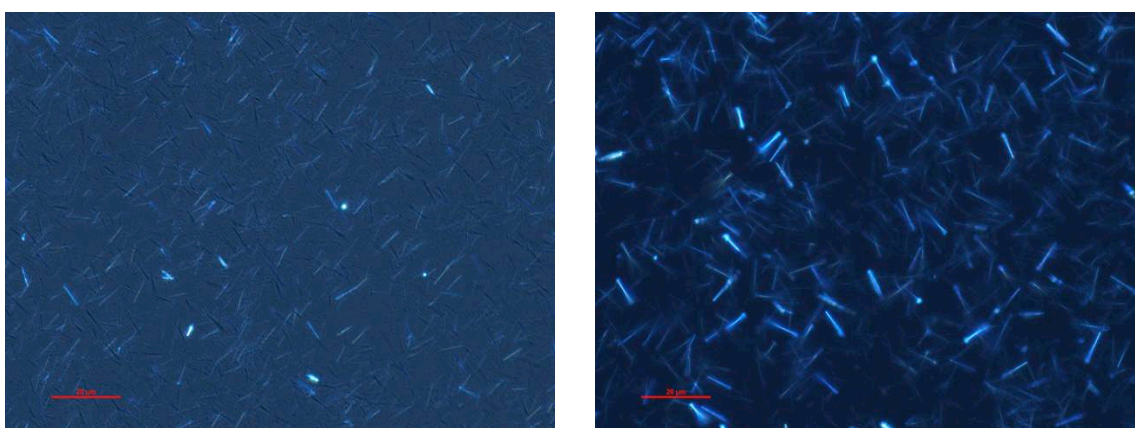
Figure 17. Annealing after 2 hours at 125ºC (left) and 4 hours at 125ºC (right)

Freshly prepared devices were then annealed at 125ºC for another 4 hours under atmospheric pressure and in N_2. Electrical characterisation was carried out in N_2 at ambient pressure using a Keithley 4200 semiconductor parameter analyser.

Figure 18 demonstrates the observed transfer characteristics of a bottom-gate, bottom-contact field-effect transistor based on the material **77**. The inset shows the schematic look of the bottom-contact transistor structure employed. The performance characteristics were obtained with the drain voltage (V_D) set to –3 V in the linear regime and –20 V in the saturation regime. The material showed p-type charge transport and its hole mobility was calculated using standard semiconductor models[32] and found to be ~10^{-4} cm^2 V^{-1} s^{-1} in the saturation modes. The threshold voltage was determined to be approximately –21 V (from the plots of $I_D^{1/2}$ against V_G). The current on/off ratio and subthreshold slope for these devices were estimated to be ~10^6 and 2 V per decade, respectively.
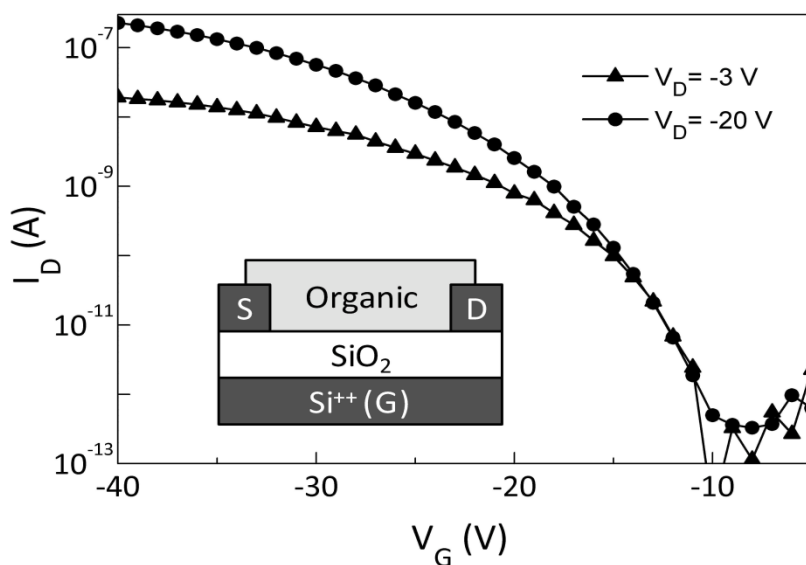
Figure 18. Performance of the transistor based on material **77**; the inset shows the schematic device structure

The relatively low observed hole mobility could be attributed partly to the deep HOMO level of **77** and partly to the less ordered polycrystalline nature of the evaporated film. However, it should be possible to manipulate the latter by additional optimisation of evaporation rates and substrate temperatures to achieve larger crystalline domains and therefore improve the device performance.

2.3. Summary

In this Chapter, the synthesis of a new type of fused oligothiophene derivative and its functionalisation with solubilising and electron withdrawing groups were presented. The electrochemical and photophysical properties of the three new materials were investigated and the results suggest that these compounds could serve as valuable components in extended structures for photonics applications. With additional appropriate functionalisation, the materials could also be incorporated in more extended conjugated structures and polymers. Regarding the latter, compounds **78** and **79** were successfully used for the synthesis of a family of such materials in subsequent research work. The details of their synthesis and results from their property investigations will be discussed in Chapters 3 and 4.

REFERENCES

1. Shirota, Y.; Kageyama, H., *Chem. Rev.* **2007,** *107*, 953-1010.

2. Mason, C. R.; Skabara, P. J.; Cupertino, D.; Schofield, J.; Meghdadi, F.; Ebner, B.; Sariciftci, N. S., *J. Mater. Chem.* **2005,** *15*, 1446.

3. Skabara, P. J.; Berridge, R.; Serebryakov, I. M.; Kanibolotsky, A. L.; Kanibolotskaya, L.; Gordeev, S.; Perepichka, I. F.; Sariciftci, N. S.; Winder, C., *J. Mater. Chem.* **2007,** *17*, 1055.

4. Xiao, K.; Liu, Y.; Qi, T.; Zhang, W.; Wang, F.; Gao, J.; Qiu, W.; Ma, Y.; Cui, G.; Chen, S.; Zhan, X.; Yu, G.; Qin, J.; Hu, W.; Zhu, D., *J. Am. Chem. Soc.* **2005,** *127*, 13281-13286.

5. He, M.; Zhang, F., *J. Org. Chem* **2007,** *72*, 442-451.

6. San Miguel, L.; Porter III, W. W.; Matzger, A. J., *Org. Lett.* **2007,** *9*, 1005-1008.

7. Li, X.-C.; Sirringhaus, H.; Garnier, F.; Holmes, A. B.; Moratti, S. C.; Feeder, N.; Clegg, W.; Teat, S. J.; Friend, R. H., *J. Am. Chem. Soc.* **1998,** *120*, 2206-2207.

8. Zhang, X.; Coté, A. P.; Matzger, A. J., *J. Am. Chem. Soc.* **2005,** *127*, 10502-10503.

9. Okamoto, T.; Kudoh, K.; Wakamiya, A.; Yamaguchi, S., *Org. Lett.* **2005,** *7*, 5301-5304.

10. Ertas, E.; Ozturk, T., *Tetrahedron Lett.* **2004,** *45*, 3405.

11. Morrison, J. J.; Murray, M. M.; Li, X. C.; Holmes, A. B.; Moratti, S. C.; Friend, R. H.; Sirringhaus, H., *Synth. Met.* **1998,** *102*, 987.

12. Osuna, R. M.; Zhang, X.; Matzger, A. J.; Hernandez, V.; Navarrete, J. T. L., *J. Phys. Chem.* **2006,** *110*, 5058-5065.

13. Kim, E.-G.; Coropceanu, V.; Gruhn, N. H.; Sanchez-Carrera, R. S.; Snoeberger, R.; Matzger, A. J.; Bredas, J.-L., *J. Am. Chem. Soc.* **2007,** *129*, 13072-13081.

14. Sun, Y.; Ma, Y.; Liu, Y.; Lin, Y.; Wang, Z.; Wang, Y.; Di, C.; Xiao, K.; Chen, X.; Qiu, W.; Zhang, B.; Yu, G.; Hu, W.; Zhu, D., *Adv. Funct. Mater* **2006,** *16*, 426-432.

15. Yamada, K.; Okamoto, T.; Kudoh, K.; Wakamiya, A.; Yamaguchi, S.; Takeya, J., *Appl. Phys. Lett.* **2007,** *90*, 072102.

16. Barbarella, G.; Favaretto, L.; Sotgiu, G.; Antolini, L.; Gigli, G.; Cingolani, R.; Bongini, A., *Chem. Mater.* **2001,** *13*, 4112-4122.

17.   Perepichka, I. F.; Perepichka, D. F.; Meng, H.; Wudl, F., *Adv. Mater.* **2005,** *17*, 2281.

18.   Okamoto, T.; Kudoh, K.; Wakamiya, A.; Yamaguchi, S., *Chem. Eur. J.* **2007,** *13*, 548-556.

19.   Zhang, X. N.; Johnson, J. P.; Kampf, J. W.; Matzger, A. J., *Chem. Mater.* **2006,** *18*, 3470.

20.   (a) San Miguel, L.; Matzger, A. J., *J. Org. Chem* **2008,** *73*, 7882-7888; (b) Suzuki, Y.; Okamoto, T.; Wakamiya, A.; Yamaguchi, S., *Org. Lett.* **2008,** *10*, 3393.

21.   Tedesco, E.; Della Salla, F.; Favaretto, L.; Barbarella, G.; Albesa-Jove, D.; Pisignano, D.; Gigli, G.; Cingolani, R.; Harris, K. D. M., *J. Am. Chem. Soc.* **2003,** *125*, 12277.

22.   Frey, J.; Bond, A. D.; Holmes, A. B., *Chem. Commun.* **2002**, 2424-2425.

23.   Sotgiu, G.; Favaretto, L.; Barbarella, G.; Antolini, L.; Gigli, G.; Mazzeo, M.; Bongini, A., *Tetrahedron* **2003,** *59*, 5083-5090.

24.   Kim, O. K.; Lee, K. S.; Huang, Z.; Heuer, W. B.; Paik-Sung, C. S., *Opt. Mater.* **2003,** *21*, 559.

25.   Sotgiu, G.; Zambianchi, M.; Barbarella, G.; Aruffo, F.; Cipriani, F.; Ventola, A., *J. Org. Chem.* **2003,** *68*, 1512.

26.   (a) Chiang, L. Y.; Shu, P.; Holt, D.; Cowan, D., *J. Org. Chem.* **1983,** *48*, 4713; (b) Fox, M. A.; Pan, H. L., *J. Org. Chem.* **1994,** *59*, 6519; (c) Skabara, P. J.; Mullen, K.; Bryce, M. R.; Howard, J. A. K.; Batsanov, A. S., *J. Mater. Chem.* **1998,** *8*, 1719.

27.   Blanchard, P.; Jousselme, B.; Frére, P.; Roncali, J., *J. Org. Chem.* **2002,** *67*, 3961.

28.   (a) Blakemore, P. R.; Marsden, S. P.; Vater, H. D., *Org. Lett.* **2006,** *8*, 773-776; (b) Tobisu, M.; Kita, Y.; Ano, Y.; Chatani, N., *J. Am. Chem. Soc.* **2008,** *130*, 15982-15989; (c) Wong, M. S.; Xia, P. F.; Zhang, X. L.; Lo, P. K.; Cheng, Y.-K.; Yeung, K.-T.; Guo, X.; Shuang, S., *J. Org. Chem.* **2005,** *70*, 2816-2819.

29.   Barbarella, G.; Favaretto, L.; Zambianchi, M.; Pudova, O.; Arbizzani, C.; Bongini, A.; Mastragostino, M., *Adv. Mater.* **1998,** *10*, 551.

30.   Kamlet, M. J.; Abboud, J. L. M.; Abraham, M. H.; Taft, R. W., *J. Org. Chem.* **1983,** *48*, 2877.

31.   Antolini, L.; Tedesco, E.; Barbarella, G.; Favaretto, L.; Sotgiu, G.; Zambianchi, M.; Casarini, D.; Gigli, G.; Cingolani, R., *J. Am. Chem. Soc.* **2000,** *122*, 9006.

32.   Zaumsiel, J.; Sirringhaus, H., *Chem. Rev.* **2007,** *107*, 1296.

CHAPTER 3

CHAPTER 3

SYNTHETIC APPROACHES TO CONJUGATED POLYMERS

3.1. Common Methods of Polymerisation

Polymeric materials are very widely used in various electronic devices. They are robust, flexible, light-weight and require inexpensive techniques for deposition and processing. Polymers are particularly useful in transistor devices, such as OTFTs, and various applications utilising photoluminescence, *e.g.*, LEDs and displays. Solar cells based on polymers contribute to a class of OPV devices known as plastic solar cells (PSC).

Polymers can be prepared using a number of known methods. The choice of polymerisation technique is often defined by the nature of the monomers, their synthetic availability and in general, desired outcome of the procedure in terms of polymer weight, regioselectivity, extent of defect formation, production scale, etc. Some of the most common polymerisation schemes will be reviewed in this Chapter. The synthesis of four new diindenodithienothiophene (DITT)-based polymers will also be discussed.

3.1.1. Polymerisations Utilising Transition Metal-based Catalysts

The ultimate goal of any polymerisation is the formation of C—C (or other) bonds between each monomer unit in a continuous manner. Since conjugated polymers are often comprised of various aromatic units, the rise of transition-metal (Pd, Ni, Ru, Cr and others) catalysed cross-coupling reactions introduced a powerful approach for formation of sp^2-sp^2 and sp^2-sp bonds between these unsaturated blocks. In fact, the use of these catalysts boosted the field of organic chemistry and made many synthetic challenges attainable. Pd-catalysis played a particular role in the development of several important synthetic approaches and the scientists who pioneered this field –

Richard Heck, Ei-ichi Negishi and Akira Suzuki – were awarded the 2010 Nobel Prize in Chemistry for their input.

The most common cross-coupling polymerisations involving transition metal-based catalysts, such as Stille, Suzuki, Kumada and Negishi, proceed according to one general cyclic mechanism, which is outlined in Scheme 22.[1] The main participants usually include: (a) a halide-bearing electrophile, X—Ar_1—X (b) an organometallic nucleophile, RM'—Ar_2—M'R and (c) Pd- or Ni-based catalyst, M(0).
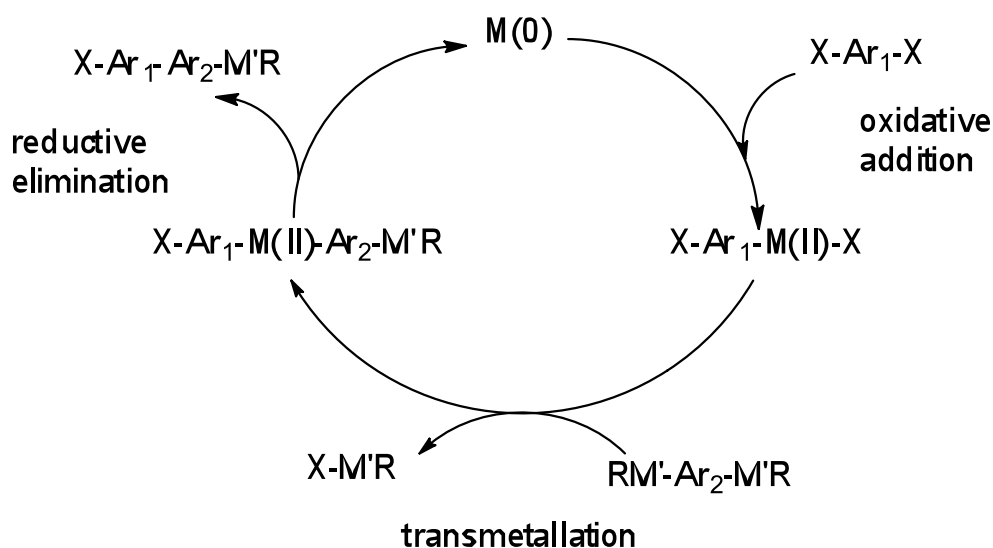
Scheme 22. General mechanism for transition metal-catalysed polymerisation

The cross-coupling proceeds in a few general steps. It is initiated with oxidative addition of the M(0)-complex to the electrophile. The organometallic nucleophile loses one of its M'R groups during the rate-determining transmetallation step, which is forced by the difference in electronegativity between M and M'. Thus, an intermediate of type X-Ar_1—M(II)—Ar_2-M'R is formed. The coupled product is then released during reductive elimination, which can be seen as a decomposition process, where the two organic parts combine and the metal M loses its two 'ligands'. The catalyst is thus reduced back to its original state and the process is repeated.

Transitional metal-based catalysts in which the metal is present in its (0) valence state, such as Pd(PPh$_3$)$_4$, Ni(COD)$_2$ are highly reactive, reliable and utilised frequently in

cross-coupling polymerisations. However, these zerovalent complexes are not stable in air (oxygen) with complete loss of efficiency upon exposure in some cases. They therefore require handling under inert atmospheres (nitrogen, argon). Other catalysts, where the metal is in its (II) oxidation state, *e.g.*, Pd(dppp)Cl$_2$, Pd(dppf)Cl$_2$, Ni(dppp)Cl$_2$ are much more stable in ambient conditions, but their reactive (0) state is then generated *in situ*, which makes the whole process less reproducible due to the stoichiometrical factor.[2]

During the cross-coupling polymerisation (copolymerisation) process with M(0)-catalysts, the amounts of monomers in relation to each other must follow strict 1:1 stoichiometry in order to avoid undesirable side reactions and blockage of the catalyst reactive site, which eventually has a negative impact on obtained yields, polymer weight and polydispersity (polymer weight distribution). When the M(II) catalysts are reduced *in situ* producing M(0), the organometallic nucleophile is consumed to some extent, adding even more uncertainty into the stoichiometric balance and must be taken into account.[2] Another factor, influencing this important balance, obviously relates to the monomers purity and should not be underestimated.

An important aspect concerning the preparation of polymers using transitional metal-based catalysts involves subsequent removal of the catalyst debris from the bulk of the material. Traces of the metal (Pd, Ni) and also phosphine, being present at the point of device performance evaluation, can cause adverse effects, such as quenching of electroluminescence, and observation of inadequate (usually poorer than anticipated) results. Therefore, additional effort should be applied to eliminate such occurrence.[3]

Additionally, the presence of active termini (*e.g.*, halogen) on the polymer chains can also trigger negative effects on device performance by creating charge traps or promoting the formation of defects.[4,5] Fortunately, in many cases these issues can be addressed by appropriate end-capping of polymers at the final stages of the polymerisation.

Copolymerisations utilising transitional metal-based catalysts take place under rather mild conditions and therefore show high tolerance towards a range of substituents on

both monomers. However, some classes of aromatic copolymers possess higher reactivity under one certain set of reaction conditions (and/or functionalities involved), than the others and there are several varieties of catalysed polymerisations that can satisfy the requirements accordingly.

3.1.1.1. Stille Polymerisation

Copolymerisation *via* the Stille cross-coupling reaction is probably the most versatile method utilised for the preparation of alternating polymers consisting of two (or more) different monomers. The method involves coupling between an organic halide, triflate or carbonyl chloride and an organotin compound in the presence of a Pd-based catalyst. Scheme 23 shows a schematic view of this process.
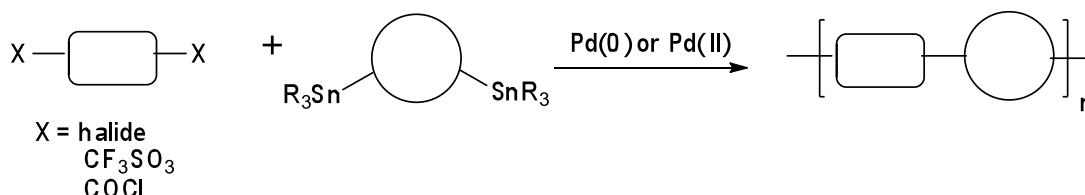
Scheme 23. Schematic Stille co-polymerisation

Stille copolymerisation is suitable for heterocycles and is predominantly successful with thiophene-based monomers, including both linked and fused types, whereas stannylated benzene derivatives show very low reactivity in this process.[1,2] Organotin compounds are generally very stable in ambient conditions and together with the fact that stannylated thiophenes are now readily synthetically available, it provides an additional advantage for their use in Stille polymerisation reactions. Thus, a large number of thiophene-containing polymers prepared by this method were reported over the recent years.[1,5,6,7,8]

The catalyst for the Stille method is usually commercially available $Pd(PPh_3)_4$ (0), which is potent enough upon oxygen-free handling, resulting in high polymer yields. As mentioned, Pd(II) catalysts, such as $Pd(PPh_3)_2Cl_2$ or $Pd(dppf)Cl_2$ may also be used, keeping in mind that the organotin derivative will be responsible for the reduction of the catalyst and additional care must be taken to balance the stoichiometry of the

monomers. The amount of Pd(II)-catalyst introduced into the reaction mixture is therefore also important.[2]

Ligands, coordinated to the metal, can migrate relatively easily and thus *in situ* addition of other ligands can be employed for optimising the reaction. For instance, in a study dedicated to optimisation of (co)polymerisation of substituted PPPs, addition of the ligand $AsPh_3$ to $Pd_2(dba)_3$ catalyst significantly increased the rate of the reaction and yielded polymers with higher molecular weights, whereas addition of ligands PPh_3 and $P(2\text{-furyl})_3$ did not produce such improvements. Ligands $P(OPh_3)$ and $P(2\text{-MeC}_6H_4)_3$ had an altogether negative impact on the catalyst, causing its degradation and thus yielding low molecular weight polymers.[2]

The choice of solvent is also important. The solvent in a polymerisation reaction has two main tasks: (a) it should be able to dissolve the final polymer and (b) should not interfere with the reactants in any destructive way, particularly towards the catalyst. THF is generally suitable for this reaction, although its low boiling point cannot allow sufficient temperatures for faster reactions. Greater polymerisation rates can be observed in higher boiling DMF, but dissolution of the final polymer in this solvent can be affected. Failure to efficiently dissolve the final polymer results in low molecular weights.[2]

Low molecular weights of obtained polymers can also be caused by bulky substituents on the monomers, despite the fact that their presence is often required for the polymer's increased solubility. In addition, steric hindrance from the substituents tend to slow down the polymerisation process.[2] Thus, in order to obtain polymers with optimal molecular weights, one must ensure the solubility of the final product through either solvent or solubilising groups, incorporated onto the monomer frame.

Stille cross-coupling polymerisation proceeds under rather mild conditions allowing tolerance towards sensitive functionalities such as amines, carbonyl, cyano- and nitro-groups, which is clearly a very beneficial feature. Despite that, the reaction times are typically rather long, sometimes stretching over days.

The recent improvements towards this factor were reported by Tierney *et al.*,[9] where a range of polymerisations of alkylated thiophene monomers *via* Stille coupling was carried out with the assistance of microwave irradiation. The group investigated performance of the classic Stille polymerisation, using the $Pd(PPh_3)_4$ catalyst. Chlorobenzene was chosen as the solvent, due to its boiling point being higher than THF, allowing heating up to 200ºC, and otherwise good compatibility with the Stille and microwave conditions. The molecular weights of the obtained polythiophenes, after 10 minutes at 200ºC under microwave irradiation, were rather high with polydispersities ranging from 2.1 to 2.9.

Other catalyst/ligand systems were also investigated, where a sterically bulky ligand $P(o\text{-tol})_3$ in combination with $Pd_2(dba)_3$ catalyst resulted in faster coupling rates and thus higher molecular weights of the final polymers. Overall, the reported results showed that the microwave-assisted Stille coupling yielded high molecular weight polymers with considerably shorter reaction times. This approach is now frequently used in various co-polymerisations[10] along with the conventional method.

3.1.1.2. Suzuki Polymerisation

Suzuki copolymerisation or polycondensation (SPC) is another well-known way to obtain alternating polymers. This method presents a powerful alternative for preparing benzene- and fluorene-containing chains (polyarylenes), where the Stille cross-coupling reaction results in failure due to very low reactivity of stannylated benzene derivatives.[1-2] However, SPC is also suitable for the preparation of thiophene-based and other polymers.[1,3,5]

In the Suzuki approach, the organometallic nucleophile consists of an aryl unit, appropriately substituted with a boronic acid or boronic ester group. The transition metal-based catalyst is often Pd(0), such as $Pd(PPh_3)_4$, although Pd(II) catalysts, *e.g.*, $Pd(OAc)_2$ and $Pd(PPh_3)_2Cl_2$ can be used for *in situ* generation of Pd(0). A schematic representation of a SPC is outlined in Scheme 24.
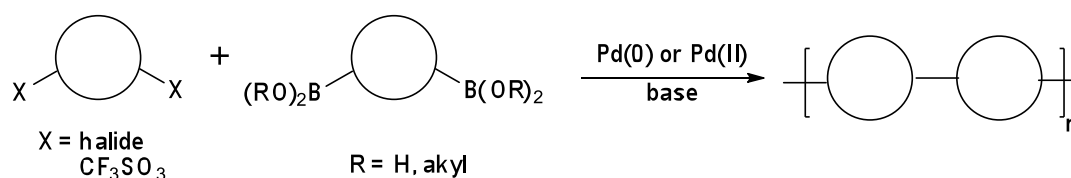
Scheme 24. Schematic representation of a SPC reaction

There are a few important key points that should be taken into account for successful polymerisation *via* SPC. Similarly to the Stille copolymerisation, 1:1 stoichiometry between the monomers must be followed and it is particularly complex in the Suzuki method, due to the chemistry of the boronic group. The boronic acids are generally more reactive but, at the same time, are more prone to dehydration with the formation of condensation products during storage or deboronation upon reaction with stronger bases, putting into risk the stoichiometric balance of the monomers. Additionally, the limited solubility of boronic acids can also be a problem. Boronic esters, on the other hand, make less reactive monomers that require stronger bases to form nucleophilic boronate salts, but are more resistant towards side-reactions and are soluble in virtually any organic solvent, thus providing more predictable polymerisations.[3] These advantages of boronic esters over the acids are therefore reflected in more frequent use of the former in the SPC route towards various fluorene-based polymers.[1, 5]

The presence of a water-soluble base, *e.g.*, K_2CO_3 or Na_2CO_3 is required during the Suzuki polymerisation (to form nuclephilic boronate salts), meaning that mixtures of solvents are used during the reaction. The organic part of the solvent mixture is commonly toluene, xylene, dioxane or THF. Hence, the mixtures are not always homogenous and use of an additional phase-transfer catalyst may be beneficial.[1, 3]

To establish a solid ground for optimisation and in the hope to mediate possible improvements, Goodson and co-workers conducted an extensive investigation of the influence of solvents, base, ligands and palladium source on molecular weights of polymers obtained *via* SPC.[11] Their study was based on the synthesis of oligophenylene-containing polymers according to the procedure below (Scheme 25).
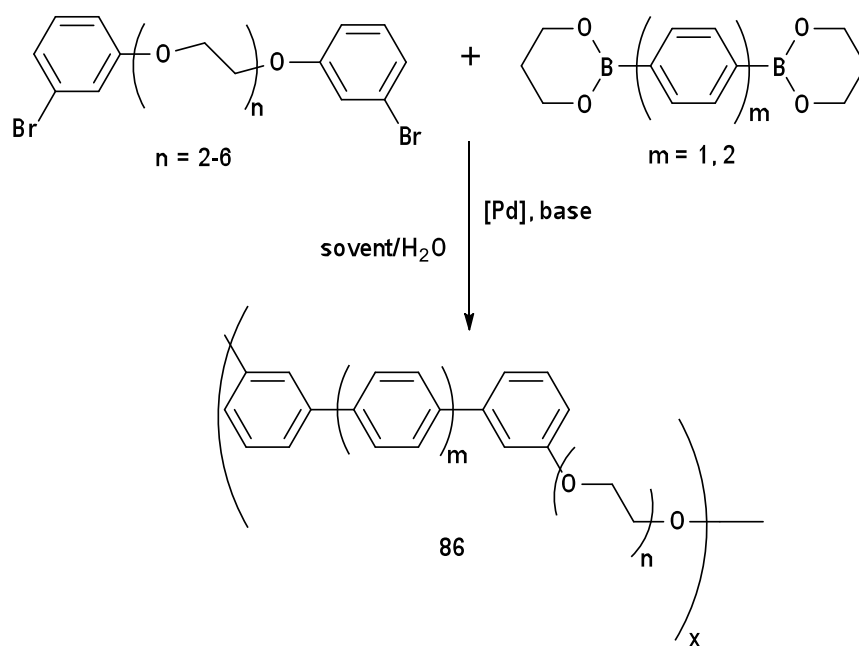
Scheme 25. SPC for study of Goodson *et al.*[11]

The outcome of their impressive work revealed that the best result was produced with solvents that could provide good solubility of the polymer, such as dichloromethane. Conversely, polymer **86** precipitated immediately in DMF and the obtained weight was then very low. Using hydroxides to generate the nucleophilic species resulted in the formation of oligomers only, confirming the instability of boronic groups in the presence of strong bases and indicating the preference towards milder reagents. A few polymerisations with the catalyst $Pd_2(dba)_3$ and a variety of added ligands were performed to explore their effect on the reaction outcome, where the bulky $P(o\text{-tol})_3$ yielded the best results. Further investigations of the most suitable Pd-source revealed that bulkier catalysts, such as $Pd(P(o\text{-tol})_3)_2$, afforded the best polymers.[11]

Intensive degassing of the solvent mixture or inert gas 'blanket' during the entire process is highly recommended, since the Pd(0)-based catalysts, $Pd(PPh_3)_4$ and $Pd[P(p\text{-tolyl})_3]_3$ that are commonly used in SPC are oxygen sensitive and suffer degradation upon exposure to air. Additionally, oxygen can promote homo-couplings between boronic acids and esters, resulting in quenching of the chain growth and yielding low molecular weight polymers.[11] On the whole, Goodson's investigation provides a comprehensive picture of the important factors influencing SPC and offers ideas for its optimisation.

Long reaction times, lasting days, as seen for Stille copolymerisation reactions, encouraged the exploration of microwave radiation assisted SPC. The reported work of Scherf *et al.*[12] shows similar results for both conventional and μW-assisted Suzuki-type polymerisations for the preparation of a 2,6-naphthylene polyketone precursor. However, the reaction times were 3 days and 10-12 minutes, respectively, illustrating a massive improvement. Syntheses of two particularly difficult 1,5-naphthylene-based polyketones were achieved only when using the microwave protocol, while the conventional method did not yield the intended products. A useful review[13] on microwave-assisted transition metal-catalysed polycondensations was recently published, accounting for accomplishments in this area.

Among the recent developments of Suzuki-type polymerisation, utilisation of chlorinated aryls, which are cheap, commercially and synthetically available, was investigated. Chlorinated aryls are generally considered to show low reactivity towards oxidative addition in transition metal-catalysed reactions. Therefore, addition of more electron-rich ligands – biaryl-based phosphines, diadamantyl phosphines and similar, is desirable to compensate for this drawback. Thus, the synthesis of polyphenylenes *via* Suzuki-type polymerisation using *meta*-dichlorinated alkyloxy-benzene was reported.[14] The catalyst used was Pd[P(p-tolyl)$_3$]$_3$ and the added ligand was Buchwald's diaryl-based phosphine (**87**), applied in a 1.0 : 2.5 ratio.

Buchwald ligand

87
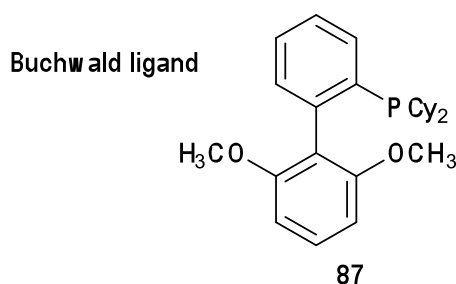
Polymerisations were carried out in a THF/water solvent mixture under reflux for 4 days, and the most successful polymers (M$_w$ ~ 15,000 and PDI < 2) were obtained with K$_3$PO$_4$ as the base. For comparison, polymerisation, carried out in the absence of the ligand, did not produce the desired polymer.

Another recent report by Tsuji and co-workers,[15] demonstrates a successful Suzuki molecular reaction of chlorinated aryls, using a new phosphine ligand, EG12-Phos, which was prepared within the group and then used in their synthesis. Investigations of the possible application of the new ligand for long-chain synthesis are underway.

3.1.1.3. Kumada Polymerisation

The Kumada method generally covers polymerisations of organomagnesium compounds (organometallic nucleophiles) with halogenated aryls in presence of Ni(II) catalysts. This type of coupling can be performed for a single monomer or cross-coupling polymerisation for the preparation of aromatic chains, *e.g.*, polyphenylenes, polycyclopentadithiophenes, polypyridines and other extended, occasionally rather complex structures with distinct electronic properties. [1,5,16]

The mechanism follows the conventional 'oxidative addition-transmetallation-reductive elimination' pattern, although the reactive Ni(0) is generated *in situ* from the Ni(II)-reagent by reaction with the Grignard derivative. Hence, the stoichiometric balance of the monomers in the cross-coupling polymerisations of this type must be calculated taking into account the amount of added catalyst.

There are few Ni(II)-catalysts that can be employed in Kumada-type polymerisations. The two most frequently used and effective reagents are Ni(dppp)Cl$_2$ (**88**) and Ni(dppe)Cl$_2$ (**89**) (Figure 19) and have been employed for both cross- and homopolymerisations. Another common catalyst, Ni(dppf)Cl$_2$ (**90**), is probably less suitable for the latter, as it has been reported to yield polymers of low molecular weights, while usage of both **88** and **89** resulted in much higher molecular weight products during the polymerisation of various 3-substituted thiophenes.[17]
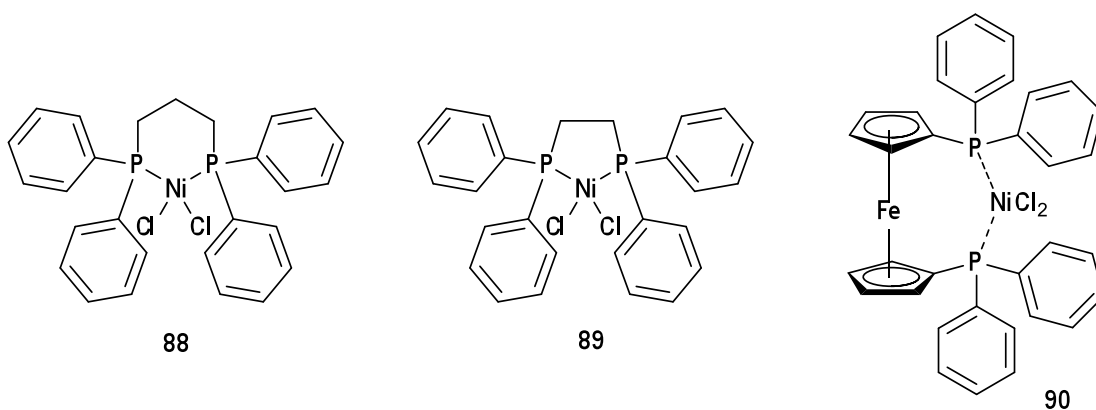
Figure 19. Common Ni(II)-catalysts. **88**: dichloro(1,3-bis(diphenylphosphino)propane) nickel; **89**: dichloro(1,3-bis(diphenylphosphino)ethane) nickel; **90**: dichloro(1,3-bis(diphenylphosphino)ferrocene) nickel

Pd(dppf)Cl$_2$ can also be utilised in Kumada copolymerisations as shown by Babudri *et al.*[18] who successfully prepared a series of copolymers using this catalyst (Scheme 26).
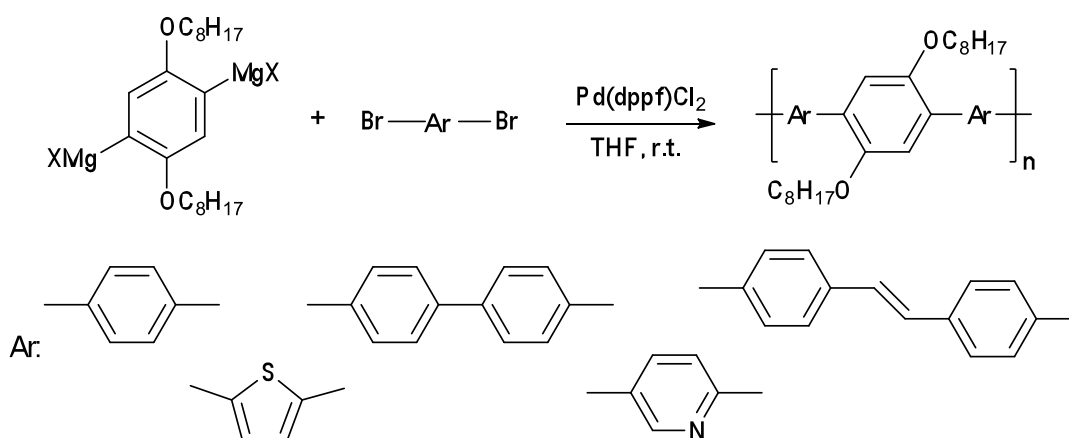
Scheme 26. Kumada co-polymerisation by Babudri *et al.*[19]

A special case of Kumada polymerisation, GRIM (Grignard Metathesis), is now an established method for the regioselective preparation of soluble polythiophenes from 3-alkylated monomers.[20,21] The electrochemical and electroluminescent properties of this class of materials are strongly dependent on the alignment of the alkyl chains on the polymer backbone, where the HT (head-to-tail) structures are referred to as regioregular and are highly preferred. In order to obtain such polymers, an efficient and regioselective strategy, involving Kumada coupling, was originally developed by McCullough *et al.*[22] and was found to yield almost entirely HT polymers.

The high degree of regioselectivity was attributed to the regiospecific lithiation of the 5-position of 2-bromo-3-alkylthiophene by LDA, which then afforded the Grignard derivative in this position. Subsequent addition of a catalytic amount of Ni(dppp)Cl₂ promoted Kumada polymerisation, where the regioregular polymer was formed.

Later, McCullough improved this method (Scheme 27) by reacting 2,5-dibromo-3-alkylthiophene with a Grignard reagent (R' = alkyl or vinyl) to obtain the reactive magnesium intermediate in one step through Grignard metathesis (GRIM). Although the Grignard intermediate was formed as a 85:15% mixture, polymerisation afforded mainly (>95%) the HT-polymer and this regioregularity was suggested to depend on the bulkiness of the Ni(dppp)Cl₂-catalyst.[20]
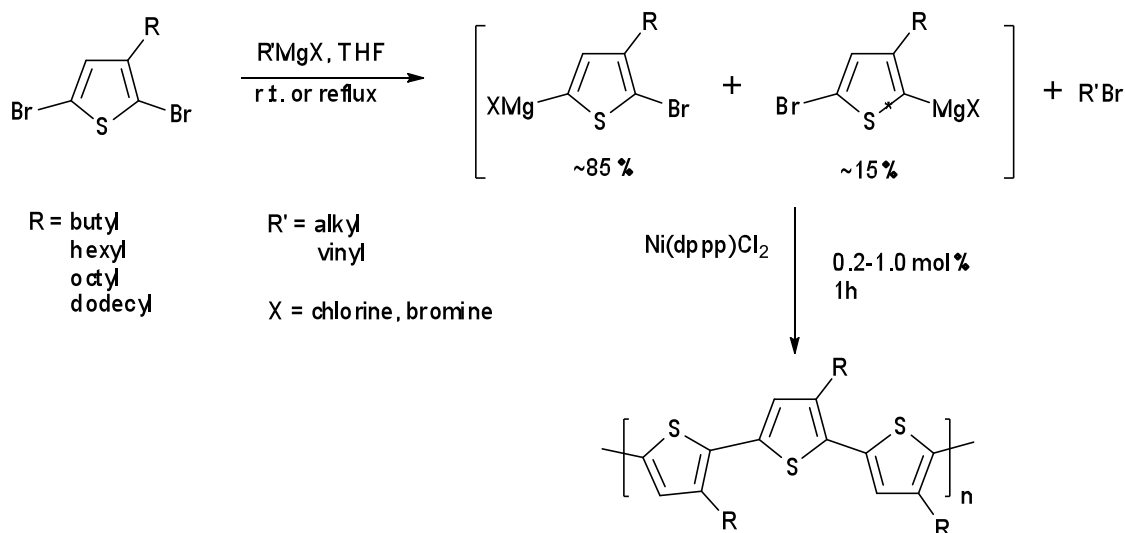
Scheme 27. General GRIM method for synthesis of HT-polythiophenes

The GRIM method has many other advantages, apart from regioselectivity. It is also fast, can proceed even at room temperatures with commercially available reagents and is probably the most utilised tool for the preparation of these promising materials.

3.1.1.4. Negishi Polymerisation

Negishi coupling is based on the reaction between organozinc compounds and halogenated aryls, catalysed by Pd(II) or Ni(II)-complexes. It can be compared to the Kumada coupling in terms of the employed catalysts and the mechanism, where the reactive zerovalent species of Pd or Ni are generated by the organometallic compound. Although Negishi coupling is a very useful tool in small molecule synthesis, preparation of conjugated polymers by this method is mainly focused on polythiophenes.

Classic Negishi coupling involves the use of Pd(II)-based catalysts, such as Pd(dppp)Cl$_2$, Pd(dppe)Cl$_2$, Pd(dppf)Cl$_2$ and PdCl$_2$(PPh$_3$)$_2$ but Ni(II)-based reagents are also rather common. The zinc derivatives can be obtained *in situ* from halo-compounds by reaction with *n*-BuLi and zinc-salts, *e.g.*, ZnCl$_2$, or direct metallation with Rieke zinc (Zn*). The latter is a highly reactive metal, prepared by the reaction between anhydrous ZnCl$_2$ and an alkali metal, usually Li, and used immediately after.[23]

Rieke zinc is readily used for the preparation of zincated 3-alkyl-thiophenes, which can further participate in a Negishi-type polymerisation to obtain both regioregular and regiorandom polymers, according to the method developed by Rieke[23] (Scheme 28).
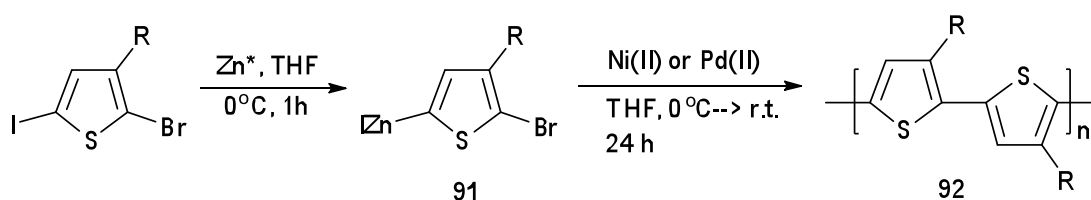
Scheme 28. Rieke polymerisation of 3-alkylthiophenes[23]

The degree of regioregularity was found to be strongly dependent on the nature of the applied catalyst. In analogy with the McCullough[20] method (section 3.1.1.3), the Ni(dppe)Cl$_2$ catalysed process resulted in almost entirely regioregular polythiophenes, whilst a decrease in the bulkiness of the ligands to PPh$_3$ and an increase in the size of the metal (Pd), diminished the percentage of the HT-polymers in the mixture to a

totally regiorandom product. Thus, the trend in regioselectivity among the four tested catalysts was proposed: Ni(dppe)Cl$_2$ > Pd(dppe)Cl$_2$ > Ni(PPh$_3$)$_4$ > Pd(PPh$_3$)$_4$.[23]

The synthesis of a polythiophene, bearing a chiral centre in the repeat unit, by the Rieke method, was also reported.[24] The group used active Zn* for the preparation of the zinc intermediate and Ni(dppe)Cl$_2$ catalyst and obtained high molecular weight polymer **93** with a regioregularity of approximately 95%. Insertion of the chiral side chains on the polythiophene was reported to promote a higher order within the structure, which in turn influences the optical properties of the material.[24]
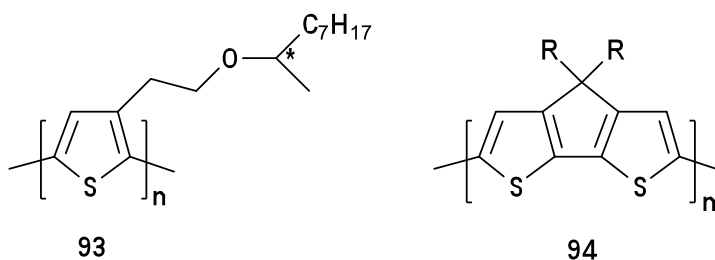
Apart from various polythiophenes, the number of publications reporting the preparation of other polymers *via* Negishi coupling is rather limited. However, Coppo *et al.*[25] investigated different polymerisation methods for the synthesis of a family of polycyclopentadithiophenes substituted with long alkyl chains (**94**). They eventually found that using Rieke zinc in a Negishi-type protocol (catalyst Ni(dppe)Cl$_2$) yielded the best results for these systems, although the molecular weights were in the moderate range.

Also, Li and co-workers[26] managed the synthesis of a rather complex binaphthyl-based system (**95**) *via* Negishi polymerisation, using Pd(PPh$_3$)$_4$ as the catalyst and applying a *n*-BuLi/ZnCl$_2$ procedure to obtain the organozinc derivative.

95
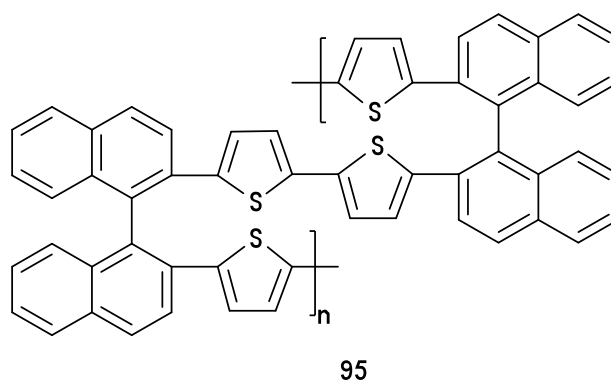
3.1.1.5. Yamamoto Polymerisation

Yamamoto polymerisation, also called dehalogenative homopolymerisation utilises mainly zerovalent Ni-complexes for the polymerisation of dihalogenated aromatics, affording π-conjugated polymers of high quality (Scheme 29).
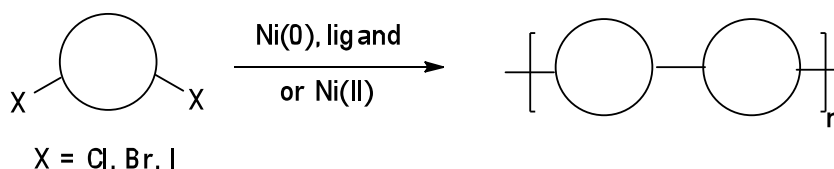
Scheme 29. Schematic representation of Yamamoto polymerisation

This method was originally reported by Yamamoto et al.[27] in 1992 and demonstrated the preparation of non-substituted polythiophenes, cyano-group bearing and alkylated polythiophenes and also polyphenylenes, using mixtures of the Ni-complex, bis(1,5-cyclooctadiene)nickel (Ni(COD)$_2$), and neutral ligands – triphenylphosphine or 2,2'-bipyridyl. Under mild reaction conditions using either DMF or toluene as the solvent and heating up to 25–100ºC for 2–48 hours, high molecular weight polymers were obtained. This approach was found to be extremely useful and was eventually employed for the synthesis of many other homopolymers, *e.g.*, poly(9,9-dialkylfluorene)s (**96**),[28] poly(9,10-dihydrophenanthrene)s (**97**), poly(2,5-pyridine) (**98**), poly(3,6-carbazole)s (**99**) and many other complex structures.[1, 5]
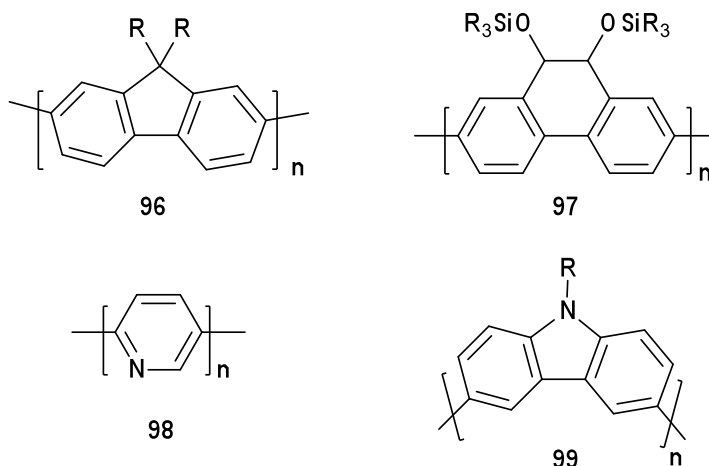
The mechanism of this homopolymerisation is different from the one using cross-coupling methods. The Ni(0)-complex acts as a dehalogenator of the X—Ar—X monomer in this reaction, enabling the formation of long chains with a tendency for high regioselectivity through the mechanism pictured in Scheme 30 below.[27,29] The main distinction of this process *versus* other catalysed polycondensations is that the Ni(0) is actually consumed as the polymerisation progresses and approximately stoichiometric amounts must be used to achieve high molecular weight products.
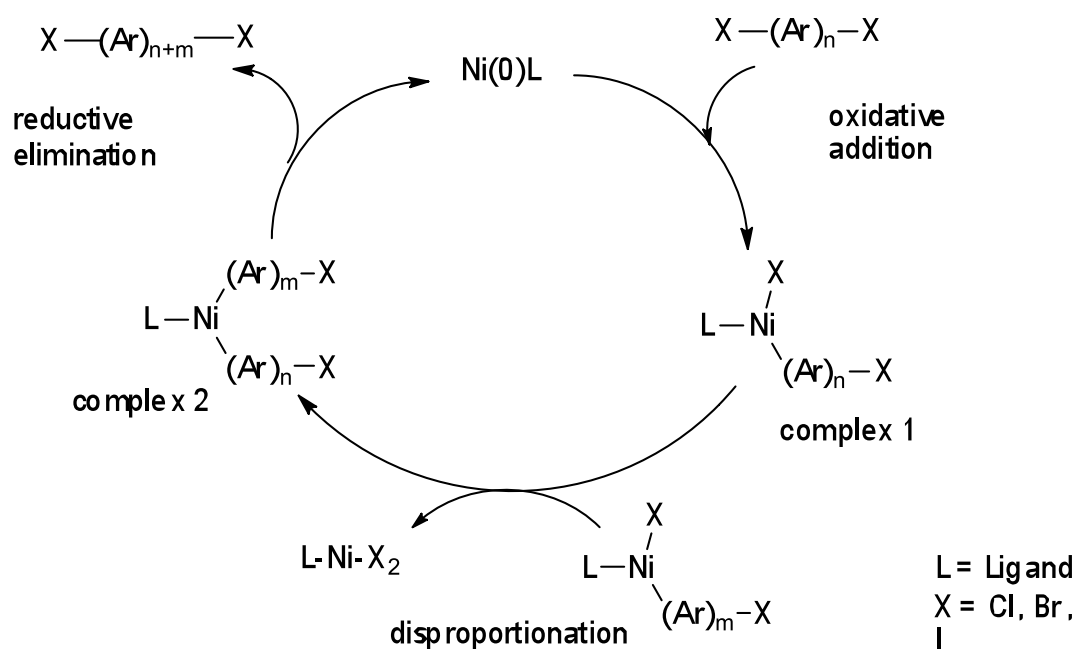
Scheme 30. General mechanism of Yamamoto polymerisation

The polymerisation sequence initiates with the oxidative addition of the C—X bond of the dihaloaromatic to the Ni(0) reagent. Subsequent recombination of complex 1 with a second molecule of complex 1 in the disproportionation step leads to complex 2. The extended compound $X—(Ar)_{n+m}—X$ is released through reductive elimination. The latter can enter the cycle again and the process is repeated as long as the supply of monomers/oligomers is present and the Ni-complex remains chemically active. Both complexes 1 and 2 can be isolated[27] if they possess sufficient stability due to the bulkiness of the aromatic, which is useful for mechanistic studies. Additionally, the formation of the Ni—C bond is believed to be favoured towards the less sterically hindered position of mono-substituted monomers, explaining a certain tendency for regioselectivity during Yamamoto polymerisation.[27]

The attraction of this method is attributed to its synthetic simplicity and mild reaction conditions, allowing straightforward synthesis of polymers bearing sensitive substituents. Another advantage of this approach is that it is a one-component process, eliminating the problematic issue of monomer stoichiometry. Hence, the method opens possibilities for the preparation of polymers with strict alternation of, *e.g.*, donor and acceptor fragments through their coupling into a two-component monomer block prior to polymerisation.

The drawback of this synthetic route includes a high sensitivity of the Ni(0) complexes towards air and moisture. In most cases, Yamamoto polymerisations require glovebox environments and neglecting this aspect can result in low molecular weights of polymers and low yields. Also, Ni(0) reagents are commonly rather expensive.

The Yamamoto method is the preferred route for the synthesis poly(9,9-dialkylfluorene)s (**96**), since the previously common $FeCl_3$ oxidative polymerisation produced low weight and poor quality polymers. Although the earlier described Suzuki method (section 3.1.1.2) is very efficient for obtaining PFs, the Yamamoto procedure yields polymers of even higher molecular weights and with a high degree of regioregularity.[28]

Ni(II)-based catalytic systems can also be used for Yamamoto polymerisations. For instance, in the synthesis of polypyridine (**98**), where NiCl$_2$ is reduced with zinc/triphenylphosphine *in situ* in order to generate the reactive Ni(0).[5,30]

Examples of microwave radiation-assisted Yamamoto polymerisation are also known. μW-assistance traditionally decreases the reaction times considerably and facilitates difficult procedures as was shown in the synthesis of polypyrazine (PPyrz).[31] Yamamoto homopolymerisation of 2,5-dibromopyrazine was performed by both conventional and microwave-assisted methods. Both protocols yielded the desired polymer in comparable yields and the reaction times were improved from two days to 10 minutes.

3.1.2. Other Methods of Polymerisation

Polymerisation methods involving catalysis by transition metal-based complexes are indeed very common tools to obtain conjugated polymers with high diversity of structures. However, they may seem synthetically demanding, elaborated and rather often require expensive reagents. These aspects can make the methods less suitable under certain circumstances and for such occasions there is a choice of alternative approaches, briefly described below.

3.1.2.1. Oxidative Polymerisation with FeCl$_3$

Oxidative polymerisation is a chemical polymerisation method mostly utilising ferric chloride (FeCl$_3$) as the reagent. This method is widely known and its main advantage is that it can afford a straightforward and cost-effective synthesis of high molecular weight homopolymers on a large scale. On the other hand, the disadvantages of this method include: (a) the formed polymer is often found in its doped state and needs dedoping,[25] which is not always convenient; (b) low controllability of the process in terms of molecular weights and polydispersities of the product, sometimes reaching values greater than 10;[25,32] (c) iron salts that remain in the polymer's bulk after the

synthesis, can have an unfavourable effect on the device performance, and extensive washing procedures must be set up to dispose of their content.[25,32]

The latter aspect is particularly significant, since a large excess of $FeCl_3$ must be used for an optimal polymerisation process, which would produce long polymer chains with at least some degree of polydispersity control. Several published sources reported $FeCl_3$/monomer ratios required for this polymerisation as high as 4-5.[25,32,33,34] The reason for such heavy $FeCl_3$ load lies in the mechanism of the process, where the reagent is consumed to form a Fe^{3+}/Fe^{2+} couple during the oxidation of the unsaturated monomer.

The mechanism of polymer growth was proposed by Andersson during his attempts to improve the regioselectivity of the oxidative polymerisation of P3ATs.[35] He suggested that the process involved an initial formation of cations or radical cations that further act as electrophiles in an electrophilic aromatic substitution with a neutral monomer (- $2H^+$) and eventually re-enter the cycle 'oxidation – chain extension' as depicted in Scheme 31.[35]
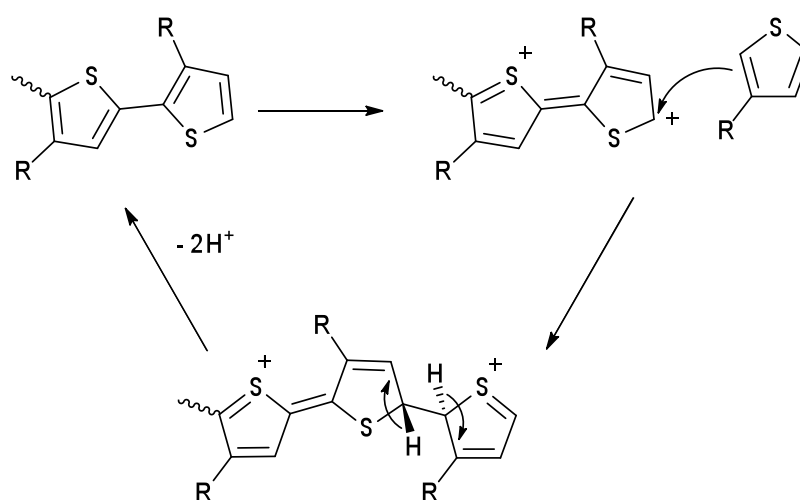
Scheme 31. Andersson's mechanism for oxidative polymerisation of 3-alkylthiophene

At the same time, he also applied a gradual addition of $FeCl_3$ slurry to the dissolved monomer rather than following the opposite order of introducing the reactants into the reaction mixture. This slight change led to a significantly improved regioselectivity of the polymerisation from almost regiorandom to *ca.* 94% content of the HT polymer.[35]

Some recent reports of polymer synthesis by oxidative polymerisation include polypyrene (**100**), thiophene/thiadiazole (**101**) and fluorene (**102**) based materials. Despite the drawbacks already mentioned, the authors emphasise the simplicity and low cost of this method.

100

101

102
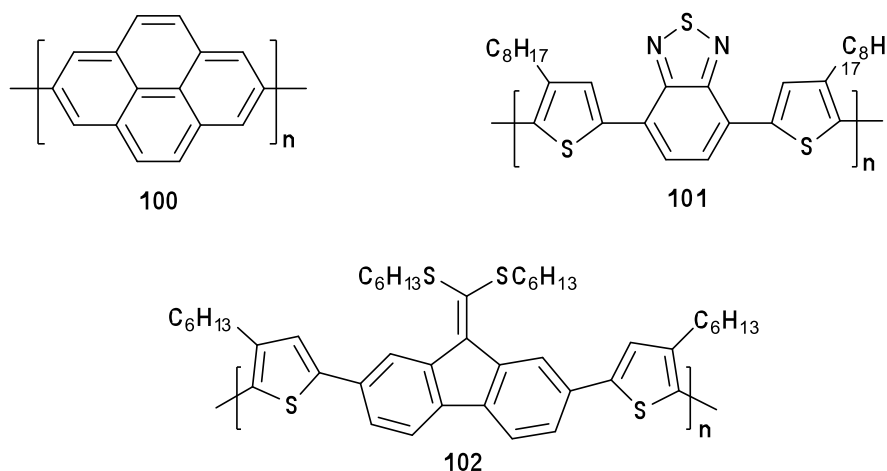
3.1.2.2. Electropolymerisation

Electropolymerisation is a technique, where deposition of the polymer occurs on the electrode surface from the monomer solution and where the initial charged precursors are generated by an applied potential rather than a catalyst. Usually, polymer film formation takes place at the anode surface, mainly platinum sheets/wires, glassy carbon or ITO glass, *via* a series of oxidation cycles.[36,37] The thickness of the formed polymer film can be easily controlled by the number of cycles, but it is also limited by the size/surface area of the electrode. An additional advantage of this method is that it offers possibilities for the instant evaluation of the polymer's properties by, *e.g.*, cyclic voltammetry.[36-37]

As mentioned, the initial charged species, radical cations (**103**), are achieved by electrochemical oxidation. Further insight on the mechanism is a rather debated subject, but it is generally agreed that it involves the formation of a dication with another charged radical monomer, followed by its re-aromatisation to a neutral dimer (**104**) through the elimination of two protons. The dimer can then be oxidised again and

merged with other charged species, thus forming a polymer chain as schematically presented in Scheme 32.[36]
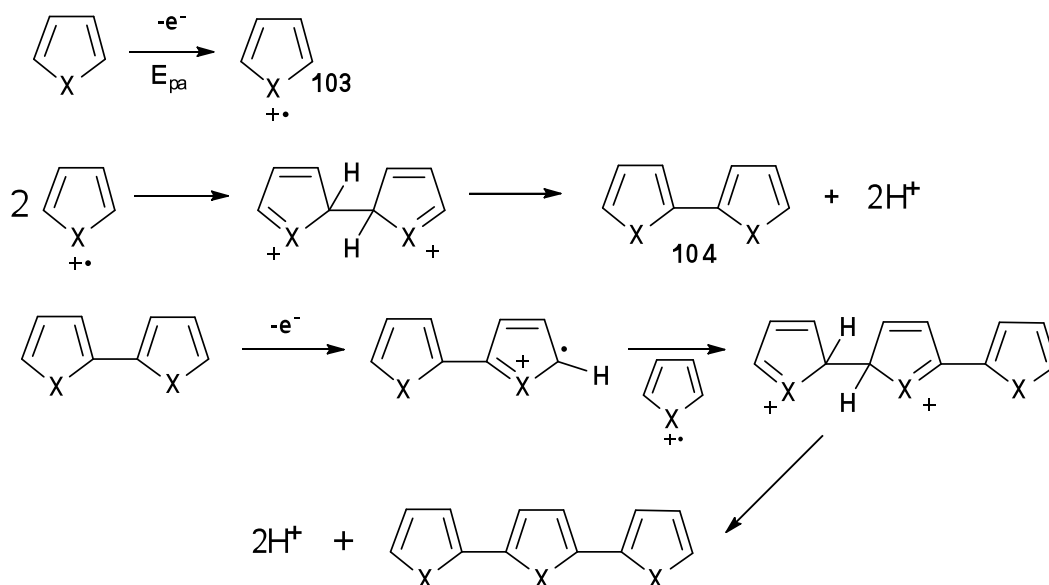
Scheme 32. Electropolymerisation mechanism for 5-membered heterocycles[36]

Electropolymerisation was commonly employed in the preparation of polythiophenes before more efficient chemical methods were developed. The technique was extensively studied towards optimal process conditions involving applied potentials, electrolytes, solvents, monomer requirements and mechanistic aspects.[36]

Electropolymerisation is still a rather common method to obtain smaller quantities of polymers or to perform simultaneous electrochemical characterisation of the polymeric material. However, preparation of more substantial amounts would require large electrode surfaces and electrolyte/solvent quantities, which can become unnecessarily costly and, thus, not very suitable for the purpose.

Electropolymerisation can be a quite cost-effective solution when other chemical polymerisation methods are not preferred for various reasons as in the case of thienopyrazines (**105**), which suffer strong complexation with Fe^{3+} upon oxidative polymerisation.[38]

R = H or alkyl

105
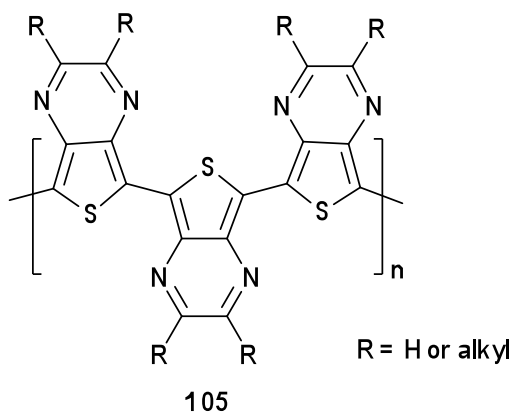
3.2. Synthesis of DITT-based Polymers

The synthesis and characterisation of three new DITT-based molecular materials (**77-79**) were discussed in Chapter 2 and further work in this direction included the synthesis of four new polymers (**106-109**), containing this block and an investigation of their electrochemical properties. Thus, the sections below will focus on the details of the synthetic part of the work and in Chapter 4 the properties of these polymers will be discussed.
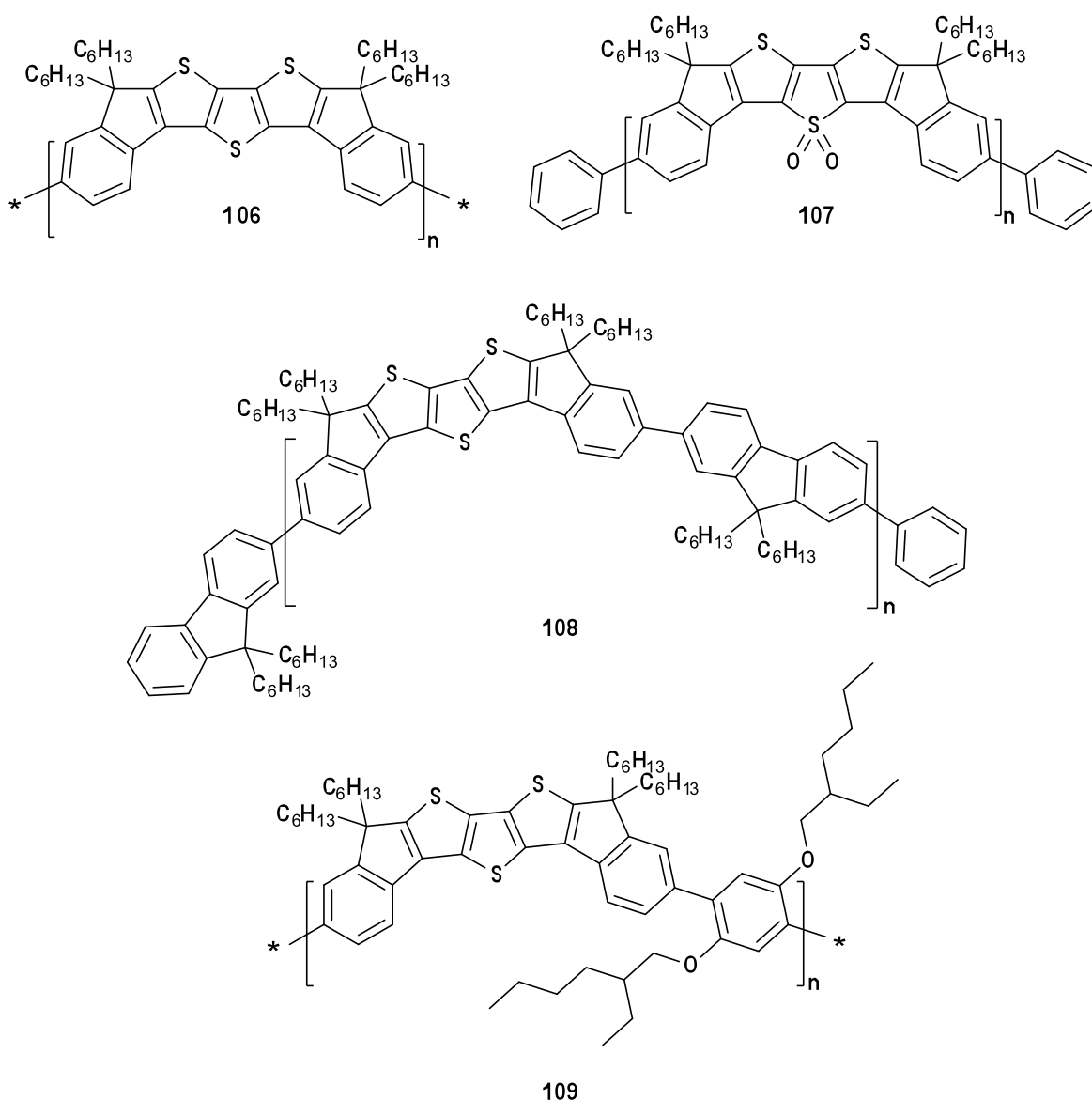
3.2.1. Synthesis of Monomers

In order to polymerise the DITT- materials **78** and **79**, appropriate bromination was carried out. It was achieved through the route outlined in Scheme 33.
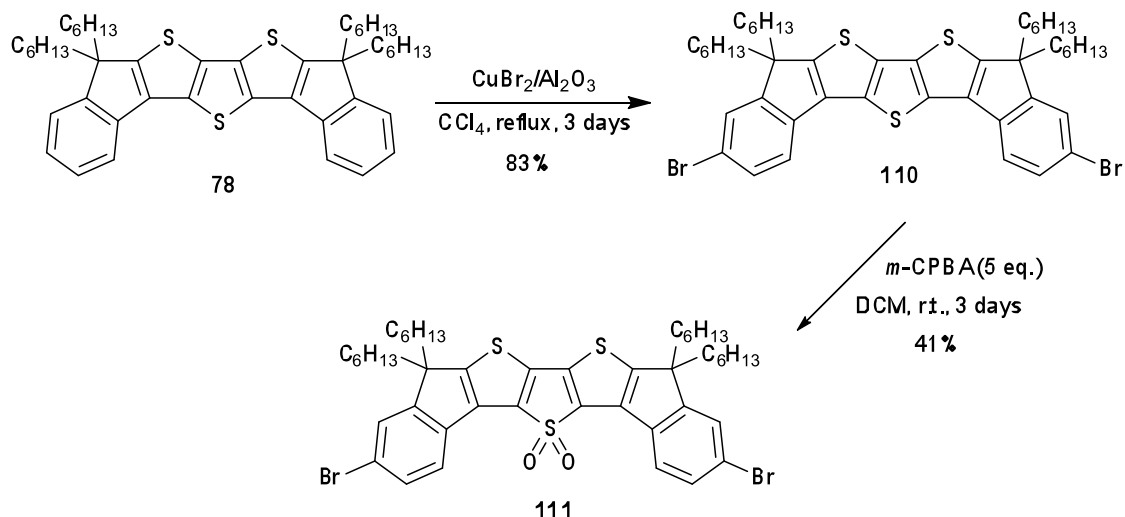
Scheme 33. Synthesis of monomers **110** and **111**

Bromination of compound **78** was performed according to a previously described method for the selective halogenation of aromatic compounds,[39] where the brominating reagent $CuBr_2$ was first deposited on alumina. After thorough drying of the reagent under vacuum with heating, it was added to **78** dissolved in CCl_4 and refluxed under N_2 for 3 days. The reaction was monitored by TLC, showing that the starting material (**78**) was still present in significant amounts after 24 hours. After an additional 2 days, the reaction was complete according to TLC and the product (**110**) was isolated in 83% yield after precipitation from dichloromethane/methanol. The new compound was analysed by ^1H and ^{13}C NMR spectroscopy, confirming the symmetry of the molecule. Mass spectrometry and elemental analysis indicated the presence of two bromine atoms per molecule. In order to ensure that bromination occurred in the desired positions, an NOE experiment was carried out.

The idea of the experiment was to irradiate the system at the resonance frequency of selected protons and see where any long-range through-space couplings with any other protons emerge. Hence, three signals were investigated, including two aromatic peaks and also one aliphatic multiplet (m), corresponding to the CH_2 protons closest to the

main core of the molecule. Irradiation of the latter showed a through-space coupling with a ^{4}J split singlet (ds) in the aromatic region as illustrated in Figure 20. This indicates the spatial proximity of the CH$_2$ unit to a single proton with only one coupling across four bonds, which allows its assignment to the C3-position. The absence of ^{3}J splitting for this signal thus confirms the C4 position of the halogen atom on the outer aromatic ring.
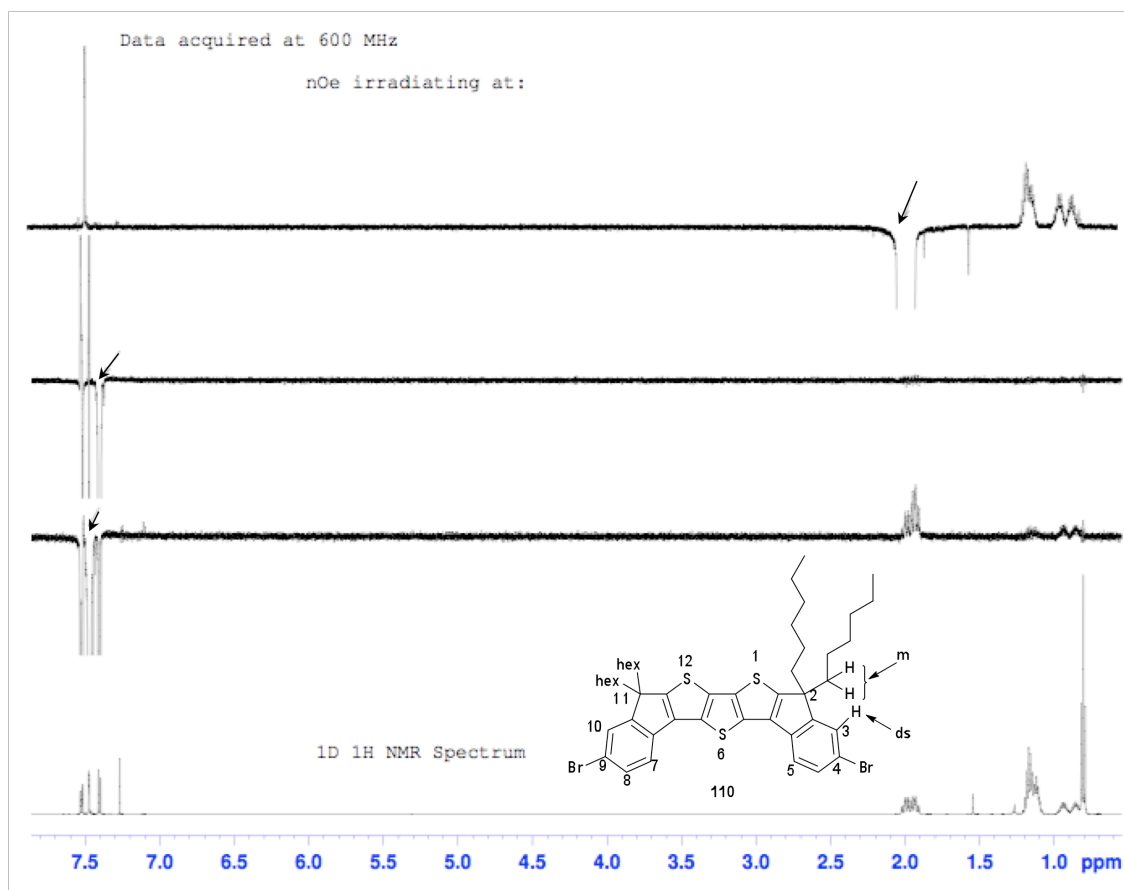
Figure 20. NOE experiment, determining the structure of compound **110**. The arrows show the investigated frequencies of the ^{1}H NMR-spectrum

The new monomer (**110**) was homopolymerised (**106**) and used together with other monomers to obtain polymers **108** and **109**.

Oxidation of **110** with an excess of *m*-CPBA at room temperature in the absence of light for 3 days, resulted in a complex mixture of products, which after purification by column chromatography (distilled petroleum ether/toluene, 3:1) and precipitation from dichloromethane/methanol, afforded highly luminescent compound **111** in 41% yield as

a bright orange solid. The new material was analysed by ^{1}H and ^{13}C NMR spectroscopy, mass spectrometry and elemental analysis. Its symmetrical structure and presence of two oxygen atoms per molecule were confirmed.

Apart from **111**, another luminescent compound was isolated during column chromatography. Followed by precipitation from dichloromethane/methanol, an orange solid was obtained in 14% yield. It was characterised by ^{1}H and ^{13}C NMR spectroscopy revealing a non-symmetric structure. Together with the results from mass spectrometry and elemental analysis, the compound was identified as a non-symmetric isomer of **111**. X-ray diffraction additionally confirmed the structure as compound **112** below.
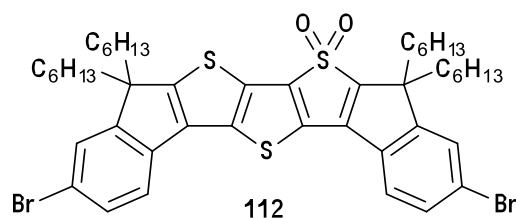
Thus, oxidation with *m*-CPBA did not show a high selectivity towards one particular sulfur atom in the core of **110**. Despite attempts to optimise the reaction through varying amounts of *m*-CPBA, temperature and times, no significant improvement was achieved. Further, compound **111** was homopolymerised *via* Yamamoto polymerisation.

In addition to the synthesis of homopolymers, the DITT-block was also copolymerised with two other monomers. One of them was 9,9-dihexylfluorene-2,7-diboronic acid (**113**) widely used in polymerisation by Suzuki cross-coupling protocol.[5,3] It was prepared according to procedures already reported[40] and then converted into the boronic ester **114** by gentle overnight reflux in toluene together with ethanediol, affording a nearly quantitative yield of compound **114** as a white solid (Scheme 34). This fluorene unit was later used together with monomer **110** to prepare polymer **108.**
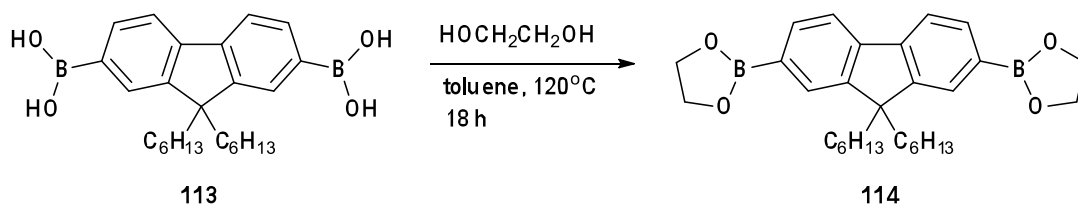
Scheme 34. Synthesis of monomer **114**

Monomer **117** was used for preparation of copolymer **109**. It can be synthesised through a halogen-lithium exchange followed by boronation.[41] However, in a separate project in the Skabara laboratory, it was obtained as a side-product during the lithiation–boronation sequence of 1,4-bis((2-ethylhexyl)oxy)benzene (**115**), along with the main product – mono-boronic acid **116** as shown in Scheme 35. Following a previously described procedure,[42] the reaction involved initial lithiation of **115** with *n*-BuLi in the presence of TMEDA at room temperature and then boronation with triisopropyl borate.
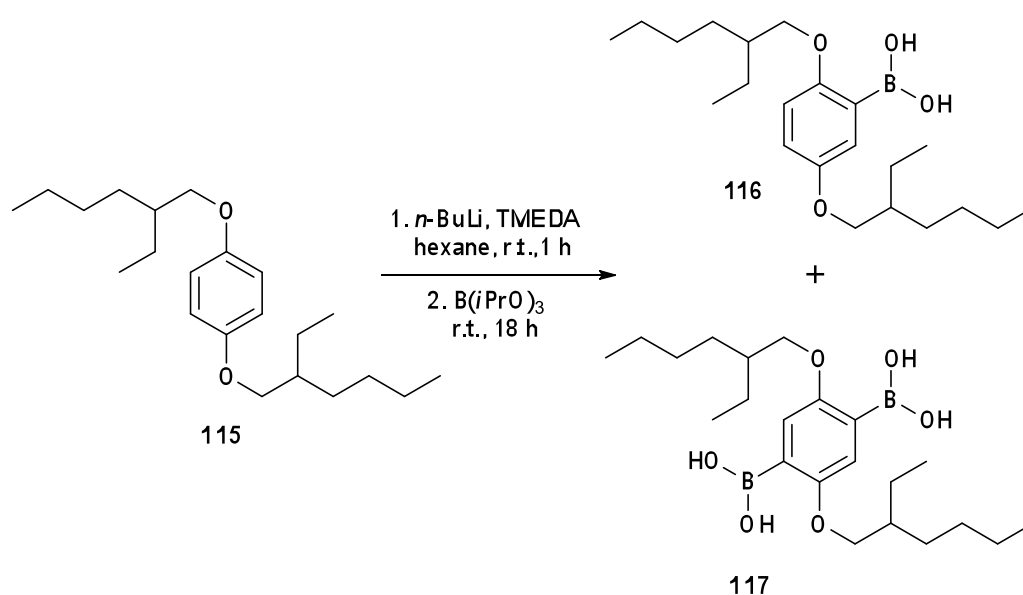
Scheme 35. Monomer **117** as a side-product from the synthesis of compound **116**

After separation of the crude product by column chromatography on silica gel (ethyl acetate/hexanes, 1:10), compound **117** was isolated in ca. 8% yield. Its structure was confirmed by ^{1}H and ^{13}C NMR spectroscopy and elemental analysis and agreed well with the reported values.

3.2.2. Synthesis of Polymer 106

Polymer **106** was prepared by a microwave-assisted Yamamoto homopolymerisation, using Ni(COD)$_2$ as the reducing agent or dehalogenator (Scheme 36).
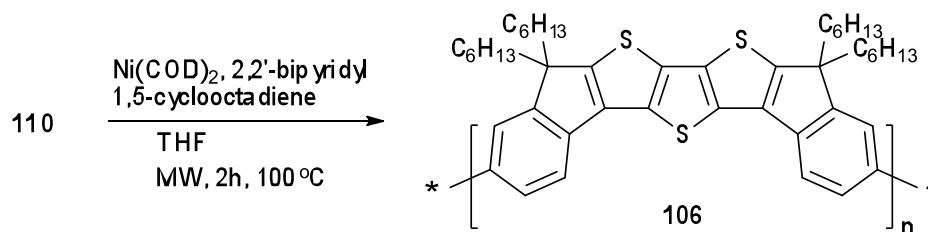
Scheme 36. Preparation of polymer **106**

Weighing and all handling of Ni(COD)$_2$ was performed in a glovebox to avoid the loss of activity of the complex through its degradation as the result of exposure to oxygen. After adding the remaining reactants, the polymerisation was conducted in a microwave oven at a temperature of 100°C for 2 hours.

The crude material, after precipitation with methanol, filtering and drying, was then subjected to Soxhlet extraction to remove more soluble oligomers and lower molecular weight fractions. The extractions were performed with methanol, acetone and finally dichloromethane (to extract the product) and lasted *ca.* 24 hours for each solvent. This was a standard work-up procedure for all four polymers.

The polymer was obtained in 51% yield and was soluble in THF, dichloromethane and chloroform. The ^{1}H NMR spectrum showed broad signals in the aromatic and aliphatic regions. The average molecular weight data were determined by absolute gel permeation chromatography (GPC) with a light scattering detector and were found to be: M_w 92,449 g mol^{-1}, M_n 17,361 g mol^{-1} and PDI 5.3.

The polydispersity index (5.3) was rather high. One explanation to this could be that the amounts of the Ni-reagent were too high (2 eq). It is reasonable to suggest that when Ni(COD)$_2$ is present in excess, a large number of shorter oligomers is generated but the decreasing amount of the available monomers cannot support the successful

growth of longer chains. Furthermore, the excessive oxidative addition of available molecules of the Ni(0) complex to both halogen termini of the monomer can lower the degree of or even block polymer growth. Hence, the average weight of the polymers obtained is lower than might have been expected and the polydispersity index is high due to the low level of uniformity among the polymer chains.

Another explanation could be in the chosen protocol of the polymerisation. The obvious advantage of the microwave-assisted process is a dramatic decrease of the reaction time, while the conventional method would normally take up to 3-4 days. However, zerovalent Ni(COD)$_2$, a rather unstable complex in ambient environment, might suffer even faster degradation under such intense reaction conditions, which could also have a negative effect on the polymer characteristics and its yield. In order to compensate for this factor (loss of catalytic activity), a somewhat higher than usual amount of the reagent was used. Thus, a combination of these two factors (amount of Ni(COD)$_2$ and the microwave protocol) was most likely the reason behind the observed molecular weight characteristics of the polymer **106**.

Preferably, the halogen groups at the ends of the polymer chains should be removed by end-capping. For this polymer, the procedure was not performed since the polymerisation was set up according to the µW-protocol and some technical aspects associated with this made additional procedures less feasible due to possible exposure to air.

3.2.3. Synthesis of Polymer 107

The homopolymer of the fluorescent monomer **111** was also obtained by Yamamoto polymerisation. Both microwave-assisted and conventional protocols were investigated. The former was performed under the conditions that were applied during the synthesis of polymer **106**. However, the yield of the polymer obtained under this protocol was very low, making further characterisation impossible due to an insufficient amount of the material.

Thus, in the next attempt the conventional method was employed and the amount of the Ni(COD)$_2$ complex was decreased to a roughly stoichiometric quantity. The reaction conditions are outlined in Scheme 37.
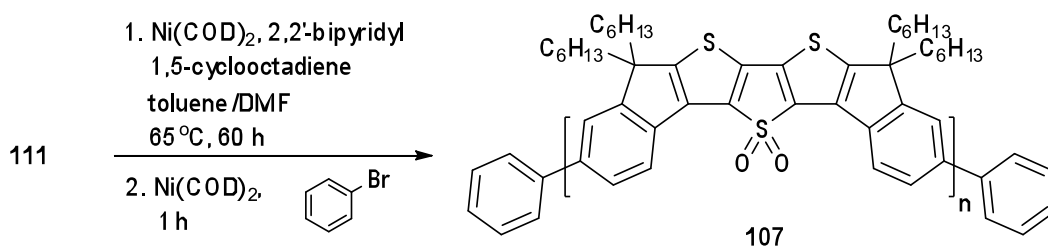
Scheme 37. Yamamoto polymerisation of **111**

The synthesis was conducted under N$_2$ and with gentle heating to 65°C. After 2.5 days, end-capping of the polymer's bromine end-groups was carried out by adding an excess of bromobenzene together with a fresh portion of Ni(COD)$_2$ complex. After the standard work up with Soxhlet extraction, the polymer was obtained as dark orange powder in 51% yield. The ^{1}H NMR spectrum showed very broad signals in the expected regions, fully overlapping possible signals from the end-cap groups. The average molecular weight characteristics were therefore determined by GPC only and were established as: M$_w$ 66,890 g mol^{-1}, M$_n$ 61,470 g mol^{-1}, PDI 1.1.

The low polydispersity index together with higher molecular weight indicated a more optimal polymerisation process under the conventional protocol. The polymer was soluble in dichloromethane, THF and chloroform. Its electrochemical and optical properties were investigated.

3.2.4. Synthesis of Polymer 108

The synthesis of polymer **108** was achieved by Suzuki cross-coupling polymerisation between the DITT-based block **110** acting as a haloaromatic electrophile and compound **114**, bearing two boronic ester groups, which after initial activation with a base (formation of the reactive salt) represented the nucleophile in this reaction.

The polymerisation was performed employing the conventional method and using 5 mol% of the catalyst Pd(PPh$_3$)$_4$, as outlined in Scheme 38. Subsequent end-capping of the polymer chains was also carried out: first by adding the mono-boronated fluorene unit to remove the bromine termini and after *ca.* 1 hour – with bromobenzene for the removal of the boronic centres.
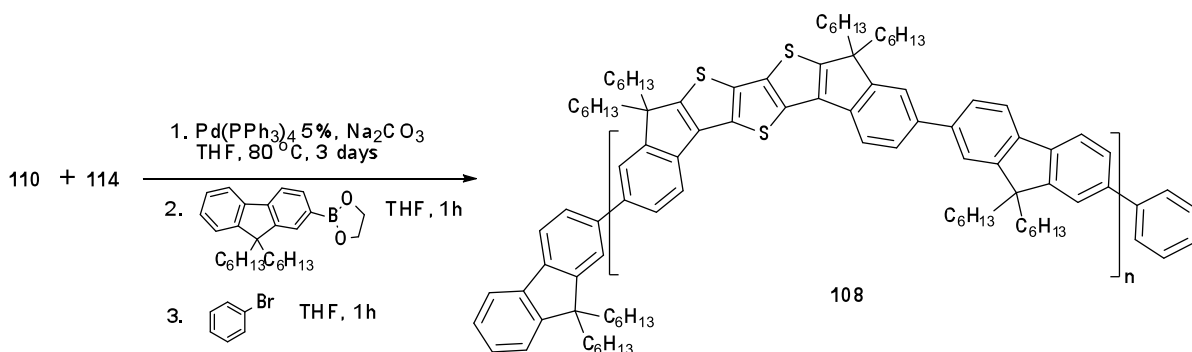
Scheme 38. Synthesis of **108** *via* Suzuki polymerisation

Standard work-up including Soxhlet extraction afforded the polymer **108** in 83% yield. The GPC results were recorded as: M$_w$ 10,931 g mol^{-1}, M$_n$ 4,976 g mol^{-1}, PDI 2.2.

The polydispersity of this material was found to be 2.2, which showed good uniformity of the obtained material, but the low molecular weight suggested that the process resulted in formation of longer oligomers rather than polymers.

There are many factors that can affect Suzuki-type cross-coupling and it is not possible to define which one of them had the most significant influence without a more detailed evaluation. However, the potency/freshness of the catalyst, stoichiometry of the monomers and efficient maintenance of the oxygen–free environment are rather vital factors and each one or a combination of these could be the cause in this particular case.

On the other hand, the bulkiness of the growing chain should also be taken into account. Both DITT and fluorene units are bearing long alkyl chains, which could potentially influence the rate and extent of the polymerisation. With this in mind, a

prolonged reaction time could result in a better outcome. Also, a higher boiling point solvent, such as toluene, would allow for polymerisation at more elevated temperatures.

3.2.5. Synthesis of Polymer 109

Within the series of DITT-based polymers, this material was obtained *via* another Suzuki cross-coupling polymerisation of **110** and **117** as illustrated in Scheme 39.
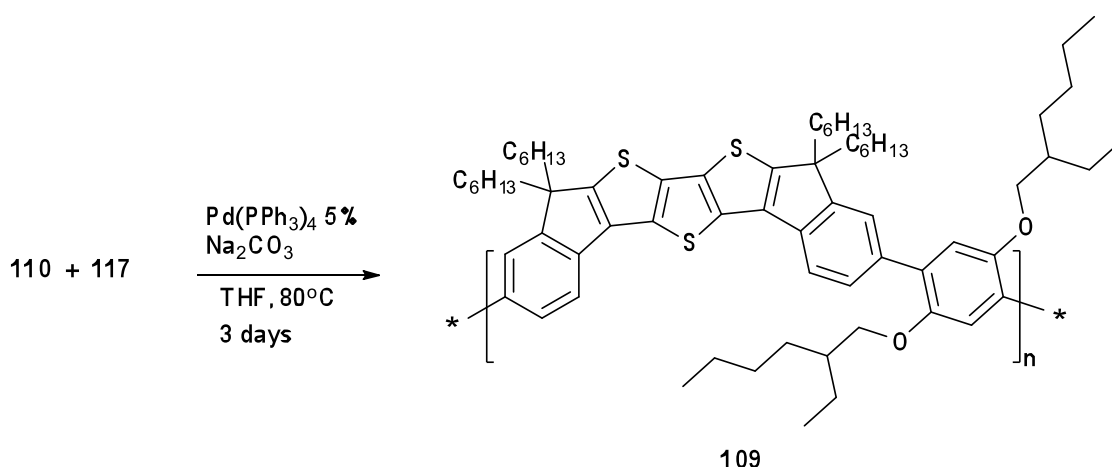
Scheme 39. Synthesis of polymer **109**

Suzuki polymerisation was performed according to the conventional procedure with 5 mol% amount of the $Pd(PPh_3)_4$. The end-capping procedure was not carried out. When the reaction time elapsed, the mixture was subjected to the standard work-up procedure, yielding 83% of the material. Analysis by GPC gave the following data: M_w 11,017 g mol^{-1}, M_n 1,310 g mol^{-1}, PDI 8.0.

The low molecular weight and high polydispersity of the material obtained are symptomatic of a non-optimised polymerisation and formation of shorter chains. The ^{1}H NMR showed broadened but clear signals in the aromatic and aliphatic regions.

Indeed, usage of the (di)boronic acids can occasionally be rather unreliable, due to their known instability towards dehydration and formation of condensation products. During the polymerisation, this may well cause stoichiometric chaos and hence, an

unsatisfactory outcome. However, monomer **117** could be considered more stable towards possible dehydration, owing to lower accessibility of the boronic centres, hindered by long and branched alkyl chains in the *ortho* positions.

At the same time, this type of substitution could slow down the polymerisation process as well, since the reactive sites, *i.e.*, the boronic groups of the monomer **117**, were sterically hindered and complicated the transmetallation step. In turn, this obstacle most likely led to a dramatic decrease of the polymerisation rate and disruptions of the polymer chain growth. As a result, the molecular weight of the isolated product (**109**) was low and was accompanied by a high polydispersity index.

In an attempt to optimise the reaction conditions, the polymerisation was repeated using toluene as the solvent and the temperature was increased to 90ºC. However, it resulted in very poor yield (3–4%) of heavier molecular weight fractions, presumably dominated by the build-up of the oligomers. Thus, it can be proposed that this kind of monomer is not very suitable to be used in cross-coupling polymerisations, despite its increased stability.

Regardless of the fact that the molecular weight characteristics of polymer **109** were not remarkably good, its electrochemical and optical properties were also investigated.

3.2.6. Summary and Conclusions

Four polymers, containing the DITT-core were synthesised either by Yamamoto homopolymerisation (**106** and **107**) or by Suzuki cross-coupling polymerisation (**108** and **109**). Table 5 summarises the methods of their preparation and molecular average data, acquired by GPC.

Table 5. Summary of preparation methods and GPC results of polymers **106-109**

Polymer	Method/Catalyst, amount	Yield, %	M_w, g mol^{-1}	PDI
106	(μW) Yamamoto/Ni(COD)$_2$, 2 eqv.	51	92,449	5.3
107	Yamamoto/Ni(COD)$_2$, 1.3 eqv.	51	66,890	1.1
108	Suzuki / Pd(PPh$_3$)$_4$, 5 mol%	83	10,931	2.2
109	Suzuki / Pd(PPh$_3$)$_4$, 5 mol%	83	11,017	8.0

A few conclusions regarding the synthesis of these four materials can be made. It is clear, that the polymerisation of DITT-based blocks alone and in combination with other units is not straightforward and requires further investigation and optimisation. Yamamoto polymerisation, in practice, showed better results using the conventional protocol and this was, to a large degree, attributed to the instability of the zerovalent Ni-complex, further aggravated by microwave irradiation. The conventional protocol can be generally quite successful with DITT-based systems, including sulfones, with appropriate control of catalyst amounts and oxygen-free conditions.

The synthesis of the bulky polymer **108** and the sterically unfavourable material **109** by Suzuki cross-coupling polymerisation pose a certain synthetic challenge towards the production of high molecular weight materials. Optimisation of these syntheses can be directed towards the use of other solvents and possibly, addition of less sterically demanding catalysts/ligands.

REFERENCES

1. Cheng, Y.-J.; Yang, S.-H.; Hsu, C.-S., *Chem. Rev.* **2009,** *109*, 5868-5923.

2. Bao, Z.; Chan, W. K.; Yu, L., *J. Am. Chem. Soc.* **1995,** *117*, 12426-12435.

3. Sakamoto, J.; Rehahn, M.; Wegner, G.; Schlüter, A. D., *Macromol. Rapid Commun.* **2009,** *30*, 653-687.

4. Graupner, W.; Leditzky, G.; Leising, G.; Sherf, U., *Physical Review B* **1996,** *54*, 7610-7613.

5. Grimsdale, A. C.; Chan, K. L.; Martin, R. E.; Jokisz, P. G.; Holmes, A. B., *Chem. Rev.* **2009,** *109*, 897-1091.

6. Perepichka, I. F.; Perepichka, D. F., *"Handbook of Thiophene-based Materials: Applications in Ogranic Electronics and Photonics"*. Wiley: 2009; Vol. One: Synthesis and Theory.

7. Zhang, S.; Guo, Y.; Fan, H.; Liu, Y.; Chen, H.-Y.; Yang, G.; Zhan, X.; Liu, Y.; Li, Y.; Yang, Y., *J. Polym. Sci. A* **2009,** *47*, 5498-5508.

8. Zhan, X.; Tan, Z.; Domarcq, B.; An, Z.; Zhang, X.; Barlow, S.; Li, Y.; Zhu, D.; Kippelen, B.; Marder, S. R., *J. Am. Chem. Soc.* **2007,** *129*, 7246-7247.

9. Tierney, S.; Heeney, M.; McCulloch, I., *Synth. Met.* **2005,** *148*, 195-198.

10. Paek, S.; Lee, J.; Lim, H. S.; Lim, J.; Lee, J. Y.; Lee, C., *Synth. Met.* **2010,** *160*, 2273-2280.

11. Murage, J.; Eddy, J. W.; Zimbalist, J. R.; McIntyre, T. B.; Wagner, Z. R.; Goodson, F. E., *Macromol.* **2008,** *41*, 7330-7338.

12. Nehls, B. S.; Füldner, S.; Preis, E.; Farrell, T.; Scherf, U., *Macromol.* **2005,** *38*, 687-694.

13. Galbrecht, F.; Bünnagel, T. W.; Scherf, U.; Farrell, T., *Macromol. Rapid Commun.* **2007,** *28*, 387-394.

14. Kandre, R.; Schlüter, A. D., *Macromol. Rapid Commun.* **2008,** *29*, 1661-1665.

15. Fujihara, T.; Yoshida, S.; Terao, J.; Tsuji, Y., *Org. Lett.* **2009,** *11*, 2121-2124.

16. Allard, S.; Forster, M.; Souharce, B.; Thiem, H.; Scherf, U., *Angew. Chem. Int. Ed.* **2008,** *47*, 4070-4098.

17. Miyakoshi, R.; Yakoyama, A.; Yokozawa, T., *J. Polym. Sci. Part A: Polym. Chem.* **2008,** *49*, 753-765.

18. Babudri, F.; Colanguili, D.; Farinola, G. M.; Naso, F., *Eur. J. Org. Chem.* **2002**, 2785-2791.

19. Babudri, F.; Farinola, G. M.; Naso, F., *J. Mater. Chem.* **2004,** *14*, 11-34.

20. Loewe, R. S.; Ewbank, P. C.; Liu, J.; Zhai, L.; McCullough, R. D., *Macromol.* **2001,** *34*, 4324-4333.

21. Perepichka, I. F.; Perepichka, D. F.; Meng, H.; Wudl, F., *Adv. Mater.* **2005,** *17*, 2281.

22. McCullough, R. D.; Lowe, R. D.; Jayaraman, M.; Anderson, D. L., *J. Org. Chem* **1993,** *58*, 904-912.

23. Chen, T.-A.; Wu, X.; Rieke, R. D., *J. Am. Chem. Soc.* **1995,** *117*, 233-244.

24. Saito, F.; Takeoka, Y.; Rukikawa, M.; Sanui, K., *Synth. Met.* **2005,** *153*, 125-128.

25. Coppo, P.; Cupertino, D. C.; Yeates, S. G.; Turner, M. L., *Macromol.* **2003,** *36*, 2705-2711.

26. Li, J.; Rajca, A.; Rajca, S., *Synth. Met.* **2003,** *137*, 1507-1508.

27. Yamamoto, T.; Morita, A.; Miyazaki, Y.; Maruyama, T.; Wakayama, H.; Zhou, Z.-h.; Nakamura, Y.; Kanbara, T.; Sasaki, S.; Kubota, K., *Macromol.* **1992,** *25*, 1214-1223.

28. Scherf, U.; List, E. J. W., *Adv. Mater.* **2002,** *14*, 477-486.

29. Yamamoto, T., *Macromol. Rapid Commun.* **2002,** *23*, 583-606.

30. Horsburgh, L. E.; Monkman, A. P.; Samuel, I. D. W., *Synth. Met.* **1999,** *101*, 113-114.

31. Yamamoto, T.; Fujiwara, Y.; Fukumoto, H.; Nakamura, Y.; Koshihara, S. Y.; Ishikawa, T., *Polymer* **2003,** *44* (4487-4490).

32. Cai, T.; Zhou, Y.; Wang, E.; Hellström, S.; Zhang, F.; Xu, S.; Inganäs, O.; Andersson, M. R., *Solar Energy Materials & Solar Cells* **2010,** *94*, 1275-1281.

33. Li, X.-G.; Liu, Y.-W.; Huang, M.-R.; Peng, S.; Gong, L.-Z.; Moloney, M. G., *Chem. Eur. J.* **2010,** *16*, 4803-4813.

34. Takagi, K.; Sugimoto, S.; Mitamura, M.; Yuki, Y.; Matsuoka, S.-i.; Suzuki, M., *Synth. Met.* **2009,** *159*, 228-233.

35. Andersson, M. R.; Selse, D.; Berggern, M.; Järvinen, H.; Hjertberg, T.; Inganäs, O.; Wennerstöm, O.; Österholm, J.-E., *Macromol.* **1994,** *27*, 6503-6506.

36. Roncali, J., *Chem. Rev.* **1992,** *92*, 711-738.

37.   Sadki, S.; Schottland, P.; Brodie, N.; Sabouraud, G., *Chem. Soc. Rev.* **2000,** *29*, 283-293.

38.   Kenning, D. D.; Rasmussen, S. C., *Macromol.* **2003,** *36*, 6298-6299.

39.   Kodomari, M.; Satoh, H.; Yoshitomi, S., *J. Org. Chem.* **1988,** *53*, 2093-2094.

40.   Perepichka, I. I.; Perepichka, I. F.; Bryce, M. R.; Pålsson, L.-O., *Chem. Commun.* **2005**, 3397-3399.

41.   Monkman, A. P.; Pålsson, L.-O.; Higgins, R. W. T.; Wang, C.; Bryce, M. R.; Batsanov, A. S.; Howard, J. A. K., *J. Am. Chem. Soc.* **2002,** *124*, 6049-6055.

42.   Rose, A.; Zhu, Z.; Madigan, C. F.; Swager, T. M.; Bulovic, V., *Nature* **2005,** *434*, 876-879.

CHAPTER 4

CHAPTER 4

PROPERTIES OF DITT-BASED POLYMERS 106-109

The DITT-based small molecules (**77-79**) are novel compounds and there are no available data for polymeric materials containing these units. Polymer **106** is comprised of the soluble monomer **78**, broadens the subject of DITT-based materials and therefore poses a certain degree of interest as a novel polymeric material.

Also, there are a limited number of reports with reference to DTT-based polymers and copolymers. Some of these were mentioned in Chapter 1 (section 1.5.4) and their main application was in photovoltaics. Thus, to the best of my knowledge, there are no reports on DTT copolymers, accommodating either 9,9-substituted fluorenes or alkyloxy-phenylene units. Polymers based on these two are widely known PPP-type materials and represent two of the most important and actively researched groups, possessing optical properties that can be utilised in light-emitting devices such as PLEDs.[1,2]

Monomer 1,4-bis((2-ethylhexyl)oxy)benzene, that was utilised for the preparation of polymer **109**, contains branched alkyloxy substituents. These groups on the benzene ring have multiple functions: (a) they increase the solubility of otherwise insoluble pristine *para*-phenylene polymer and longer branched chains have more effect *versus* the unbranched analogues, (b) they lower the glass transition temperature and (c) they red-shift the absorption and emission maxima. Regarding the emission characteristics, unsubstituted PPP films absorb and emit in the ultra-violet region (~300 nm and ~375 nm, respectively), which is not suitable for the fabrication of stable PLEDs.[1] Substitution of the benzene ring with alkyloxy chains red-shifts the emission to some extent (depending on the degree of substitution within the polymer chain) but not sufficiently to cross the minimum for human eye perception.[2] Thus, substantial effort was put into altering the emission wavelength through copolymerisation with numerous derivatives and phenylene monomers bearing alkyloxy chains (mostly in *para*-positions) are rather common solubilising and red-shifting representatives.[2-3]

Methylene linkages between the flexible phenylene units give a higher degree of planarisation in PPPs (*i.e.*, effective conjugation) and make a class of LPPP-polymers. Polyfluorene (PF) belongs to the variety of PPP in which the methylene bridging occurs between every second pair of benzene rings. PFs are valued for their hole-transporting properties and bright blue emission in the visible region (~430 nm), which makes them highly suitable for applications in light-emitting devices[2] and solar cells.[4] The continuous research and investigations of fluorene-containing polymers are mainly directed towards overcoming the difficulties associated with the blue emitters, such as colour instability due to the formation of defects and subsequent quenching of the blue emission.[2] Manipulation of the rather wide optical band gap (~3 eV) of PFs is another interesting pursuit for both light-emitting and light-harvesting purposes.

The appearance of emission bands in the green/yellow region, unacceptable for optimal device operation, is the common problem with these promising materials and it was discovered that the build-up of fluorenone defects is responsible for this.[1-2] Formation of fluorenone can potentially occur at the stages from synthesis to device fabrication and operation, by oxygen contamination. Additionally, the problem of aggregation is enhanced in conjunction with this defect. The most effective approach to combat these two issues is therefore substitution of both methylene protons to hinder the reactivity through the linkage. Various alkyl, alkyloxy and aryl substituents have been introduced in the 9-positions of fluorene.[2] One of the first and widely known substituted fluorene bears two hexyl chains in the 9-position – 9,9-dihexylfluorene. A homopolymer of this monomer exhibits a well-resolved vibronic emission spectrum with a slight blue-shift of the emission maximum to *ca*. 420 nm.[5]

Copolymerisation, often *via* Suzuki cross-coupling polymerisation,[3] dilutes the fluorene content and helps to decrease the problem of defect formation. Additionally, copolymerisation offers the possibilities to manipulate the emission wavelength and to alter the band gap of the polymer. This aspect is particularly interesting when introducing heterocyclic monomers as the resulting optoelectronic characteristics are often intermediate of what both repeat units have to offer. It should also be noted that the human eye is not very sensitive to the emission from pristine PF and a red-shift of up to 50 nm is a rather valuable visual improvement.[1] Consequently, there are ample

reports on the subject of copolymers bearing 9,9-substituted fluorene units.[2] In this work the 9,9-dihexylfluorene comonomer was used to synthesise polymer **108** and then investigate the property changes in relation to the homopolymer of TH-DITT (**106**).

Regarding the oxidation of the thiophene sulfur atom to a sulfone functionality, an extensive work by Barbarella *et al.*[6] showed the strong dependence of optical properties on the degree of torsional restriction within the thiophene backbone of the material. The group investigated a range of both linked[7] and fused thiophene-based[8,9,10] structures. However, to the best of my knowledge, there are no reported polymers comprised solely of DTT-units, bearing a central *S,S*-dioxy group. Nonetheless, polymer **107** presented in this work is one such polymer and its properties will be discussed in the sections below. Regarding copolymers containing the DTT sulfone derivative, only one report presenting an alternating copolymer with 3-alkylthiophene was found.[11]

Synthetic routes to polymers **106-109** were discussed in Chapter 3. The four polymers were further characterised in terms of their optical properties, electrochemical behaviour, thermal stability and physical attributes. These results will be presented and discussed in the sections of this Chapter.

4.1. Optical Properties (Absorption and Emission)

The solution UV-visible absorption and emission spectra of polymers **106-109** were recorded in chloroform and the former are presented in Figure 21 together with the absorption spectrum of compound **78** for better visualisation of the main spectral features.
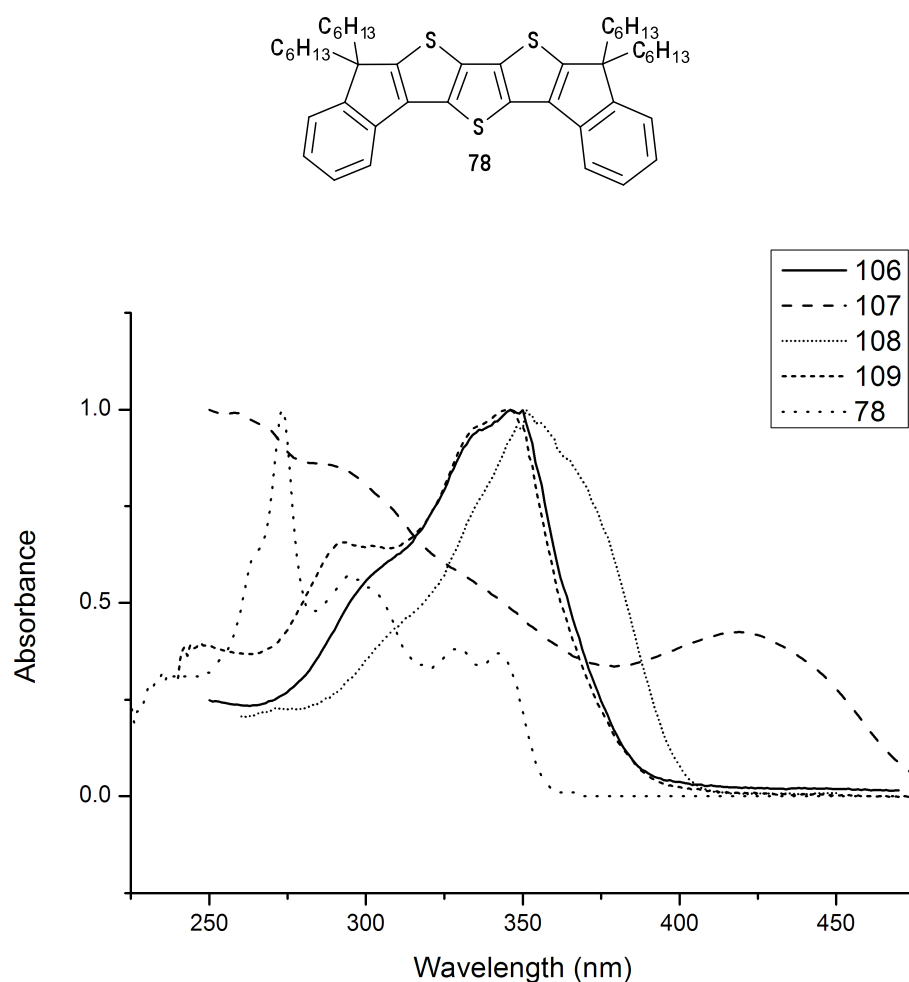
Figure 21. Absorption spectra of polymers **106-109** and monomer **78** in chloroform solution

Thin films of the polymers were prepared on silica substrates by spin-coating from concentrated (15 mg/ml) chloroform solutions and their solid-state absorption and emission properties were also studied. The complete set of optical data obtained for the four polymers is summarised in Table 6 and the spectra are presented for each polymer separately in Figures 22-25 below.

Table 6. Optical data of polymers **106-109**

	$\lambda_{abs,\ max}$ / nm	Optical $E_g{}^b$ / eV	$\lambda_{em,\ max}$ / nm	PLQY^d (solution)	PLQY^d (film)
106	346 (334)^a	3.20 (388 nm)	413 (406)^c	0.20	0.05
107	423 (419)^a	2.58 (480 nm)	529 (523)^c	0.04	0.07
108	351 (351)^a	3.09 (401 nm)	406 (406)^c	0.49	0.04
109	345 (336)^a	3.19 (389 nm)	409 (418)^c	0.32	0.03

^{a}Absorption maxima of films (nm). ^{b}Optical band gaps determined from the onset of the highest wavelength absorption band by $E_g = hc/\lambda_{onset}$ and given in eV. ^{c}Emission maxima of films (nm). ^{d}Photoluminescence quantum yield.

Polymer **106** showed a broad absorption maximum at 346 nm in chloroform solution and it was red-shifted by 73 nm in comparison with the monomer **78** (Figure 21). This red-shift indicates an increase in the effective conjugation within the polymer backbone. The onset of the polymer absorption edge (388 nm) gave an optical band gap of 3.20 eV, which was lower than the optical HOMO-LUMO gap of the monomer **78** (3.40 eV). The emission spectrum (Figure 22) of the dilute chloroform solution of **106** showed a maximum at 413 nm, which is also red-shifted (by 37 nm) in comparison with the monomer ($\lambda_{em,\ max}$ = 376 nm for **78**). A low intensity peak at shorter wavelength (387 nm) corresponds to a vibronic relaxation as the result of the presence of higher energy excited states (excitons).

A thin film of polymer **106** showed a small blue-shift (12 nm) and further broadening of the entire absorption band and the peak in comparison to its solution spectrum, but otherwise was of the same behaviour as illustrated in Figure 22. The emission spectrum of the thin-film appeared similar to the solution state spectrum, with a vibronic peak at 387 nm and a 7 nm blue-shift of the maximum ($\lambda_{em,\ max}$ = 406 nm). At longer wavelengths, the spectrum was broadened with a rough structure, possibly indicating the formation of aggregates.

The blue-shifts in absorption/emission in the solid state and the vibronic peaks are rather characteristic of more planar polymers, such as LPPPs or PFs,[1] and confirms the structural features (planarity) of the novel polymer **106**.
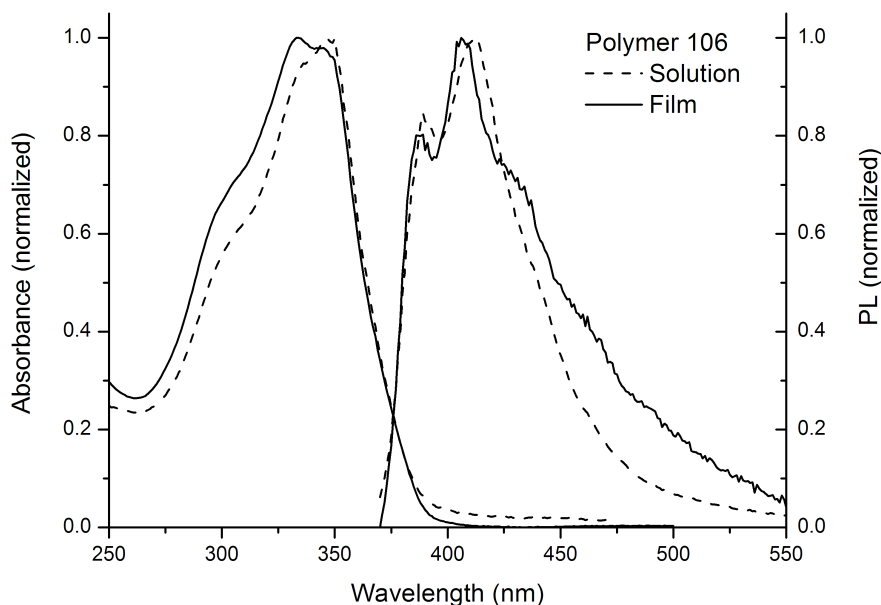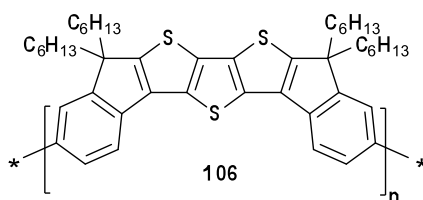
Figure 22. Absorption and emission (λ_{exc} = 360 nm) spectra of polymer **106**

The increase in conjugation through polymerisation, evident from both absorption and emission spectra, was clearly beneficial for the optical properties of this material, since the molecular compound **78** had a very poor PLQY in solution (0.004) and no emission was recorded for its films. The higher PL efficiency (or PLQY) values for both solution state and thin-film samples of the polymer **106** (0.20 and 0.05, respectively) suggest more efficient radiative dissipation of energy in the excited states, facilitated by the increased ability to delocalise these charged species within the polymeric network. However, despite the notable improvements, the solution PLQY was still in a rather moderate range and in the solid state the emission was quenched to only 5%, most likely due to aggregation (formation of close interchain interactions in the ground state), which is known to cause a dramatic decrease in PL efficiencies.[12]

Co-polymerisation of **78** with 9,9-dihexylfluorene units (**114**) caused some difference in the absorption pattern of the resulting polymer **108** in comparison with the homopolymer **106**. The solution absorption band of **108** appeared broad and extended

over longer wavelengths. However, its rather sharp maximum emerged at 351 nm (Figure 21), which was only a 5 nm bathochromic shift from that of **106** and blue-shifted by *ca*. 35 nm if compared with poly(9,9-dihexylfluorene).[5] The optical band gap of 3.09 eV, estimated from the onset of the absorption edge, was therefore expectedly wider than for poly(9,9-dihexylfluorene) (~2.91 eV). At the same time, the fluorene influence is noticeable since the optical band gap of the DITT homopolymer **106** is even wider (opt. E_g = 3.20 eV). However, the band gaps of these three polymers are roughly of the same order.

Polymer **108** showed almost the same absorption trend in thin film form, with only minor broadening of the absorption band ($\lambda_{abs, max}$ = 351 nm) in comparison with its solution spectrum (Figure 23).
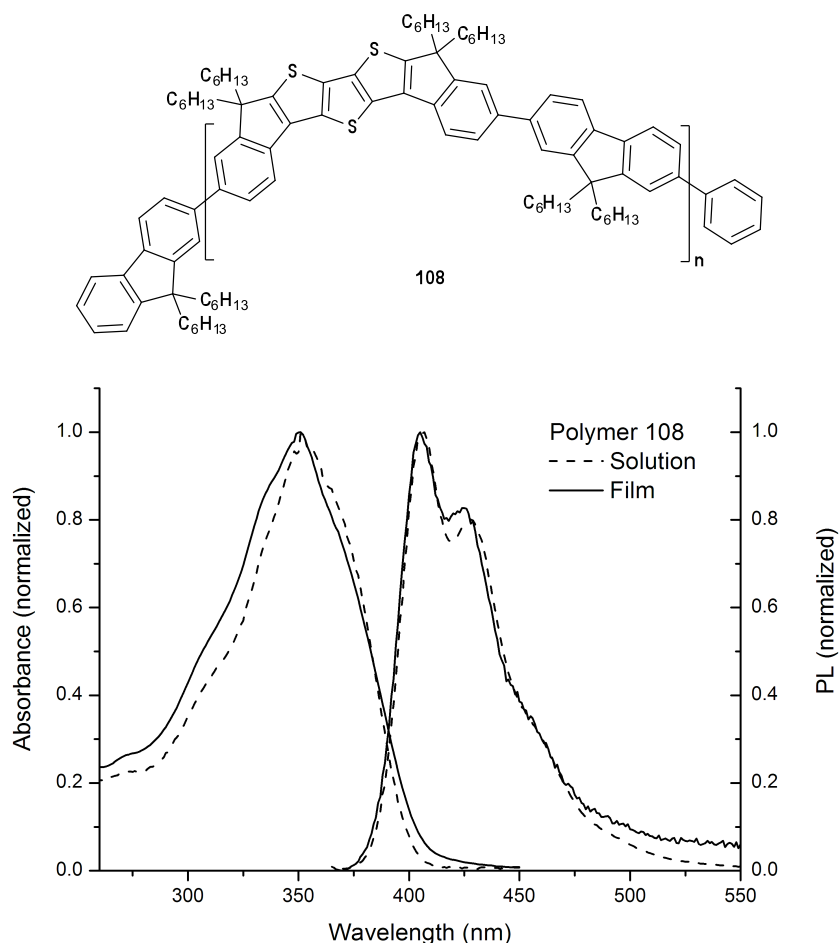
Figure 23. Absorption and emission (λ_{exc}= 360 nm) spectra of polymer **108**

Both solution and thin-film emission spectra of polymer **108** exhibited vibronic structures with a low intensity peak at *ca.* 425 nm in solution and 429 nm as a film, a recognisable feature, caused by the fluorene units.[1] The recorded maxima at 406 nm were comparable with the emission patterns observed for the homopolymer **106**, which also means a blue-shift from the reference poly(9,9-dihexylfluorene) maxima of *ca.* 420 nm (for solution state and thin-film).[5] This suggests that the radiative process involves higher energy excitons and then mainly originates at the TH-DITT sites.

The thin-film emission band of **108** closely resembled its solution spectrum and was only slightly broadened in the longer wavelength region. At the same time, the absence of resolved emission bands in the green or yellow regions was a sign of a certain degree of colour stabilisation and freedom from the fluorenone-defect. Endcapping, carried out at the synthesis stage, could also have played a positive role in suppressing the defect formation.

The solution PL efficiency of **108** was significantly higher (0.49) than that of the polymer **106**, solely consisting of the DITT-units (0.20), indicating that the inclusion of fluorene units into the polymer chain induced higher rates of exciton relaxation through radiative pathways. For comparison, 9,9-dihexylfluorene homopolymer has a PLQY of 0.58 and the value obtained for the new polymer (**108**) can be considered to be quite similar.

Although it is not evident from the Figure 23, the solid state emission suffered from quenching, most likely caused by the formation of aggregates, and showed a greater than 12-fold decrease in the PLQY (to 0.04). However, it should be noted that aggregates form presumably due to the increased tendency of the TH-DITT blocks to interact through strong interchain contacts, rather than through the fluorenone defect, which is apparent from the observed stable blue emission.

Further examination of changes in the optical properties, induced by other comonomers, was performed with polymer **109**, accommodating both TH-DITT and 1,4-bis((2-ethylhexyl)oxy)benzene units. The solution absorption spectrum (Figure 21) was closely related to that of **106**, including the maximum detected at 345 nm. The

absorption shoulder at shorter wavelength (292 nm) was even more pronounced (than what was seen for **106**), indicating that the UV-light promoted excitation was to a large degree focused around the TH-DITT core, masking a less intense contribution from the 1,4-bis((2-ethylhexyl)oxy)benzene units in approximately the same region. This pattern could be expected, bearing in mind the high polydispersity index of this low molecular weight material (**109**) and, hence, possibly higher inherent content of DITT *versus* 1,4-bis((2-ethylhexyl)oxy)benzene units.

The optical band gap of **109** was estimated to be 3.19 eV and could be considered the same within the margins of the band gap that was calculated for **106**, suggesting that the incorporation of the benzo-comonomer did not change the absorption characteristics in any significant way. On the other hand, it is not entirely unexpected since both comonomers absorb light at roughly the same energies.[2]

The solid-state absorption spectrum of **109** (Figure 24) showed a small blue-shift (9 nm), minor broadening of the absorption maximum peak and increased intensity of the higher energy shoulder, but otherwise had the same pattern as the solution state spectrum.

Emission of the solution peaked in the "short" blue region, at 409 nm, which was consistent with expectations and close to the maxima observed for **106** and **108**. In contrast, no resolved vibronic structure of the emission spectrum of **109** was detected probably due to some loss of planarity, accompanied by the insertion of the alkyloxy-phenylene units. The same tendency was observed for the solid-state emission, which possessed a rough structure and broadening in the longer wavelengths region. It should be mentioned that PPPs commonly do not show vibronic spectra as the result of large torsion angles between the monomers within the polymer chain.[1]

109
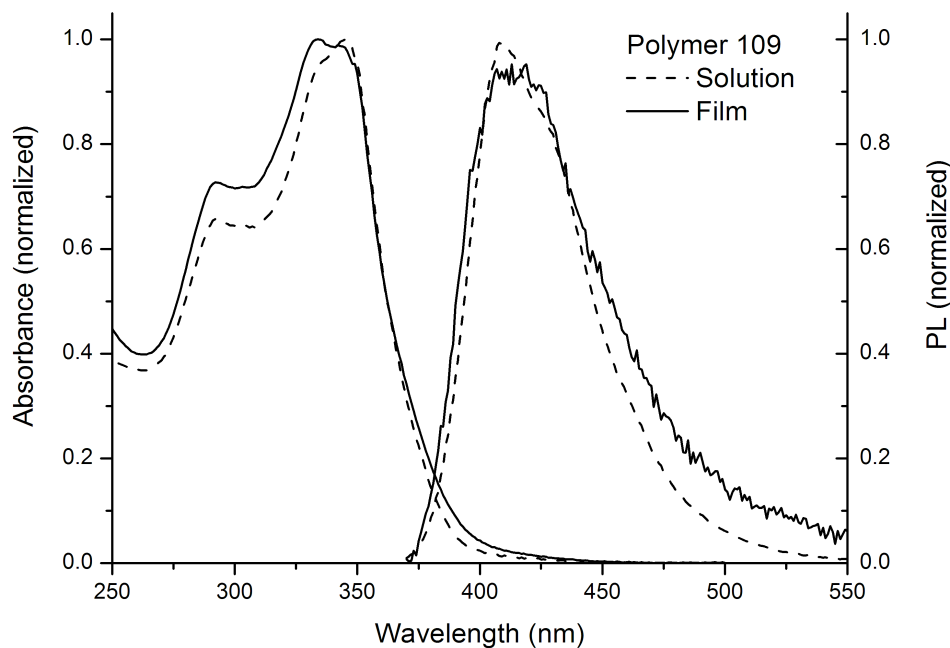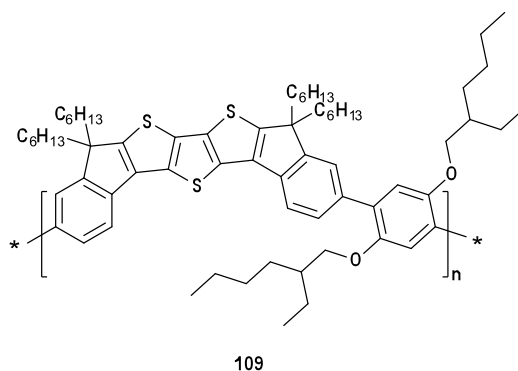
Figure 24. Absorption and emission (λ_{exc}= 360 nm) spectra of polymer **109**

The contribution of the benzo-units was also reflected in the increased solution PLQY (to 0.32) *versus* the homopolymer **106**. However, it was notably lower than that observed with the fluorene-containing **108** and could be attributed to structural effects most likely caused by the steric demands of the substituted phenylene-comonomer and leading to a decrease in radiative decay.

In analogy with **106** and **108**, the solid state emission was also affected by the formation of ground state aggregates and consequently seen as a dramatic decrease of PL efficiency to only 3% (0.03).

The sulfone-based polymer **107** is a somewhat different material in relation to the other three polymers, taking into account that its monomer **79** had lost the aromaticity of the inner fused thiophene core as the result of the sulfone group insertion. Hence, its optical properties demonstrated significant differences as well. More precisely, **107** had a broad solution absorption band over the region of 250-475 nm. The absorption peak at 423 nm was similar to its monomer (**79**) absorption behaviour and the red-shift of the polymer's absorption maximum was almost negligible (4 nm). This observation indicates that there is no conjugation between the DITT repeat units within the polymer chains of **107** and the effective conjugation length, otherwise reflected in significant red-shifts of the absorption maxima, is therefore very limited.

A solvatochromic study of the monomer (Chapter 2) had previously revealed that its absorption peak at 419 nm could be attributed to the intramolecular charge transfer (ICT). It was therefore reasonable to propose that the absorption maximum of the polymer at 423 nm had the same origin, which expectedly brought the optically determined band gap of **107** to almost the same value as that of its monomer **79** (2.58 eV and 2.60 eV, respectively).

The thin-film absorption spectrum of **107** exhibited marginal differences from the solution data as illustrated in Figure 25.
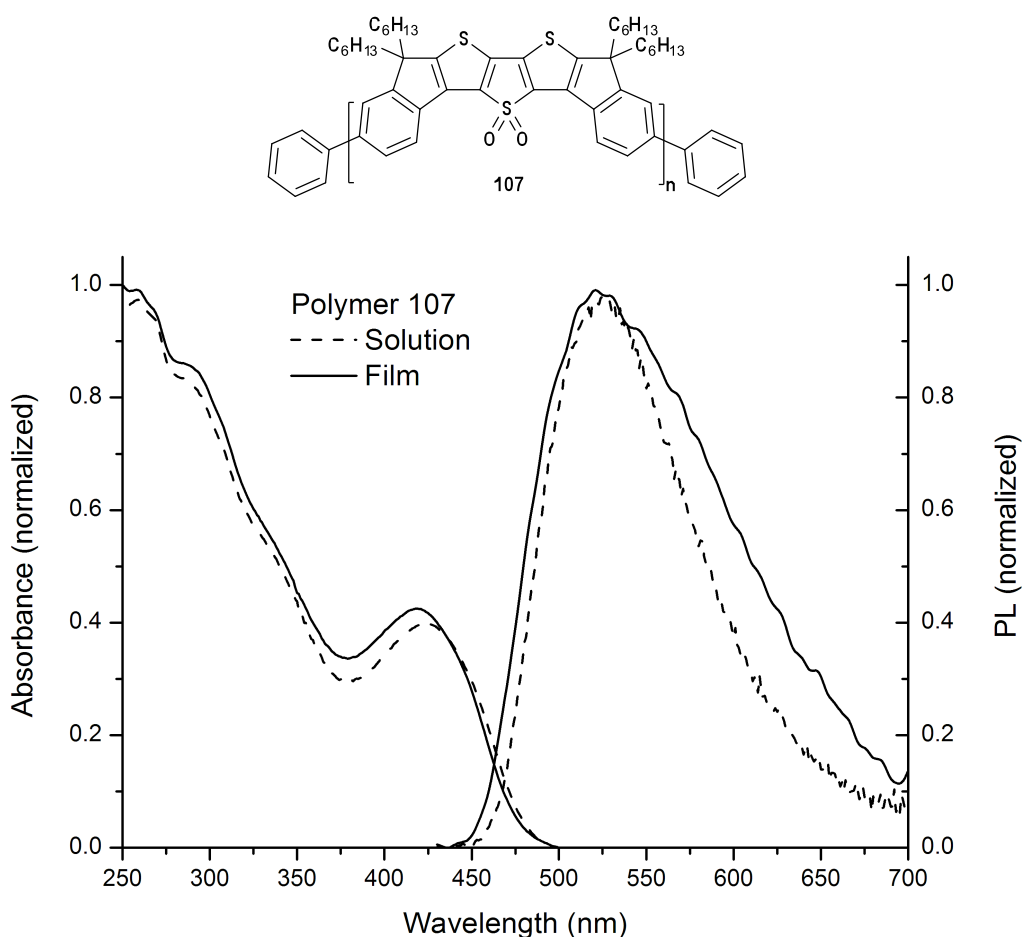
Figure 25. Absorption and emission (λ_{exc}= 360 nm) spectra of polymer **107**

The emission spectra of both solution state and thin-film samples showed peaks at the same wavelength ($\lambda_{em,max}$ = 523 nm) and also matched the emission maxima of the monomer **79** ($\lambda_{em,max}$ = 524 nm). These results demonstrated that despite the fact that absorption of light in **107** occurs over a broad region, the radiative relaxation process mainly takes the path through the *S,S*-dioxy dithienothiophene core, in very much the same way as it has been shown for analogous molecular materials.[8]

However, the emission intensity was unexpectedly weak, both in solution and film, reflected by the low PLQY values, which were estimated to be 0.04 and 0.07 in solution and solid state, respectively. This could probably be due to fast relaxation of the excited fragments through vibrational or rotational (non-radiative) pathways, rather than *via* the generation of visible emission.

Low PL efficiencies in the solid state had already been witnessed for TH-DITT-based polymers, assigned to efficient interchain interactions that led to the formation of aggregates or excimers, which are known to reduce PLQYs. Accompanying S···O and C···O interactions, typical for *S,S*-dioxides,[8] could further aggravate this problem. Concerning polymer **107**, these could be particularly disadvantageous for its solutions, in which the polymer chain has increased rotational flexibility and the prevalence of chalcogen interactions could result in twists between repeat units within the chain. In the excited state, these twisted arrangements could further suffer from vibrational motions and eventually lead to extensive quenching of the emission. Thus, the higher PLQY (0.007) observed in the thin-film of **107**, could be attributed to the existence of relatively ordered domains, allowing a certain degree of radiative decay, while its solutions demonstrated widespread quenching of this process. Additionally, the energetic disorder as the result of the intense absorption over a broad region might have contributed to various traps that quench the emission (probably even more in solution).

Furthermore, time resolved measurements confirmed the poor emitting properties of this polymer, showing fast bi-exponential decays in both solution state and thin-film (Figure 26 and Table 7). The radiative emissive states were short lived with average lifetimes of 236 ps and 1.4 ns for solution and film, respectively.
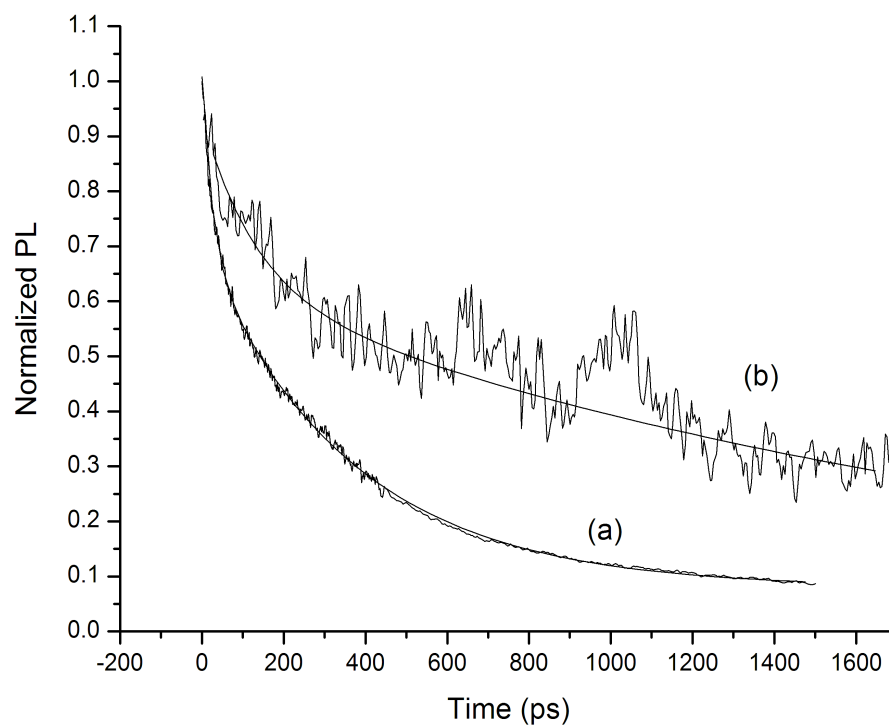
Figure 26. Time resolved decay spectra of **107**: (a) in solution (with fit), at $\lambda_{exc}= 400$ nm; (b) in thin film (with fit), at $\lambda_{exc}= 400$ nm.

Table 7. Results of time resolved spectroscopy for **107** in solution and thin film (obtained from the fitted graphs)

107	$A_1{}^a$	τ_1 (ps)^b	$A_2{}^a$	τ_2 (ps)^b	τ_{av} (ps)^c
Solution	0.31	25.69	0.62	365.40	252.16
Film	0.31	129.27	0.62	2136.15	1467.19

^{a}A$_1$ and A$_2$ are fitted exponentials. ^{b}Fluorescence life time.
^{c}Calculated according to $\tau_{av} = A_1\tau_1 + A_2\tau_2 /(A_1 + A_2)$

It is evident from the above data, that the radiative decay in solution was faster (shorter lifetime) than that of the film, which was also consistent with the observed PLQY values.

4.2. Electrochemical Properties (Cyclic Voltammetry)

The electrochemical properties of the polymers **106–109** were investigated by cyclic voltammetry (CV), using dichloromethane as the solvent; the results are collated in Table 8.

The supporting electrolyte was tetrabutylammonium hexafluorophosphate (0.1 M) and the potentials were referenced against the ferrocene/ferrocenium redox couple. Glassy carbon was used as the working electrode with platinum and silver wires as the counter and pseudo-reference electrodes, respectively. Oxidation and reduction cycles were performed separately to avoid complications in the CV due to possible side-products arising from irreversible and quasi-reversible processes.

The electrochemical HOMO-LUMO gaps (band gaps) were calculated from the differences in the onsets of the first oxidation and reduction peaks. Using data referenced to the ferrocene/ferrocenium redox couple, HOMO and LUMO energies were calculated by subtracting the onsets from the HOMO of ferrocene, which has a known value of –4.8 eV.

Table 8. CV results for **106-109**

	E_{ox} / V	E_{red} / V	HOMO[a] / eV	LUMO[a] / eV	Echem E_g / eV
106	0.72 / 0.56	-2.14^i	-5.29	-3.10	2.31
107	0.54 / 0.52	-2.11^i	-5.27	-2.90	2.37
108	0.71 / 0.63	-2.10^i	-5.37	-2.86	2.51
109	0.80 / 0.65	-2.06^i	-5.40	-2.87	2.52
	$1.05 / 0.88^{qr}$				

[a]HOMO and LUMO values were calculated from the onset of the first peak of the corresponding redox wave and referenced to ferrocene, which has a HOMO of -4.8 eV. [i]Irreversible peak. [qr]Quasi-reversible peak.

Polymer **106** displayed reversible oxidation ($E_{ox}^{1/2}$ = 0.64V) and irreversible reduction peaks (E_{red} = –2.14 V, Table 8 and Figure 27). In comparison with its monomer **78**, the

oxidation potential was almost the same ($E_{ox}^{\frac{1}{2}}$ = 0.68 V for **78**), indicating that the radical cations were localised on the repeat units.
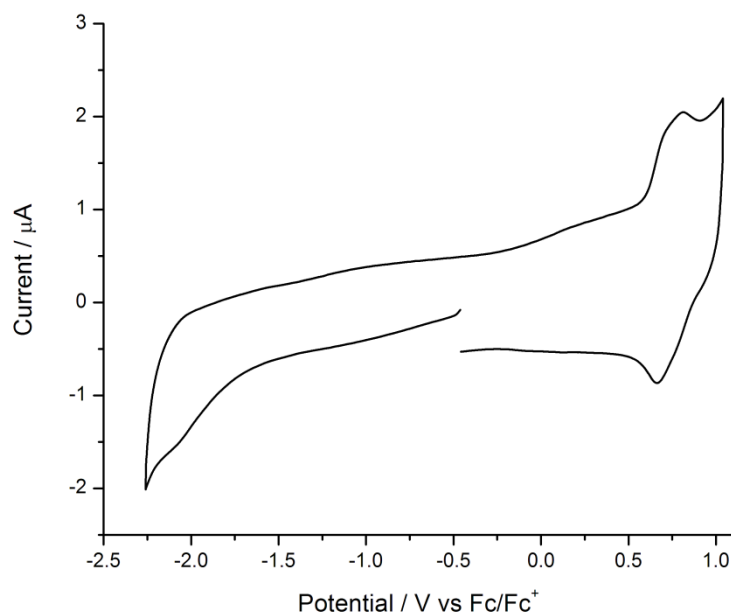
Figure 27. CV of polymer **106**

On the other hand, reduction of **106** occurred at a less negative potential (E_{red} = −2.95 V for **78**), demonstrating some degree of stabilisation through the extended conjugation within the polymer backbone. Consequently, the less negative reduction potential gave a significantly decreased electrochemical band gap of the polymer with the value of 2.31 eV *versus* 3.5 eV for the HOMO-LUMO gap of the monomer. However, taking into consideration the wider optically determined band gap (which indicates the longest conjugation path), it could be concluded that the electrochemical processes are focused in the centre of each unit, where the oxidation occurs through the α-positions of the indene subunits, stabilised by the resonance within one monomer.

Polymer **107** was not readily susceptible to electrochemical processes and gave very weak peaks for both oxidation and reduction as seen in Figure 28. CV with more concentrated solutions did not help to achieve more defined spectra. This may be the result of structural effects, gained with the polymerisation of **79**, which also inflicted dramatic changes in the optical properties of this material.
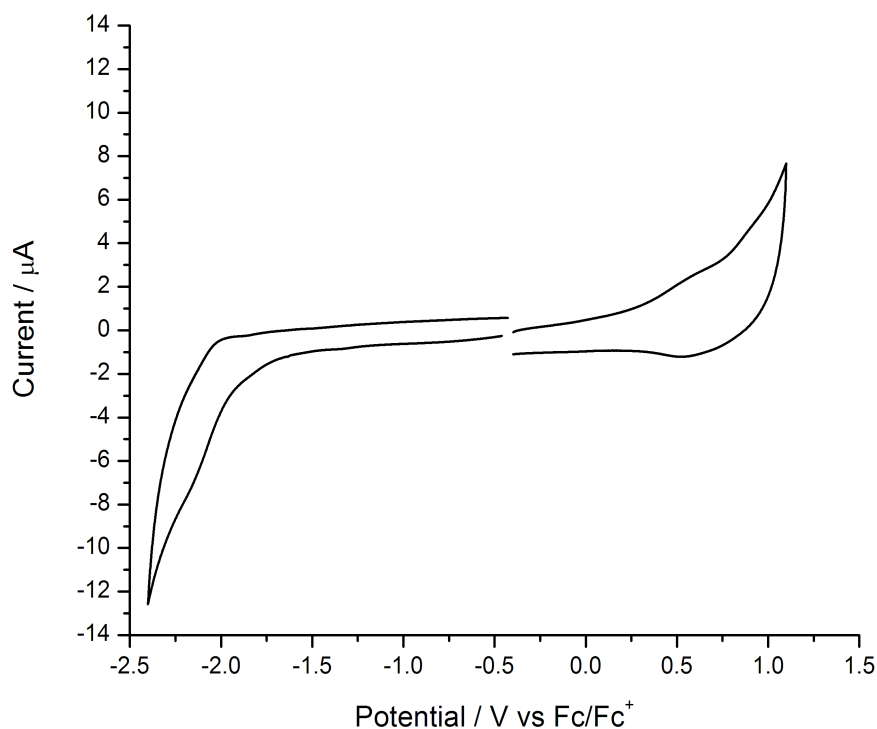
Figure 28. Oxidation and reduction of polymer **107**

Oxidation of **107** was found to be reversible ($E_{\mathrm{ox}}^{1/2} = 0.53$ V) and at lower potentials than its monomer ($E_{\mathrm{ox}}^{1/2} = 1.00$ V for **79**). Such a decrease would be consistent with the increase in effective conjugation within the polymer chains. However, its photophysical characteristics suggest conformational perturbations and, thus, possible deviations in the electrochemical behaviour due to different mechanisms for the distribution of charges. Furthermore, the reduction of **107** was found irreversible ($E_{\mathrm{red}} = -2.11$ V), which contrasted with the reversibility observed in its monomer **79** ($E_{\mathrm{red}}^{1/2} = -1.99$ V). A more negative potential was recorded for the polymer, which demonstrated a greater resistance towards reduction. This observation can additionally support the impression that the electrochemistry of the polymer had little resemblance with what was found for its monomer.

The electrochemical band gap of **107** was calculated from the onsets of oxidation and reduction to 2.37 eV and it was relatively close to the optical estimate of 2.58 eV.

Copolymer **108**, containing alternating TH-DITT (**78**) and 9,9-dihexylfluorene units, showed one reversible oxidation wave ($E_{ox1}^{1/2}$ = 0.67 V) and an irreversible reduction (E_{red} = –2.10 V), as shown in Figure 29. Both oxidation and reduction potentials and their stability were very similar to the electrochemical characteristics of the TH-DITT homopolymer **106**, suggesting that the fluorene units do not participate in these processes.
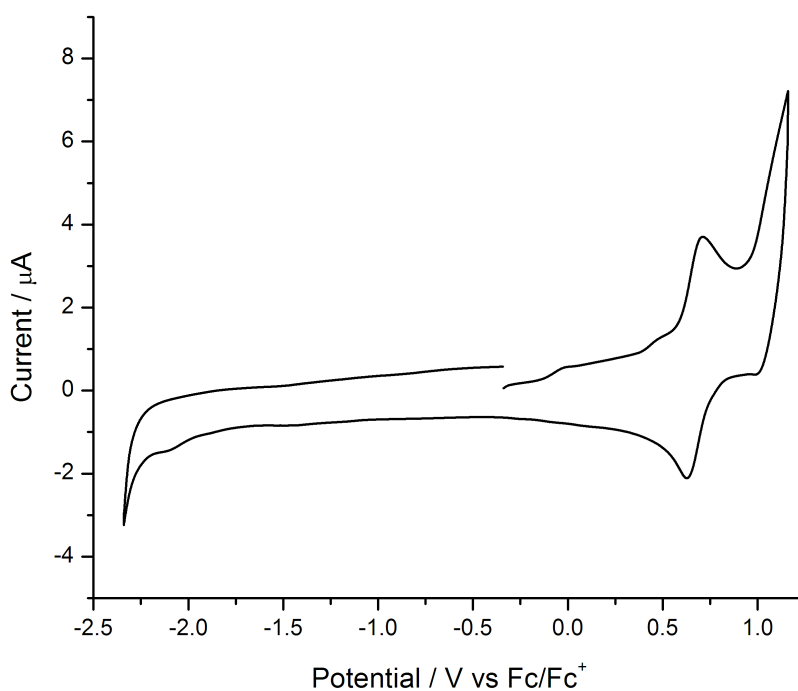
Figure 29. CV of polymer **108**

The oxidation and reduction potentials of the homopolymer poly(9,9-dihexylfluorene) were reported in the literature[5] at 0.81 V and –2.28 V, respectively, giving the HOMO level of –5.61 eV and the LUMO of –2.52 eV. Comparing these figures with the HOMO and LUMO values obtained for copolymer **109** (–5.37 eV and –2.86 eV respectively, Table 8), it is clear that the former was brought higher and the latter was substantially lowered as the result of copolymerisation. These observations are rather useful for the purpose of tuning the HOMO and LUMO levels of PFs.

The electrochemical band gap of **108** was calculated to be 2.51 eV, which is wider than that of **106**, but considerably smaller than what was reported for poly(9,9-dihexylfluorene) (3.09 eV). Taking into account that the optically estimated band gap of **108** was 3.09 eV this could confirm that the electrochemical behaviour of this polymer is dominated by the DITT monomer and the observed change in the optical properties was associated with the inclusion of the 9,9-dihexylfluorene monomers.

The CV of polymer **109** was different from the two other related polymers (**106** and **108**), showing one reversible ($E_{ox1}^{1/2}$ = 0.73 V) and one quasi-reversible ($E_{ox2}^{1/2}$ = 0.97 V) oxidation wave (Figure 30). The former was rather similar to the oxidation pattern of **106** and could be assigned to the oxidation of the DITT monomer. The quasi-reversible wave at higher oxidation potential could be ascribed to the contribution from the 1,4-bis((2-ethylhexyl)oxy)benzene units. This peak was not fully reversible, probably due to an unknown side reaction.
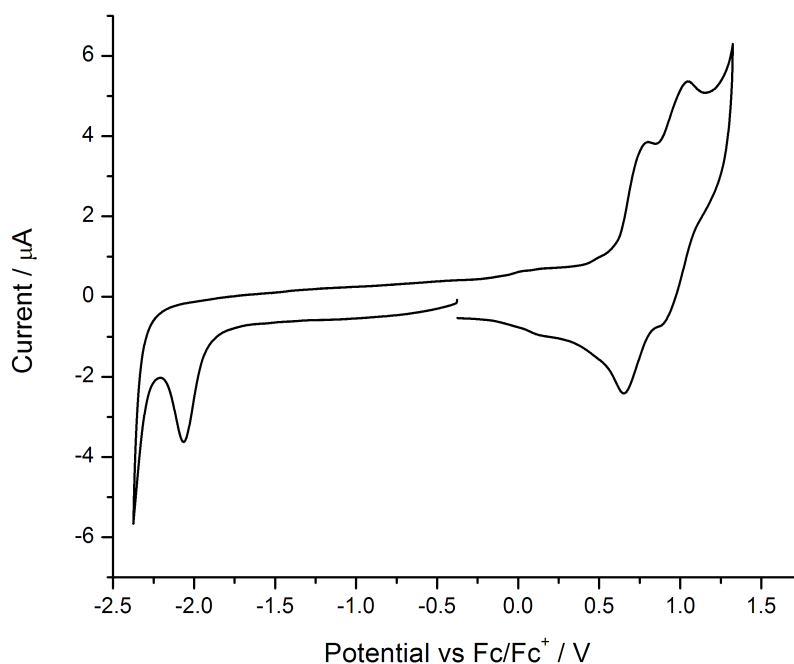
Figure 30. CV of polymer **109**

Reduction showed one irreversible peak (E_{red} = −2.06 V), which was consistent with the electrochemical behaviour dominated by DITT-units. Oxidation and reduction

potentials gave values for HOMO and LUMO (Table 8) that were significantly different from the estimates for the 1,4-bis((2-ethylhexyl)oxy)benzene comonomer (*ca.* –5.7 eV and –2.3 eV,[13] respectively). Thus, in the copolymer **109**, the HOMO is raised and the LUMO is lowered.

The electrochemical band gap of **109** was estimated to be 2.52 eV and was in close agreement with the values obtained for polymer **108**, in the same way governed by DITT monomers. In fact, the electrochemical data of both **108** and **109** are rather similar, apart from the higher oxidation potential of the latter, which brings its HOMO levels to a slightly deeper level. This can generally imply that the TH-DITT block, incorporated into the polymer backbone of known aromatic blue-emitters (and hole-transporters) is capable of modifying the HOMO and LUMO levels, which can be of high importance at the device design stage.

In general, the HOMO-levels of the four new polymers were found to be rather low, ranging between –5.40 eV and –5.27 eV, and the calculated band gaps were relatively wide as well. These observations could suggest good environmental stability, *i.e.*, resistance towards oxygen and moisture.

4.3. Thermal and Physical Properties (TGA and DSC)

The thermal stability of polymers **106-109** was determined by the thermal gravimetric analysis (TGA). Their physical properties were also investigated by differential scanning calorimetry (DSC). The data acquired for these materials are summarised in Table 9 along with their average molecular weight values.

Table 9. Physical data obtained by TGA and DSC, GPC results for polymers **106-109**

	$T_d{}^a$ / °C (-10 % wt)	$T_g{}^b$ / °C	M_w, g mol^{-1}	PDI
106	411.2	191.9	92,449	5.3
107	359.0	192.6	66,890	1.1
108	423.7	181.8	10,931	2.2
109	411.7	112.9	11,017	8.0

^{a}TGA. ^{b}DSC.

The four polymers were characterised as thermally stable materials, exhibiting high degradation temperatures (T_d), determined at 10% weight loss upon heating. Polymer **107** had the lowest T_d of 359ºC and the other three (**106**, **108** and **109**) were stable at temperatures well over 400ºC (Table 9).

All four polymers were found to be of the amorphous kind, *i.e.*, showing no sharp melting or crystallisation peaks in the DSC trace, as would be expected for crystalline materials. This means that they are rather disordered in their solid state and possess no three dimensional arrangements. Thus, the DSC measurements showed only glass to rubber transitions (T_g).

The glassy state of an amorphous polymer is defined by frozen conformational movements in rather random and disordered arrangements. The polymer in this state is stiff and breakable under applied force, *i.e.*, behaves like glass. During heating, the polymer can undergo a transition to the rubbery state, bringing about significant changes in its physical properties. The polymer mass then becomes softer, more elastic

and tolerant to, *e.g.*, forced stretching.[14] Knowing the T_g of a polymeric semiconducting material is useful during the fabrication of electronic devices, when thermal cycling or treatments (*e.g.*, annealing) are required. The performance of devices (*e.g.*, TFTs) can be significantly improved after appropriate thermal procedures.[6]

The polymers **106-108** showed glass transitions in a narrow temperature range (180-190ºC), indicating a similar degree of restriction of molecular movements. The T_g of **108** was somewhat lower (181.8ºC), ascribed to its lower molecular weight in comparison with **106** and **107**.

For polymer **109**, a substantial decrease of T_g was observed, which was consistent with (a) low molecular weight and high PDI (8.0) of this material, since the multiple ends of the polymer chains tend to demand more free volume to accommodate their higher flexibility and (b) the presence of the branched alkyl chains, which increase the free volume of the polymer and thus, allowing a higher extent of rotational motions with increasing temperature, thus bringing the T_g to lower values. Generally, structural features of a polymer allowing high rotational freedom (large free volume) lower the observed temperatures for glass transition.

4.4. Summary and Conclusions

On the whole, polymers **106**-**109** are amorphous and thermally stable materials.

Polymers **106**, **108** and **109** show increased conjugation within the polymer chains, indicated by the significant red-shift in their absorption in comparison to the TH-DITT monomer **78**. Polymer **107** shows broadening of the absorption band, which almost overlaps with the ICT peak, assigned to the effect produced by the sulfone moieties within the monomer units (**79**). However, the negligible red-shift of the polymer's absorption maximum and close similarity to the monomer's absorption spectrum indicate a very limited effective conjugation within the polymer chain.

The blue emitters – polymers **106**, **108** and **109** exhibit an increase in solution PLQYs in comparison with their molecular 'parent' compound **78** and its copolymerisation with 9,9-dihexylfluorene was particularly beneficial in this sense.

A dramatic drop in the PL efficiencies of thin films of these three polymers, associated with aggregation, can now be seen as their typical feature. The formation of aggregates is most likely caused by strong interchain interactions, facilitated by the increased *S*-density in the entire polymeric network. This prevalence could probably be advantageous from the charge transport point of view, however it certainly has a detrimental impact on their solid-state emissive properties. The incorporation of other moieties into the TH-DITT polymer backbone, both 9,9-dihexylfluorene (polymer **108**) and 1,4-bis((2-ethylhexyl)oxy)benzene (polymer **109**), do not seem to influence this matter, thus leading to the conclusion that the most efficient absorption (excitation) and emission (radiative relaxation) processes are strongly controlled by the structural characteristics of the main DITT core.

The optical properties of polymer **107** are surprisingly poor in relation to the observed intense emissive character of the molecular sulfone derivative **79**. Some additional investigations could help to elucidate the aspects causing such dramatic transformations. These might include emission measurements at different concentrations, in different solvents (to exclude or find presence of excimers) and with

excitation at other energies (wavelengths). For thin-films – other preparation techniques (solvent, deposition method) could influence the quality of the final samples.

Regarding the electrochemical properties, polymer **106** exhibits strong resemblance to the characteristics observed for its monomer **78**, despite the extension of the effective conjugation. The CV results of materials **108** and **109** demonstrate that their electrochemical behaviour is to a large degree dominated by the TH-DITT units. On the other hand, copolymerisation of **78** resulted in notable changes in the HOMO and LUMO energies of the two copolymers in comparison with the values reported for their corresponding homopolymers. Also, the band gaps of these three polymers are rather similar with differences within *ca*. 0.2 eV.

The electrochemistry of the polymer **107** is to a considerable extent deviated from the main electrochemical features of its monomer **79**, suggesting that a new redox pathway takes place, *e.g.*, through the indene segments along the chains. The band gap of this material is in the same range as the values estimated for the other members of this family.

Rather wide band gaps of all four polymers and low HOMO-levels can indicate good environmental stability. Additionally, no visual changes in the colour and texture of the four were noticed after 6 months of storage under ambient conditions.

REFERENCES

1.	Skotheim, T. A.; Reynolds, J. R., *"Conjugated Polymers"*. CRC Press: 2007.

2.	Grimsdale, A. C.; Chan, K. L.; Martin, R. E.; Jokisz, P. G.; Holmes, A. B., *Chem. Rev.* **2009,** *109*, 897-1091.

3.	Sakamoto, J.; Rehahn, M.; Wegner, G.; Schlüter, A. D., *Macromol. Rapid Commun.* **2009,** *30*, 653-687.

4.	Cheng, Y.-J.; Yang, S.-H.; Hsu, C.-S., *Chem. Rev.* **2009,** *109*, 5868-5923.

5.	Chen, S.-H.; Shiau, C.-S.; Tsai, L.-R.; Chen, Y., *Polymer* **2006,** *47*, 8436-8443.

6.	Perepichka, I. F.; Perepichka, D. F., *"Handbook of Thiophene-based Materials: Applications in Ogranic Electronics and Photonics"*. Wiley: 2009; Vol. One: Synthesis and Theory.

7.	Barbarella, G.; Favaretto, L.; Zambianchi, M.; Pudova, O.; Arbizzani, C.; Bongini, A.; Mastragostino, M., *Adv. Mater.* **1998,** *10*, 551.

8.	Barbarella, G.; Favaretto, L.; Sotgiu, G.; Antolini, L.; Gigli, G.; Cingolani, R.; Bongini, A., *Chem. Mater.* **2001,** *13*, 4112-4122.

9.	Sotgiu, G.; Favaretto, L.; Barbarella, G.; Antolini, L.; Gigli, G.; Mazzeo, M.; Bongini, A., *Tetrahedron* **2003,** *59*, 5083-5090.

10.	Sotgiu, G.; Zambianchi, M.; Barbarella, G.; Aruffo, F.; Cipriani, F.; Ventola, A., *J. Org. Chem.* **2003,** *68*, 1512.

11.	Catellani, M.; Boselli, B.; Luzzati, S.; Tripodi, C., *Thin Solid Films* **2002,** *403* (66-70).

12.	Farchioni, R.; Grosso, G., *Organic Electronic Materials. Conjugated Polymers and Low Molecular Weight Organic Solids*. Springer: 2001.

13.	Yang, Y.; Pei, Q.; Heeger, A., *J. Appl. Phys.* **1996,** *79*, 934.

14.	Cowie, J. M. G., *Polymers: Chemistry and Physics of Modern Materials*. Intertext Books: 1973.

CHAPTER 5

CHAPTER 5

SUMMARY AND FURTHER PERSPECTIVES
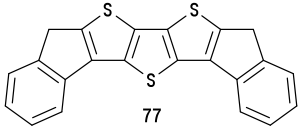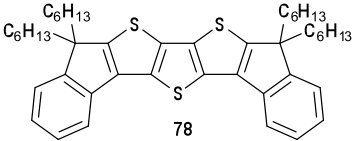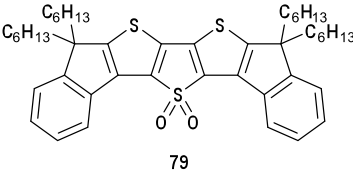
This work was dedicated to developing synthetic routes towards new semiconducting materials, incorporating the fused thiophene-moiety DTT, and investigating the properties of these rather complex compounds and their polymers.

DTT is a fused trimer of thiophene and is a rigid and flat molecule with the ability to induce the formation of highly ordered π-stacked arrangements, facilitated by an increased C:H ratio and density of sulfur, which is in turn achieved through the fusion of thiophene rings. As a component of more complex compounds (or monomers), DTT contributes to an increased degree of overall planarity of the molecule, which promotes the establishment of close intermolecular interactions (*e.g.*, π-stacking) and, hence, more efficient charge transport within the bulk of the material.

This building block was successfully derivatised, producing materials with high hole mobilities, suitable for OFET application. It was also implemented as a donor component of D-A polymers for photovoltaic applications (see Chapter 1).

DTT on its own exhibits no remarkable optical characteristics, but these can be manipulated with additional functionalisation of the system. For instance, the DTT-sulfone (*S,S*-dioxide) shows strong fluorescence in the green region, reaching 75% PLQY in solution, which is attributed to its rigid core structure with no conformational flexibility or rotational freedom.[1,2] A number of DTT-based sulfones linked with thiophenes and benzene-rings are known and these have been extensively studied. This sulfone-family presents an interesting class of DTT-based molecular emitters over a wide range of colours.[2,3]

Table 10. Data summary for compounds **77-79**
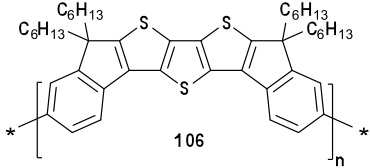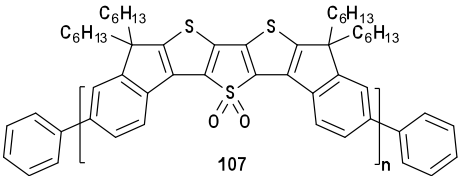
Material	$\lambda_{abs,max}$ (nm)	Optical $E_g{}^a$ (eV)	ε (dm^3/mol cm)	$\lambda_{em,\,max}$ (nm)	PLQY solution/ film	E_{ox} (V)	E_{red} (V)	HOMO^b (eV)	LUMO^b (eV)	Echem E_g (eV)
77	284	3.4	34 300	373	0.01/–	0.72^i	-2.68^i	-5.4	-2.1	3.3
78	273	3.4	56 600	376	0.004/–	0.71/0.64	-2.95^i	-5.4	-1.9	3.5
79	419	2.6	32 100	524	0.72/0.14	1.04/0.96	-2.03/1.95	-5.7	-2.9	2.8

^{a}Optical HOMO-LUMO gaps determined from the onset of the highest wavelength absorption band (and given in eV).
^{b}HOMO and LUMO values were calculated from the onset of the first peak of the corresponding redox wave and referenced to ferrocene, which has a HOMO of -4.8 eV.
^{i}Irreversible peak.

Table 11. Summary of physical and optical data for polymers **106-109**

Material, M_w (g mol^{-1}) / PDI	T_d, °C (-10 %wt)	T_g, °C	$\lambda_{abs,max}$ solution/film (nm)	Optical E_g [a] (eV)	$\lambda_{em, max}$ solution/film (nm)	PLQY solution/film
92,449 / 5.3	411.2	191.9	346 / 334	3.2	413 / 406	0.20 / 0.05
66,890 / 1.1	359.0	192.6	423 / 419	2.58	529 / 523	0.04 / 0.07
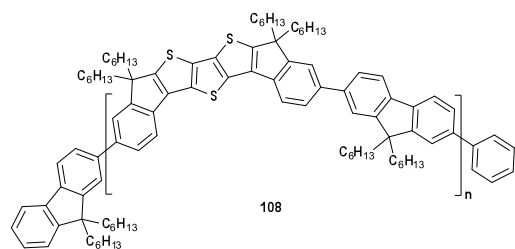
| | 423.7 | 181.8 | 351 / 351 | 3.09 | 406 / 406 | 0.49 / 0.04 |

108

10,931 / 2.2
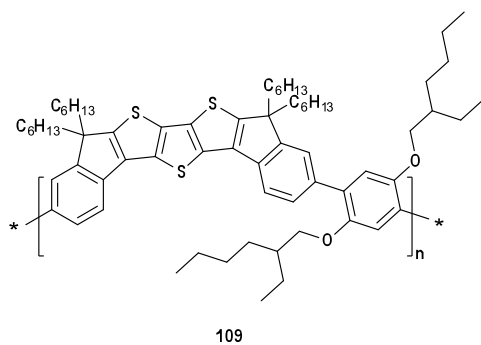
| | 411.7 | 112.9 | 345 / 336 | 3.19 | 409 / 418 | 0.32 / 0.03 |

109
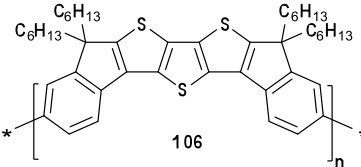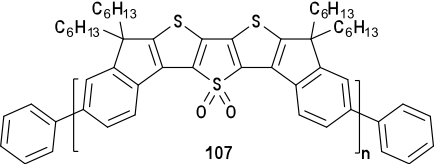
11,017 / 8.0

[a] Optical HOMO-LUMO gaps determined from the onset of the highest wavelength absorption band (and given in eV).

Table 12. Summary of electrochemical data for polymers **106-109**

Material	E_{ox} (V)	E_{red} (V)	HOMO[b] (eV)	LUMO[b] (eV)	Echem E_g (eV)
106	0.72 / 0.56	-2.14[i]	-5.29	-3.10	2.31
107	0.54 / 0.52	-2.11[i]	-5.27	-2.90	2.37

0.71 / 0.63	-2.10^{i}	-5.37	-2.86	2.51

108
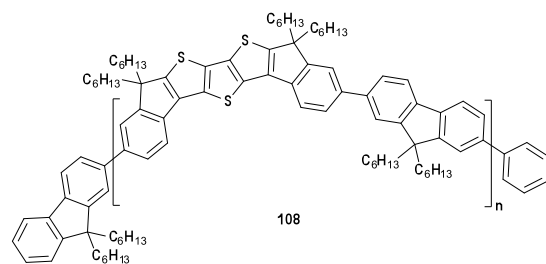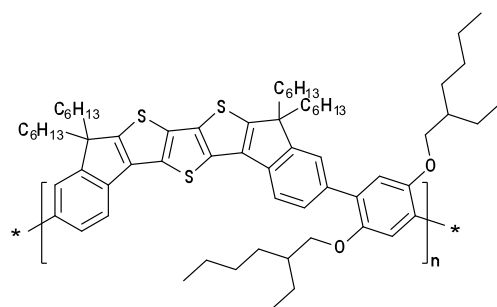
0.80 / 0.65	-2.06^{i}	-5.40	-2.87	2.52
$1.05 / 0.88^{qr}$				

109

[b]HOMO and LUMO values were calculated from the onset of the first peak of the corresponding redox wave and referenced to ferrocene, which has a HOMO of -4.8 eV.
[i]Irreversible peak.
[qr]Quasi-reversible peak

In this work, the DTT block was utilised as a central core in larger aromatic systems (materials **77-79**), bearing indene units on its both sides (diindenodithienothiophenes, DITTs). The low solubility of the unsubstituted parent compound (**77**) was greatly improved with the introduction of four alkyl chains (**78**). The *S,S*-dioxide of this system (**79**) was also prepared to evaluate the emitting properties of a more extended DTT-sulfone. The synthesis of these materials and evaluation of their properties were discussed in Chapter 2. Table 10 summarises the results obtained along with their chemical structures.

The hole mobility of the parent compound **77** was found to be rather low ($\sim 10^{-4}$ cm^2 V^{-1} s^{-1}), in the initial attempts of OFET device fabrication. Potentially, this value can be increased with appropriate optimisation of the fabrication process. High PL efficiency of the material **79** in solution (0.72), typically for DTT-based *S,S*-dioxides,[1] was quenched to much lower values in its solid state (0.14), thus rendering the possibilities for OLED fabrication not viable.

However, these molecular semiconducting materials would be useful in extended structures to assist with more efficient intermolecular organisation, or as planar conjugated spacers. Their role as comonomers was also found effective for tuning of the HOMO and LUMO levels of other optically active systems (Chapter 4). Additionally, the DITT-sulfone (**79**) could possibly be used as a fluorescent marker for biomolecules, in analogy with previously reported work from the Barbarella group.[3]

There are a scarce number of reports, regarding the polymers containing the DTT-block, probably reflecting the synthetic challenge associated with the preparation of the monomers. Thus, further work in this direction was conducted with the polymerisation of the soluble monomers **78** and **79**. The former was also copolymerised with 9,9-dihexylfluorene and 1,4-bis((2-ethylhexyl)oxy)benzene.

Polymerisation aimed to extend the conjugation between these molecular blocks and thus amend the optical and electrochemical properties of individual molecular compounds. In turn, copolymerisation is an efficient way to obtain interesting variations in the properties of known polymers. Also, polymeric materials are

generally more convenient for unambiguous production of thin and flexible films, which is a cost effective way of manufacturing lightweight devices.

Homopolymers of **78** and **79** were prepared *via* Yamamoto polymerisation (**106** and **107**) and the copolymers **108** and **109** were obtained by Suzuki cross-coupling polymerisation (Chapter 3). The GPC analysis of the four new materials revealed that, on the whole, both procedures would require further optimisation to achieve more uniform and/or higher molecular weight materials. Property evaluation of the polymers **106-109** was presented and discussed in Chapter 4. Their structures and the summary of their molecular, physical, optical and electrochemical characteristics are collated in Tables 11 and 12.

Polymerisation of the monomer **78** was clearly advantageous for its otherwise very weak emissive properties, *e.g.*, solution state PLQY of **106** was measured to be 50 times higher than that of the monomer. Copolymerisation with the other two monomers had an even more pronounced effect, showing solution PLQYs of 49% for **108** and 32% for **109** (*versus* 0.4% for **78**, see Table 11). The PL of the thin films was, as the result of aggregate formation, dramatically quenched for all three polymers, which effectively eliminated the possibilities for their further application in thin-film based PL devices.

It was also noticed that HOMO and LUMO levels showed interesting dynamics upon copolymerisation, where the former reached higher levels and the latter was lowered. These are valuable observations to keep in mind for potential work with other materials.

Regarding the polymer **107** (homopolymer of the strongly fluorescent monomer **79**), its unexpectedly poor emission characteristics both in solution state and thin-film clearly demonstrate that polymerisation enhanced the rate and occurrence of non-radiative decay mechanisms. Thus, the original intension to implement this polymer in photonic devices now does not seem reasonable. However, since the polymer shows a broad absorption spectrum (*i.e.*, excitation), there would be some practical sense to investigate its use in organic solar cells.

155

Electrochemical characterisation showed that the three polymers, containing monomer **78**, were to a large degree governed by this unit and only a slight decrease in oxidation potentials was observed. The electrochemically determined band gaps of the three materials were found to be smaller, mainly due to the less negative reduction potentials. The CV of the sulfone-based polymer deviated significantly from what was observed for its monomer **79**, suggesting that the redox processes in **107** take place through other sites than in the simple structure of **79**.

These amorphous polymers showed good thermal stability and their relatively wide band gaps could suggest a certain degree of environmental stability as well. Possible alternative applications of these polymers could include UV-light sensors, equipped with fluorescence detectors.

REFERENCES

1.   Barbarella, G.; Favaretto, L.; Sotgiu, G.; Antolini, L.; Gigli, G.; Cingolani, R.; Bongini, A., *Chem. Mater.* **2001,** *13*, 4112-4122.

2.   Tedesco, E.; Della Salla, F.; Favaretto, L.; Barbarella, G.; Albesa-Jove, D.; Pisignano, D.; Gigli, G.; Cingolani, R.; Harris, K. D. M., *J. Am. Chem. Soc.* **2003,** *125*, 12277.

3.   Sotgiu, G.; Zambianchi, M.; Barbarella, G.; Aruffo, F.; Cipriani, F.; Ventola, A., *J. Org. Chem.* **2003,** *68*, 1512.

CHAPTER 6

CHAPTER 6

EXPERIMENTAL

6.1. General

For all reactions that required anhydrous conditions, glassware was dried in an oven at 120°C.

Microwave assisted reactions were performed in a Biotage Initiator microwave oven.

Column chromatography was performed with commercially available solvents, using VWR silica gel (40-63 μm). Thin layer chromatography (TLC) was performed using aluminium plates precoated with Merck silica gel 60 (F_{254}) and visualized by ultra-violet radiation and/or iodine vapor.

The chemicals were purchased from Sigma-Aldrich and used without further purification, unless stated otherwise. 2-Bromo-1-indanone was purified by column chromatography using silica gel (dichloromethane/petroleum ether, 2:1, then dichloromethane). Potassium *tert*-butoxide was purchased from AlfaAesar (97%,), Ni(COD)$_2$ from Strem and its all handling was performed in a glovebox.

Anhydrous solvents were obtained from a PureSolv solvent purification system.

Known compounds are indicated by a reference to a previous literature procedure.

^{1}H NMR spectra were recorded on AVANCE/DPX 400 and AVANCE 400 instruments at 400 MHz and on AVANCE/DRX500 instrument at 500 MHz; and ^{13}C NMR at 100 MHz; chemical shifts (δ_H) are given in parts per million (ppm). Peak multiplicities are denoted by s (singlet), d (doublet), t (triplet), q (quartet) and m (multiplet) or by a combination of these: dd (doublet of doublets), dt (doublet of triplets), td (triplet of doublets), br m (broad multiplet) with coupling constants (J) given in Hertz (Hz).

Melting points were taken using a Stuart Scientific apparatus and are uncorrected.

Elemental analyses were conducted on a Perkin Elmer 2400.

Electron impact mass spectra were recorded on a TraceGC – FinniganPolaris Q.

ES mass spectra were recorded on a ThermoFinnigan LCQ DUO.

Infrared spectra were recorded on a Perkin Elmer Spectrum One FT-IR spectrometer (thin film deposited onto a diamond plate). Only selected absorptions (v_{max}) are reported.

Solution absorption spectra were recorded on a UNICAM UV 300 instrument in chloroform. Varian Cary 300 UV-Vis absorption spectrometer was used for polymer thin film absorption measurements.

X-ray crystallography was performed on a Nonius KappaCCD diffractometer.

GPC, TGA and DSC instruments and methods are described in separate sections of this Chapter.

6.2. Synthetic Procedures and Data

82. 2,2'-(Thiophene-3,4-diylbis(sulfanediyl))bis(2,3-dihydro-1*H*-inden-1-one)

Method A
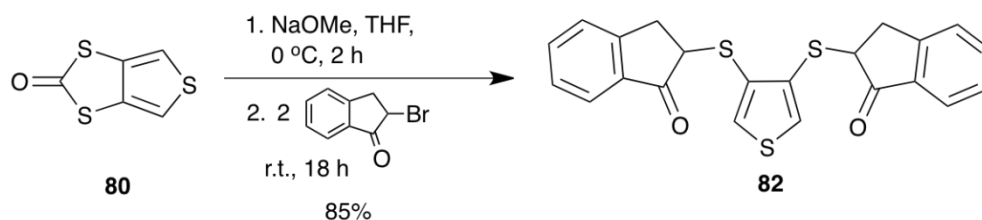
Thieno[3,4-*d*][1,3]dithiol-2-one **80**[1] (1.77 g, 10.15 mmol) was dissolved in dry THF (450 ml) and cooled to 0°C under N_2. Sodium methoxide (25 wt% sol in MeOH, 4.76 ml, 20.81 mmol) was added (mixture turned milky yellow) and the mixture was stirred for 1 hour. Purified 2-bromo-1-indanone (4.5 g, 21.32 mmol) was added, the mixture allowed to reach room temperature and then the reaction stirred for 18 hours. The solvent was removed, the remaining solid dissolved in dichloromethane (350 ml), washed with water (5 × 100 ml), dried over $MgSO_4$, filtered and evaporated. The crude product was subjected to column chromatography on silica gel (petroleum ether/ethyl acetate, 2:1), yielding 3.51 g (85%) of the desired compound **82** as a pale yellow viscous oil.

Method B
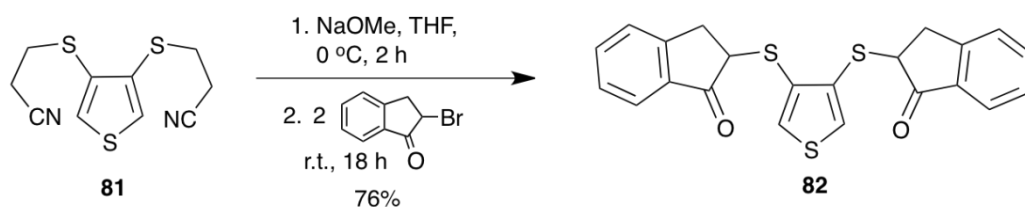
3,3'-(Thiophene-3,4-diylbis(sulfanediyl))dipropanenitrile **81**[2,3] (4.70 g, 0.019 mol) was dissolved in dry THF (500 ml) and cooled to 0°C under N_2. Sodium methoxide (25 wt% sol in MeOH, 8.92 ml, 0.039 mmol) was added (mixture turned milky yellow) and

the mixture was stirred for 1 hour. Purified 2-bromo-1-indanone (8.42 g, 0.040 mol) was added, the mixture allowed to reach room temperature and then the reaction stirred for 18 hours. The solvent was removed, the remaining solid dissolved in dichloromethane (1200 ml), washed with water (5 × 400 ml), dried over MgSO$_4$, filtered and evaporated. The crude product was subjected to column chromatography on silica gel (petroleum ether/ethyl acetate, 2:1), yielding 5.88 g (76%) of the desired compound **82** as a pale yellow viscous oil.

^{1}H NMR 500 MHz (CDCl$_3$) δ 7.79 (1H, d, ^3J = 7.5 Hz, ar H), 7.78 (1H, d, ^3J = 7.5 Hz, ar H), 7.61 (2H, t, ^3J = 7.5 Hz, ar H), 7.46 (1H, s, thiophene H), 7.43 (1H, s, thiophene H), 7.40 (4H, m, ar H), 4.20 (1H, dd, $^3J_1$ = 7.8 Hz, $^3J_2$ = 3.4 Hz, —S—C<u>H</u>—), 4.19 (1H, dd, $^3J_1$ = 7.8 Hz, $^3J_2$ = 3.4 Hz, —S—C<u>H</u>—), 3.62 (2H, dd, ^2J = 17.7 Hz, ^3J = 7.8 Hz, —C<u>H</u>$_2$—), 3.16 (1H, dd, $^3J_1$ = 17.7 Hz, $^3J_2$ = 3.4 Hz, —C<u>H</u>$_2$—), 3.15 (1H, dd, $^3J_1$ = 17.7 Hz, $^3J_2$ = 3.4 Hz, —C<u>H</u>$_2$—) ppm (as a mixture of diastereomers). **^{13}C NMR** 100 MHz (CDCl$_3$) δ 202.0, 201.9, 152.0, 135.40, 135.36, 135.2, 131.5, 131.4, 128.9, 128.8, 127.9, 126.38, 126.35, 124.6, 49.8, 49.7, 34.40, 34.37 ppm (as a mixture of diastereomers). **MS (EI$^+$)** m/z 408.0314 (M$^+$). **IR** 1/λ = 2923 (sp^{3}C—H), 1698 (C=O), 1594 (aromatic C=C), 1092 (S=C), 848 and 746 (aromatic C—H) cm^{-1}.

77. [1,2-*b*:2′,1′-*g*]Dihydrodiindeno-(dithieno)-[3,2-*b*:2,3-*d*]-thiophene (DITT)
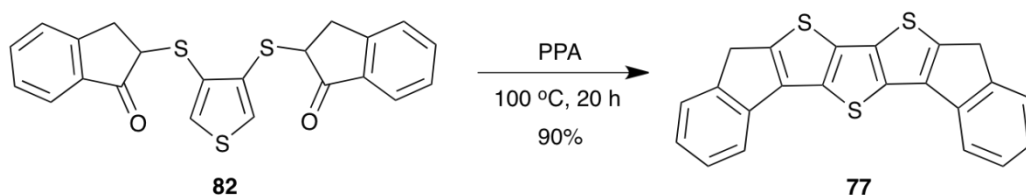
2,2'-(Thiophene-3,4-diylbis(sulfanediyl))bis(2,3-dihydro-1*H*-inden-1-one) **82** (1.55 g, 3.79 mmol) was placed in a round-bottomed flask along with polyphosphoric acid (30 g), heated to *ca.*100°C under N$_2$ and stirred at this temperature for 20 hours. Water (400 ml) was added and the product was extracted with dichloromethane (5 × 400 ml), washed with water (3 × 300 ml), dried over MgSO$_4$, filtered and evaporated. The crude product was dissolved in boiling in toluene (*ca.* 400 ml) with charcoal, filtered through

a silica plug and left to crystallize, yielding 1.27 g (90%) of the product **77** as pale fine needle-like crystals. The product can be sublimed at 220°C and 0.3 mm Hg.

[For the work up on a larger scale (2–2.5 g and more load of starting material) it can be more convenient to add water to the reaction mixture and filter off the precipitate, dry it, dissolve in boiling toluene with some charcoal powder and filter it hot. Reduce the solvent volume and cool down slowly. The crystals start forming as soon as the temperature drops by 10-15 degrees from the boiling point of toluene.]

M. p. decomposes at 268°C. **^{1}H NMR** 400 MHz (CDCl$_3$) δ 7.65 (2H, d, ^3J = 8.0 Hz, ar H), 7.55 (2H, d, ^3J = 8.0 Hz, ar H), 7.45 (2H, t, ^3J = 8.0 Hz, ar H), 7.28 (2H, dt, ^3J = 8.0 Hz, ^4J = 1.2 Hz, ar H), 4.00 (4H, s, —C$\underline{H}_2$—) ppm. **^{13}C NMR** not recorded due to the very low solubility of the material. **MS (EI$^+$)** m/z 372.0107 (M$^+$). **IR** $1/\lambda$ = 1602 (aromatic C=C), 1440 (sp^{3}C—H), 1183 (S=C), 754 (aromatic C—H) cm^{-1}. **Anal. calcd.** for (C$_{22}$H$_{12}$S$_3$): C, 70.9; H, 3.3; S, 25.8%. Found: C, 70.8; H, 3.0; S, 26.0%.

78. [1,2-*b*:2′,1′-*g*]Dihexyldiindeno-(dithieno)-[3,2-*b*:2,3-*d*]-thiophene (TH-DITT)

Method A:
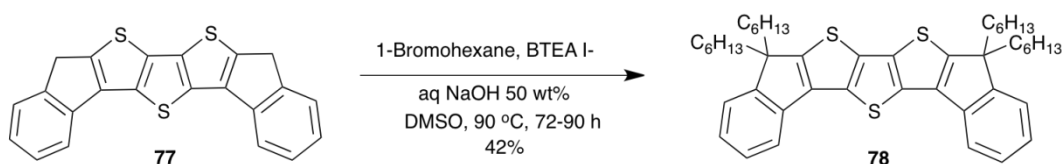
[1,2-*b*:2′,1′-*g*]Dihydrodiindeno-(dithieno)-[3,2-*b*:2,3-*d*]-thiophene **77** (50 mg, 0.134 mmol), benzyltriethylammonium iodide (BTEAI, *ca.* 10 mg), 1-bromohexane (0.15 ml, 1.072 mmol) and DMSO (11.5 ml) were placed in a round-bottomed flask and degassed for 20 minutes with N$_2$. Degassed aqueous NaOH solution (50 wt%, 0.1 ml) was added dropwise to the flask and the mixture was heated to 90-95°C until all of the solid dissolved; the mixture was then left to stir for a further 72 hours. The reaction was monitored by TLC (petroleum ether). When most of the starting material was

converted, the mixture was poured over a saturated solution of ammonium chloride (15 ml) and extracted with dichloromethane (3 × 25 ml). The organic layers were washed with water (3 × 25 ml), dried over MgSO$_4$, filtered and evaporated. The crude product was subjected to column chromatography on silica gel (petroleum ether) yielding 40 mg (42%) of the product **78** as pale viscous oil.

^{1}H NMR 400 MHz (CDCl$_3$) δ 7.58 (2H, d, ^{3}J = 7.2 Hz, ar H), 7.39 (2H, dt, ^{3}J = 7.2 Hz, ^{4}J = 0.8 Hz, ar H), 7.35 (2H, d, ^{3}J = 7.2 Hz, ar H), 7.27 (2H, dt, ^{3}J= 7.2 Hz, ^{4}J = 0.8 Hz, ar H), 1.99 (8H, m, Ar—C$\underline{H}_2$—alkyl), 1.22-0.84 (32H, br m, alkyl CH$_2$), 0.80 (12H, t, ^{3}J = 6.8 Hz, CH$_3$) ppm. **^{13}C NMR** 100 MHz (CD$_2$Cl$_2$) δ 154.3, 153.8, 137.6, 137.5, 134.8, 131.9, 127.2, 125.4, 122.8, 119.5, 57.0, 40.3, 31.9, 29.9, 24.4, 22.9, 14.1 ppm. **MS (FAB$^+$)** m/z 709.393 (M+H)$^+$. **IR** 1/λ = 2929 and 2857 (sp^{3}C—H), 1602 (aromatic C=C), 1457 (sp^{3}C—H), 1177 (S=C), 752 (aromatic C—H) cm^{-1}.

Method B:
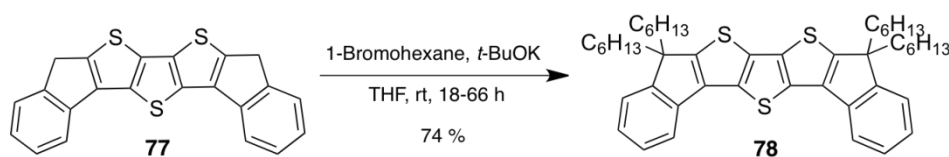
[1,2-*b*:2′,1′-*g*]Dihydrodiindeno-(dithieno)-[3,2-*b*:2,3-*d*]-thiophene **77** (2.5 g, 6.711 mmol) was placed in a round-bottomed flask and flushed with N$_2$. 1-Bromohexane (9.43 ml, 67.11 mmol) and dry THF (125 ml) were added and the mixture was additionally purged with N$_2$. Solution of potassium *tert*-butoxide (33.56 mmol, 3.77 g) in dry THF (140 ml) was added to the mixture at room temperature with vigorous stirring during 2 hours. Initially, the addition of potassium *tert*-butoxide solution produced bright yellow-orange colour of the reaction mixture and when the alkylation was complete the colour changed to pale yellow. The mixture was stirred at least overnight at room temperature and then filtered through a silica plug and the solvent was evaporated. The residue was dissolved in dichloromethane (1 L) and washed with water (3×400 ml), dried over MgSO$_4$, filtered and the solvent was evaporated. The crude product was subjected to column chromatography on silica gel (distilled

petroleum ether, b.p. 40-60°C) and further recrystallised from boiling acetone yielding 3.52 g (74%) of the product **78** as white grainy crystals.

M. p. 95-97°C. **^{1}H NMR** 400 MHz (CDCl$_3$) δ 7.58 (2H, d, ^3J = 7.2 Hz, ar H), 7.39 (2H, dt, ^3J = 7.2 Hz, ^4J = 0.8 Hz, ar H), 7.35 (2H, d, ^3J = 7.2 Hz, ar H), 7.27 (2H, dt, ^3J= 7.2 Hz, ^4J = 0.8 Hz, ar H), 1.99 (8H, m, Ar—C$\underline{H}_2$—alkyl), 1.22-0.82 (32H, br m, alkyl CH$_2$), 0.80 (12H, t, ^3J = 6.8 Hz, CH$_3$) ppm. **^{13}C NMR** 100 MHz (CD$_2$Cl$_2$) δ 153.9, 153.2, 137.3, 137.1, 134.4, 131.6, 126.9, 125.0, 122.3, 119.3, 56.6, 39.9, 31.5, 29.6, 24.0, 22.6, 14.0 ppm. **MS (FAB$^+$)** m/z 709.394 (M+H)$^+$. **IR** 1/λ = 2926 and 2856 (sp^{3}C—H), 1605 (aromatic C=C), 1467 (sp^{3}C—H), 1182 (S=C), 753 (aromatic C—H) cm^{-1}. **Anal. calcd**. for (C$_{46}$H$_{60}$S$_3$): C, 77.9; H, 8.5; S, 13.6%. Found: C, 78.0; H, 8.7; S, 13.9%.

79. [1,2-*b*:2′,1′-*g*]Dihexyldiindeno-(dithieno)-[3,2-*b*:2,3-*d*]-*S,S*-dioxy-thiophene (TH-DITT-O$_2$)
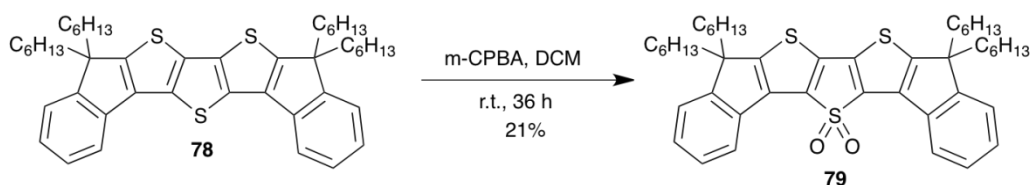
[1,2-*b*:2′,1′-*g*]Dihexyldiindeno-(dithieno)-[3,2-*b*:2,3-*d*]-thiophene **78** (90 mg, 0.127 mmol) and meta-chloroperoxybenzoic acid (270 mg, 1.27 mmol) were dissolved in dry dichloromethane (11 ml) and stirred for 36 hours at room temperature. The mixture was poured over a saturated solution of sodium sulfite Na$_2$SO$_3$ (30 ml) and the product extracted with dichloromethane (150 ml). The organic layer was washed with water (3 × 50 ml) and brine (60 ml), dried over MgSO$_4$, filtered and evaporated. The crude product was subjected to column chromatography on silica gel (dichloromethane/petroleum ether, 1:3) and precipitated with acetonitrile yielding 20 mg (21%) of **79** as a bright yellow powder.

M. p. 72-74°C. **^{1}H NMR** 400 MHz (CD$_2$Cl$_2$) δ 7.70 (2H, d, ^3J = 7.2 Hz, ar H), 7.43-7.33 (6H, m, ar H), 1.98 (8H, m, Ar—C$\underline{H}_2$—alkyl), 1.28-0.88 (32H, br m, alkyl CH$_2$), 0.83 (12H, t, ^3J = 7.0 Hz, CH$_3$) ppm. **^{13}C NMR** 100 MHz (CD$_2$Cl$_2$) δ 156.7, 154.1, 140.2, 138.3, 135.3, 134.1, 127.8, 127.0, 123.0, 121.5, 57.5, 39.9, 31.8, 29.8, 24.5, 22.9, 14.1 ppm. **MS (FAB$^+$)** m/z 741.384 (M+H)$^+$. **IR** 1/λ = 2929 and 2852 (sp^{3}C—H), 1679 (aromatic C=C), 1314 and 1141 (-SO$_2$-), 754 (aromatic C—H) cm^{-1}. **Anal. calcd.** for (C$_{46}$H$_{60}$O$_2$S$_3$): C, 74.5; H, 8.2; O, 4.3; S, 13.0%. Found: C, 74.0; H, 7.9; S, 12.5%.

83. Diethyl 3,5-dibromodithieno[3,2-*b*:2',3'-*d*]thiophene-2,6-dicarboxylate
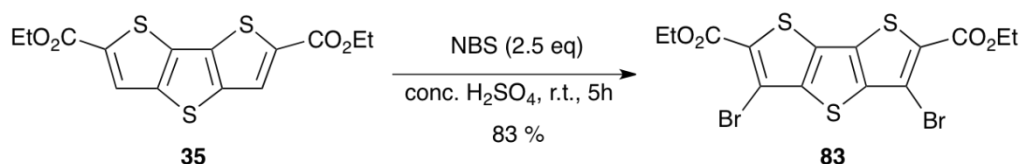
Diethyl dithieno[3,2-*b*:2',3'-*d*]thiophene-2,6-dicarboxylate **35**[4] (1 g, 2.94 mmol) was dissolved in conc. H$_2$SO$_4$ (10 ml) and recrystallised NBS (1.31 g, 7.35 mmol) was added. The mixture was stirred at room temperature and absence of light for 5 hours. Then it was poured over ice and the precipitate was filtered off and washed with more H$_2$O. The crude product was dried overnight, then dissolved in hot toluene, filtered through silica plug and recrystallised (toluene) affording 1.22 g (83%) of the product **83** as fine pale yellow crystals.

M. p. 230-232°C. **^{1}H NMR** 400 MHz (CDCl$_3$) δ 4.46 (4H, q, ^3J = 7.2 Hz, C$\underline{H}_2$), 1.44 (6H, t, ^3J = 7.2 Hz, C$\underline{H}_3$) ppm. **^{13}C NMR** 100 MHz (CDCl$_3$) δ 160.6, 146.1, 132.5, 129.3, 110.5, 62.0, 14.3 ppm. **MS (FAB$^+$)** m/z 498.815 (M+H)$^+$. **Anal. calcd.** for (C$_{14}$H$_{10}$O$_4$S$_3$Br$_2$): C, 33.8; H, 2.0; Br, 32.1; O, 12.8; S, 19.3%. Found: C, 33.6; H, 1.7; Br, 32.4; S, 19.2%.

110. TH-DITT-Br$_2$
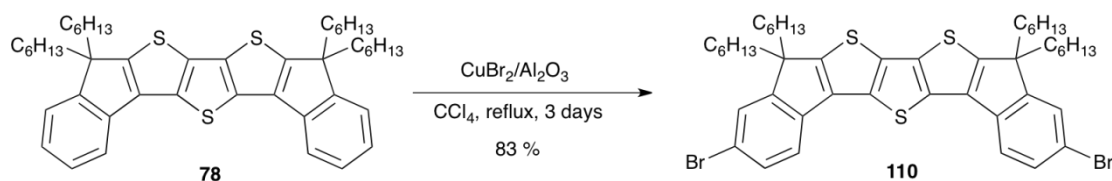
CuBr$_2$/Al$_2$O$_3$: To a solution of copper (II) chloride dihydrate (10 g) in distilled water (30 ml) neutral alumina (20 g, Sigma-Aldrich, type 507c) was added at room temperature. The water was evaporated using a rotary evaporator at 75°C and under reduced pressure. The residue was dried under vacuum (4.5 mm Hg) at 115°C for 3 days.

[1,2-*b*:2′,1′-*g*]Dihexyldiindeno-(dithieno)-[3,2-*b*:2,3-*d*]-thiophene **78** (4.0 g, 5.65 mmol), CuBr$_2$/Al$_2$O$_3$ (34 g, 0.0508 mol) and CCl$_4$ (300 ml, freshly distilled from CaH$_2$) were placed in a round-bottomed flask and purged with N$_2$. The mixture was refluxed for 3 days. The solid was filtered off and washed with CCl$_4$. Evaporation of the solvent and following precipitation by dichloromethane/methanol yielded 4.08 g (83%) of **110** as a white powder. Crystals could be obtained by slow evaporation of dichloromethane/ethyl acetate.

M. p. 170-172°C. **^{1}H NMR** 400 MHz (CDCl$_3$) δ 7.53 (2H, dd, ^3J = 8.0 Hz, ^4J = 1.6 Hz, —CH=C<u>H</u>—CBr=), 7.47 (2H, ds, ^4J = 1.6 Hz, =CH—CBr=C<u>H</u>—C–), 7.40 (2H, d, ^3J = 8.0 Hz, –C—C<u>H</u>=CH—CBr=), 1.96 (8H, m, Ar—C<u>H$_2$</u>—alkyl), 1.22-0.84 (32H, br m, alkyl CH$_2$), 0.80 (12H, t, ^3J = 7.0 Hz, CH$_3$) ppm. **^{13}C NMR** 100 MHz (CDCl$_3$) δ 156.0, 153.6, 136.2, 136.1, 134.6, 131.5, 130.0, 125.7, 120.4, 119.3, 56.9, 39.8, 31.5, 29.5, 24.0, 22.6, 14.0 ppm. **MS (FAB$^+$)** m/z 866.205 (M+H)$^+$. **IR** 1/λ = 2922 and 2846 (sp^{3}C—H), 1601 (aromatic C=C), 1465 (sp^{3}C—H), 1180 (S=C), 815 (aromatic C—H), 561 (C—Br) cm^{-1}. **Anal. calcd**. for (C$_{46}$H$_{58}$Br$_2$S$_3$): C, 63.7; H, 6.7; Br, 18.4; S, 11.1%. Found: C, 63.6; H, 6.9; Br, 18.4; S, 11.2%.

111 and **112**. TH-DITT-O$_2$-Br$_2$
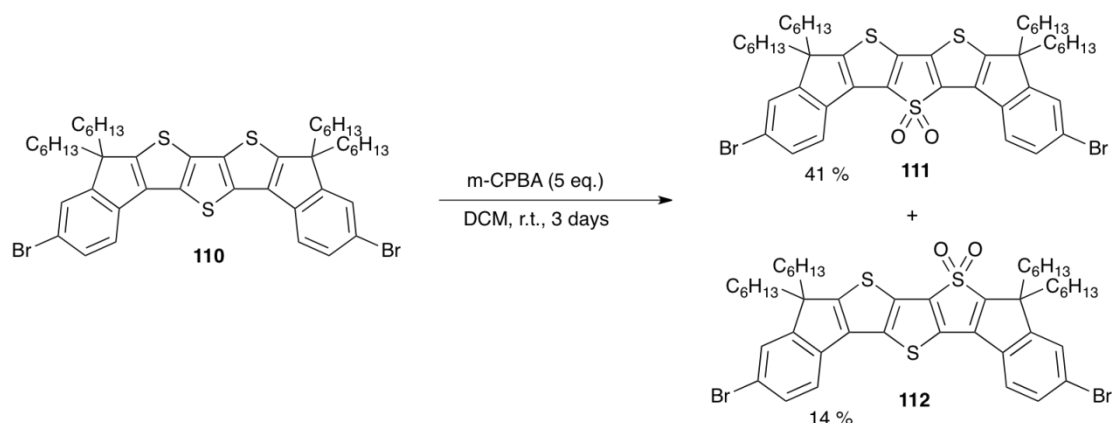
TH-DITT-Br$_2$ **110** (4.8 g, 5.536 mmol) and *m*-CPBA (77%, 27.68 mmol, 6.353 g) were placed in a round-bottomed flask, flushed with N$_2$ and dissolved in dry dichloromethane (480 ml). The mixture was stirred at room temperature, with absence of light for 3 days and then poured into saturated solution of Na$_2$SO$_3$ and extracted with more dichloromethane. The organic fraction was washed with water (3×500 ml) and brine, dried over MgSO$_4$, filtered and evaporated. The crude product was subjected to column chromatography on silica gel (distilled petroleum ether/toluene, 3:1) affording two products. Further precipitation of each from dichloromethane/methanol yielded 2.02 g (41%) of the main product **111** as a bright yellow-green powder and 0.69 g (14%) of the other product **112** as a yellow-orange powder.

Product **111**:

M. p. 189-191°C. **^{1}H NMR** 400 MHz (CDCl$_3$) δ 7.59 (2H, d, ^3J = 8.0 Hz, –C—C$\underline{H}$=CH—CBr=), 7.52 (2H, dd, ^3J = 8.0 Hz, ^4J = 1.6 Hz, —CH=C$\underline{H}$—CBr=), 7.44 (2H, ds, ^4J = 1.6 Hz, =CH—CBr=C$\underline{H}$—C–), 1.91 (8H, m, Ar—C$\underline{H}_2$—alkyl), 1.26-0.87 (32H, br m, alkyl CH$_2$), 0.83 (12H, t, ^3J = 7.0 Hz, CH$_3$) ppm. **^{13}C NMR** 100 MHz (CDCl$_3$) δ 156.0, 155.5, 139.8, 137.3, 133.8, 133.7, 130.7, 125.8, 122.8, 121.1, 57.4, 39.5, 31.5, 29.5, 24.2, 22.6, 14.0 ppm. **MS (FAB$^+$)** m/z 898.301 (M+H)$^+$. **IR** 1/λ = 2915 and 2860 (sp^{3}C—H), 1568 (aromatic C=C), 1464 (sp^{3}C—H), 1314 and 1144 (-SO$_2$-), 822 (aromatic C—H), 555 (C—Br) cm^{-1}. **Anal. calcd**. for (C$_{46}$H$_{58}$Br$_2$O$_2$S$_3$): C, 61.5; H, 6.5; Br, 17.8; S, 10.7; O, 3.6%. Found: C, 61.4; H, 6.6; Br, 17.9; S, 10.9; O, 3.2%.

Product **112**:

M. p. 196-198°C. **^{1}H NMR** 400 MHz (CDCl$_3$) δ 7.61 (1H, dd, ^{3}J = 8.0 Hz, ^{4}J = 1.6 Hz, C5 ar H), 7.54 (1H, dd, ^{3}J = 8.0 Hz, ^{4}J = 1.6 Hz, C9 ar H), 7.52 (1H, ds, ^{4}J = 1.6 Hz, C3 ar H), 7.49 (1H, ds, ^{4}J = 1.6 Hz, C11 ar H), 7.46 (1H, d, ^{3}J = 8.0 Hz, C6 ar H), 7.37 (1H, d, ^{3}J = 8.0 Hz, C8 ar H), 2.26 (2H, dt, ^{3}J$_1$ = 13 Hz, ^{3}J$_2$ = 3.8 Hz, Ar—2C$\underline{H}_2$—alkyl), 1.96 (6H, m, Ar—12&2C$\underline{H}_2$—alkyl), 1.35-0.85 (32H, br m, alkyl CH$_2$), 0.81 (12H, t, ^{3}J = 7.0 Hz, CH$_3$) ppm. **^{13}C NMR** 100 MHz (CDCl$_3$) δ 157.8, 156.2, 155.3, 147.0, 140.7, 137.3, 134.8, 134.7, 133.6, 132.3, 130.33, 129.7, 125.6, 125.5, 123.3, 122.3, 120.0, 119.5, 59.9, 56.9, 39.3, 37.4, 31.0, 30.9, 29.0, 28.9, 23.7, 23.5, 22.1, 13.5 ppm. **MS (FAB$^+$)** m/z 899.203 (M+H)$^+$. **IR** 1/λ = 2909 and 2845 (sp^{3}C—H), 1572 (aromatic C=C), 1456 (sp^{3}C—H), 1310 and 1143 (-SO$_2$-), 818 (aromatic C—H), 538 (C—Br) cm^{-1}. **Anal. calcd**. for (C$_{46}$H$_{58}$Br$_2$O$_2$S$_3$): C, 61.5; H, 6.5; Br, 17.8; S, 10.7; O, 3.6%. Found: C, 61.2; H, 6.4; Br, 18.1; S, 10.4; O, 3.8%.

117. (2,5-Bis((2-ethylhexyl)oxy)-1,4-phenylene)diboronic acid
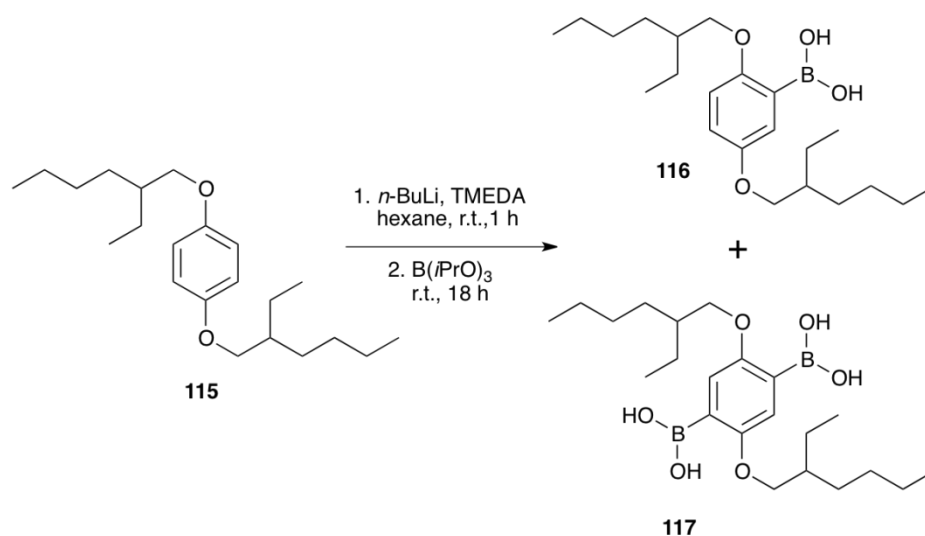
n-BuLi (2.4 M in hexanes, 30 mL, 0.072 mol) was added dropwise at room temperature to the solution of 1,4-bis(2-ethylhexyl)oxy)benzene **115** (19.39 g, 0.058 mol) and TMEDA (19.5 mL) in dry hexane (78 ml). The reaction was stirred at room temperature for 16 hours before being cooled down to 0°C. Triisopropyl borate (40 ml, 0.173 mol) was added. The reaction mixture was warmed to room temperature and

stirred for 5 h before quenching with water. The product was extracted with diethyl ether. The combined extracts were washed with water and dried over MgSO$_4$. The solvent was removed and the residue was subjected to column chromatofraphy on silica gel (ethyl acetate/hexanes, 1:10). Two fractions were collected and after evaporation of the solvent, afforded the boronic acid **116** as a viscous oil (16.52 g, 75%) and diboronic acid **117** (1.97 g, 8%) as a off white solid. Diboronic acid **117** was recrystallized from acetone hexane mixture prior the Suzuki cross-coupling polymerisation. The analysis data were in agreement with those reported elsewhere.[5]

M. p. (**117**) 135-137°C. **^{1}H NMR** (**117**) 400 MHz (DMSO) δ 7.77 (4H, s, O$\underline{H}_2$), 7.20 (2H, s, ar Hs), 3.90 (4H, d, ^3J = 5.6 Hz, –O–C$\underline{H}_2$), 1.68 (2H, m, –OCH$_2$–C$\underline{H}$–(CH$_2$)$_2$), 1.5–1.2 (16H, m, 2×8 C$\underline{H}_2$), 0.90 (12 H, m, 4×3 C$\underline{H}_3$) ppm. **^{13}C NMR** (**117**) 100 MHz (DMSO) δ 157.0, 117.8, 70.7, 30.0, 28.4, 23.4, 22.4, 13.9, 10.9 ppm. **Anal. calcd**. for (C$_{22}$H$_{40}$B$_2$O$_6$): C, 62.6; H, 9.6%. Found: C, 62.1; H, 9.6%.

106. Poly(TH-DITT), μW Yamamoto polymerisation
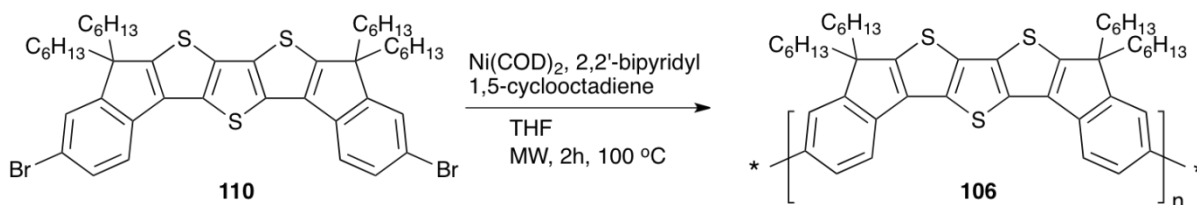
Ni(COD)$_2$ (193 mg, 0.70 mmol) was weighted out and placed in a flask together with TH-DITT-Br$_2$ **110** (300 mg, 0.35 mmol) and 2,2'-bipyridyl (109 mg, 0.70 mmol) in a glove box. 1,5-cyclooctadiene (0.09 ml, 0.70 mmol) and dry THF (20 ml) were added. The reaction was conducted in a microwave for 2 hours at 100°C. The reaction mixture was poured into methanol and allowed to precipitate in fridge overnight. The precipitate was filtered off into a thimble and subjected to Soxhlet extraction using methanol, acetone and dichloromethane in this order and for 24 hour each. The dichloromethane fraction was collected and solvent evaporated. The residue was dissolved in small amount of dichloromethane and precipitated with methanol yielding 125 mg (51%) of the polymer **106** as a yellow-brown powder.

^{1}H NMR 400 MHz (CDCl$_3$) δ 7.8-7.5 (m, aromatic protons), 2.27-1.83 (broad signal, Hs closest to the aromatic moieties), 1.37-0.93 (br m, alkyl protons), 0.88-0.61 (m, terminal CH$_3$s) ppm. **GPC**: M$_n$ 17,361 g mol^{-1}, M$_w$ 92,449 g mol^{-1}, PDI 5.3. **TGA**: T$_d$ 411.2ºC. **DSC**: T$_g$ 191.9ºC. **Anal. calcd**. for (C$_{46}$H$_{60}$S$_3$): C, 77.9; H, 8.5; S, 13.6%. Found: C, 77.0; H, 8.1; S, 12.8%.

107. Poly(TH-DITT-O$_2$), Yamamoto polymerisation
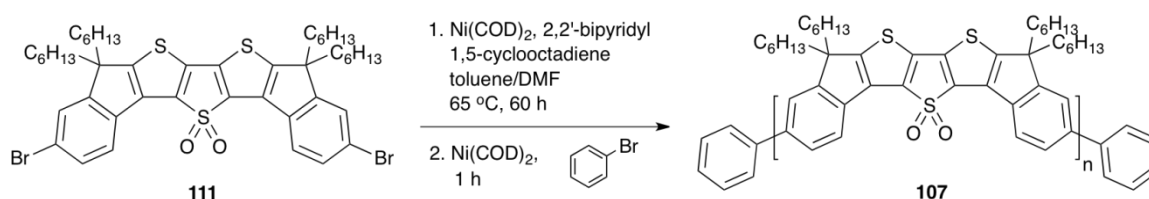
TH-DITT-O$_2$-Br$_2$ **111** (250 mg, 0.278 mmol) was dissolved in anhydrous toluene (4 ml) and added dropwise to a flask containing solution of Ni(COD)$_2$ (103 mg, 0.375 mmol), 2,2'-bipyridyl (58 mg, 0.373 mmol) and 1,5-cyclooctadiene (0.045 ml) in anhydrous DMF (5 ml). The mixture was stirred under nitrogen and with absence of light for 60 hours at 65ºC. Bromobenzene (0.03 ml, 0.278 mmol) and solution of Ni(COD)$_2$ (76 mg, 0.278 mmol) in DMF were added and the reaction was stirred for an additional hour. The mixture was then poured into methanol and allowed to precipitate in the fridge. The resulting precipitate was filtered off into a thimble and subjected to Soxhlet extraction using methanol, acetone and dichloromethane in this order and for 24 hour each. The dichloromethane fraction was collected and solvent evaporated. The residue was dissolved in small amount of dichloromethane and precipitated with methanol yielding 105 mg (51%) of the final product **107** as a yellow-brown powder.

^{1}H NMR 400 MHz (CDCl$_3$) δ 8.1-6.4 (br m, aromatic protons), 2.7-0,1 (broad signals, alkyl protons) ppm. **GPC**: M$_n$ 61,470 g mol^{-1}, M$_w$ 66,890 g mol^{-1}, PDI 1.1. **TGA**: T$_d$ 359.0ºC. **DSC**: T$_g$ 192.6ºC. **Anal. calcd**. for (C$_{46}$H$_{60}$O$_2$S$_3$): C, 74.5; H, 8.2; S, 13.0%. Found: C, 65.3; H, 6.7; S, 6.1% (the sample was suspected to undergo incomplete combustion, therefore, large deviations from the theoretical values were obtained).

108. Poly(TH-DITT-*alt*-9,9-dihexylfluorene), Suzuki cross-coupling polymerisation
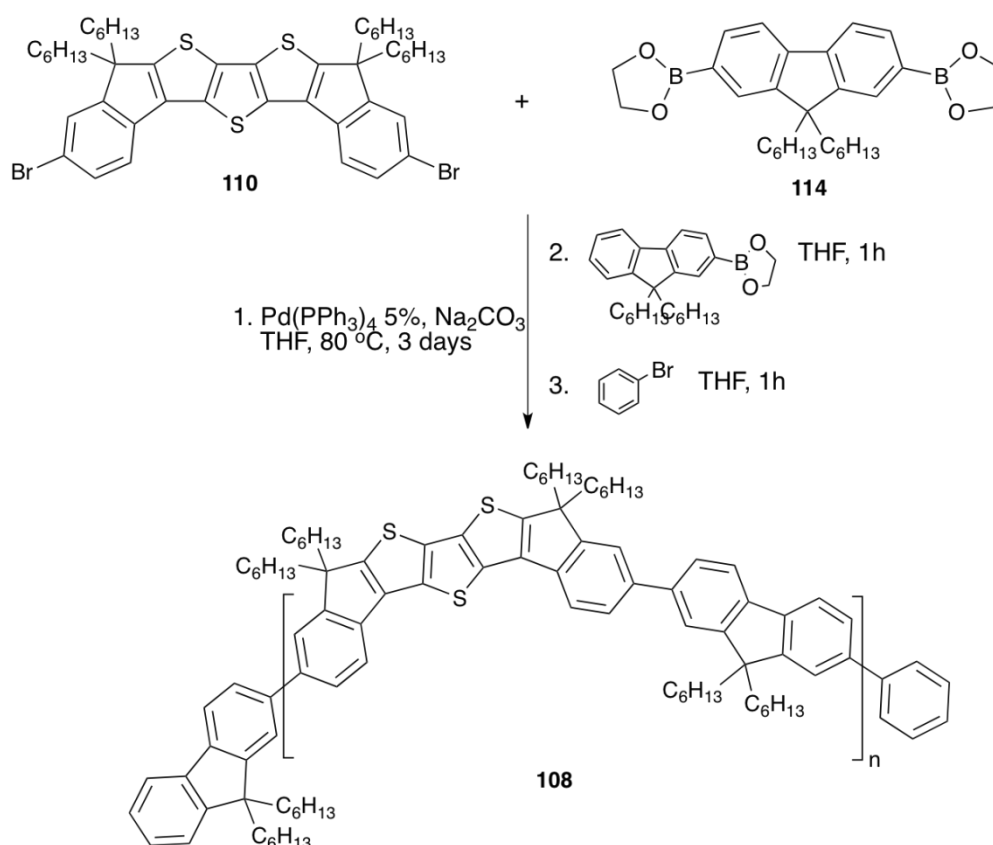
TH-DITT-Br$_2$ **110** (300 mg, 0.35 mmol), Pd(PPh$_3$) (20 mg, 0.0175 mmol) and 2,2'-(9,9-dihexyl-9H-fluorene-2,7-diyl)bis(1,3,2-dioxaborolane) **114** (166 mg, 0.35 mmol) were placed in a round-bottomed flask, purged with N$_2$ and dissolved in dry THF (10 ml). 2M solution of Na$_2$CO$_3$ (0.84 ml, 1.68 mmol) was added, the mixture was heated to 80°C and stirred at this temperature for 3 days. Solution of 2-(9,9-dihexyl-9H-fluoren-2-yl)-1,3,2-dioxaborolane (132 mg, 0.35 mmol) in dry THF (1 ml) was added to the reaction and stirred for 1 hour followed by addition of bromobenzene (0.037 ml, 0.35 mmol) and stirring for additional hour. The final mixture was poured into methanol and allowed precipitate in fridge overnight. The precipitate was filtered off into a thimble and subjected to Soxhlet extraction using methanol, acetone and dichloromethane in this order and for 24 hour each. The dichloromethane fraction was collected and solvent evaporated. The residue was dissolved in small amount of dichloromethane and precipitated with methanol yielding 303 mg (83%) of the final product **108** as a pale brown powder.

¹H NMR 400 MHz (CDCl₃) δ 7.91-7.6 (br m, aromatic Hs), 2.24-1.92 (broad signal, Hs closest to the aromatic moieties), 1.33-0.93 (br m, alkyl protons), 0.92-0.67 (m, terminal CH₃s) ppm. **GPC**: M_n 4,976 g mol^{-1}, M_w 10,931 g mol^{-1}, PDI 2.2. **TGA**: T_d 423.7ºC. **DSC**: T_g 181.8ºC. **Anal. calcd**. for ($C_{71}H_{92}S_3$): C, 81.9; H, 8.9; S, 9.2%. Found: C, 80.4; H, 8.4; S, 7.6%.

109. Poly(TH-DITT-*alt*-(2,5-bis((2-ethylhexyl)oxy)-1,4-phenylene)), Suzuki cross-coupling polymerisation

109
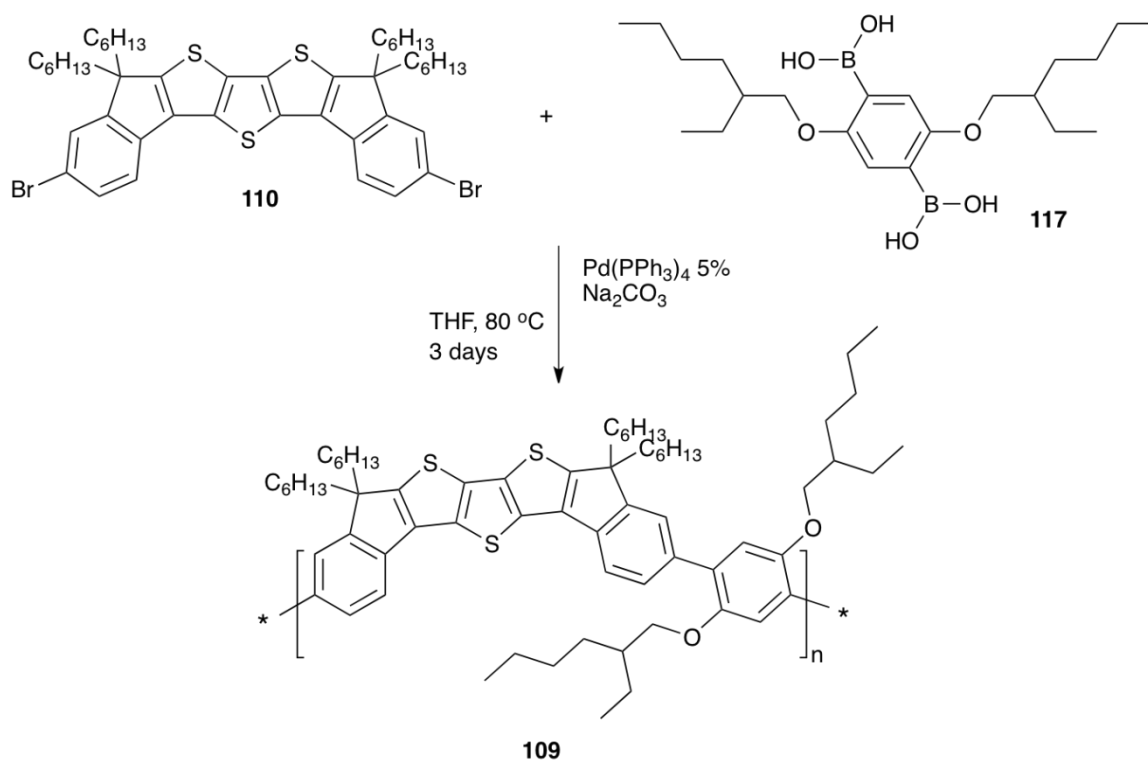
TH-DITT-Br₂ **110** (300 mg, 0.35 mmol), Pd(PPh₃) (20 mg, 0.0175 mmol) and (2,5-bis((2-ethylhexyl)oxy)-1,4-phenylene)diboronic acid **117** (148 mg, 0.35 mmol) were placed in a round-bottomed flask, purged with N₂ and dissolved in dry THF (10 ml). 2M solution of Na₂CO₃ (0.84 ml, 1.68 mmol) was added, the mixture was heated to 80°C and stirred at this temperature for 3 days. The mixture was poured into methanol and allowed precipitate in fridge overnight. The precipitate was filtered off into a thimble and subjected to Soxhlet extraction using methanol, acetone and dichloromethane in this order and for 24 hour each. The dichloromethane fraction was

collected and solvent evaporated. The residue was dissolved in small amount of dichloromethane and precipitated with methanol yielding 300 mg (83%) of the final product **109** as a medium brown powder.

^{1}H NMR 400 MHz (CDCl$_3$) δ 7.76-7.31 and 7.16-7.00 (m, aromatic protons), 4.0-3.75 (m, Hs on branched alkyl chains closest to O), 2.20-1.84 (broad signal, Hs closest to the aromatic moieties), 1.76-0.93 (br m, other alkyl protons), 0.92-0.60 (m, terminal CH$_3$s) ppm. **GPC**: M$_n$ 1,310 g mol^{-1}, M$_w$ 11,017 g mol^{-1}, PDI 8.0. **TGA**: T$_d$ 411.7°C. **DSC**: T$_g$ 112.9°C. **Anal. calcd**. for (C$_{68}$H$_{96}$O$_2$S$_3$): C, 78.4; H, 9.3; S, 9.2%. Found: C, 82.1; H, 8.8; S, 8.2%.

6.3. MALS-SEC/GPC (Multi-angle Light Scattering Size Exclusion Chromatography/Gel Permeation Chromatography)

The instrument package was supplied by Optokem and comprised the following equipment: (i) a Jones Chromatography 760 series Solvent D-Gasser, (ii) a Waters 515 HPLC pump operating at room temperature, (iii) a Jasco AS-950 autosampler with 50 position sample racks, (iv) a column oven, (v) a set of three Styragel HR 2, HR 4 and HR 6 designation 7.8 x 300 mm GPC columns, and (vi) two detectors connected in a serial configuration: a multi-angle light scattering detector (mini-Dawn) supplied by Wyatt Technology and an interferometer refractomer detector (Optilab DSP) supplied by Wyatt Technology.

THF was the mobile phase, the column oven temperature was set to 30º C, and the flow rate was 1 ml/min. The samples were prepared for injection by dissolving 10 mg of polymer in 1 ml of HPLC grade THF and filtered off with an Acrodisc® 0.2 μm PTFE membrane. 0.2 ml of this mixture was then injected, and data were collected for 40 min. The wavelength used was 690 nm. The dn/dc value used was 0.184 (poly(styrene)/THF). Astra for Windows was used to collect and process the signals transmitted from the detectors to the computer and to produce the molar mass distribution plots.

6.4. Cyclic Voltammetry

Cyclic voltammetry measurements were performed on a CH Instruments 660A Electrochemical Workstation with iR compensation, using anhydrous dichloromethane as the solvent for oxidation and tetrahydrofuran as the solvent for reduction (as stated).

The supporting electrolyte was tetrabutylammonium hexafluorophosphate (0.1 M) and the potentials were referenced against the ferrocene/ferrocenium redox couple. Glassy carbon was used as the working electrode with platinum and silver wires as the counter and pseudo-reference electrodes, respectively. Oxidation and reduction cycles were

performed separately to avoid complications in the CV due to possible side products arising from irreversible and quasi-reversible processes.

The electrochemical HOMO-LUMO gaps were calculated from the differences in the onsets of the first oxidation and reduction peaks. Using data referenced to the ferrocene/ferrocenium redox couple, HOMO and LUMO energies were calculated by subtracting the onsets from the HOMO of ferrocene, which has a known value of –4.8 eV.

6.5. PLQY Measurements

6.5.1. Solutions

Solution photoluminescence quantum yields of the samples were measured by preparing a sample in chloroform with the same absorbance at 360 nm as a standard solution of quinine sulphate in 0.5 M sulphuric acid.

The emission spectrum was then measured in a Jobin Yvon Horiba FluoroMax (molecular materials) or Jobin Yvon Spex FluoroMax 2^{TM} (polymers) spectrometers with an excitation wavelength $\lambda_{ecx} = 360$ nm, in triplicate.

6.5.2. Films

Thin films of all materials were prepared by spin coating on quartz substrates from their concentrated chloroform solutions.

The photoluminescence quantum yields of the films were determined using a Kimmon Helium-Cadmium CW laser, operating at 325 nm to excite the sample and an integrating sphere to collect the resulting emission following the method of Greenham *et al*.[6]

6.6. Time Resolved Spectroscopy of 79 and 107 (Fluorescence Lifetime Measurements)

The lifetime of a photoluminescent molecule is determined by the rate of radiative and non-radiative decay processes dissipating the excited state energy. The PLQY is equal to the ratio of the radiative rate to the sum of radiative and non-radiative rates. By combining measurements of PLQY and fluorescence lifetime in solutions and thin films it is possible to obtain more information about the impact of molecular interactions.

Time resolved fluorescence measurements were performed by the time correlated single photon counting (TCSPC) technique. A pulsed nitride laser diode at 393 nm was used to excite the sample of **79** and the resulting emission passed through a monochromator and detected a micro-channel plate-photomultiplier. The time delay between the excitation pulse and the photon detection is converted into a voltage pulse. The amplitude of pulses is then plotted on a histogram and decay statistics can be calculated. Decay curves were fitted by iterative reconvolution of the instrument response function with one or two exponential decay functions, as described below.

For the compound **79** in solution with emission collected at the peak of the fluorescence signal at 376 nm and at longer wavelengths (600 nm) the fluorescence signal decays were described by a mono exponential decay function:

$$S_F(t) = A_1 \exp(-t/\tau) + B$$

Where τ is the fluorescence lifetime and B is a constant.

For the films of **79** with emission collected at the peak at 524 nm and at longer wavelength (600 nm), the fluorescence signal decays were described by a bi-exponential decay function:

$$S_F(t) = A_1 \exp(-t/\tau_1) + A_2 \exp(-t/\tau_2) + B$$

The average PL lifetime is defined by:

$$\tau_{av} = A_1\tau_1 + A_2\tau_2 \, /(A_1 + A_2)$$

For the polymer **107**, the time resolved measurements of solution and thin film were performed by the similar method, described above. The sample was excited by a pulsed nitride laser diode at 400 nm. The emitted photons, resolved in terms of time and position, were detected by a Streak camera. When coupled with a spectrograph, the emission is simultaneously resolved as a function of time and wavelength.

The signals for both solution and thin film emission were described by bi-exponential decay function and the average lifetimes (τ_{av}) were calculated according to the equation above.

6.7. Thermal Characterisation (TGA and DSC)

6.7.1. TGA

Polymer degradation temperatures (T_d) were determined on a Perkin Elmer Thermogravimetric Analyser TGA7 under a flow of helium (20 ml/min). The temperature was raised at the rate of 10ºC/min to 500ºC. The data were processed using Pyris Series Software and each T_d was recorded at 10% weigh loss.

6.7.2. DSC

Glass transition temperatures of polymers were determined using the TA Instruments DSC Q1000 under a flow of nitrogen (20 ml/min) and the data were processed with TA Instruments Universal Analysis 200 software.
Typical method used:

1. Equilibrate at 25ºC.
2. Isothermal for 1.0 min.
3. Ramp 10.0ºC/min to 220ºC.
4. End of cycle 1.

5. Isothermal for 1.0 min.
6. Ramp 10.0ºC/min to -20ºC.
7. End of cycle 2.
8. Isothermal for 1.0 min.
9. Ramp 10.0ºC/min to 400ºC.
10. End of cycle 3.
11. End of method.

REFERENCES

1. (a) Chiang, L. Y.; Shu, P.; Holt, D.; Cowan, D., *J. Org. Chem.* **1983,** *48*, 4713; (b) Fox, M. A.; Pan, H. L., *J. Org. Chem.* **1994,** *59*, 6519; (c) Skabara, P. J.; Mullen, K.; Bryce, M. R.; Howard, J. A. K.; Batsanov, A. S., *J. Mater. Chem.* **1998,** *8*, 1719.

2. Ertas, E.; Ozturk, T., *Tetrahedron Lett.* **2004,** *45*, 3405.

3. Blanchard, P.; Jousselme, B.; Frére, P.; Roncali, J., *J. Org. Chem.* **2002,** *67*, 3961.

4. Frey, J.; Bond, A. D.; Holmes, A. B., *Chem. Commun.* **2002**, 2424-2425.

5. Monkman, A. P.; Pålsson, L.-O.; Higgins, R. W. T.; Wang, C.; Bryce, M. R.; Batsanov, A. S.; Howard, J. A. K., *J. Am. Chem. Soc.* **2002,** *124*, 6049-6055.

6. Greenham, N. C.; Samuel, I. D. W.; Hayes, G. R.; Phillips, R. T.; Kessener, Y.; Moratti, S. C.; Holmes, A. B.; Friend, R. H., *Chem. Phys. Lett.* **1995,** *241*, 89-96.

LIST OF PUBLICATIONS

1. Irina Afonina, Peter J. Skabara, Filipe Vilela, Alexander L. Kanibolotsky, John C. Forgie, Ashu K. Bansal, Graham A. Turnbull, Ifor D. W. Samuel, John G. Labram, Thomas D. Anthopoulos, Simon J. Coles and Michael. B. Hursthouse *Synthesis and Characterisation of New Diindenothienothiophene (DITT) Based Materials*, J. Mat. Chem., **2010**, *20*, 1112-1116.

2. Irina Afonina, Simon J. Coles, Michael B. Hursthouse, Alexander L. Kanibolotsky and Peter J. Skabara *10,11-dihydrodiindeno[1,2-b:2',1'-d]-thiophene,* Acta Cryst., **2008**, *E64*, 167.

APPENDIXES

A-1. X-ray Data of Compound 77

Table 1. Crystal data and structure refinement for **77**

Identification code	**77**
Empirical formula	$C_{22}H_{12}S_3$
Formula weight	372.50
Temperature	120(2) K
Wavelength	0.71073 Å
Crystal system	Monoclinic
Space group	P2(1)/c
Unit cell dimensions	a = 15.8475(14) Å a= 90º.
	b = 15.8514(14) Å b= 98.498(6)º.
	c = 6.9724(4) Å g = 90º.
Volume	1732.3(2) Å^3
Z	4
Density (calculated)	1.428 Mg/m^3
Absorption coefficient	0.429 mm^{-1}
F(000)	768
Crystal size	0.45 x 0.02 x 0.01 mm^3
Theta range for data collection	3.22 to 27.49º.
Index ranges	-20<=h<=20, -20<=k<=20, -8<=l<=9
Reflections collected	19708
Independent reflections	3940 [R(int) = 0.1068]
Completeness to theta = 27.49º	99.1 %
Absorption correction	Semi-empirical from equivalents
Max. and min. transmission	0.9957 and 0.8305
Refinement method	Full-matrix least-squares on F^2
Data / restraints / parameters	3940 / 0 / 227
Goodness-of-fit on F^2	1.104
Final R indices [I>2sigma(I)]	R1 = 0.1079, wR2 = 0.2576
R indices (all data)	R1 = 0.1583, wR2 = 0.2819
Extinction coefficient	0.013(4)
Largest diff. peak and hole	1.393 and -0.864 e. Å^{-3}

Special details

Table 2. Atomic coordinates (x 10^4) and equivalent isotropic displacement parameters (Å^2x 10^3) for **77**

	x	y	z	U(eq)
C(1)	2012(4)	3217(4)	1690(8)	20(1)
C(2)	2335(4)	2405(3)	1814(8)	19(1)
C(3)	3237(4)	2380(4)	2023(9)	20(1)
C(4)	3583(4)	3185(4)	2103(9)	22(1)
C(5)	4536(4)	3180(4)	2340(9)	24(1)
C(6)	4713(4)	2235(4)	2417(9)	25(1)
C(7)	5490(4)	1813(4)	2653(9)	30(2)
C(8)	5488(5)	934(5)	2692(10)	34(2)
C(9)	4714(5)	479(4)	2485(11)	36(2)
C(10)	3936(5)	895(4)	2261(9)	27(1)
C(11)	3935(4)	1777(4)	2214(8)	22(1)
C(12)	1108(4)	3242(4)	1450(8)	20(1)
C(13)	763(4)	2439(4)	1378(8)	20(1)
C(14)	-149(4)	2451(4)	1074(8)	20(1)
C(15)	-456(4)	3260(4)	981(9)	23(1)
C(16)	-1423(4)	3291(4)	653(9)	26(1)
C(17)	-1625(4)	2353(4)	609(8)	22(1)
C(18)	-2418(4)	1973(4)	378(9)	27(1)
C(19)	-2455(5)	1087(4)	338(10)	31(2)
C(20)	-1712(5)	605(4)	575(9)	27(1)
C(21)	-909(4)	992(4)	819(9)	26(1)
C(22)	-869(4)	1873(4)	833(9)	22(1)
S(1)	2819(1)	3973(1)	1875(2)	25(1)
S(2)	1531(1)	1647(1)	1599(2)	21(1)
S(3)	332(1)	4021(1)	1195(2)	24(1)

U(eq) is defined as one third of the trace of the orthogonalized U^{ij} tensor.

Table 3. Bond lengths [Å] and angles [º] for **77**

C(1)-C(2)	1.383(8)	C(2)-C(1)-C(12)	113.2(5)
C(1)-C(12)	1.417(8)	C(2)-C(1)-S(1)	112.0(5)
C(1)-S(1)	1.745(6)	C(12)-C(1)-S(1)	134.9(5)
C(2)-C(3)	1.415(9)	C(1)-C(2)-C(3)	113.1(5)
C(2)-S(2)	1.743(6)	C(1)-C(2)-S(2)	112.1(5)
C(3)-C(4)	1.387(8)	C(3)-C(2)-S(2)	134.8(5)
C(3)-C(11)	1.454(8)	C(4)-C(3)-C(2)	111.5(5)
C(4)-C(5)	1.495(9)	C(4)-C(3)-C(11)	108.1(5)
C(4)-S(1)	1.731(6)	C(2)-C(3)-C(11)	140.4(6)
C(5)-C(6)	1.524(9)	C(3)-C(4)-C(5)	112.8(5)
C(6)-C(7)	1.389(9)	C(3)-C(4)-S(1)	113.1(5)
C(6)-C(11)	1.421(9)	C(5)-C(4)-S(1)	134.1(5)
C(7)-C(8)	1.393(10)	C(4)-C(5)-C(6)	100.7(5)
C(8)-C(9)	1.411(11)	C(7)-C(6)-C(11)	120.4(6)
C(9)-C(10)	1.386(10)	C(7)-C(6)-C(5)	129.3(6)
C(10)-C(11)	1.398(9)	C(11)-C(6)-C(5)	110.3(5)
C(12)-C(13)	1.384(8)	C(6)-C(7)-C(8)	118.7(7)
C(12)-S(3)	1.734(6)	C(7)-C(8)-C(9)	120.9(7)
C(13)-C(14)	1.429(9)	C(10)-C(9)-C(8)	120.9(7)
C(13)-S(2)	1.740(6)	C(9)-C(10)-C(11)	118.5(7)
C(14)-C(15)	1.369(8)	C(10)-C(11)-C(6)	120.7(6)
C(14)-C(22)	1.454(9)	C(10)-C(11)-C(3)	131.2(6)
C(15)-C(16)	1.516(9)	C(6)-C(11)-C(3)	108.1(5)
C(15)-S(3)	1.726(6)	C(13)-C(12)-C(1)	111.4(5)
C(16)-C(17)	1.520(8)	C(13)-C(12)-S(3)	112.3(5)
C(17)-C(18)	1.382(9)	C(1)-C(12)-S(3)	136.2(5)
C(17)-C(22)	1.410(9)	C(12)-C(13)-C(14)	112.2(5)
C(18)-C(19)	1.407(9)	C(12)-C(13)-S(2)	113.1(5)
C(19)-C(20)	1.393(10)	C(14)-C(13)-S(2)	134.6(5)
C(20)-C(21)	1.400(9)	C(15)-C(14)-C(13)	111.4(5)
C(21)-C(22)	1.397(9)	C(15)-C(14)-C(22)	108.6(5)
		C(13)-C(14)-C(22)	140.1(6)
		C(14)-C(15)-C(16)	112.4(5)
		C(14)-C(15)-S(3)	113.8(5)
		C(16)-C(15)-S(3)	133.8(5)
		C(15)-C(16)-C(17)	100.2(5)

C(18)-C(17)-C(22)	121.4(6)	C(21)-C(22)-C(17)	120.1(6)
C(18)-C(17)-C(16)	127.9(6)	C(21)-C(22)-C(14)	131.7(6)
C(22)-C(17)-C(16)	110.7(6)	C(17)-C(22)-C(14)	108.2(5)
C(17)-C(18)-C(19)	118.2(6)	C(4)-S(1)-C(1)	90.3(3)
C(20)-C(19)-C(18)	120.9(7)	C(13)-S(2)-C(2)	90.2(3)
C(19)-C(20)-C(21)	120.7(6)	C(15)-S(3)-C(12)	90.3(3)
C(22)-C(21)-C(20)	118.6(6)		

Symmetry transformations used to generate equivalent atoms
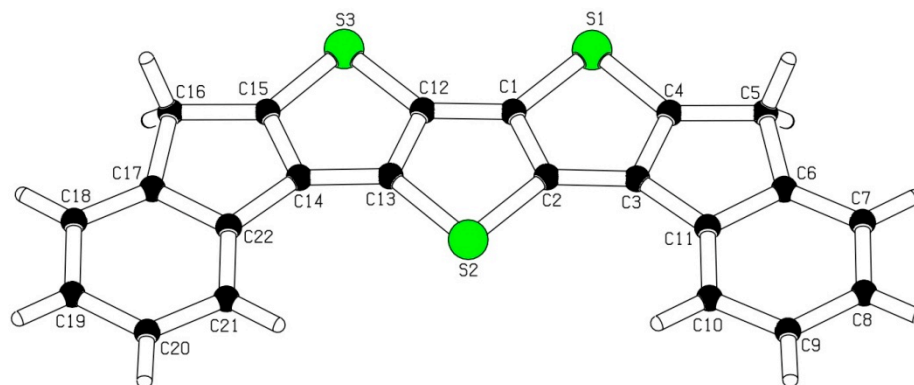
Table 4. Anisotropic displacement parameters (Å^2 x 10^3) for **77**

	U^{11}	U^{22}	U^{33}	U^{23}	U^{13}	U^{12}
C(1)	26(3)	16(3)	18(3)	6(2)	1(2)	2(2)
C(2)	30(3)	13(3)	15(3)	5(2)	6(2)	-2(2)
C(3)	26(3)	14(3)	22(3)	-2(2)	5(2)	0(2)
C(4)	30(3)	15(3)	20(3)	1(2)	3(2)	0(2)
C(5)	26(3)	21(3)	24(3)	-2(2)	5(2)	-6(3)
C(6)	26(3)	32(3)	17(3)	1(3)	1(2)	1(3)
C(7)	29(4)	37(4)	22(3)	-2(3)	1(3)	1(3)
C(8)	34(4)	37(4)	32(4)	1(3)	5(3)	19(3)
C(9)	43(5)	26(4)	39(4)	0(3)	8(3)	8(3)
C(10)	33(4)	24(3)	24(3)	-2(3)	3(3)	7(3)
C(11)	27(3)	23(3)	15(3)	2(2)	3(2)	2(3)
C(12)	27(3)	14(3)	18(3)	4(2)	6(2)	5(2)
C(13)	29(3)	12(3)	18(3)	7(2)	4(2)	3(2)
C(14)	28(3)	23(3)	10(3)	1(2)	1(2)	0(3)
C(15)	29(3)	19(3)	19(3)	1(2)	1(2)	0(3)
C(16)	31(4)	23(3)	22(3)	2(2)	4(3)	2(3)
C(17)	30(3)	18(3)	18(3)	1(2)	7(2)	3(3)
C(18)	22(3)	35(4)	25(3)	0(3)	9(3)	-2(3)
C(19)	29(4)	35(4)	30(4)	-5(3)	7(3)	-3(3)
C(20)	38(4)	22(3)	23(3)	1(3)	7(3)	-3(3)
C(21)	32(4)	19(3)	28(3)	1(3)	11(3)	3(3)
C(22)	28(3)	23(3)	17(3)	5(2)	8(2)	3(3)
S(1)	29(1)	15(1)	30(1)	0(1)	5(1)	-2(1)
S(2)	26(1)	15(1)	21(1)	0(1)	5(1)	1(1)
S(3)	29(1)	15(1)	26(1)	1(1)	4(1)	2(1)

The anisotropic displacement factor exponent takes the form: $-2p^2[h^2a^{*2}U^{11} + ... + 2\,h\,k\,a^*b^*\,U^{12}]$

A-2. X-ray Data of Compound *112*

Table 1. Crystal data and structure refinement for **112**

Identification code	**112**
Empirical formula	$C_{46}H_{58}Br_2O_2S_3$
Formula weight	898.92
Temperature	120(2) K
Wavelength	0.71073 Å
Crystal system	Monoclinic
Space group	P2(1)/c
Unit cell dimensions	a = 11.367(2) Å a= 90°.
	b = 12.002(2) Å b= 99.687(7)°.
	c = 32.790(6) Å g = 90°.
Volume	4409.4(14) Å^3
Z	4
Density (calculated)	1.354 Mg/m^3
Absorption coefficient	2.016 mm^{-1}
F(000)	1872
Crystal size	0.4 x 0.06 x 0.02 mm^3
Theta range for data collection	2.92 to 27.50°.
Index ranges	-11<=h<=14, -14<=k<=14, -42<=l<=42
Reflections collected	34665
Independent reflections	8461 [R(int) = 0.1808]
Completeness to theta = 27.50∞	83.4 %
Absorption correction	Semi-empirical from equivalents
Max. and min. transmission	0.952 and 0.742
Refinement method	Full-matrix least-squares on F^2
Data / restraints / parameters	8461 / 0 / 482
Goodness-of-fit on F^2	1.019
Final R indices [I>2sigma(I)]	R1 = 0.1343, wR2 = 0.2932
R indices (all data)	R1 = 0.2712, wR2 = 0.3739
Largest diff. peak and hole	1.066 and -0.701 e.Å^{-3}

Special details

Table 2. Atomic coordinates (x 10^4) and equivalent isotropic displacement parameters ($\approx^2$x 10^3) for **112**.

	x	y	z	U(eq)
C(1)	158(12)	3068(10)	-2075(4)	35(3)
C(2)	-687(12)	3839(11)	-2170(4)	39(3)
C(3)	-1301(12)	3750(11)	-2601(4)	37(3)
C(4)	-915(12)	2884(10)	-2808(4)	38(3)

C(5)	-2299(13)	4274(11)	-2871(4)	38(3)
C(6)	-3024(12)	5176(11)	-2814(4)	41(4)
C(7)	-3899(13)	5468(12)	-3146(4)	45(4)
C(8)	-4055(14)	4870(13)	-3513(5)	53(4)
C(9)	-3336(12)	3987(11)	-3569(4)	40(3)
C(10)	-2487(13)	3682(11)	-3255(4)	41(4)
C(11)	-1527(13)	2770(11)	-3242(4)	43(4)
C(12)	-2092(12)	1618(11)	-3329(4)	41(4)
C(13)	-2874(12)	1236(13)	-3024(4)	48(4)
C(14)	-3188(14)	9(13)	-3055(5)	56(4)
C(15)	-3917(14)	-397(12)	-2749(5)	53(4)
C(16)	-4228(14)	-1618(12)	-2784(4)	51(4)
C(17)	-4829(15)	-2093(14)	-2447(5)	69(5)
C(18)	-716(14)	3032(12)	-3570(4)	52(4)
C(19)	-133(14)	4187(13)	-3520(5)	58(4)
C(20)	708(12)	4385(12)	-3826(5)	50(4)
C(21)	1229(13)	5537(14)	-3804(5)	57(5)
C(22)	2055(14)	5822(13)	-3396(5)	60(4)
C(23)	2602(14)	6982(13)	-3374(5)	59(5)
C(24)	735(10)	3091(11)	-1655(3)	31(3)
C(25)	310(11)	4009(10)	-1451(4)	33(3)
C(26)	874(11)	4138(12)	-1042(4)	39(4)
C(27)	1712(11)	3308(10)	-931(4)	31(3)
C(28)	902(12)	4871(12)	-690(4)	40(3)
C(29)	228(12)	5835(11)	-658(4)	36(3)
C(30)	464(13)	6415(12)	-284(4)	45(4)
C(31)	1288(13)	6033(11)	40(4)	41(4)
C(32)	1971(13)	5078(11)	6(4)	44(4)
C(33)	1747(13)	4504(12)	-365(4)	46(4)
C(34)	2373(12)	3441(10)	-492(4)	36(3)
C(35)	3735(12)	3598(11)	-470(4)	42(4)
C(36)	4034(12)	4690(12)	-673(4)	49(4)
C(37)	5208(10)	4613(12)	-847(4)	43(4)
C(38)	5597(12)	5785(13)	-973(5)	56(4)
C(39)	6620(13)	5723(14)	-1219(5)	57(4)
C(40)	7051(15)	6865(16)	-1328(5)	81(6)
C(41)	2105(12)	2477(10)	-198(4)	39(3)
C(42)	2651(14)	1370(12)	-275(5)	56(4)

C(43)	2412(17)	531(12)	41(5)	69(5)
C(44)	3062(18)	-573(14)	25(5)	79(6)
C(45)	2710(20)	-1259(16)	-319(5)	96(7)
C(46)	3514(14)	-2305(11)	-354(5)	54(4)
O(1)	-77(8)	1057(8)	-2413(3)	50(3)
O(2)	1369(8)	2284(8)	-2646(3)	55(3)
S(1)	257(3)	2164(3)	-2494(1)	43(1)
S(2)	1864(3)	2413(3)	-1325(1)	42(1)
S(3)	-828(3)	4714(3)	-1772(1)	40(1)
Br(1)	-5227(2)	5347(2)	-3960(1)	67(1)
Br(2)	1576(1)	6868(1)	539(1)	49(1)

U(eq) is defined as one third of the trace of the orthogonalized U^{ij} tensor.

Table 3. Bond lengths [Å] and angles [°] for **112**.

C(1)-C(2)	1.332(17)	C(24)-S(2)	1.737(13)
C(1)-C(24)	1.421(17)	C(25)-C(26)	1.394(17)
C(1)-S(1)	1.770(12)	C(25)-S(3)	1.743(12)
C(2)-C(3)	1.473(18)	C(26)-C(27)	1.384(17)
C(2)-S(3)	1.704(13)	C(26)-C(28)	1.447(17)
C(3)-C(4)	1.355(17)	C(27)-C(34)	1.514(17)
C(3)-C(5)	1.458(18)	C(27)-S(2)	1.711(13)
C(4)-C(11)	1.480(18)	C(28)-C(33)	1.381(19)
C(4)-S(1)	1.766(15)	C(28)-C(29)	1.401(18)
C(5)-C(6)	1.393(18)	C(29)-C(30)	1.399(17)
C(5)-C(10)	1.429(18)	C(30)-C(31)	1.372(19)
C(6)-C(7)	1.390(19)	C(31)-C(32)	1.399(18)
C(7)-C(8)	1.386(19)	C(31)-Br(2)	1.899(14)
C(8)-C(9)	1.369(19)	C(32)-C(33)	1.384(18)
C(8)-Br(1)	1.895(15)	C(33)-C(34)	1.553(19)
C(9)-C(10)	1.339(18)	C(34)-C(35)	1.549(19)
C(10)-C(11)	1.541(19)	C(34)-C(41)	1.569(17)
C(11)-C(12)	1.532(18)	C(35)-C(36)	1.533(18)
C(11)-C(18)	1.561(19)	C(36)-C(37)	1.540(17)
C(12)-C(13)	1.517(18)	C(37)-C(38)	1.55(2)
C(13)-C(14)	1.51(2)	C(38)-C(39)	1.526(18)
C(14)-C(15)	1.485(18)	C(39)-C(40)	1.52(2)
C(15)-C(16)	1.508(19)	C(41)-C(42)	1.505(19)
C(16)-C(17)	1.507(19)	C(42)-C(43)	1.503(19)
C(18)-C(19)	1.53(2)	C(43)-C(44)	1.52(2)
C(19)-C(20)	1.517(18)	C(44)-C(45)	1.40(2)
C(20)-C(21)	1.50(2)	C(45)-C(46)	1.57(2)
C(21)-C(22)	1.54(2)	O(1)-S(1)	1.418(10)
C(22)-C(23)	1.52(2)	O(2)-S(1)	1.441(9)
C(24)-C(25)	1.417(17)		

C(2)-C(1)-C(24)	114.2(11)	C(20)-C(21)-C(22)	115.2(13)
C(2)-C(1)-S(1)	112.4(10)	C(23)-C(22)-C(21)	115.5(13)
C(24)-C(1)-S(1)	133.2(11)	C(25)-C(24)-C(1)	109.6(11)
C(1)-C(2)-C(3)	112.4(11)	C(25)-C(24)-S(2)	110.1(8)
C(1)-C(2)-S(3)	114.0(10)	C(1)-C(24)-S(2)	140.1(10)
C(3)-C(2)-S(3)	133.6(11)	C(26)-C(25)-C(24)	113.8(11)
C(4)-C(3)-C(5)	108.1(12)	C(26)-C(25)-S(3)	134.6(11)
C(4)-C(3)-C(2)	113.3(12)	C(24)-C(25)-S(3)	111.7(9)
C(5)-C(3)-C(2)	138.3(12)	C(27)-C(26)-C(25)	111.0(12)
C(3)-C(4)-C(11)	114.3(13)	C(27)-C(26)-C(28)	107.8(11)
C(3)-C(4)-S(1)	111.1(10)	C(25)-C(26)-C(28)	141.2(14)
C(11)-C(4)-S(1)	134.5(10)	C(26)-C(27)-C(34)	112.5(11)
C(6)-C(5)-C(10)	120.0(13)	C(26)-C(27)-S(2)	113.9(10)
C(6)-C(5)-C(3)	132.2(12)	C(34)-C(27)-S(2)	133.3(10)
C(10)-C(5)-C(3)	107.8(11)	C(33)-C(28)-C(29)	121.6(13)
C(7)-C(6)-C(5)	116.9(13)	C(33)-C(28)-C(26)	109.9(13)
C(8)-C(7)-C(6)	121.3(14)	C(29)-C(28)-C(26)	128.5(13)
C(9)-C(8)-C(7)	121.6(14)	C(30)-C(29)-C(28)	116.7(13)
C(9)-C(8)-Br(1)	119.2(11)	C(31)-C(30)-C(29)	121.3(14)
C(7)-C(8)-Br(1)	119.0(11)	C(30)-C(31)-C(32)	121.8(13)
C(10)-C(9)-C(8)	118.6(13)	C(30)-C(31)-Br(2)	119.1(10)
C(9)-C(10)-C(5)	121.5(13)	C(32)-C(31)-Br(2)	119.0(11)
C(9)-C(10)-C(11)	129.1(13)	C(33)-C(32)-C(31)	117.1(14)
C(5)-C(10)-C(11)	109.2(12)	C(28)-C(33)-C(32)	121.4(14)
C(4)-C(11)-C(12)	112.2(11)	C(28)-C(33)-C(34)	110.2(12)
C(4)-C(11)-C(10)	100.2(11)	C(32)-C(33)-C(34)	128.4(14)
C(12)-C(11)-C(10)	111.3(12)	C(27)-C(34)-C(35)	112.9(10)
C(4)-C(11)-C(18)	114.0(12)	C(27)-C(34)-C(33)	99.5(10)
C(12)-C(11)-C(18)	109.3(10)	C(35)-C(34)-C(33)	112.8(11)
C(10)-C(11)-C(18)	109.7(11)	C(27)-C(34)-C(41)	112.9(11)
C(13)-C(12)-C(11)	115.0(11)	C(35)-C(34)-C(41)	110.9(10)
C(14)-C(13)-C(12)	114.0(11)	C(33)-C(34)-C(41)	107.2(10)
C(15)-C(14)-C(13)	115.2(12)	C(36)-C(35)-C(34)	112.1(11)
C(14)-C(15)-C(16)	114.7(12)	C(35)-C(36)-C(37)	112.2(12)
C(17)-C(16)-C(15)	116.2(12)	C(36)-C(37)-C(38)	110.3(11)
C(19)-C(18)-C(11)	113.8(11)	C(39)-C(38)-C(37)	111.9(12)

| C(20)-C(19)-C(18) | 112.4(12) | C(40)-C(39)-C(38) | 112.6(13) |
C(21)-C(20)-C(19)	113.6(12)	C(42)-C(41)-C(34)	114.8(11)
C(43)-C(42)-C(41)	110.4(11)	O(2)-S(1)-C(4)	111.7(6)
C(42)-C(43)-C(44)	114.5(13)	O(1)-S(1)-C(1)	112.0(6)
C(45)-C(44)-C(43)	117.6(18)	O(2)-S(1)-C(1)	112.4(6)
C(44)-C(45)-C(46)	115.9(18)	C(4)-S(1)-C(1)	90.7(6)
O(1)-S(1)-O(2)	115.8(6)	C(27)-S(2)-C(24)	91.1(6)
O(1)-S(1)-C(4)	111.6(6)	C(2)-S(3)-C(25)	90.4(6)

Symmetry transformations used to generate equivalent atoms

Table 4. Anisotropic displacement parameters ($\approx^2$x 10^3) for **112**.

	U^{11}	U^{22}	U^{33}	U^{23}	U^{13}	U^{12}
C(1)	40(9)	18(7)	47(8)	-5(6)	8(6)	-1(7)
C(2)	44(9)	28(8)	46(8)	1(6)	9(7)	10(7)
C(3)	39(9)	24(8)	43(8)	-6(6)	-7(6)	-8(7)
C(4)	46(9)	19(8)	49(8)	-3(6)	5(7)	-19(7)
C(5)	50(10)	23(8)	41(8)	2(6)	11(7)	4(7)
C(6)	54(10)	31(9)	37(8)	-1(6)	4(7)	-4(8)
C(7)	39(9)	36(9)	60(9)	-11(7)	6(7)	-3(7)
C(8)	71(11)	40(10)	48(9)	7(7)	7(8)	11(9)
C(9)	49(9)	33(9)	36(8)	2(6)	-2(6)	-7(8)
C(10)	47(10)	36(9)	41(8)	5(7)	9(7)	1(7)
C(11)	62(10)	37(9)	27(7)	-3(6)	1(6)	3(8)
C(12)	49(9)	32(9)	37(7)	1(6)	-12(6)	12(7)
C(13)	31(9)	66(12)	46(8)	14(7)	6(6)	15(8)
C(14)	57(11)	51(11)	65(10)	-3(8)	27(8)	10(9)
C(15)	61(11)	41(10)	59(10)	-5(8)	15(8)	-17(8)
C(16)	63(11)	49(11)	42(8)	4(7)	10(7)	-2(8)
C(17)	69(12)	74(13)	70(11)	-9(9)	25(9)	-28(10)
C(18)	64(11)	43(10)	45(8)	-9(7)	4(7)	11(8)
C(19)	69(11)	56(11)	50(9)	15(8)	15(8)	7(9)
C(20)	35(9)	52(11)	61(10)	13(8)	4(7)	1(8)
C(21)	46(10)	72(13)	57(10)	8(8)	19(8)	16(9)
C(22)	60(11)	60(12)	60(10)	16(9)	11(8)	10(9)
C(23)	56(11)	57(11)	67(10)	21(9)	24(8)	16(9)
C(24)	23(7)	38(8)	28(6)	-9(6)	-7(5)	-11(6)

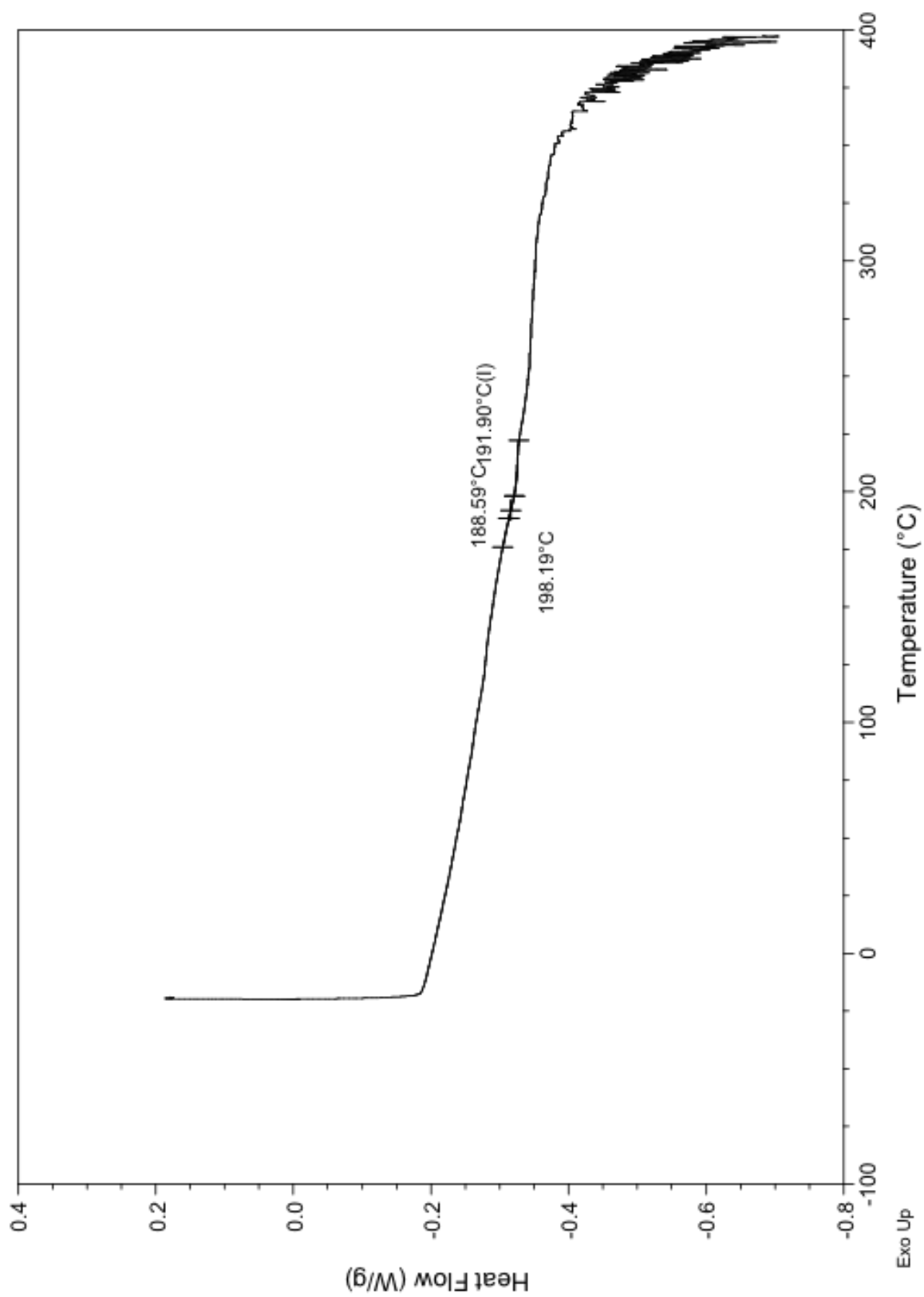|						
C(25)	30(8)	26(8)	37(7)	8(6)	-7(6)	11(6)
C(26)	18(8)	59(10)	38(8)	-1(7)	0(5)	-21(7)
C(27)	29(8)	17(7)	44(7)	5(6)	-4(6)	-5(6)
C(28)	39(9)	38(9)	45(8)	-7(7)	17(7)	-6(8)
C(29)	34(8)	30(8)	42(8)	-3(6)	1(6)	-17(7)
C(30)	46(10)	39(9)	52(9)	-6(7)	14(7)	-5(8)
C(31)	55(10)	12(8)	57(9)	12(6)	12(7)	-5(7)
C(32)	55(10)	30(9)	43(8)	-3(6)	0(7)	-11(8)
C(33)	54(10)	45(10)	38(8)	4(7)	7(7)	-26(8)
C(34)	51(10)	17(7)	38(7)	6(6)	0(6)	13(7)
C(35)	50(10)	37(9)	41(8)	0(6)	11(7)	-5(7)
C(36)	34(9)	53(10)	57(9)	-11(8)	-3(7)	-6(8)
C(37)	11(7)	61(11)	53(8)	5(7)	-5(6)	-7(7)
C(38)	35(9)	73(12)	60(10)	-21(9)	6(7)	-11(8)
C(39)	39(10)	68(12)	61(10)	-2(9)	-1(7)	-5(9)
C(40)	53(12)	125(18)	68(12)	14(11)	19(9)	-3(12)
C(41)	47(9)	22(8)	46(8)	6(6)	0(6)	-13(7)
C(42)	65(11)	50(11)	55(9)	8(8)	17(8)	-1(9)
C(43)	110(15)	26(10)	81(12)	-16(8)	41(11)	-5(10)
C(44)	116(17)	51(12)	67(12)	7(9)	4(11)	-33(11)
C(45)	160(20)	72(15)	55(11)	1(10)	10(12)	-40(15)
C(46)	82(12)	19(8)	64(10)	-9(7)	25(9)	0(8)
O(1)	49(6)	48(7)	52(6)	4(5)	6(5)	10(5)
O(2)	44(7)	70(7)	52(6)	-2(5)	13(5)	7(5)
S(1)	50(3)	43(3)	36(2)	-3(2)	6(2)	2(2)
S(2)	39(2)	45(2)	41(2)	-3(2)	3(2)	-1(2)
S(3)	45(2)	37(2)	38(2)	-3(2)	5(2)	2(2)
Br(1)	59(1)	86(1)	49(1)	-2(1)	-5(1)	20(1)
Br(2)	51(1)	53(1)	43(1)	-8(1)	8(1)	-5(1)

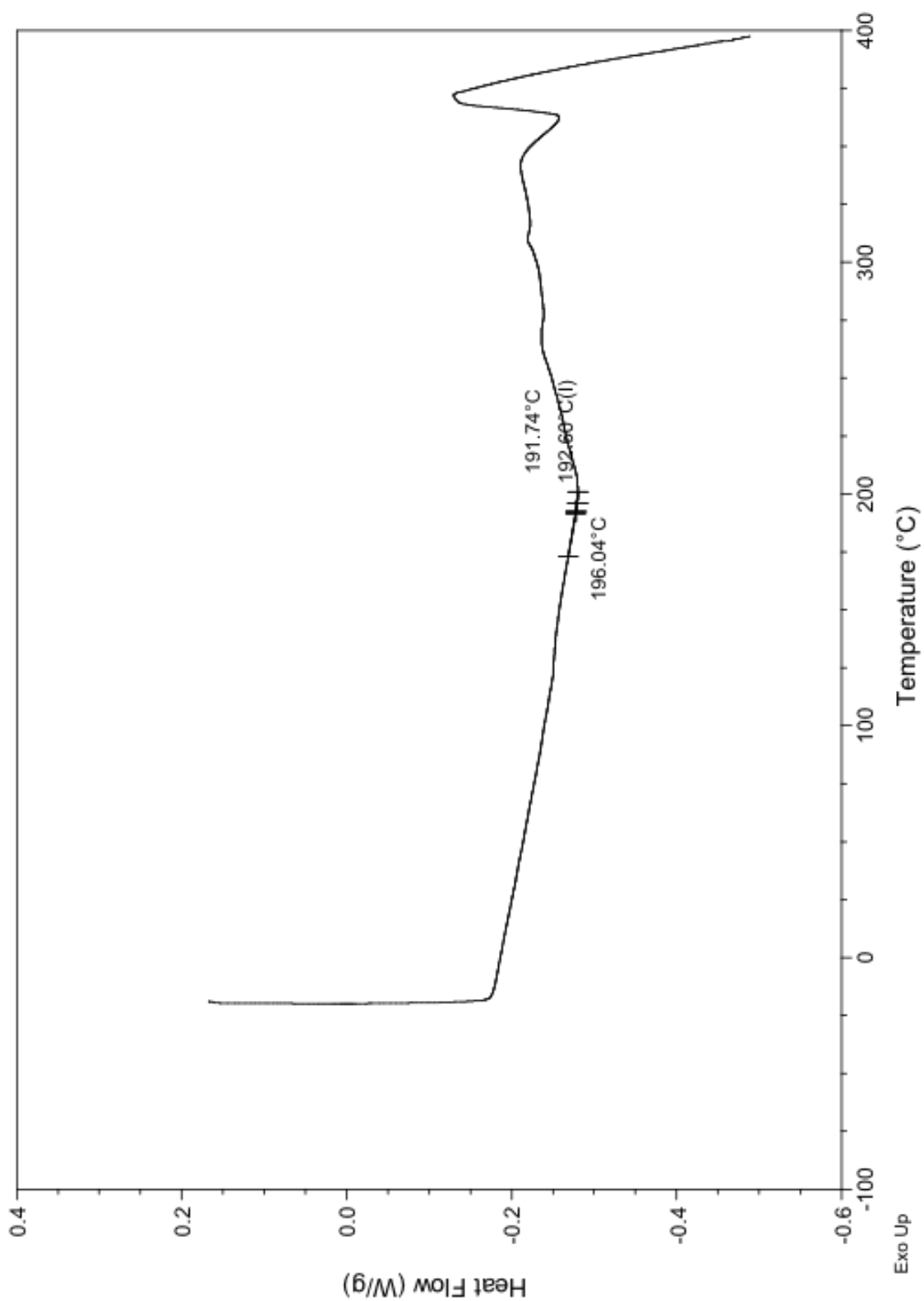The anisotropic displacement factor exponent takes the form: $-2p^2[h^2a^{*2}U^{11} + ... + 2\,h\,k\,a^*\,b^*\,U^{12}]$.
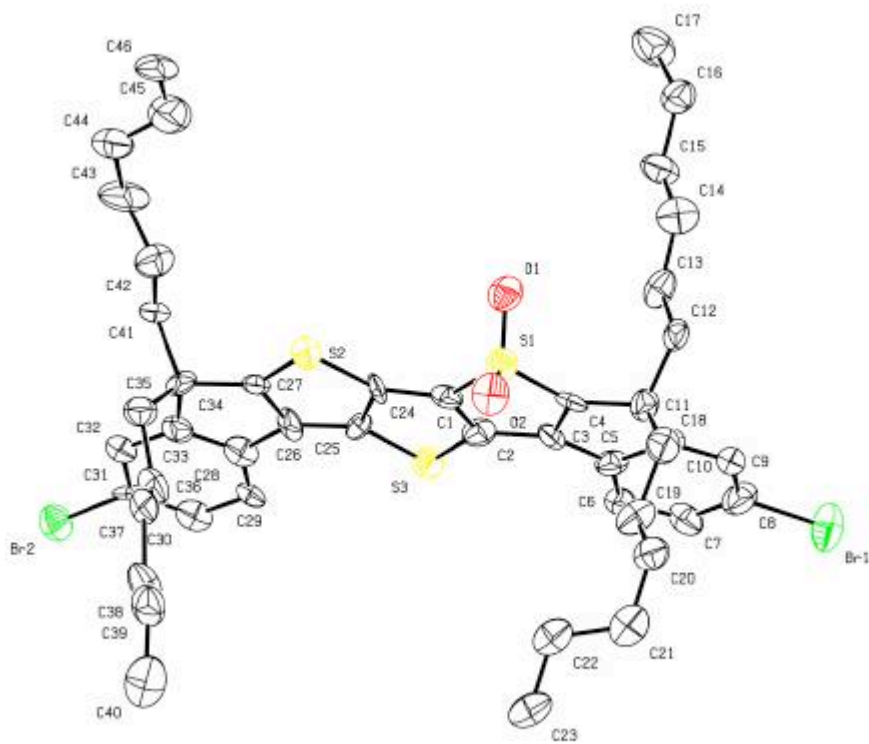
A-3. NOE-Experiment of Compound 110

Data acquired at 600 MHz
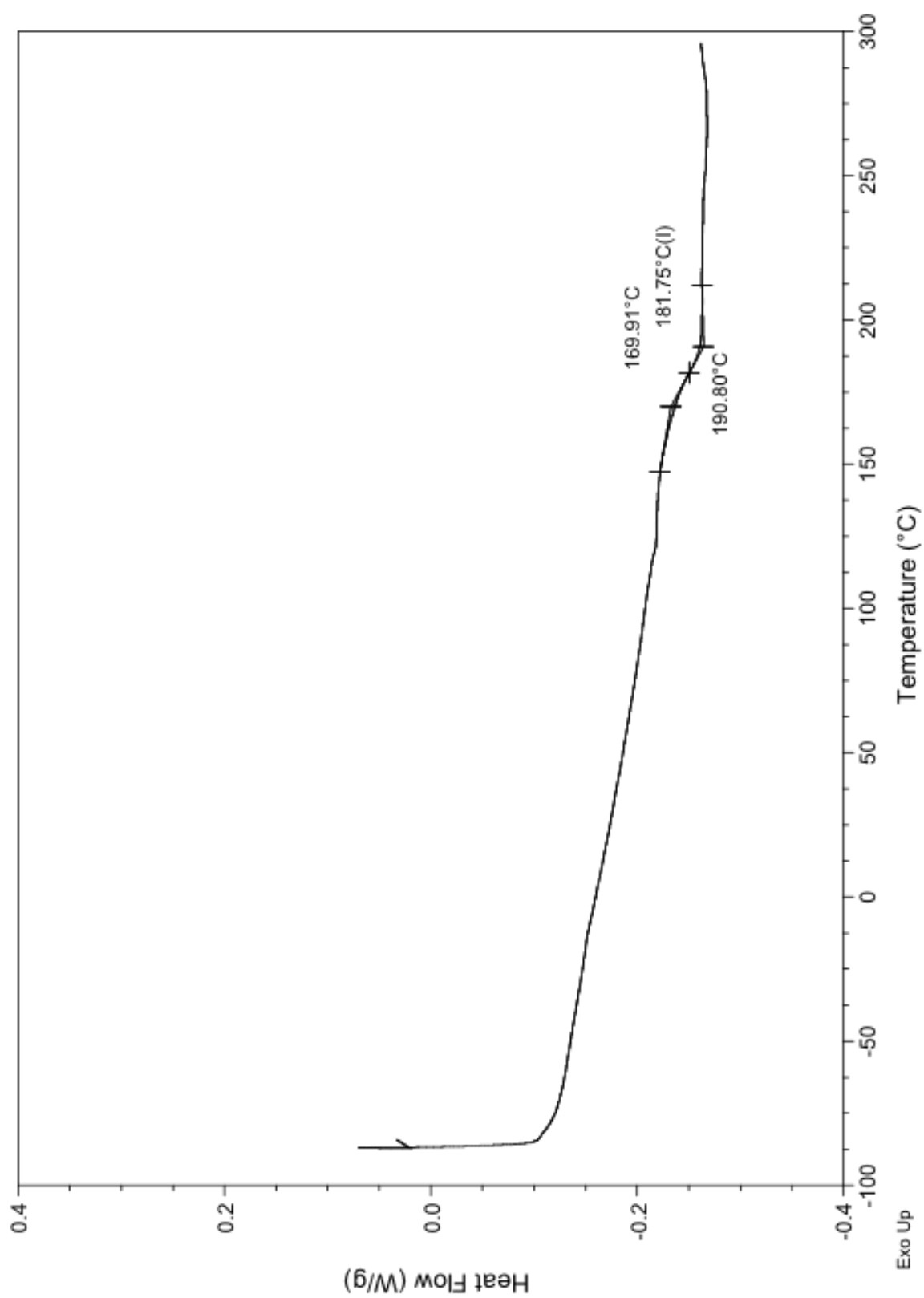
nOe irradiating at:

1D 1H NMR Spectrum
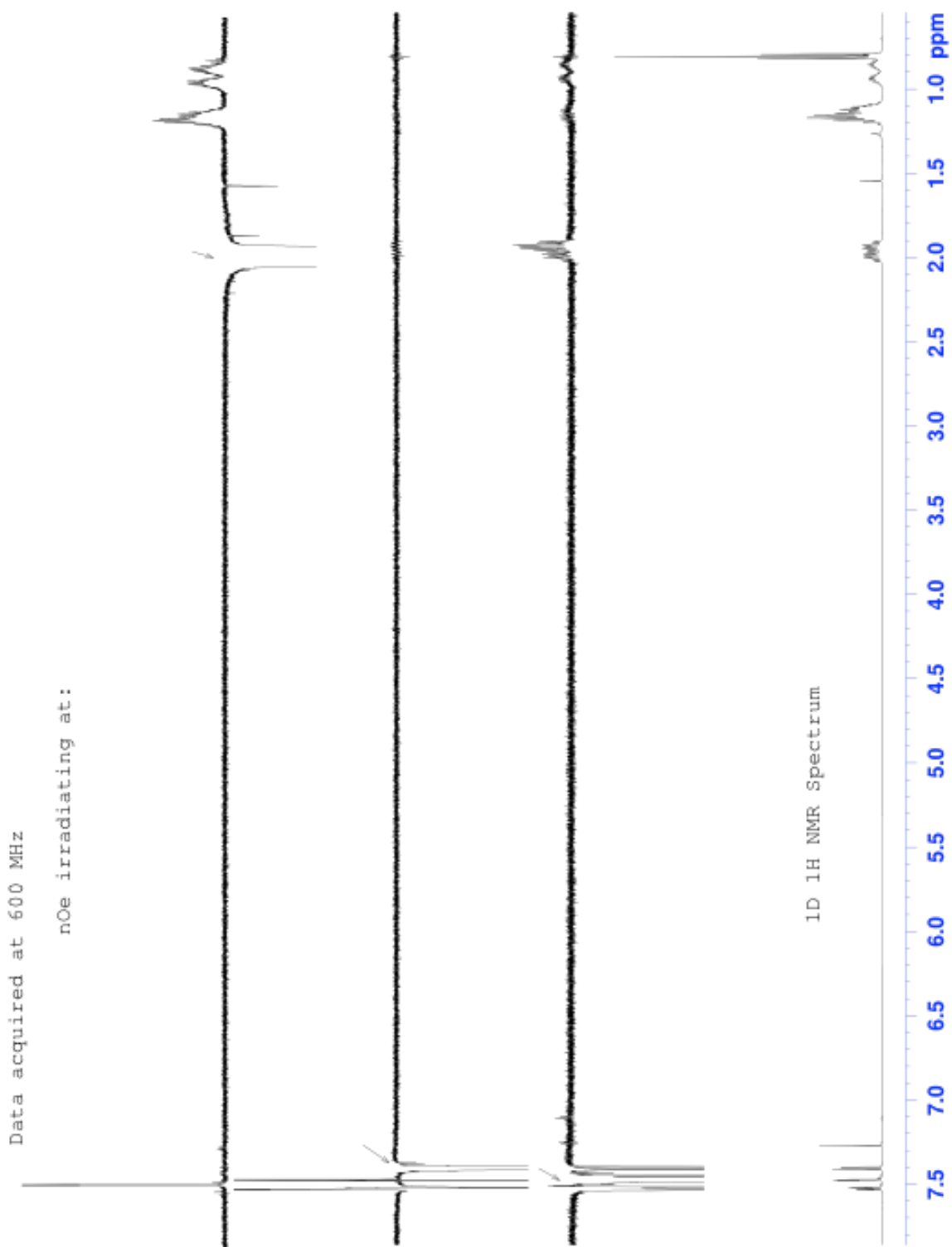
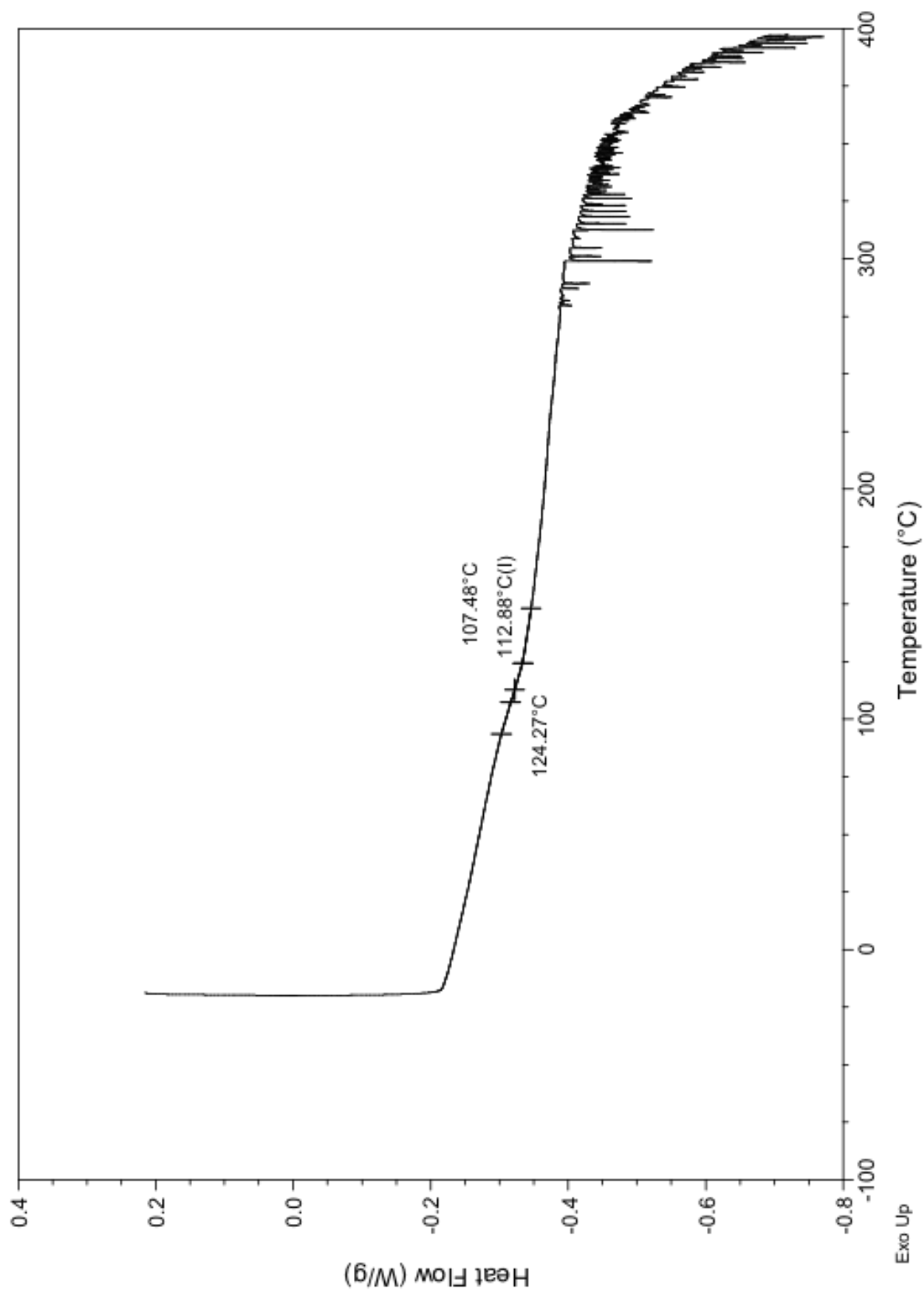## A-4. DSC Trace of Polymer *106*

A-5. DSC Trace of Polymer 107

A-6. DSC Trace of Polymer 108

*A-7. DSC Trace of Polymer **109***

A-8. TGA of Polymers *106-109*